



Dissertation

Spectral and Thermodynamic Properties of Organic Exciplexes.

Sadia Asim

Graz, im Dezember 2011

zur Erlangung des akademischen Grades des Doktors
der technischen Wissenschaften

Doktoratsstudium der Technischen Wissenschaften im
Technische Universität Graz „Institut für Physikalische und
Theoretische Chemie“

Betreuer:

O.Univ.-Prof. Dipl.-Chem. Dr. Günter Grampp

to My Loving Parents
to Sweet Abdulah
to Asim Mansha

Contents

1. Introduction	1
2. Theoretical Perspective	5
2.1. Mechanism of Fluorescence Quenching	5
2.2. Historical Background of Exciplex	7
2.3. Excimer Stability	7
2.3.1. Excitation Resonance Interaction	7
2.3.2. Intermolecular Charge Transfer	8
2.3.3. MO Theoretical Calculations	8
2.3.4. Arrangement in Pairs and Intra Molecular Excimers	8
2.3.5. Triplet-Triplet Annihilation, Electron Transfer and Stable Dimeric Cations	8
2.4. Exciplex Stability	9
2.4.1. A.Weller's Mechanism for Exciplex Formation	9
2.4.2. M.G.kuz'min Mechanism for Exciplex Formation	11
2.4.3. Electronic Structure of Exciplex	14
2.4.4. the Farid and Gould Model	16
2.5. Types of Exciplex	18
2.6. Thermodynamic Parameters and Kinetics of Exciplexes	19
2.6.1. Calculation of Average Emission Frequencies	19
2.6.2. A.Weller's Calculations Scheme	20
2.6.3. Calculation of Diffusion-Coefficient	25
2.6.4. Calculation of Activation Enthalpy of Diffusion	25
2.6.5. Calculation of Diffusion Rate Constant	25
2.6.6. The Kuz'min Calculation Scheme	27
2.6.7. Band Parameters Obtained from Excited Emission Spectra	34
2.6.8. Fluorescence Lifetimes and Quantum Yields of Exciplex and Fluorophore	36
2.6.9. Calculation of Gibbs Energy of Electron Transfer Using Rehm-Weller Equation	41
2.7. Factors Effecting Solution Dynamics of Exciplexes	43
2.8. Electron Donor and Acceptor – Electrochemical and Photophysical Properties	47
2.9. Energy Transfer and Electron Transfer in Photoinduced Electron Transfer	48
3. Experimental	51
3.1. Solvents	51

3.1.1. Propylacetate/Butyronitrile Mixture	53
3.2. Reactants	53
3.2.1. Fluorophores	54
3.2.2. Quenchers	54
3.3. Absorption Spectroscopy	54
3.4. Fluorescence Spectroscopy	56
3.4.1. Fluoromax:	56
3.4.2. Thermally Insulated Box With Cuvette Holder:	56
3.4.3. Temperature Regulating Liquids and Thermometers:	58
3.4.4. Light Guide Arrangement Inside the Fluoromax:	59
3.4.5. Light Lost by Liquid Light Guide	61
3.5. Time Resolved Fluorescence Spectroscopy	61
3.5.1. Time Correlated Single Photon Counting (TCSPC)	62
3.5.2. Phase-Modulation Fluorometry	72
3.6. Sample Preparation	77
4. Results and Discussion	79
4.1. Spectral Shifts	80
4.1.1. 1-Cyanonaphthalene/Hexamethylbenzene Exciplex System(1-CN/HMB)	80
4.1.2. 2,3-Dicyanonaphthalene/Hexamethylbenzene Exciplex System(2,3- DCN/HMB)	83
4.1.3. N,N-dimethylaniline and biphenyl System (DMA/BP)	83
4.1.4. Pyrene and N,N'-bis(dimethylamino)diphenylmethane system(PY/DMDPM)	85
4.1.5. N-alkylated Carbazoles with Dicyanobenzenes	88
4.2. Fluorophore and Exciplex Peak Intensities	88
4.2.1. Fluorophore peak intensities in absence of quencher	88
4.2.2. Ratio of Exciplex Peak Intensity to the Fluorophore Peak Intensity in Presence of Quencher	91
4.3. Exciplex Energetics–Band Parameters Obtained from Excited Emission Spectra:	96
4.3.1. Energy of zero-zero Transitions and Gauss Broadening of Vibronic Level	96
4.3.2. Huang-Rhys Factor (S) and Energy of Dominant High-Frequency Vibration	102
4.4. Fluorescence Life Times	105
4.4.1. Fluorescence Lifetime of Fluorophore	105
4.4.2. Fluorescence Lifetime of Exciplex	108
4.5. Equilibrium constant for exciplex formation	110
4.6. Extent of charge transfer between donor and acceptor	112
4.7. Parameters appearing in Kuzmin's equations:	114
4.8. Enthalpy of Exciplex Formation	119
4.9. Entropy of Exciplex Formation	122
4.10. Gibb's Energy of Exciplex Formation	124
5. Conclusions and Outlooks	127

5.1. Concluding Remarks	127
5.2. Outlook	129
A. Appendix	131
A.1. Spectral Shifts	131
A.1.1. 1-cyanonaphthalene/hexamethylbenzene Exciplex System (1-CN/HMB)	131
A.1.2. 2,3-dicyanonaphthalene/hexamethylbenzene Exciplex System(2,3-DCN/HMB)	134
A.1.3. N,N'-dimethylaniline and biphenyl System (DMA/BP)	137
A.1.4. Pyrene and N,N'-bis(dimethylamino)diphenylmethane system(PY/DMDPM)	140
A.1.5. N-alkylated Carbazoles With Dicyanobenzenes	143
A.2. Exciplex Energetics–Band Parameters Obtained from Excited Emission Spectra:	144
A.2.1. Energy of zero-zero transitions and Gauss broadening of Vibronic level	144
A.2.2. Huang-Rhys factor (S) and energy of dominant high-frequency vibration	144
A.3. Fluorescence Life Times	147
A.3.1. Fluorescence Lifetime of Exciplex	147
A.4. Parameters appearing in Kuzmin’s equations:	150
A.5. Enthalpy of exciplex formation	151
B. Acronyms	155
Bibliography	157

List of Tables

3.1. Solvents With Some Fundamental Physical Properties	52
3.2. Fluorophores With Some Fundamental physical Properties	55
3.3. Fundamental physical Properties of Quenchers	56
3.4. Instrumental Configuration and Parameters of the SPT Equipment	70
3.5. Pulse Energies Characteristic of Flash Lamp	73
4.1. Spectral Shift of Exciplex.	82
4.2. Data of N-Alkylcarbazol/Dicyanobenzenes.	90
4.3. Fluorophore Peak Intensity in Absence of Quencher.	91
4.4. Ratio of Exciplex Peak Intensity to Fluorophore Peak Intensities in Presence of Quencher in Various Solvents.	92
4.5. Zero-zero Transition Energy.	98
4.6. Gauss Broadening of Vibronic Level.	100
4.7. Difference of Shift Values with Respect to Non-Polar Solvent for 1-CN/HMB.	101
4.8. Huang-Rhys Factor as a Function of Solvent Polarity for all Exciplex Systems.	102
4.9. Energy of Dominant High-Frequency Vibration as a Function of Solvent Polarity for all Exciplex Systems.	104
4.10. Fluorescence Lifetimes of Fluorophores as a Function of Solvent Polarity.	106
4.11. Fluorescence Lifetimes for Exciplex System 1-CN/HMB as a Function of Solvent Polarity.	108
4.12. Equilibrium Constant for Exciplex Formation and Extent of Charge Transfer Between Donor and Acceptor for Exciplex System 1-CN/HMB as a Function of Solvent Polarity.	111
4.13. Kuzmin's Parameters Used in Further Calculations.	115
4.14. Dipole Moment for 1-CN/HMB Exciplex.	117
4.15. Enthalpy of Exciplex Formation for 1-CN/HMB Exciplex System.	120
4.16. Entropy of Exciplex Formation for 1-CN/HMB Exciplex System.	123
4.17. Gibb's Energy of Exciplex Formation for 1-CN/HMB Exciplex System.	125
A.1. Fluorescence Lifetimes for Exciplex System 2,3-DCN/HMB as a Function of Solvent Polarity.	147
A.2. Fluorescence Lifetimes for Exciplex System DMA/BP as a Function of Solvent Polarity.	148
A.3. Fluorescence Lifetimes for Exciplex System DMA/BP as a Function of Solvent Polarity.	149
A.4. Fluorescence Lifetimes for Exciplex System PY/DMDPM as a Function of Solvent Polarity.	150

List of Figures

2.1. General Reaction Scheme for Photo Induced Electron Transfer Reactions	6
2.2. Molecular Orbital Description of Exciplex and Ground State Complexes.	10
2.3. General Potential Curve Representing Conventional Exciplex	17
2.4. General Potential Curve Representing Bonded Exciplex	18
2.5. Reaction Scheme for A.Weller's Model.	21
2.6. Reaction Scheme for M.G. Kuz'min Model	27
2.7. Figure Showing Kuzmin's Fitting Parameters	35
2.8. Pictorial Representation of Fluorescence Lifetimes.	38
2.9. Thermodynamic Pathway for Photoinduced Electron Transfer	42
2.10. Dynamic Interconversion of Various Species in Solution	44
2.11. Effects of Solvent Polarity on Photoinduced Electron Transfer Reactions.	47
2.12. Effects of Solvent Polarity on Energetics of Electron Transfer.	48
2.13. Energy Transfer Versus Electron Transfer.	49
3.1. Structures of the Fluorophore Used in the Present Studies.	54
3.2. Structures of the Quenchers Used in the Present Studies.	55
3.3. Fluoromax with Temperature Regulating Assembly	57
3.4. Picture of Fluoromax with Temperature Regulating Assembly	58
3.5. Thermally Insulated Box with Cuvette Holder	59
3.6. Calibration Curve For Temperature Regulating Assembly	60
3.7. Normal Cuvette Holder Inside the Fluoromax	60
3.8. Cuvette with Light Guide Arrangement Inside the Fluoromax	61
3.9. light Lost by Liquid Light Guide	62
3.10. Simplified Scheme of a Time Correlated Single Photon Counting Fluorometer	63
3.11. Leading-edge Timing Versus Constant-fraction Timing	67
3.12. Formation of Constant Fraction Signal	68
3.13. Voltage Ramp Generated by Time-to-amplitude Converter (TAC)	68
3.14. Configuration of SPT Instrument	69
3.15. Phase and modulation of Fluorescence in Response to Intensity-modulated Excitation Using Single Frequency	74
3.16. Diagram for Basic Setup of Modulation	75
3.17. Original Data recorded on DSO	76
4.1. Fluorescence Spectra of 1-CN and 1-CN/HMB Exciplex in Butylacetate	81
4.2. Fluorescence Spectra of 2,3-DCN and 2,3-DCN/HMB Exciplex in Toluene	84
4.3. Spectral Shifts for 2,3-DCN/HMB	85
4.4. Fluorescence Spectra of DMA and DMA/BP Exciplex in Butylacetate	86

4.5.	Fluorescence Spectra of PY and PY/DMDPM Exciplex in Propylacetate/Butyronitrile Solvent Mixture with $x_p = 0.9$ Propylacetate.	87
4.6.	Spectral Shifts for PY/DMDPM	88
4.7.	Fluorescence Spectra of Carbazoles and DCB Exciplex in Tetrahydrofuran	89
4.8.	Ratio of Peak Intensities of Exciplex to Fluorophore in the Presence of Quencher for 1-CN/HMB.	93
4.9.	Ratio of Peak Intensities of Exciplex to Fluorophore in the Presence of Quencher for 2,3-DCN/HMB and N-alkylated Carbazoles/Dicyanobenzenes.	94
4.10.	Ratio of Peak Intensities of Exciplex to Fluorophore in the Presence of Quencher for DMA/BP.	94
4.11.	Ratio of Peak Intensities of Exciplex to Fluorophore in the Presence of Quencher for PY/DMDPM.	95
4.12.	Exciplex Emission Spectra Obtained After Fitting to Kuzmin's Model of Self-consistent Polarization.	97
4.13.	Energy of Zero-Zero Transition as a Function of Temperature.	99
4.14.	Extent of Charge Transfer as a Function of Refractive Index and Exciplex Spectral Shift with Respect to Fluorophore for Exciplex System 1-CN/HMB	114
4.15.	Dependence of Destabilization Energy on Various factors.	116
4.16.	Dependence of $(H_{22}^{\circ} - H_{11}^{\circ})$ on Various Factors	119
4.17.	Dependence of (H_{12}) on Various Factors	119
4.18.	Reciprocal Temperature Dependence of $\ln(\phi'/\phi)$ for the Exciplexes of 1-CN/HMB.	121
4.19.	Dependence of Gibb's Energy of Electron Transfer on Various Factors for the Exciplexes of 1-CN/HMB.	126
A.1.	Emission spectra of 1-CN with HMB in solvents with ϵ from 1.91 to 2.42	131
A.2.	Emission spectra of 1-CN with HMB exciplex in solvents with ϵ from 4.18 to 9.74	132
A.3.	Emission spectra of 1-CN with HMB in solvents with ϵ from 10.43 to 19.09	133
A.4.	Emission spectra of 2,3-CN with HMB in solvents with ϵ from 1.91 to 6.0	134
A.5.	Emission spectra of 2,3-CN with HMB in solvents with ϵ from 6.06 to 10.43	135
A.6.	Emission spectra of 2,3-CN with HMB in solvents with ϵ from 11.61 to 19.09	136
A.7.	Emission spectra of DMA with BP in solvents with ϵ from 1.91 to 4.18	137
A.8.	Emission spectra of DMA with BP in solvents with ϵ from 4.91 to 10.43	138
A.9.	Emission spectra of DMA with BP in solvents with ϵ from 11.61 to 19.09	139
A.10.	Emission spectra of PY with DMDPM in solvents with ϵ from 1.91 to 6.0	140
A.11.	Emission spectra of PY with DMDPM in solvents with ϵ from 6.06 to 10.43	141
A.12.	Emission spectra of PY with DMDPM in solvents with ϵ from 11.61 to 19.09	142
A.13.	Emission spectra of N-alkylated carbazoles with dicyanobenzenes in solvents tetrahydrofuran.	143
A.14.	Gauss Broadening of Vibronic Level vs. Temperature	144
A.15.	Spectral Huang-Rhys Factor as a Function of Temperature for all Exciplex Systems.	145

A.16. Energy of Dominant High-Frequency Vibration as a Function of Temperature for all Exciplex.	146
A.17. Graph between ν_{max} and $f - 1/2f'$ for 1-CN/HMB Exciplex System. . .	151
A.18. Reciprocal temperature Dependence of $\ln(\phi'/\phi)$ for the exciplexes of 1-CN/HMB.	152
A.19. Reciprocal temperature Dependence of $\ln(\phi'/\phi)$ for the exciplexes of 1-CN/HMB.	153

Abstract

This work presents the spectral and thermodynamic properties of organic exciplexes in organic solvents over a range of temperature (from 253 to 338 K). The steady state and time resolved techniques were used to find the emission intensities and fluorescence lifetimes of fluorophores and exciplexes. First of all the peak positions, peak shifts and peak intensities of both fluorophores and exciplexes were compared with each other as a function of solvent polarity and temperature. Later in order to obtain the band parameters representing the energetics of exciplexes the data was fitted to the Kuz'min's model of self-consistent polarization. Next step was the evaluation of lifetimes of fluorophores and exciplexes. Then the thermodynamic parameters were calculated and compared by using the kinetic models proposed by A.Weller and M.G.Kuz'min.

In the end of work it was concluded that soon after the exciplex formation the solvent molecules rearrange themselves around it and they may stabilize or destabilized the reactant exciplex. In case of non polar solvents the solvent stabilization between the ion pair state is weak and therefore the donor and acceptor of exciplex remain tightly held together due to the absence of significant solvent stabilization. Resultantly stronger exciplex with larger stability is observed in non polar solvents.

Zusammenfassung

In dieser Arbeit werden spektrale und thermodynamische Eigenschaften von Exciplexen organischer Moleküle untersucht. Die Untersuchungen erfolgten in zahlreichen organischen Lösungsmitteln unterschiedlicher Polarität und jeweils in einem Temperaturbereich von 253 bis 338 K. Steady-state und zeitaufgelöste Single-Photon Counting Fluoreszenzmessungen sind zur Bestimmung der Exciplexintensitäten, sowie von Lebensdauern der Fluorophore und der Exciplexe herangezogen worden. Genaue Untersuchungen der Bandenlage und der Bandenverschiebungen sowie deren Intensität wurden jeweils als Funktion der unterschiedlichen Lösungsmittel und der Temperatur angestellt. Die erhaltenen Ergebnisse sind mit Hilfe des theoretischen Modells nach Kuzmin interpretiert und dargestellt. Die thermodynamischen Daten sind sowohl nach dem Kuzmin Modell als auch mit dem Modell nach Weller interpretiert worden.

Es konnte gezeigt werden, dass die Solventrelaxation nach der Exciplexbildung für die Stabilität der jeweiligen Exciplexe eine besondere Rolle spielt. In unpolaren Lösungsmitteln ist nur eine schwache Wechselwirkung auf, während in polaren Lösungsmitteln die Exciplexe eine größere Stabilität aufweisen, was sich in den thermodynamischen Größen, wie Enthalpie und Entropie wieder spiegelt.

Acknowledgments

According to Ludwig Wittgenstein “Knowledge is in the end based on acknowledgment.” In the light of this quote I will like to thanks to my parents, family, friends, teachers and all other relations who make me able to finish this task. All of them could not be mentioned here but I would like to thanks all of them by saying “ thank you every one from core of my heart for making me accomplish this goal. With out your help and support I was unable to manage it.” Some people are really very special and I will like to admit that because of their extra support, patience and generosity I was able to manage this task.

First of all I will like to thank to almighty GOD for bestowing me with good health and series of opportunities to reach at this stage. After GOD I am able to reach this stage due to my parents. Ami, papa I love you alot. I am feeling very proud to say thanks to you. I can never forget your love and support for me. Ami I find that your arms were always open when I needed a hug. Your heart understood when I needed a friend. Your strength and love has guided me and gave me wings to fly. Papa in my view point you are the person who catch me before I fall rather you give me enough courage to try again, you clean my tears, give me enough courage and strength to make my own way, scolds me when I did some mistake and you shines with pride when I get succeed. Then I will like to thanks to my brothers and sisters as they prove to be a great support for me.

I would like to express my profound gratitude to Prof. Grampp for giving me a chance to work with him. Here I am feeling that the my vocabulary is insufficient to write acknowledgment for you. Your gentle, caring and inspirational personality helps me to learn alot from you. Your enthusiasm and passion for work serves to be a great source of inspiration for me. I find you always available when I need help and guidance. Your polite nature and freedom of though make the working atmosphere very comfortable for me. Here I will says a big thanks to Mrs. Jutta Grampp due to he charming and joyful personality. I will ever remember her as she helps me to settle in the new atmosphere.

I feel pleasure to thanks to some of my teachers Prof. M. Shahid Ansari as he supervise

me in MPhil and he make me learn lots of things about physical chemistry and especially he makes me learn how to work in lab. I will also like to mention Prof. M.S. Subhani here because he makes me learn the basics of photochemistry and this proves to be very strong foundation for my further work in photochemistry.

A deep thanks goes to Arnulf Rospeinter for his proper guidance and incredible help in the start of my studies. Especially his help in LaTeX and writing complex LaTeX programs for me because as a result of this I was able to save my lots of time. I will also like to thanks to Prof. Stephan Landgraf as he was always their to solve any problem relating the instrument. His expertise in electronics and user friendly softwares makes me feel comfortable when I working. With out his help I can only dream of working in lab. I am also grateful to him as he make the Single Photon Counting and the Frequency Modulation running for me when I need it.

Big thanks go to Hilde Freißmuth, Helmut Eisenköbl, Herbert Lang, and Marion Hofmeister. All of them make things running for me during my stay by providing me chemicals, solvents, glassware, internet facility, mechanical and electric help and also helping me in administrative issues. With their help I was able to work relaxedly and with more efficiency.

My Pakistani colleagues (Asim, Zahid, Faiza, Rashida, Tajamal, tahir and Noureen) were lovely people as with them I never miss my home. I can never forget the parties which we have together. Their presence never make me feel that I am away from my home country. Here I will like to thanks to my colleagues (Boryana, Daniel, Kenneth, Truong, Kraiwan, Kunal and Christine). They all were very patient and polite with me. I have lots of good memories form them. I have learned alot about from these all people.

Now I will like to mention two loveliest people of my life Asim and Abdullah. I feel my self incomplete with out them . Here I will agree with Thomas Jefferson for his saying that “The happiest moments of my life have been the few which I have passed at home in the bosom of my family”. Asim’s expertises in photochemistry and his caring nature makes me feel that I am not alone rather I find him holding my hand on every step of life. His love and support makes difficult things easy for me. His passion for cooking and tea along with light chitchat makes my weekends very special. You really prove to be my best friend and I can proudly say that “you are infact the best friend I ever have”. Abdullah you are most the beautiful gift of GOD for me. Ever I was tired your smiles make me fresh again. From you I have learned how to love unconditionally not expecting anything

in return, how to be innocent and how to enjoy the small things in life. I will say that Asim and Abdullah you both are behind my achievement and success and I would never be able to paid for the support and strength you both give me ··· so THANKYOU! you both have made my life worthwhile.

In the end I will like to thank to Higher Education Commission (HEC) of Pakistan for their financial help and support.

1. Introduction

To my self I am only a child
playing on the beach, while vast
oceans of truth lie undiscovered
before me

(Isaac Newton)

Interactions between the electron donor and acceptor in ground state results in the formation of charge transfer (CT) complex which is characterized by the appearance of a new absorption band at lower energies. An exciplex is formed as a result of bimolecular interactions between an excited fluorophore (acting as acceptor (A)) and a ground state quencher acting as electron donor (D) and vice versa.¹ In 1963 exciplexes were reported for the first time.² Previously the classical mechanism of electron transfer, based on the model proposed by the Marcus^{3,4} was used to describe the electron transfer from donor to the excited acceptor after preliminary reorganization of reactants and media. This electron jump provides degenerate electronic term for reactants and products along with the subsequent relaxation of the products and the media. Later it was concluded^{5,6} that electron transfer between donor and excited acceptor involves transient formation of exciplex and a gradual shift of electron density from donor to acceptor and change in the nuclear coordinates of reactants and media, rather than a diabatic jump.⁷ Thus the formation of exciplex occurs with the change in the electronic structure of excited fluorophore and quencher, at the same time changes in medium reorganization also occur.^{8,9}

Exciplexes are very important excited state complexes and they appear as transient species in many photochemical reactions particularly photoinduced electron transfer reactions.^{6,10} Usually a strong binding energy in the range of 20 - 80 kJ/mol, charge transfer nature, relatively long lifetimes and moderate stabilities are characteristics of exciplexes. Exciplex formation is often indicated by the appearance of a broad structureless emission band. Emission from the exciplex is predicted by vertical Frank-Condon allowed transitions from a minimum on an excited-state surface to a low lying repulsive ground state surface. Emission from exciplex may not be observed if there is a significant nuclear change during the transition to the low-lying ground state surface. Such non-emitting

exciplexs have properties similar to the contact ion pairs.

In present thesis the fluorescence spectra were recorded from 253 to 340 K by using fluorescence spectrometer and the temperature was regulated by a home built thermally insulated box with cuvette holder inside it. Details about the construction of this box and about the calibration of the light guides attached with this box are discussed in the experimental portion of this thesis. Following are the important points of discussion in the present document. The exciplex systems of 1-cyanonaphthalene with hexamethylbenzene (1-CN/HMB), 2,3-dicyanonaphthalene with hexamethylbenzene (2,3-DCN/HMB), biphenyl with N,N'-dimethyl aniline (BP/DMA), pyrene with 4,4'-bis(dimethylamino)diphenyl methane (PY/DMADM), N-methyl carbazole with 1,2-dicyanobenzene (NMC/1,2-DCB), N-methyl carbazole with 1,3-dicyanobenzene (NMC/1,3-DCB), N-methylcarbazole with 1,4-dicyanobenzene (NMC/1,4-DCB), and N-ethylcarbazole with 1,2-dicyanobenzene (NEC/1,2-DCB) are discussed as a function of solvent polarity and temperature.

- Appearance of fluorophore peak along with the red shift in the wavelength due to exciplex formation is discussed in first part of results and discussion. Later on the shift of exciplex peak with respect to fluorophore is discussed. No change was observed in excitation wavelength upon addition of quencher. Decrease in the intensity of fluorescence peak and appearance of a broad structureless band towards bathochromic side represents the exciplex formation. All the exciplex formed are dipolar because they all are red shifted. Peak positions of both the exciplex and fluorophore, and the spectral shift of exciplex with respect to fluorophore are discussed as a function of solvent polarity and temperature. From the relation between these parameters it is observed that with the increase of solvent polarity the exciplex is destabilized. Solvent's orientation and distortion polarization are responsible for the thermochromic shifts. Exciplex is stabilized with the increase of temperature if the distortion polarization dominates, and if the solvent's orientation dominates then the exciplex is destabilized with the increase of temperature.
- Later in discussion the exciplex energetics-band parameters obtained from the excited emission spectra are discussed as a function of solvent polarity and temperature. The isolated emission spectra of all exciplexes of different systems were fitted according to the kuzmin's model of self-consistent polarization,^{11 12} . All these fittings were done over a range of temperature i.e from 253 till 340 K. Energy of zero-zero transitions, gauss broadening of vibronic level, huang-rhys factor and energy of dominant high-frequency vibration are the band parameters obtained from the fitting of equation 2.110. All these parameters represent the energetics and stability of exciplex. For all the exciplex systems these parameters does not show same behavior for increase of solvent polarity and temperature. Reasons for different behavior of these parameters are discussed in section 4.3

of results and discussion.

- Then the fluorescence lifetimes for fluorophore and exciplex are discussed in 4.4. Measurements were done using frequency modulation and single photon counting technique. Fluorophore lifetimes were measured by using frequency modulation and the single photon counting was used to evaluate the exciplex lifetimes. The aim of measuring lifetime was to calculate the entropy of exciplex formation and the equilibrium constant for complex formation. The lifetimes were measured at 297 K and it was assumed that it remains constant for all temperature range used for exciplexes. The effects of local environment and solvent polarity on the lifetimes is discussed in this portion. Lifetimes for 1-CN/HMB in solvents of different polarity are only discussed here

- Then equilibrium constant for exciplex formation is discussed in section 4.5. Variation of equilibrium constant for exciplex formation with solvent polarity is discussed in this section. Effect of donor and acceptor, electronegativities of donor and acceptor, and ionization energies of reacting molecules on the equilibrium constant are also discussed in this section.

- Extent of charge transfer is the ability of donor to transfer the electrons to the acceptor. This parameter cannot be calculated according to the Weller's mechanism. According to Kuz'min the exciplex systems can be classified according to the extent of charge transfer as the full charge transfer and the partial charge transfer. Partial charge transfer exciplexes are those for whom the value of extent of charge transfer is less than one and the full charge transfer exciplexes are those which have the value for extent of charge transfer greater than one. 1-CN/HMB system is discussed in this section and this system was found to be full charge transfer exciplex. Reason for this behavior and the factors effecting the extent of charge transfer are discussed in the section 4.6.

- Destabilization energy, m , difference between the matrix element coupling of charge transfer and locally excited state ($H_{22}^o - H_{11}^o$) and matrix element coupling between the locally excited and charge transfer states (H_{12}) are some of the parameters which are appearing in the Kuzmin's equations. In section 4.7 these parameters are discussed as a function of solvent polarity and temperature. Various other factors effecting these parameters are also discussed in this section. These factors are used for further calculation of entropy, enthalpy and entropy of exciplex formation. Calculation of Exciplex dipole moment by the solvatochromic method and the factors effecting it are also discussed here. Later the value of dipolemoment is used to calculate the value of m .

- Two kinetic schemes proposed by A.Weller and M.G.Kuz'min are compared in the last part of discussion. Mathematical equations and kinetic schemes of these two models are discussed in sections 2.6.2 and 2.6.6. Calculation and comparison of the enthalpy of exciplex formation is made in section 4.9. Later in this section the various other factors

effecting the entropy of exciplex formation are also discussed. The entropy of exciplex formation was also calculated and compared by using both the models, also the effect of other factors like ratio of quantum yield of exciplex emission and fluorophore emission in the presence of quencher, quencher concentration, ratio of radiative lifetimes of exciplex to fluorophore, ratio of non radiative lifetimes of exciplex to fluorophore and enthalpy of exciplex formation on the enthalpy values are also discussed. In the last part (section 4.10) Gibb's energy of exciplex formation was calculated from both the models and then comparison was made between the values obtained.

2. Theoretical Perspective

Knowledge is of no value unless
you put it into practice.

(Anton Chekhov)

This chapter aims to give a bit of theoretical back ground about the work presented in the upcoming chapters. Excited state charge transfer can be studied by many techniques like Lasers,^{7,13,14} flash photolysis,^{2,15,16} transient dc-photo current methods.¹⁷⁻¹⁹ Here steady state and the time resolved fluorescence techniques are used to study the fluorescence behavior of exciplex systems therefore the theoretical background contains information about the mechanism of fluorescence quenching with emphases on exciplex formation. The M.G.Kuz'min and A.Weller's model for calculations of thermodynamic parameters, exciplex energetics and the factors affecting the fluorescence behavior are discussed.

2.1. Mechanism of Fluorescence Quenching

When a fluorophore (A), present as a solute in solution, is excited by photons it goes to the electronically and vibronically excited state. Now its electronic and geometrical structure is different from the ground state and resultantly there is a difference in interactions with the environment and molecules near by it. This excited molecule returns to the lowest vibrational level of its first excited state by means of vibrational relaxation. The various possible interactions of such an excited fluorophore are represented in figure 2.1 The excited fluorophore returns to ground state either by radiative or by non radiative transitions¹. Radiative transitions the fluorophore can return to the ground state either by directly emitting light i.e by fluorescence (fl), by interconversion (ic), or by intersystem crossing (isc). If another solute (D) is also present in system then the fluorophore can react in forming another non-fluorescing specie (AD)²⁰ 2. In another situation $^1(A^{\delta\pm}D^{\delta\pm})$ is formed between excited fluorophore and quencher. The formation of exciplex is usu-

¹ The non-radiative transitions are not of interest here, so that's why they are not discussed further.

² The electron transfer quenching between 'F' and 'D' resulting into the formation of ion radicals also comes under this heading.²⁰

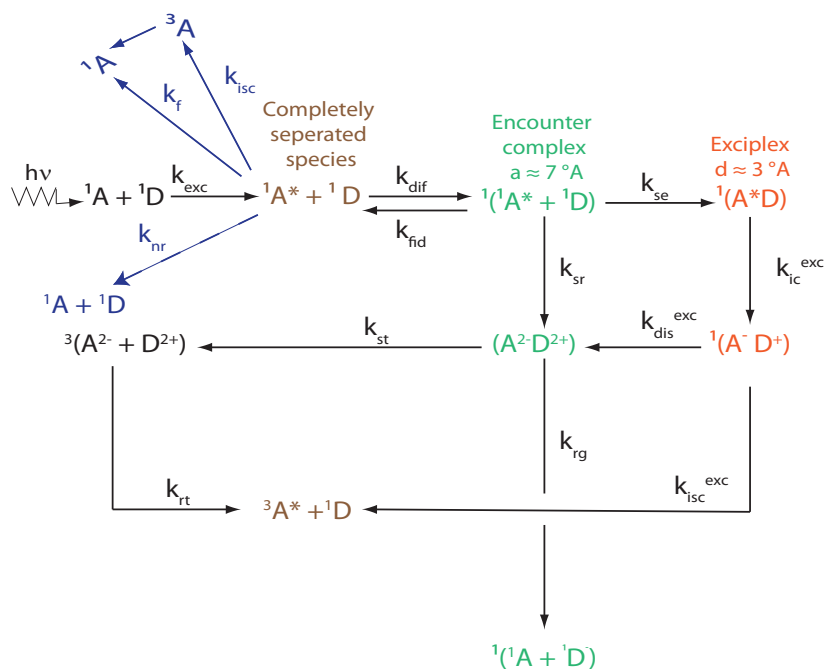


Figure 2.1.: General reaction scheme for photo induced electron transfer reactions of electron donor (D) and acceptor (A) systems. Blue arrowheads represents those reactions which are not directly involved in quenching and they are part of classical photo physics. The black arrow heads represent those reactions which implicate directly into the quenching process. Also f = fluorescence, ic = interconversion, exc = excitation, nr = non-radiative, dif = diffusion, fid = free induction decay, se = singlet exciplex, sr = singlet radical, rg = radical ground, dis = disinterigation, st = singlet triplet, rt = radical triplet.

ally accompanied by the appearance of a new usually red shift fluorescence band. This decrease in the intensity of fluorophore is known as quenching. The excited state fluorescence quenching can occur dynamically (the reactant must approach each other either by diffusion or, in the presence of potential fields, in combination with migration).

All processes represented in figure 2.1 determine the molecular fluorescence lifetime of the fluorophore (τ) and it's quantum yield (ϕ)¹.

$$\frac{1}{\tau} = k_{nr} + k_r + k_{isc} \quad (2.1)$$

$$\phi = \frac{k_r}{k_{nr} + k_r + k_{isc}} \quad (2.2)$$

¹ These relationships are very general. In the upcoming chapters the lifetimes of fluorophore and exciplex will be explained in details.

2.2. Historical Background of Exciplex

Formation of excited state charge transfer complexes (excimers and exciplexes) are subject of interest for all photo chemists.² These excited state complexes are important because they are transient in many of photo reactions, particularly in photo induced electron transfer reactions.²¹⁻²³ The term excimer represents atomic or molecular dimer aggregates which are unstable in ground state, but are stable under electronic excitation. The name excimer was given to the excited state dimers by Stevens and Hutton.²⁴ The first simplest excimer reported is Helium (He_2)²⁵ ¹. Later on many other excimers were reported ².

Exciplexes on the other hand are excited state charge transfer complexes which dissociate in the ground state. They are hetero-excimer formed in the excited singlet state by one-to-one association of electron donor (D) and acceptor (A) molecule. They don't differ in principal from excited stable ground state complexes. They were reported first time in 1963.² In former times the exciplex was recognized as hetero-excimers. The term exciplex was used for the first time by Walker, Bedner and Lumry^{28,29} ³. First time the exciplex formation was observed between different but similar molecules such as pyrene and its methyl derivatives.^{30,31} Where as in 1963 Leonhardt and Weller observed exciplexes between two entirely dissimilar components such as pyrene and dimethyl aniline.² Later on exciplex formation was observed and reported in many systems.⁴

2.3. Excimer Stability

Various possible mechanisms are available for the formation of excimers some are mentioned below:

2.3.1. Excitation Resonance Interaction

In this mechanism the excimer is stabilized due to the delocalization of the excitation among both components and Pyrene excimer is attributed to this mechanism:³²

¹ For He excimer, emission from upper state to the ground state produces continuum extending from 600 to 1000 Å in the far UV region. Thus a broad and diffuse emission appears bearing all characteristics of excimer.

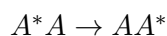
² Excimers formed as a result of interactions between the excited and unexcited aromatic compounds had been considered by Kautsky²⁶ and in 1954, Kasper and Förster²⁷ reported excimers of pyrene in it's condensed solution.

³ They used the term exciplex in connection with polar solvent effects on fluorescence spectra of indole, where, however, the existence of a well defined complex as the emitting species may be doubtful.

⁴ Exciplex formation may occur either by an excited acceptor with an unexcited donor or vice versa.¹⁰

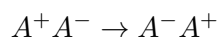
$A^* + D \rightarrow (A^- D^+)$ (e.g A = perylene, D = dimethyl aniline)

$D^* + A \rightarrow (D^+ A^-)$ (e.g D = pyrene, A = 1,4-dicyanobenzene)



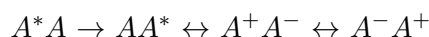
2.3.2. Intermolecular Charge Transfer

According to the Ferguson³³ excimers are formed as a result of intermolecular charge transfer. According to him symmetrical resonance hybrids are formed:



2.3.3. MO Theoretical Calculations

These calculations were done by assuming the symmetrical sandwich geometry of excimer.³⁴ From these calculations it has become clear that neither the resonance hypothesis nor the charge transfer hypothesis alone is sufficient to explain the stability of excimer state. Infact they both contribute to the excimer state¹, therefore the exciplex formation is represented as:



2.3.4. Arrangement in Pairs and Intra Molecular Excimers

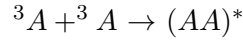
In crystals, the aromatic molecules are arranged in pairs or in other suitable geometries which are favorable for excimer formation.³⁵ Whereas in composite molecules intra molecular excimers are formed. Here two or more aromatic residues are linked together by a flexible $-(CH_2)_n-$ chains of suitable length. $n = 3$ for diphenyl alkanes series,³⁶ poly vinyl carbazole,³⁷ $n = 8$ ³⁸ for $py - (CH_2)_n - py$ ².

2.3.5. Triplet-Triplet Annihilation, Electron Transfer and Stable Dimeric Cations

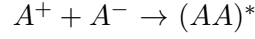
The most common mechanism of excimer formation is interaction of molecule in its lowest excited singlet state with another in its ground state. Triplet-triplet annihilation may result in excimer formation as:

¹ MO calculations are not very accurate because of the trans annular mode of interaction and also due to the limitation that exact value of the inter planar distance is not experimentally accessible.

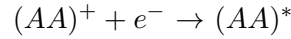
² This exciplex might be stabilized due to strong resonance interactions between pyrene nuclei.



Similarly electron transfer between radical anion and radical cation can also result in excimer formation and is represented as:³⁹



Also the stable dimeric cations may also form excimers by electron capture:⁴⁰



2.4. Exciplex Stability

Exciplex formation explained by A.Weller, M.G Kuz'min and S.Farid et.al is discussed here. A.Weller and M.G Kuz'min proposed conventional models whereas S.Farid et.al introduces some modification to the conventional models.

2.4.1. A.Weller's Mechanism for Exciplex Formation

In 1963, when exciplex was reported for the first time it was mentioned that they don't differ principally from the excited stable ground state. The stability of this excited state complex was attributed to the interaction between the no bond ground state and polar excited state.⁴¹



S_{ad}^* denotes the overlap integral between the lowest anti bonding orbital (a^*) of acceptor and the highest bonding orbital (d) of the donor. Also this interaction exhibits a destabilizing effect on the excited charge transfer state and is expressed as.⁴²

$$U_{dest} = \frac{(\alpha - E_{CT}^{\circ} S_{ad}^*)^2}{E_{CT}^{\circ}} \quad (2.4)$$

Where α is the Hamiltonian matrix element between the zero order complex ground and excited states and E_{CT}^* is the energy of the pure charge transfer state. The energy of charge transfer complex state in majority of cases is closer to the lowest excited singlet state of components therefore the locally excited states must also be included in the general description of excited state.^{43,44}



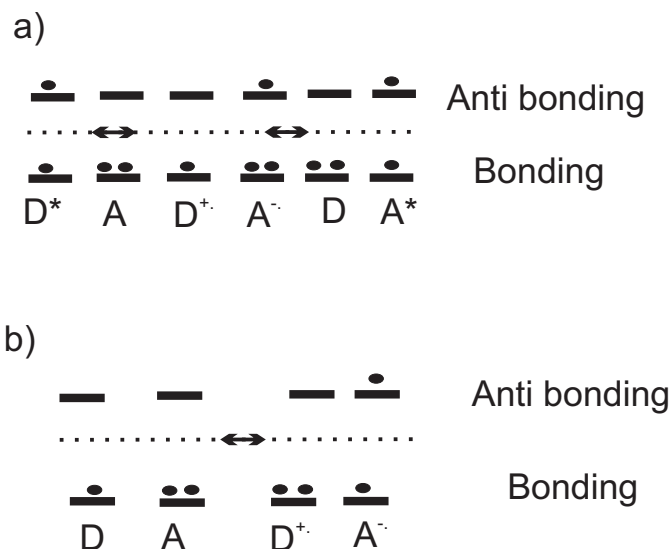


Figure 2.2.: Molecular orbital description of (a) exciplexes and (b) ground-state complexes.⁴⁵

Thus the interaction with the charge transfer states depend upon the overlap integrals S_{ad} and S_{ad}^{**} , where S_{ad} is the overlap integral between the highest bonding orbitals and S_{ad}^{**} is between the lowest anti bonding orbitals (figure 2.2) These overlap integrals lead to the stabilization of the exciplex state by an amount U_{stab} ¹.

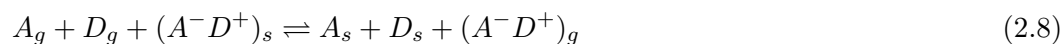
These considerations are applied first of all to the gas phase where the energy of the “pure” charge transfer exciplex state above the separated ground state components is given by the following expression:

$$E_{CT}^{\circ} = IP_D - EA_A - C \quad (2.6)$$

In above equation IP_D is the donor’s ionization potential and EA_A is the acceptor’s electron affinity and ‘C’ is the coulomb’s attraction energy at equilibrium distance. Thus the energy of any exciplex E_e in any solvent is given by the following equation:

$$E_e = E_{CT}^{\circ} + U_{dest} - U_{stab} - \Delta H_e^{sol} \quad (2.7)$$

The enthalpy of solvation, ΔH_e^{sol} , is associated with the following equilibrium:



¹ The U_{stab} increases as the charge transfer state comes closer in energy to the locally excited states.

The subscript ‘g’ and ‘s’ appearing in the above equation represent gas phase and solution respectively. As the dominating factor for exciplex formation is solvation therefore the following equation can be written:

$$\Delta H_e^{sol} = \frac{\mu^2}{\rho^3} \left[\frac{\epsilon - 1}{2\epsilon + 1} - \frac{d \ln \epsilon}{d \ln T} \frac{3\epsilon}{(2\epsilon + 1)^2} \right] \quad (2.9)$$

μ is the dipole moment of the exciplex, ρ is the equivalent radius of Kirkwood-Onsager continuum mode, which is applied here, ϵ is the static dielectric constant.

2.4.2. M.G.kuz'min Mechanism for Exciplex Formation

kuz'min made several modifications in the classical mechanism. For better understanding it is necessary to have idea about both mechanisms.

- **Classical Mechanism:** This mechanism was proposed by Marcus in 1956.^{3,4} According to this, a diabatic electronic jump occurs from the electron donor to acceptor after preliminary reorganization of the reactants and the media¹. As a result of it degenerate electronic terms are obtained for the reactants and products along with subsequent relaxation of the products and media.

- **Real Mechanism:** This mechanism was proposed several years ago^{5,46-48} and according to this the electron transfer between the excited molecules present in the kinetic region² involves a gradual shift of electron density from donor to the acceptor molecules along with change in the nuclear coordinates of the reactants and media rather than a diabatic electron jump.

The electronic and geometric structures of exciplex strongly depends upon the interaction of excited donor (D)–acceptor (A) complex with solvents and also on the driving force ($-\Delta G_{et}$) for electron transfer between D and A, e.g a very rapid and extended structured exciplex is formed for pyrene (A) and N,N-dimethyl aniline (D) in polar solvents whereas the same compounds show very slow formation and a sandwiched shape exciplex in non-polar solvents.⁴⁹ The electronic wave function of an exciplex is a linear combination of wave functions of locally excited (A^*D) and completely charge transfer (A^-D^+) states so

$$\psi = a\psi(A^*D) + b\psi(A^-D^+) \quad (2.10)$$

¹ The term media refers to the solvent molecules surrounding the reactants.

² Kinetic region is the region for endergonic and slightly exergonic reactions with Gibb's energy of electron transfer $\Delta G_{et} > -15 \text{ kJmol}^{-1}$.⁶

2. Theoretical Perspective

The ratios of coefficients ‘a’ and ‘b’ depend on the energy gap between (A^*D) and (A^-D^+) states ¹ and the charge interaction (β). If the effect of solvent polarization is neglected then the enthalpy of exciplex formation ΔH_{EX} and the degree of electron transfer δ in the exciplex are expressed by the following equations:

$$\Delta H_{EX} \approx \frac{\Delta H_{et}}{2} - \left[\left(\frac{\Delta H_{et}}{2} \right)^2 + (\beta)^2 \right]^{(1/2)} \quad (2.11)$$

$$\delta \approx \frac{1}{1 + \left[\frac{\Delta H_{et}}{2} + \left(1 + \left(\frac{\Delta H_{et}}{2\beta} \right)^2 \right)^{1/2} \right]^2} \quad (2.12)$$

M.G Kuz'min shows that in the region $-\beta < \Delta H_{EX} < \beta^6$ the stabilization of an exciplex is provided by the exchange interaction rather than by the difference between the orbital energies of donor and acceptor and the electrostatic interaction thus in this region the locally excited state influences considerably to the electronic structure of the exciplex ². The dipole moment of such an exciplex is much smaller than the dipole moment of a contact radical ion pair . The dissociation of exciplex into contact radical ion pair is hindered by the stabilization energy and therefore prolonged lifetimes are observed ³. Such exciplexes are thus similar to the ground state charge transfer complexes when the complete charge transfer state has a much higher energy than the corresponding ground state ($\Delta G > 100kJmol^{-1}$) and the wave function is given as:

$$\psi = a\psi(AD) + b\psi(A^-D^+) \quad (2.13)$$

In above equation $a \gg b$. After discussing A.Weller and M.G Kuz'min's models it can be summarized that the exciplex is stabilized due to the overlap between either the highest bonding orbitals or the lowest anti bonding orbitals. If the mixing is between the bonding or anti bonding orbitals of the locally excited state and the radical ion pair then the exciplex is stabilized (E_{stab}). On the other hand there is interaction between the singlet charge transfer state and the ground state, involving the mixing of antibonding with bonding orbitals then result is loss of energy (E_{dest}). Thus the net energy change

¹ i.e The ratio of ‘a’ and ‘b’ depends upon the enthalpy of excited state electron transfer.

² This situation persists even if coefficients a and b are comparable or even $a > b$.

³ This explanation is for exciplexes in polar media because as solvent polarity increases the exciplex dissociates into radical ion pairs. No such problem is observed in non-polar solvents as they accelerates the exciplex emission band, with relatively high enthalpy and equilibrium constant of exciplex formation and strong shift of exciplex emission relative to the parent excited molecules $h\nu \approx 2\Delta H_{EX}$.

ΔE_{EX} is given by their difference as :

$$\Delta E_{EX} = E_{stab} - E_{dest} \quad (2.14)$$

The free energy change of exciplex formation involves the orbital stabilization term, ionization energy E_1 of the electron donor species, the electron affinity E_{EA} of an acceptor,⁵⁰ the excitation energy E^* , the coulombic interaction between the excited species and the ground state molecule ($E_{CEX} = z_D z_A e_o^2 / d_{EX}$) and the energy of exciplex solvation ($E_{EX_{solv}} = \mu^2(\epsilon - 1) / [\rho^3(2\epsilon + 1)]$)^{45,50,51} .

$$\Delta E_{EX} = E_1 - E_{AA} - E^* - \Delta E_{EX} - E_{EX_{solv}} + E_{CEX} \quad (2.15)$$

Where d_{EX} is the distance between the exciplex constituents, z_D and z_A are the unit charges of donor and acceptor respectively, μ is the dipole moment of the exciplex, ρ is its radius and ϵ is the permittivity of the solvent.

An exciplex can dissociate into a solvent-separated ion pair ($D^+ \cdots A^-$) that can be stabilized by interaction with solvent molecules, or it can form a contact ion pair $D^+ A^-$ as a result of electron transfer between the constituents of exciplex when the orbital interaction is not strong enough to favor the exciplex structure.^{51,52} The energy free terms for these species (ΔG_{SSIP} and ΔG_{CIP} where SSIP denotes solvent separated ion pair, and CIP denotes contact ion pair) involve the coulombic and solvation energies.⁵¹

$$\Delta G_{SSIP} = E_1 - E_{EA} - E^* + E_{SSIP_{solv}} + E_{CSSIP} \quad (2.16)$$

$$\Delta G_{CIP} = E_1 - E_{EA} - E^* - E_{SSIP_{solv}} + E_{CCIP} \quad (2.17)$$

Where $E_{SSIP_{solv}} = z_D z_A e_o^2 [(1 \times r_D + 1/r_A)(1 - 1/\epsilon)]/2$, $E_{CSSIP} = z_D z_A e^2 / \epsilon d_{SSIP}$, $E_{CIP_{solv}} = \mu^2(\epsilon - 1) / [\rho^3(2\epsilon + 1)]$ and $E_{CCIP} = z_D z_A e^2 / d_{CIP}$. When the two constituents of the exciplex ion pair have electric charges of opposite sign, the coulombic and solvation energy terms for SSIP are negative. In polar solvents, where $(E_{SSIP_{solv}} + E_{CSSIP}) < (-\Delta E_{EX} - E_{EX_{solv}} + E_{CEX})$, the exciplex dissociates into a solvent separated ion pair. Similarly contact ion pair formation is favored when $(-E_{CIP_{solv}} + E_{CCIP}) < (-\Delta E_{EX} - E_{EX_{solv}} + E_{CEX})$. However, for an encounter pair in which the two species have the same charge sign, $(E_{SSIP_{solv}} + E_{CSSIP})$, E_{CCIP} and E_{CEX} are all positive; hence if the exciplex stabilization energy ΔE_{EX} is sufficiently large, exciplex formation is more probable than creation of either a solvent-separated or a contact ion pair, and exciplex emission can be observed. This simplified emission clearly indicates that the dynamic interconversion between encounter pairs such as the exciplex and contact or solvent-separated ion-pairs

is strongly influenced by interactions with the solvent molecules.

2.4.3. Electronic Structure of Exciplex

When an exciplex is formed due to combination of two neutral species then the electronic interaction taking place in it is expressed by the linear combination of wave functions of all the possible states and ions given as:⁵³

$$\psi_{EX} = c_0\psi_0(AD) + c_1\psi_1(A^-D^+) + c_1''\psi_1''(A^+D^-) + c_2\psi_2(A^*D) + c_2''\psi_2''(AD^*) \quad (2.18)$$

The first term represents the ground state interaction, the second and third terms represent the charge transfer states and the second last and last term of above equation describes the energy transfer states. The coefficients (c_0 , c_1 , c_1'' , c_2 and c_2'') appearing in above equation represents the relative contributions of the state. If the 'A' is only acceptor and on neglecting the ground state interactions, the exciplex wave function simplifies as:

$$\psi_{EX} = c_1\psi_1(A^-D^+) + c_2\psi_2(A^*D) + c_2''\psi_2''(AD^*) \quad (2.19)$$

If the coefficient c_2 is smaller relative to the other two coefficients then the charge transfer character of the exciplex is rather large and resultantly it dissociates into a radical ion pair, especially in polar solvents¹. The vertical Franck-condon allowed transitions from a minimum on an excited state potential surface to a low-lying repulsive ground state surface results in emission from exciplexes. If there is a significant change in the molecular geometry upon transition to the ground, then luminescence may not be observed; rather, other processes, such as dissociation into a solvent-separated radical ion-pair or some chemical reaction may occur. If $c_1 \gg c_2$ then the exciplex can be an emitting specie, or its separation can occur via the formation of an excited acceptor and the ground state of donor.

Now if it is considered that the 'A' is the only acceptor and only it is the photo-excited specie in the system then the above equation 2.18 simplifies as:

$$\psi_{EX} = c_0\psi_0(AD) + c_1\psi_1(A^-D^+) + c_2\psi_2(A^*D) \quad (2.20)$$

¹ When an excited state transition metal complex is present in exciplex then the two constituents have either the same or different electric charge and therefore the role of polar solvent can be rather different in the two cases. Thus the solvent polarity can assist the creation of an inorganic exciplex consisting of two species with the same sign of electric charge.

Extent of charge transfer is determined by the values of coefficients c_1 and c_2 . The fractional charge transfer in the exciplex can be defined as c_1^2 .⁵⁴ ¹ The exciplex formed is essentially a contact radical-ion pair ($A^- + D^+$) if c_1 approaches unity.⁵⁵ The extent of mixing among the various basis states of equation 2.19 depends upon the magnitudes of the appropriate electronic coupling matrix elements, which can be rather large for exciplex species ².

Analysis of Radiative Data The radiative rate constant can be given by the following equation:

$$k_f = \frac{64\pi^2}{3hc^3} f(n) \nu_f^3 |\hat{M}|^2 \quad (2.21)$$

Where ν_f is the average emission frequency for fluorophore. The refractive index factor $f(n)$ is given as:

$$f(n) = n \left(n^2 + \frac{2}{3} \right)^2 \quad (2.22)$$

$|\hat{M}|$ is the electronic transition moment for the emission process,⁵⁷ it depends upon the electronic nature of the initial and final states involved in the emission process and mathematically it is given as:

$$\hat{M} = \langle \psi_{EX} | \hat{\mu} | \psi_G \rangle \quad (2.23)$$

$\hat{\mu}$ is the dipole moment vector operator and ψ_G is the ground state formed upon emission. for the limiting case when the contribution of the locally excited state to the exciplex is minimal (i.e $c_2 \approx 0$ in equation number 2.20), f_{CT} ³ is essentially unity and the exciplex is a pure ion pair. The transition moment under these circumstances, \hat{M}_{A-D+} , arises from mixing of a small amount of ion-pair character into the ground state and should depend upon the emission frequency approximately as indicated below

$$\hat{M}_{A-D+} = -\frac{H_{01}\Delta\hat{\mu}}{h\nu_f} \quad (2.24)$$

¹ This is correct only if ψ_2 , ψ_3 and ψ_5 are orthogonal.

² The equation number 2.20 can be used to represent the charge transfer excited state of any AD system. For example, the extent of charge transfer is also an important issue in linked donor/acceptor systems.⁵⁶ As a result of the large through-bond couplings which are sometimes found in such systems, it is important to be able to assess the possibility of mixing among locally excited and pure ion-pair states in these cases too.

³ f_{CT} is known as the fractional charge transfer and it can be defined as C_1^2 .⁵⁴

Where $\Delta\hat{\mu}$ is the difference between the static dipole moments of the pure ion-pair state $\psi_1(A^{\cdot-}D^{\cdot+})$ and the neutral state $\psi_0(AD)$, here assumed to be orthogonal, and H_{01} is the electronic matrix element coupling these states¹. Thus, \hat{M}_{A-D^+} should decrease as $h\nu_f$ increases. When an exciplex is essentially a pure radical ion-pair, the radiative transition to the essentially nonionic ground state is an intermolecular electron-transfer process and is thus expected to have a relatively small value of \hat{M} . In contrast, for the other limiting case of a pure locally excited state, the transition moment, $\hat{M}_{A^{\cdot}}$, corresponds to an allowed intra molecular process and is therefore relatively large compared to \hat{M}_{A-D^+} . As the energy of $\psi_1(A^{\cdot-}D^{\cdot+})$ increases, the energy of exciplex emission should increase, the contribution to the exciplex of locally excited state $\psi_2(A^*D)$ should also increase, and so, therefore, should the magnitude of \hat{M} .

2.4.4. the Farid and Gould Model

In conventional model the term exciplex describes the product of a photo induced electron transfer reaction with variable extent of charge transfer and is represented in equations 2.18 and 2.19. These conventional radical ion pair /exciplex model forms the basis of the well known Rhem-Weller description of photoinduced electron kinetics^{8,9} and can also provide a quantitative description of the electronic properties of exciplexes.⁵⁸ I.R. Gould and coworkers were able to find some exceptions in the charge transfer quenching like quenching of cyanoaromatics by pyridine. Quenching of 9,10-dicyanonaphthalene by pyridine was already pointed out by Jacques and coworkers²; according to them the observed reactivity differences were assigned to the exceptionally high coulombic stabilization of the n-donor radical ion pairs.^{59,60} On further investigation, I.R.Gould and coworkers find that the previous explanation of coulombic stabilization was insufficient to explain the reaction kinetics; i.e the conventional electron-transfer model was unsatisfactory too³. Therefore a new mechanism of charge transfer quenching based on covalent bond formation was proposed. This mechanism shows that how the conventional model represented in equation 2.20 is modified to explain all the exceptions previously pointed out. The unpaired electrons are localized on the individual radical ions in the conventional model. On the other hand, if the electrons can spin pair to form a covalent bond, then a bonded charge-transfer state ($A^{\cdot-} - D^{\cdot+}$) would result. The wave function to describe

¹ H_{01} is usually denoted as V in the electron transfer literature.

² They observed a general increase in the efficiency of quenching by pyridine and related n-donors compared to the corresponding π -donors such as substituted benzenes.

³ Specially the Pyridine quenches the fluorescence of 9,10-dicyanonaphthalene with a rate constant that approaches the diffusion-controlled limit even through formation of a radical ion pair in this case is endothermic more than ~ 0.6 eV!⁶¹

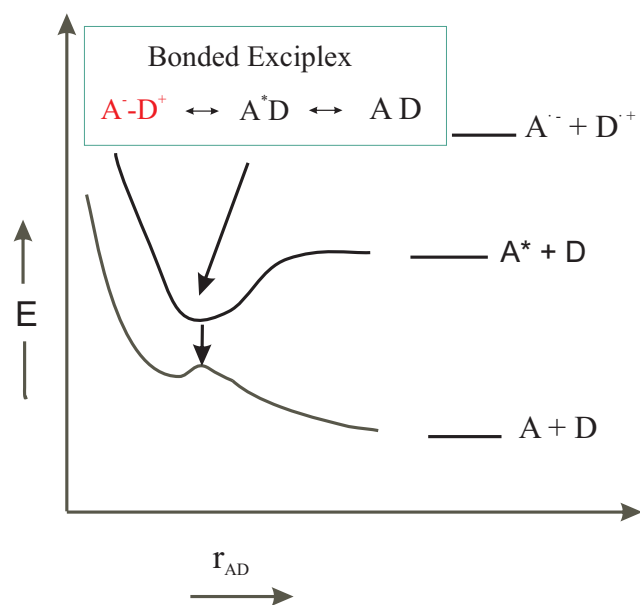


Figure 2.3.: Scheme representing energies of conventional exciplex as a function of separation distance.⁶¹

this “bonded exciplex” is given by the following equation:⁶¹

$$\psi_{EX} = c_0\psi_0(AD) + c'_1\psi'_1(A^- - D^+) + c_2\psi_2(A^*D) \quad (2.25)$$

Above equation is different from the equation 2.20 by the replacement of ($A^- + D^+$) with ($A^- - D^+$). There are many similarities between the conventional exciplex and the bonded exciplex like both have charge-transfer character. The ground state interactions between the donor and acceptor is repulsive at the geometry of the excited state in both of them. They can also decay to ground state to regenerate the starting materials. An important similarity in both type of exciplexes is that they can potentially lead to new stable organic products. The most important difference between them is that with decreasing separation distance the covalent bonding interaction leading to the bonded exciplex can significantly lower the energy of the charge-transfer state compared to the non bonded radical ion pair state (figure 2.3 and 2.4). In turn, this can allow a quenching reaction that would otherwise be energetically forbidden. In addition to the formation of new intermediate, the most important feature of the bonded exciplex structure is obviously formation of a new covalent bond. There is a wide range of bond-forming organic reactions that are initiated by photo induced single electron transfer. The bonded exciplex model properly accounts for excited-state quenching and radiation less decay behavior of the

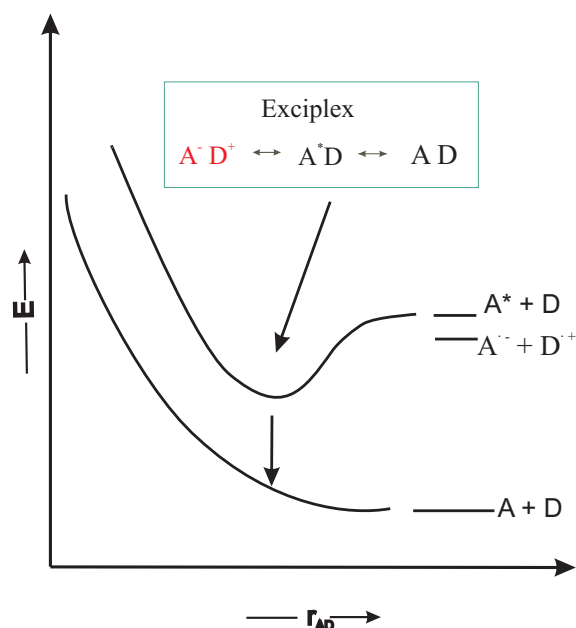


Figure 2.4.: Scheme representing energies of bonded exciplex as a function of separation distance. This potential curve shows that as the separation distance approaches the van der Waals contact the covalent bonding interaction can result in a product that is much lower in energy than that of the locally excited state ($A^* + D$) even when the energy of non bonded radical ions ($A^{\cdot-} + D^{\cdot+}$) is much higher than the locally excited state.⁶¹

quenching products¹. This model was supported by the combinational experimental and DFT computational studies by I.R.Gould and coworkers².

2.5. Types of Exciplex

On the basis of equation 2.9 appearing in Weller's mechanism exciplexes are divided into following three types:

a) **Type I** These are the excited donor acceptor complexes and have

$$U_{dest} > U_{stab} \approx 0 \text{ so that } E_e > E_{CT}^o - \Delta H_e^{sol} \quad (2.26)$$

¹ Thus the bonded exciplex may represent many important previously unidentified intermediates in many of organic photo induced electron transfer reactions.

² These studies shows a curve crossing between the ground state and the low-energy bonded exciplex state, manifested by a deviation from purely repulsive behavior on the ground state surface (figure2.3 and 2.4).

b) Type II These are charge-transfer exciplexes and have

$$U_{dest} \approx U_{stab} \approx 0 \text{ so that } E_e \approx E_{CT}^{\circ} - \Delta H_e^{sol} \quad (2.27)$$

c) Type III These are mixed excimers and exciplexes and have

$$U_{dest} > U_{stab} \approx 0 \text{ so that } E_e < E_{CT}^{\circ} - \Delta H_e^{sol} \quad (2.28)$$

This classification is formulated for the singlet state exciplexes and it can be used for triplet-state by considering that for triplet state $U_{dest} = 0$ because of the difference in multiplicity between the no-bond ground and charge transfer excited states. The experimental verification of previously mentioned classification has been found to be considerably facilitated by using the polarographic half-wave oxidation and reduction potentials E_D^* and E_A^{red} with IP_D and EA_A because they are linearly related to each other. So equation 2.6 becomes as:

$$E_{CT}^* = E_D^{ox} - E_A^{red} + (\Delta G_{D+}^{sol} + \Delta G_{A-}^{sol} - C) \quad (2.29)$$

Where ΔG_{D+}^{sol} and ΔG_{A-}^{sol} are the solvent free energies associated with the processes.

$$D_g + D_s^+ \rightleftharpoons D_s + D_g^+ \quad (2.30)$$

$$A_g + A_s^- \rightleftharpoons A_s + A_g^- \quad (2.31)$$

where the subscript 'g' and 's' represents gas phase and solvent in which the oxidation and reduction potentials have been determined.

2.6. Thermodynamic Parameters and Kinetics of Exciplexes

2.6.1. Calculation of Average Emission Frequencies

In order to proceed further the first step is to calculate the average emission frequencies. The value of average fluorescence frequency ν_f can be calculated using the Strickler-Berg formula⁶² and it is given as:

$$\nu_f = \left(\frac{\int \nu^{-2} I_{\lambda} d\nu}{\int \nu^{-5} I_{\lambda} d\nu} \right)^{1/3} \quad (2.32)$$

In above equation I_λ is the emission frequency expressed in photons per unit time per unit wavelength. The energy of ion-pair state relative to the neutral and locally excited states varies with the solvent polarity and thus the intermolecular and intra molecular coordinates also change and thus the H_{11} varies with the nuclear coordinates¹. Similarly the E_{EX} and \hat{M} are also effected. As discussed before that when f_{CT} is essentially unity then \hat{M} is equivalent to \hat{M}_{A-D^+} (mentioned earlier in equation 2.24). Under this condition the correct value of fluorescence frequency of exciplex ν'_{EX} can be obtained from the following formula:⁸

$$\nu_{EX} = \left(\frac{\int \nu^{-2} I_\lambda d\nu}{\int \nu^{-3} I_\lambda d\nu} \right) \quad (2.33)$$

Here two models presented by A.Weller and M.G.Kuz'min are described in detail as these are used for calculations. These two models are described separately for better understanding as:

2.6.2. A.Weller's Calculations Scheme

According to Weller, exciplexes always appear at the longer wavelength than the excited state, differ from the ground state complex and dissociates into their constituent molecules.^{63,64} The kinetic scheme given in figure number 2.5 represents the formation and decay of exciplex. A.Weller model is based on the calculations published by Th.Förster in 1965. These calculations for the better understandings are divided into various parts:

Calculation of Enthalpy and Entropy of Exciplex Formation^{63,64} The concentration dependence of quantum yields of fluorophore (ϕ) and exciplex (ϕ') are given by the following equation:

$$\phi = \phi_m \frac{1}{1 + \frac{C_h}{C}} \quad (2.34)$$

$$\phi' = \phi'_m \frac{1}{1 + \frac{C_h}{C}} \quad (2.35)$$

Where ϕ_m is the intensity at $C \rightarrow 0$ and ϕ'_m is the intensity at $C \rightarrow \infty$. C is concentration of quencher. According to scheme number 2.5 $C_h^2 \phi_m$ and ϕ'_m are given by the following

¹ H_{11} is the energy of the purely ionic state A^-D^+ .

² C_h is the half-value concentration.

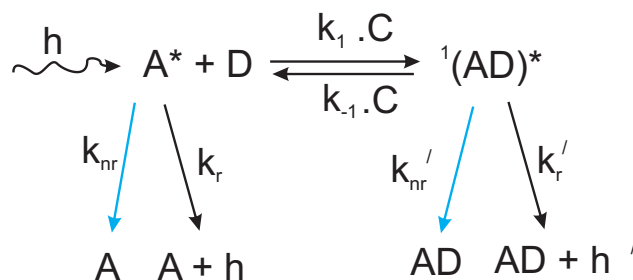


Figure 2.5.: Reaction scheme for A.Weller's model. In this scheme $h\nu =$ incident light used for photo excitation. A = fluorophore (electron acceptor), D = quencher (electron donor), $k_1 =$ rate constant for exciplex formation, $k_{-1} =$ rate constant for exciplex decay, $k_{nr} =$ non-radiative rate constant for excited fluorophore, $k_r =$ radiative rate constant for excited state fluorophore, $k_{nr}' =$ non radiative rate constant for exciplex, $k_r' =$ radiative rate constant for exciplex.

expressions:

$$\phi_m = \frac{k_r}{k_{nr} + k_r} \quad (2.36)$$

$$\phi'_m = \frac{k'_r}{k'_{nr} + k'_r} \quad (2.37)$$

$$C_h = \frac{k_{nr} + k_r}{k_1} \frac{k'_r + k'_{nr} + k_{-1}}{k'_r + k'_{nr}} \quad (2.38)$$

Following two cases are observed for the value of C_h

CASE I (low temperature range) Here $k_{-1} \ll k'_r + k'_{nr}$ so

$$C_h = \frac{k_r + k_{nr}}{k_1} \quad (2.39)$$

CASE II (high temperature range) Here $k_{-1} \ll k'_r + k'_{nr}$ so

$$C_h = \frac{k_r + k_{nr}}{k'_r + k'_{nr}} \frac{k_{-1}}{k_1} \quad (2.40)$$

Using this approximation thermodynamic enthalpy ΔH_{EX}^* and entropy ΔS_{EX}^* of exciplex formation can be calculated. ¹

All the rate constants appearing in scheme number 2.5 are exponentially sensitive to

¹ The value of C_h is very sensitive to temperature.

2. Theoretical Perspective

temperature so following Arrhenius type equations result:

$$k_{nr}(T) = N_{nr} e^{-\frac{E_{nr}}{RT}} \quad (2.41)$$

$$k'_{nr}(T) = N_{nr} e^{-\frac{E'_{nr'}}{RT}} \quad (2.42)$$

$$k_1(T) = N_1 e^{-\frac{E_1}{RT}} \quad (2.43)$$

$$k_{-1}(T) = N_{-1} e^{-\frac{E_{-1}}{RT}} \quad (2.44)$$

After rearranging equations 2.36 and 2.37, and after putting values from equations 2.41, 2.42 following equation results:

$$\frac{1}{\phi(T)} - 1 = \frac{N_{nr}}{k_r} e^{-\frac{E_{nr}}{RT}} \quad (2.45)$$

Now rearranging equation number 2.38 and putting values from equation numbers 2.34 2.35, 2.41, 2.42, 2.43, 2.44 following equation results:

$$C_h = \frac{k_R}{\phi_m N_1} e^{\frac{E_1}{RT}} + \frac{\phi'_m N_{-1} k_r}{\phi_m n_1 k'_r} e^{-\frac{E_{-1} - E_1}{RT}} \quad (2.46)$$

Putting the values into equation number 2.34 and 2.35 following expressions are obtained:

$$\phi_m(T) = \frac{1}{1 + \frac{N_{nr}}{k_r} e^{-\frac{E_{nr}}{RT}}} \quad (2.47)$$

$$\phi'_m(T) = \frac{1}{1 + \frac{N'_{nr}}{k'_r} e^{-\frac{E'_{nr'}}{RT}}} \quad (2.48)$$

Where E_{nr} and $E'_{nr'}$ are the activation energies for non radiative decay process of fluorophore and exciplex respectively. Dividing equation 2.34 by the equation 2.35 following

equation results¹:

$$\frac{\phi'}{\phi} = \frac{\phi'_m}{\phi_m} \frac{1 + \frac{C}{C_h}}{1 + \frac{C_h}{C}} = \frac{\phi'_m}{\phi_m} \frac{C}{C_h} = \frac{k'_r k_1 C}{k_r (k'_r + k'_{nr} + k_{-1})} \quad (2.49)$$

Another evaluation method has been used by Stevens and Ban. They use envelop area on the existence of an isobestic point for the fluorescence spectra. Such isobestic point occur here as with corresponding absorption spectral fluorescence yield $\phi(\lambda_i)$ of the solution at a particular wavelength λ_i in the overlapping area of two components, and it is independent of concentration. According to equation 2.34 and 2.35 it can be represented as:

$$\overline{\phi(\lambda_i)} = \phi(\lambda) + \phi'(\lambda) = \frac{C_h \phi_m(\lambda) + C \phi'_m(\lambda)}{C_h + C} \quad (2.50)$$

Above equation 2.50 is independent of concentration for those ϕ_i which fulfill following situation:

$$\phi_m(\lambda_i) = \phi'_m(\lambda_i) \quad (2.51)$$

Stevens and Ban have observed that such isobestic points occurring at constant concentration and constant temperature. Thus it is temperature dependent at constant concentration. Th.Förster find that it is only an approximation and is only valid for concentrations in the range of half-value concentration C_h . They also prove that the maximum quantum yield ϕ_m and ϕ'_m are temperature independent following:

$$\overline{d\phi(\lambda_i)} = \frac{\phi_m(\lambda_i) - \phi'_m(\lambda_i)}{(C_h + C)^2} c d C_h + \frac{C_h d\phi_m(\lambda_i) + c d\phi'_m(\lambda_i)}{C_h + C} = 0 \quad (2.52)$$

Condition in equation 2.52 is neither for $C_h \ll C$ nor for $C \gg C_h$. Since the second term of equation 2.52 predominates and the temperature dependence of the half-value concentration is equal to that of $\phi_m(\lambda_i)$ or $\phi'_m(\lambda_i)$. In more cases the temperature dependence of the half-value concentration is greater than the maximum of quantum yields so equation number 2.52 takes the form of equation number 2.51 again². In the temperature range of the association equilibrium Stevens and Ban calculate enthalpy and entropy of

¹ This is the procedure used by Birks, Tusk and Munor. Here the fluorescence spectra are measured at single concentration.

² Thus equation number 2.52 holds in intermediate area in which C_h runs through an maximum.

2. Theoretical Perspective

exciplex formation by using the following equation:

$$\ln \frac{1}{C} \frac{\phi'(\lambda_i)}{\phi(\lambda_i)} = \frac{\Delta S_{EX}^*}{R} - \frac{\Delta H_{EX}^*}{RT} \quad (2.53)$$

For the limiting case it follows from the equation number 2.34, 2.35, 2.36, 2.37 and 2.46 as:

$$\ln \frac{1}{C} \frac{\phi'(\lambda_i)}{\phi(\lambda_i)} = \ln \left(\frac{k_r + k_{nr'}}{k_r + k_{nr}} \right) + \ln \left(\frac{k_{-1}}{k_1} \right) = \ln \left(\frac{k_r' + k_{nr'}}{k_r + k_{nr}} \right) + \frac{\Delta S^*}{R} - \frac{\Delta H_{EX}^*}{RT} \quad (2.54)$$

ΔH_{EX}^* can be calculated from the slope of the above equation but for calculation of ΔS_{EX}^* , lifetimes appearing in the equation are required.

Calculation Equilibrium Constant for Exciplex Formation⁶⁴ A.Weller described a term conversion constant in the reaction mechanism and it is defined as:

$$x = \frac{k_1 \tau_o}{1 + k_{-1} \tau_o'} \quad (2.55)$$

Where k_1 = rate constant for exciplex formation and τ_o = lifetime for excited fluorophore; k_{-1} = rate constant for exciplex decay and τ_o' = lifetime for exciplex decay. With the knowledge of parameters in equation 2.55 the equilibrium constant for complex formation can be calculated as:

$$x = \frac{\tau_o'}{\tau_o} \leq \frac{k_1}{k_{-1}} = K_c \quad (2.56)$$

Calculation of Gibb's Energy of Exciplex Formation⁶⁴ Under the condition that association reaction proceeds, following equation holds:

$$k_c(ber) = 4\phi N_A (D_A + D_D)^a \quad (2.57)$$

Where N_A = Avogadro's number, D_A, D_D = Diffusion constants for acceptor and quencher, a = encounter distance (can be determined from equation Onsager cavity radius⁶⁵). Now with the knowledge of the parameters the ΔG_{EX}^* is calculated using the following equation:

$$\left[\frac{\tau_o}{x} - \frac{1}{k_c(ber)} \right] \frac{1}{\tau_o'} = \frac{1}{K_c} = \exp \left(\frac{\Delta G_{EX}^*}{RT} \right) \quad (2.58)$$

2.6.3. Calculation of Diffusion-Coefficient

The diffusion rate constant can be determined using the Stokes-Einstein relationship:⁶⁶

$$D = \frac{kT}{6\pi\eta} \left[\frac{1}{a_A} + \frac{1}{a_D} \right] \quad (2.59)$$

Where a_A and a_D are the radii of acceptor and donor respectively and η is the solvent viscosity. The radii of acceptors and donor were calculated by using the approach described in reference.⁶⁷ Briefly, in this approach the radius is a mean elliptical radius obtained from the semi axes of an ellipsoid cavity containing the molecule. This cavity is the smallest surface subscribing the optimized molecular geometry by means of density functional calculations using the B3LYP functional and the 6-311+G** basic set. If the fluorescence decays mono-exponentially, the stationary rate constant (k_{stat})¹ is identified with the rate obtained from the slope of its semi-logarithmic representation. The observed quenching rate constant is defined as:

$$R_{obs} = \frac{k_{obs}}{4\pi D} \quad (2.60)$$

k_{obs} is the observed experimental quenching rate constant². The value of R_{obs} is the characteristic distance between donor and quencher at which the reaction occurs.

2.6.4. Calculation of Activation Enthalpy of Diffusion

Activation enthalpy of diffusion can be calculated using the following equation:⁶⁸

$$\ln k_{diff} = \ln k_{diff}^{\circ} - \frac{\Delta H_{diff}^{\dagger}}{RT} \quad (2.61)$$

2.6.5. Calculation of Diffusion Rate Constant

Equation used for the calculation of k_{diff} is given as:⁶⁸

$$k_{diff} = \frac{8000RT}{3\eta} \quad (2.62)$$

¹ Value of k_{stat} can be calculated by using the equation $k_{stat} = \frac{8\pi\Gamma\left(\frac{3}{4}\right)}{\Gamma\left(\frac{1}{4}\right)}(aD^3)^{1/4}$. Thus the diffusion-controlled rate constant k_{stat} depends on diffusion coefficient as $D^{3/4}$ and $\eta^{-3/4}$ on solvent viscosity.

² Value of k_{obs} can be obtained from the Stern-volmer equation as: $\frac{\tau_0}{\tau} = 1 + k_{obs}[Q]$.

2. Theoretical Perspective

This equation holds if $a_A = a_D$, where a_A and a_D are the radius of fluorophore and exciplex respectively.

Calculation of Repulsion Energy in the Ground State⁶⁴ Following equation is used for the calculation of repulsion energies δE_{rep} :

$$\delta E_{rep} = {}^1\Delta E_{o,o} + \Delta H_{EX}^* - h\nu_c^{max} \quad (2.63)$$

In above equation ${}^1\Delta E_{o,o}$ is the singlet energy for fluorophore.

Solvent Dependence of ΔH_{EX}^* ⁶⁴ According to A.Weller if the emission frequencies of fluorophore and exciplexes are independent of temperature then following equation is obtained:

$$\log \frac{\phi'}{\phi \cdot C} = Constant + \log \frac{k_1 \tau'_o}{1 + k'_q \tau'_o} \quad (2.64)$$

As the solvent polarity increases the exciplex dissociates into radical ion pairs. This is because that rate constant k'_q (appearing in the denominator)¹ increases with ϵ and the result is shortened life span of τ'_o and it is represented by τ' as:

$$\tau' = \frac{\tau'_o}{1 + k'_q \tau'_o} \quad (2.65)$$

Now instead of equation 2.64 following equation is obtained:

$$\frac{\phi'}{\phi \cdot C} = Constant + \log \frac{k_1 \tau'_o}{1 + k'_q \tau'_o + k_{-1}^o \tau'_o} \quad (2.66)$$

Thus the temperature dependence in the high temperature range is given as:

$$\frac{d \log \left(\frac{\phi'}{\phi \cdot C} \right)}{d \left(\frac{1}{T} \right)} = -\Delta H_c - \frac{k'_q}{k'_q + k_{-1}^o} (E_{-1} - E'_q) \quad (2.67)$$

Where E_{-1} and E'_q are the activation energies of these reactions. In polar solvents $E_{-1} > E'_q$ and accordingly $k'_q \geq K'_c$, therefore at high temperatures the following situation occurs:

$$-\Delta H_{EX} = E_{-1} - E_1 \quad (2.68)$$

¹ k'_q is the changed (increased) rate constant for exciplex dissociation with the increase of solvent polarity.

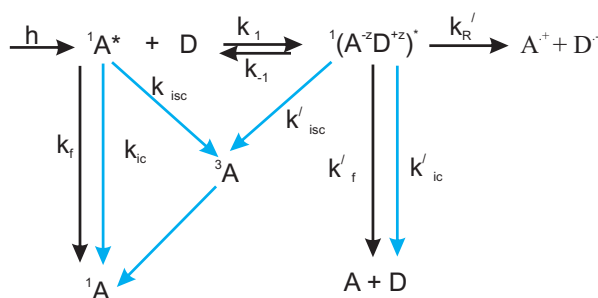


Figure 2.6.: In above scheme $h\nu$ = Incident light used for photo excitation. A = fluorophore (electron acceptor under consideration), D= electron donor under consideration, k_1 = rate constant for exciplex formation, k_{-1} = rate constant for exciplex dissociation, k_f = rate constant of emission for fluorophore, k_{ic} = rate constant of interconversion, k_{isc} = rate constant of intersystem crossing for fluorophore, k'_f = rate constant of emission for exciplex, k'_{ic} = rate constant of interconversion for exciplex, k'_{isc} = rate constant of intersystem crossing for exciplex, k'_R = rate constant of exciplex dissociation into radical ions, $\Delta H_{EX}^* = \Delta H_1^\ddagger - \Delta H_{-1}^\ddagger$.

Thus at the highest attainable temperature where $K'_c \ll k'_q$, equations 2.67 and 2.68 takes the following form:

$$\frac{d \log \left(\frac{\phi'}{\phi \cdot C} \right)}{d \left(\frac{1}{T} \right)} = E'_q - E_1 \quad (2.69)$$

Thus it is proved that with increasing the solvent polarity value of enthalpy of exciplex formation decreases.

2.6.6. The Kuz'min Calculation Scheme

The kinetic scheme, 2.6, must be understood first because the reversible excited state complexation reaction taking place is described by it. According to Kuz'min the Exciplexes are of two types ¹. He suggest two different schemes for the calculation of kinetic and thermodynamic parameters. These two schemes are discussed as under:

Partial Charge Transfer Exciplex They are characterized by the strong overlapping of their emission spectra with those of parent fluorophore. Here $z < 1$. Where 'z' is the parameter which describes the extent of charge transfer. The calculation scheme is subdivided into several parts for convenience in understanding

¹ This classification is done on the basis of extent of charge transfer between the donor (D) and acceptor(A).

Calculation of Enthalpy and Entropy of Exciplex Formation⁶⁹ According to scheme 2.6 the following equations are used to describe the ratios of quantum yields of the exciplex (ϕ') and fluorophore emission in the presence (ϕ) and in the absence (ϕ_o) of quencher¹.

$$\frac{\phi_o}{\phi} = \left[1 + \frac{k_1 \tau_o [D]}{1 + k_{-1} \tau'_o} \right] \quad (2.70)$$

$$\frac{\phi'}{\phi} = \left[\frac{\left(\frac{k'_f}{k_f} \right) \left(\frac{k_1}{k_{-1}} \right) [D]}{1 + \left(\frac{1}{k_{-1} \tau'_o} \right)} \right] \quad (2.71)$$

In above equations [D] is the concentration of donor (quencher). τ'_o and τ_o are the lifetimes of exciplex and excited fluorophore respectively ²

The rate constants appearing in the scheme 2.6 are represented by the following equations:

$$\ln k_1 = \ln k_1^o - \frac{\Delta H_1^\ddagger}{RT} \quad (2.72)$$

$$\ln k_{-1} = \ln k_{-1}^o - \frac{\Delta H_{-1}^\ddagger}{RT} \quad (2.73)$$

$$\ln \left(\frac{1}{\tau'_o} \right) = \ln k'_o - \frac{\Delta H_{EX}^\ddagger}{RT} \quad (2.74)$$

ΔH_{EX}^\ddagger is the apparent (average) enthalpy of activation for the exciplex decay ³ The enthalpy (ΔH_{EX}^*) and entropy (ΔS_{EX}^*) of exciplex formation can be determined from the temperature dependence of the relative quantum yields of fluorescence from the exciplex and fluorophore $\left(\frac{\phi'}{\phi} \right)$ and from the fluorophore in the absence and presence of quencher $\left(\frac{\phi_o}{\phi} \right)$. The mathematical expressions for rate constants are already mentioned (from equation number 2.72 to 2.74) so, according to the scheme 2.6 the equations used to

¹ The relative quantum yields of fluorescence $\left(\frac{\phi'}{\phi} \right)$ and $\left(\frac{\phi_o}{\phi} \right)$ can be calculated from the ratios $\left(\frac{W'}{W} \right)$ and $\left(\frac{W_o}{W} \right)$ of area under the corrected spectrum of exciplex W' (on the wavenumber scale) and the fluorophore in the absence and (W_o) and presence of quencher (W).

² The mathematical equations for life times are as: $\tau_o = \frac{1}{k_f + k_{ic} + k_{isc}}$ and $\tau'_o = \frac{1}{k'_f + k'_{ic} + k'_{isc}}$.

³ ΔH_{EX}^\ddagger is the enthalpy of activation for the reactions having rate constants $k'_f, k'_{ic}, k'_{isc}, k'_R$ and $(k'_f + k'_{ic} + k'_{isc} + k'_R) = k'$.

determine the activation and thermodynamic parameters are given as:

$$\ln \left[\frac{\left(\frac{\phi_o}{\phi} - 1 \right)}{\tau_o [D]} \right] = \ln k_1 - \ln (1 + k_{-1} \tau_o') = \ln k_1^\circ - \frac{\Delta H_1^\ddagger}{RT} \quad (2.75)$$

$$\ln \left[1 + \left(\frac{k_{-1}^\circ}{k_o'} \right) \exp \left\{ - \frac{(\Delta H_{-1}^\ddagger - \Delta H_{EX}^\ddagger)}{RT} \right\} \right] = A + \frac{C}{T} - \ln \left[1 + B \exp \left(\frac{D}{T} \right) \right] \quad (2.76)$$

Where

$$A = \ln k_f^\circ \quad (2.77a)$$

$$B = \frac{k_{-1}^\circ}{k_o'} \quad (2.77b)$$

$$C = \frac{\Delta H_1^\ddagger}{R} \quad (2.77c)$$

$$D = \frac{\Delta H_{EX}^\ddagger - \Delta H_{-1}^\ddagger}{R} \quad (2.77d)$$

$$\ln \left(\frac{\left(\frac{\phi'}{\phi} \right)}{[D]} \right) = \ln \left(\frac{k_f'}{k_f} \right) + \ln \left(\frac{k_1}{k_{-1}} \right) - \ln \left(1 + \frac{1}{k_{-1} \tau_o'} \right) = \ln \left(\frac{k_f'}{k_f} \right) + \ln \left(\frac{k_1^\circ}{k_{-1}^\circ} \right) - \frac{\Delta H_{EX}^*}{RT} \quad (2.78)$$

$$- \ln \left[\left\{ 1 + \frac{k_o'}{k_{-1}^\circ} \exp \left(\frac{\Delta H_{-1}^\ddagger - \Delta H_{EX}^\ddagger}{RT} \right) \right\} \right] = A' + \frac{C'}{T} - \ln \left[1 + B' \exp \left(\frac{D'}{T} \right) \right] \quad (2.79)$$

Where

$$A' = \ln \left(\frac{k_f'}{k_f} \right) + \ln \left(\frac{k_1^\circ}{k_{-1}^\circ} \right) \quad (2.80a)$$

$$B' = \frac{k_o'}{k_{-1}^\circ} = \frac{1}{B} \quad (2.80b)$$

$$C' = - \frac{\Delta H_{EX}^*}{R} \quad (2.80c)$$

$$D' = \frac{\Delta H_{-1}^\ddagger - \Delta H_{EX}^\ddagger}{R} = -D \quad (2.80d)$$

2. Theoretical Perspective

When the ratios $\left(\frac{\phi'}{\phi}\right)$ and $\left(\frac{\phi_o}{\phi}\right)$ reach a maximum value near a temperature of $T_{max} \approx -\frac{D}{\ln B} = -\frac{D'}{\ln B'}$ the fitting of the dependence of $\left(\frac{\phi'}{\phi}\right)$ and $\left(\frac{\phi_o}{\phi}\right)$ on $\frac{1}{T}$ to equations 2.76 and 2.79 gives the following expressions for the exciplex formation enthalpy, and the activation enthalpy of exciplex formation and decay.

$$\Delta H_{EX}^* = -C'R, \quad \Delta H_1^\ddagger = -CR, \quad \Delta H_{-1}^\ddagger = \Delta H_1^\ddagger - \Delta H_{EX}^* = (C' - C)R \quad (2.81)$$

$$\left(\Delta H_R^\ddagger - \Delta H_{-1}^\ddagger\right) = RD = -RD' \quad (2.82)$$

$$\Delta H_{EX}^* = \Delta H_{-1}^\ddagger + DR = \Delta H_{-1}^\ddagger - D'R = (C' - C + D)R = (C' - C - D')R \quad (2.83)$$

In order to estimate the entropy of exciplex formation ΔS_{EX}^* and the entropy of exciplex formation ΔS_1^\ddagger and decay ΔS_{-1}^\ddagger , it is necessary to know the ratio of exciplex to fluorophore emission rate constants $\left(\frac{k'_f}{k_f}\right)$ and the temperature dependence of the diffusion rate constant in a given solvent¹. The equations used for the calculation of the entropy values are given as:

$$\Delta S_{-1}^* = \Delta S_{EX}^* - \Delta S_1^\ddagger = \left[A' + A - \ln k_{diff}^o - \ln \left(\frac{k'_f}{k_f}\right) \right] R \quad (2.84)$$

$$\Delta S_{EX}^* = \left[A' - \ln \left(\frac{k'_f}{k_f}\right) \right] R \quad (2.85)$$

$$\ln \left(\frac{k_{-1}^o}{k_o}\right) = B = \frac{1}{B'} \quad (2.86)$$

$$\Delta S_{-1}^\ddagger - \Delta S_{EX}^\ddagger = R \ln B = -R \ln B' \quad (2.87)$$

$$\begin{aligned} \Delta S_{EX}^\ddagger &= \Delta S_{-1}^\ddagger - R \ln B = \left[A' + A - \ln B - \ln k_{diff}^o - \ln \left(\frac{k'_f}{k_f}\right) \right] R \\ &= \Delta S_{-1}^\ddagger + R \ln B' = \left[A' + A + \ln B' - \ln k_{diff}^o - \ln \left(\frac{k'_f}{k_f}\right) \right] R \end{aligned} \quad (2.88)$$

¹ Equation used to calculate the diffusion rate constant is $\ln k_{diff} = \ln k_{diff}^o - \frac{\Delta H_{diff}^\ddagger}{RT}$. Where $\ln k_{diff}$ is the diffusion rate constant, ΔH_{diff}^\ddagger is the enthalpy of diffusion. The equation used to calculate the activation enthalpy of diffusion is $k_{diff} = \frac{8000RT}{3\eta}$.

Sometimes both branches of temperature dependence are not found for $\left(\frac{\phi'}{\phi}\right)$ $\left(\frac{\phi_o}{\phi}\right)$ because the T_{max} for the complex of interest may not be accessible experimentally¹. Under these conditions it is impossible to calculate the activation parameters and only the ΔS_{EX}^* and ΔH_{EX}^* can be determined. Under the conditions when $t_{-1} \gg 1$ the following approximations are valid:

$$\ln \left(\frac{\phi'}{\phi} \right) = \ln \left([D] \frac{k'_f}{k_f} \right) + \frac{\Delta S_{EX}^*}{R} - \frac{\Delta H_{EX}^*}{RT} \quad (2.89)$$

The equation 2.89 is used further to calculate the values of ΔS_{EX}^* and ΔH_{EX}^* , respectively. Value of ΔH_{EX}^* can be obtained directly from the slope of graphs $\ln \left(\frac{\phi'}{\phi} \right) \frac{1}{T}$ but the value of $\ln \left([D] \frac{k'_f}{k_f} \right)$ is required for the calculation of ΔS_{EX}^* . $[D]$ is the concentration of quencher and the $\left(\frac{k'_f}{k_f} \right)$ can be calculated using the following equation:⁷⁰

$$\left(\frac{k'_f}{k_f} \right) \approx \left(\frac{\nu_{EX}}{\nu_f} \right)^3 (1 - 0.9z) \quad (2.90)$$

parameter 'z' appearing in above equation is known as the extent of charge transfer². Following is the equation used to calculate the value of 'z':⁷⁰

$$h\Delta\nu + \Delta H_{EX}^* = z^2 \{a + m[f(\epsilon) - f(n^2)]\} \quad (2.91)$$

$h\Delta\nu$ is difference of average emission frequencies of fluorophore and the exciplex³. $f(\epsilon)$ ⁴ and $f(n^2)$ can be calculated using the following formulae:⁷⁰

$$f(\epsilon) = \left[\frac{(\epsilon - 1)}{2(\epsilon + 2)} \right] \quad (2.92)$$

$$f(n^2) = \left[\frac{(n^2 - 1)}{2(n^2 + 2)} \right] \quad (2.93)$$

Here 'ε' and 'n' are the dielectric constant and the refractive index of solvents used. 'm'

¹ Usually the T_{max} is lower than the range of temperature reached experimentally.

² It is this parameter which tells the amount of charge transfer between donor and acceptor.

³ Mathematically this difference is represented as: $h(\nu_f - \nu_{EX})$.⁶⁹

⁴ The formula used for the calculation of $f(\epsilon)$ is known as the Lorentz and Debye function.

appearing in above equation 2.92 can be calculated as:

$$m = \left(\frac{\mu_{EX}^2}{\rho^3} \right) \quad (2.94)$$

Where ρ is the radius of exciplex solvation shell and it can be calculated using the equation of Onsager cavity radius:⁶⁵

$$\rho_{EX} = (r_i)_A + (r_i)_D \quad (2.95)$$

¹ And

$$r_i = \left[\frac{3M_i}{4\pi\delta N_L} \right] \quad (2.96)$$

Here M_i is the molar mass, δ is the density. μ_{EX} appearing in equation 2.94 is the dipole moment of exciplex and it can be determined from the fluorescence solvatochromic shifts by using the following equation:⁷¹

$$\nu_{EX} = \nu_{EX}(0) - \left(\frac{2\mu_{EX}^2}{hc\rho^3} \right) \left\{ f - \frac{1}{2}f \right\} \quad (2.97)$$

Where

$$\left\{ f - \frac{1}{2}f \right\} = \left[\frac{(\epsilon - 1)}{(2\epsilon + 1)} - \frac{(n^2 - 1)}{(4n^2 + 2)} \right] \quad (2.98)$$

and $\nu_{EX}(0)$ is the hypothetical gas phase exciplex fluorescence maximum.

Calculation of Apparent(average) Enthalpy of Activation for Exciplex Decay⁶⁹

Using the same high temperature approximation as used before in equation number 2.89 the average enthalpy of exciplex decay (ΔH_{EX}^\ddagger) can be calculated by using the following equation:

$$\ln \left(\frac{\phi_o}{\phi} - 1 \right) = \ln \left\{ [D] \left(\frac{k_1^o}{k_{-1}^o} \right) \left(\frac{k'_o}{\tau_o} \right) \right\} - \frac{(\Delta H_{EX}^* + \Delta H_{EX}^\ddagger)}{RT} \quad (2.99)$$

Calculation of Rate Constant for Exciplex Formation⁶⁹ Following equation is used for the calculation of rate constant for exciplex formation k_1 :

$$\ln k_1 = \ln k_1^o - \frac{\Delta H_1^\ddagger}{RT} \quad (2.100)$$

¹ subscript A and D represents the fluorophore and quencher respectively.

The value of k_1° and ΔH_1^\ddagger appearing in above equation can be calculated by using the following equation:

$$\ln \left\{ \frac{\left(\frac{\phi_o}{\phi} - 1 \right)}{\tau_o[D]} \right\} = \ln k_1^\circ - \frac{\Delta H_1^\ddagger}{RT} \quad (2.101)$$

Strongly Polar Exciplexes These resemble the contact radical-ion pairs and are characterized by almost complete charge transfer. Here $z > 1$. Formation of this type of exciplex is easily observed in non-polar solvents, but as the solvent polarity increases, the quantum yield and lifetime of fluorescence decreases and they dissociate into radical ion pairs. Here also the calculation scheme is sub-divided into several parts in order to make it easily understandable.

Calculation of Enthalpy of Exciplex Formation Following is the equation used for the calculation of enthalpy of exciplex formation ΔH_{EX}^* :⁷²

$$\Delta H_{EX}^* \approx (H_{22}^\circ - H_{11}^\circ) + a - mf(\epsilon_{293})1.4 \quad (2.102)$$

Value of 'm' and $(H_{22}^\circ - H_{11}^\circ)$ ¹ can be calculated by using the following equation:⁷²

$$(H_{22}^\circ - H_{11}^\circ) = H_{12} \left[\frac{\left(\frac{1}{z} - 1 \right)^{\frac{1}{2}} - 1}{\left(\frac{1}{z} - 1 \right)^{\frac{1}{2}}} \right] + 2zmf(\epsilon) \quad (2.103)$$

All parameters appearing in above equation are described previously. The parameter 'a' appearing in equation 2.102 is known as the destabilization energy and it can be calculated as:⁶⁹

$$a = H_{22}^\circ - H_{11}^\circ - \left\{ \frac{H_{12}}{\left(\frac{1}{z} - 1 \right)^{\frac{1}{2}}} \left(\frac{1}{z} - 2 \right) \right\} - 2zmf(\epsilon) \quad (2.104)$$

¹ $(H_{22}^\circ - H_{11}^\circ)$ are the energies of ψ_1 and ψ_2 of the exciplex.

The equation used to calculate the parameter ‘z’ appearing in the previous equation⁶⁹ is:

$$h\Delta\nu = \left\{ \frac{H_{12}}{\left(\frac{1}{z} - 1\right)^{\frac{1}{2}}} \right\} - z^2 mf(n^2) \quad (2.105)$$

Where H_{12} is the matrix element coupling charge transfer and the locally excited states and the equation used to calculate this parameter is given as:

$$H_{12} = \left(\frac{1}{z} - 1\right)^{\frac{1}{2}} [h\Delta\nu - z^2 mf(n^2)] \quad (2.106)$$

Calculation of Gibbs Energy of Exciplex Formation ΔG_{EX}^* is known as the Gibbs energy of exciplex formation and it can be calculated by using the following equation:⁷²

$$\Delta G_{EX}^* \approx (H_{22}^{\circ} - H_{11}^{\circ}) + a - mf(\epsilon_{293})(P - QT) \quad (2.107)$$

The parameters ‘Q’ and ‘P’ appearing in above equation can be calculated as:⁷²

$$\left[\left\{ \frac{\frac{(\epsilon - 1)}{(2(\epsilon + 2))}}{\frac{(\epsilon_{293} - 1)}{(2(\epsilon_{293} + 2))}} \right\} [1.4 - 0.0013 T] \right] = P - QT \quad (2.108)$$

Calculation of Entropy of Exciplex Formation ΔS_{EX}^* is known as the entropy of exciplex formation and it can be calculated as:⁷²

$$\Delta S_{EX}^* \approx -m_{293} f(\epsilon_{293}) 0.00013T \quad (2.109)$$

2.6.7. Band Parameters Obtained from Excited Emission Spectra

Direct information on the values of vertical energy gap between singlet and ground states $\Delta E_{CR} = h\nu'_o$ and other parameters necessary for discussion of the behavior of radiation less transition can be obtained from the exciplex emission spectra. For better understanding of these parameters figure 2.7 must be considered. In order to get the band

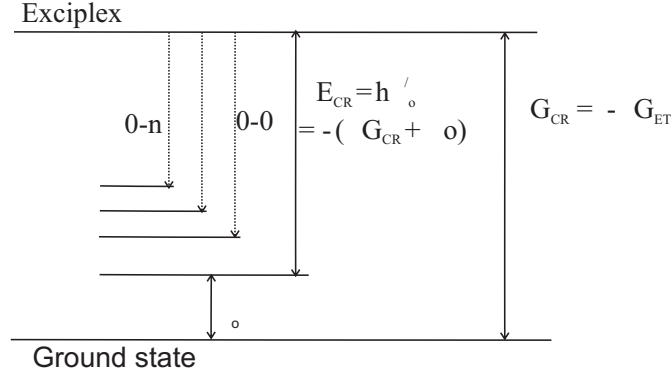


Figure 2.7.: Figure showing the Kuzmin's fitting parameters. In this figure 0-0 is the transition from zero vibronic level of exciplex to the zero vibronic level of the ground state, λ_o is the reorganization energy of solvent and other low frequency (classical) modes, ΔE_{CR} is the the energy gap between singlet excited and ground state. ΔG_{ET} is the gibb's energy of electron transfer.¹¹

parameters following equation is used,^{11,12}

$$\frac{I(\nu')}{I_o} = \sum_m \left[\exp(-S) \left(\frac{S^m}{m!} \right) \times \exp \left[-\frac{(h\nu'_o - h\nu' - mh\nu_v)^2}{2\sigma^2} \right] \right] \quad (2.110)$$

The exciplex emission spectra obtained as a function of a number of photons per unit frequency interval vs energy of emitted photons per unit frequency interval vs energy emitted photons $h\nu'$ is fitted to above equation to obtain the required parameters. In this equation emission band is represented as a sum of vibronic transitions with Gaussian band shapes. Here ν'_o is a frequency of 0 – 0 transition, $S = \frac{\lambda_v}{h\nu_v}$ is the Huang-Rhys factor,⁷³ λ_v is the internal reorganization energy associated with the average vibrational frequency of this mode, and σ is a width of the vibronic bands. This expression is completely equivalent mathematically to the another expression commonly used by many authors,⁷⁴⁻⁷⁵⁻⁷⁸ for charge transfer (CT) transitions.

$$\frac{I(\nu')}{\nu'} = \left(\frac{64\pi^4 n^3}{3h^3 c^3} \right) V_{10}^2 (\Delta\mu)^2 (4\pi\lambda_o k_B T)^{-1/2} \times \sum_m \left[\exp(-S) \left(\frac{S^m}{m!} \right) \right] \exp \left[-\frac{(\Delta G_{CR} + \lambda_o + h\nu' + mh\nu_v)^2}{4\lambda_o k_B T} \right] \quad (2.111)$$

If the energy gap between the charge transfer state and ground (G) states $\Delta E_{CR} = h\nu'_o = -(-\Delta G_{CR} + \lambda_o)$ and $\sigma^2 = 2\lambda_o k_B T$. Here V_{10} is the matrix matrix element cou-

pling charge transfer and ground states, $\Delta G_{CR} = -\Delta G_{ET}$, $\Delta\mu$ is the difference in the dipole moment between these states, and λ_o is the reorganization energy of solvent and other low frequency (classical) modes. But the physical nature of these expressions is quite different. Equation 2.110 corresponds to the spectral envelop formed by Gauss broadening of the vibronic bands to thermal fluctuations of the medium reorganization in the initial state solely. In the case of solids and liquids the inhomogeneous broadening is caused by the various kinds of intermolecular interactions besides the medium reorganization. therefore σ is related also to many other factors and its value should exceed $2\lambda_o k_B T^{1/2}$. In contrast, the energy gap ΔE_{CR} and the energy of 0-0 transition, $h\nu'_o$, are related to directly to the medium reorganization energy (2.7). The separation of σ and λ_o provides more correct description of the exciplex emission spectra.

Gould already noted⁷⁹ that the fitting of equation 2.111 to experimental emission spectra provides the sum $(\Delta G_{CR} + \lambda_o) = -\Delta E_{CR} = -h\nu'$ with much better accuracy than that of ΔG_{CR} and λ_o separately. In combined fitting to absorption and emission spectra, Stokes shift dominates in the determination of λ_o and the obtained values of λ_o can differ from $\frac{\sigma^2}{2k_B T}$. The individual fitting to absorption and emission spectra provides the value of $\lambda_o = \frac{\sigma^2}{2k_B T}$ because the spectral envelop is defined by the width of vibronic bands, and information on actual reorganization energy is missed. This indicates that that inhomogeneous broadening is substantially exceeds the medium reorganization broadening. Radiation less and radiative transitions probability depends on quantum coordinates and related parameters $h\nu, \lambda_v, \sigma$, and ΔE_{CR} rather than on classical coordinates and parameters λ_o and ΔG_{CR} . Thus the values of ΔG_{CR} and λ_o , obtained from combined fitting of absorption and emission spectra, are inapplicable for the evaluation of radiation less or radiative decay parameters.

2.6.8. Fluorescence Lifetimes and Quantum Yields of Exciplex and Fluorophore

In present discussion fluorescence lifetimes are required in order to get the value of ΔS_{EX}^* . For better understanding of results it is necessary to have an idea about the theory of lifetimes and quantum yields

Fluorescence Lifetimes⁸⁰⁻⁸² Absorption and emission processes are almost always studied on populations of molecules and the properties of the supposed typical members of the population are deduced from the macroscopic properties of the process. Generally the behavior of an excited population of fluorophore is described by using the following

equation:

$$\frac{dn^*}{dt} = -n^*\Gamma + f(t) \quad (2.112)$$

In above equation n^* is the number of excited elements at time t , Γ is the rate constant of emission and $f(t)$ is an arbitrary function of the time, describing the time course of the excitation. The dimensions of Γ are sec^{-1} (transition per molecule per unit time). If the excitation occurs at $t = 0$, the last equation, takes the form

$$\frac{dn^*}{dt} = -n^*\Gamma \quad (2.113)$$

and describes the decrease in excited molecules at all further times. Integration results in following equation¹:

$$n^*(t) = n^*(0)exp(-\Gamma t) \quad (2.114)$$

If a population of fluorophore are excited, the lifetime is the time it takes for the number of excited molecules to decay to $\frac{1}{e}$ or 36% of the original population according to:

$$\frac{n^*(t)}{n^*(0)} = e^{-\frac{t}{\tau}} \quad (2.115)$$

In most cases of interest, it is virtually impossible to predict priori the excited state lifetime of a fluorescent molecule. The true molecular lifetime, i.e, the lifetime one expects in the absence of any excited state deactivation processes - can be approximated by the Strickler-Berg (SB) equation:⁶²

$$\frac{1}{\tau_r} = k_r = 8\pi 10^5 \ln(10) \frac{c n_D^2}{N_L} \frac{\int F(\nu) d\nu}{\int \nu^{-3} F(\nu) d\nu} \int \nu^{-1} \epsilon(\nu) d\nu \quad (2.116)$$

τ_r and k_r stands for the radiative lifetime and rate constant respectively², c is the speed of light in vacuum, n_D is the refractive index of the solvent at 589 nm - D line of sodium, but a more exact equation should take into account the change in the refractive index with the absorption and emission wavelength, which would not lead to a major correction in our case but has to be seriously considered when approaching the ultraviolet region. N_L is the Loschmidt number, $F(\nu)$ is the fluorescence spectrum and $\epsilon(\nu)$ is the absorption

¹ Where Γ equals to the life time τ .

² In this version of SB equation apparently no mirror symmetry between absorption and fluorescence is used, although it is deeply rooted in the principals from which it is derived.

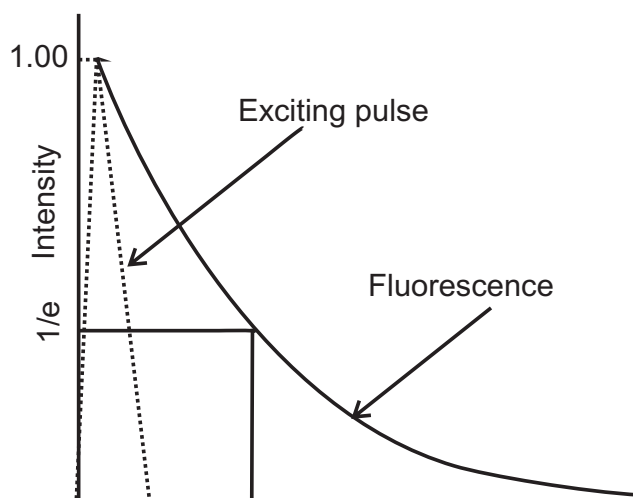


Figure 2.8.: Intensity decay representing fluorescence lifetime

spectrum. The lifetime and quantum yield for a given fluorophore are often dramatically affected by its environment. Examples of this fact would be NADH which in water has a lifetime of ≈ 0.4 ns but bound to dehydrogenases can be as long as 9 ns.^{83,84} Excited state lifetimes have traditionally been measured using either the impulse response or the harmonic response method. In principal both methods have the same information content. These methods are also referred to as either the “time domain method” or the “frequency domain method”. In impulse (or pulse) method the sample is illuminated with a short pulse of light and the intensity of the emission versus time is recorded. Originally these short light pulses were generated using flash lamps which had width on the order of several nanoseconds. Modern laser sources can now routinely generate pulses with widths on the order of picoseconds or shorter. As shown in the intensity decay figure, the fluorescence lifetime, t , is the time at which the intensity has decayed to $1/e$ of the original value. The decay of the intensity with time is given by the relationship:

$$I_t = \alpha e^{-\frac{t}{\tau}} \quad (2.117)$$

Where I_t is the intensity at time t , α is a normalization term (the pre-exponential factor) and τ is the lifetime. If the decay is single exponential and if the lifetime is long compared to the exciting light then the lifetime can be determined directly from the slope of the curve. If the lifetime and the excitation pulse width are comparable some type of decon-

olution method must be used to extract the lifetime¹. If the decay is multi exponential, the relation between the intensity and time after excitation is given by:

$$I(t) = \sum \alpha_i e^{-\frac{t}{\tau_i}} \quad (2.118)$$

Quantum Yields⁸⁵ If all the quenching processes are first order with respect to the excited state, then for any fluorescent species, the quantum yield, Q, may be represented by the following equation:

$$Q = \frac{k_f}{(k_f + \sum_i k_i)} \quad (2.119)$$

where k_f is the first-order rate constant for the direct emission of fluorescent radiation by the excited state, and the set of k_i are the first order rate constants for the various deactivation processes. The observed fluorescent lifetime, τ is given as:

$$\tau = \frac{1}{(k_f + \sum_i k_i)} \quad (2.120)$$

So that

$$k_f = \frac{Q}{\tau} \quad (2.121)$$

Now the equation 2.119 can be written as:

$$Q^{-1} = 1 + k_f^{-1} \sum_i k_i \quad (2.122)$$

If it is assumed that k_f is independent of temperature (at least in the region between 0° and 70°), then the temperature dependence of the quantum yield may be expressed as:

$$Q^{-1} - 1 = k_f^{-1} \sum_i f_i \exp\left(\frac{-E_i}{RT}\right) \quad (2.123)$$

Where f_i is the frequency factor for the i th deactivation process and involves the entropic component of the corresponding free energy of activation, E_i is the activation energy for

¹ Great effort has been made to deconvolve the effect of the exciting pulse on the observed fluorescence decay. With the advent of very fast laser pulses these deconvolution procedures become less important for most lifetime determinations although they are still required whenever the lifetime is of comparable duration to the light pulse.

the i th deactivation process. If only one deactivation process is significant,

$$Q^{-1} - 1 = \frac{f}{k_f} \exp\left(\frac{-E}{RT}\right) \quad (2.124)$$

in which case $\ln(Q^{-1} - 1)$ should vary linearly with $\frac{1}{T}$. E may be computed directly from the slope of this line. If two or more deactivation processes with significantly different activation energies are present, then curvature will be apparent in plots of $\ln(Q^{-1} - 1)$ vs. $\frac{1}{T}$. In this case, interpretation of the data is considered more difficult.

A second special case, however, is of interest. If only two deactivation processes are important, one of which is temperature independent ($E_o = 0$) and the other temperature dependent ($E_1 > 0$), then the equation 2.123 reduce to

$$Q^{-1} - 1 = \frac{f_o}{k_f} + \frac{f_1}{k_f} = \exp\left(\frac{-E}{RT}\right) = \alpha_o + \alpha_1 \exp\left(\frac{-E_1}{RT}\right) \quad (2.125)$$

The parameters α_o , α_1 and E_1 can be calculated by the following two ways:

• **Procedure 1:** Differentiating the equation 2.125 with respect to $\frac{1}{T}$ results as:

$$\frac{\partial Q^{-1}}{\partial\left(\frac{1}{T}\right)} = -\left(\frac{\alpha_1 E_1}{R}\right) \exp\left(\frac{-E_1}{RT}\right) \quad (2.126)$$

$$\ln\left(-\frac{\partial Q^{-1}}{\partial\left(\frac{1}{T}\right)}\right) = \ln\left(\frac{\alpha_1 E_1}{R}\right) - \left(\frac{E_1}{RT}\right) \quad (2.127)$$

In this case $\frac{\partial Q^{-1}}{\partial\left(\frac{1}{T}\right)}$ can be estimating by drawing tangents to a plot of Q^{-1} vs. $\frac{1}{T}$ at

various values of $\frac{1}{T}$. Then a logarithmic plot of $\frac{\partial Q^{-1}}{\partial\left(\frac{1}{T}\right)}$ vs. $\frac{1}{T}$ should be linear with

a slope equal to $\frac{E_1}{R}$. The difficulty with this procedure lies in the inaccuracy involved in drawing tangents to the curve. Alternatively, the Q^{-1} vs. $\frac{1}{T}$ data may be fitted to a polynomial function and the derivative taken directly, but because the data are basically exponential, often polynomial fits are very unsatisfactory. Once the E_1 has been determined, equation 2.125 indicates that a plot of $(Q^{-1} - 1)$ vs. $\exp\left(\frac{-E_1}{RT}\right)$ should yield a straight line whose slope is equal to α_1 and whose intercept is α_o .

•Procedure 2: Equation 2.125 may be rewritten as:

$$\ln[(Q^{-1} - 1) - \alpha_o] = \ln\alpha_1 - \left(\frac{E_1}{RT}\right) \quad (2.128)$$

and an empirical value of α_o selected such that plots of $\ln[(Q^{-1} - 1) - \alpha_o]$ vs. $\frac{1}{T}$ are linear¹.

2.6.9. Calculation of Gibbs Energy of Electron Transfer Using Rehm-Weller Equation

⁸⁶Thermodynamic relationships representing the electromotive forces of oxidation and reductions of excited-state donor and acceptor are given as:

$$E^\circ\left(\frac{D^+}{D^*}\right) = E^\circ\left(\frac{D^+}{D}\right) - E_{\infty} \quad (2.129)$$

Values of $\left(E^\circ\frac{D^+}{D^*}\right)$, according to above equation are smaller than $\left(E^\circ\frac{D^+}{D}\right)$, thus showing that the excited state is much better electron donor than the ground state. Also

$$E^\circ\left(\frac{A^*}{A^-}\right) = E^\circ\left(\frac{A}{A^-}\right) + E_{\infty} \quad (2.130)$$

Here the excited state is better electron acceptor compared to the ground state because $E^\circ\left(\frac{A^*}{A^-}\right)$ is more positive than $E^\circ\left(\frac{A}{A^-}\right)$. Equations below represents the relationship between the gas-phase energy term and the redox potentials:

$$IP = E^\circ\left(\frac{D^+}{D}\right) - \Delta G_{D^+} + constant \quad (2.131)$$

$$EA = E^\circ\left(\frac{A}{A^-}\right) - \Delta G_{A^-} + constant \quad (2.132)$$

In above equations ΔG_{D^+} and ΔG_{A^-} are the solvation terms for D^+ and A^- respectively. The overall energy change for the uphill pathway involving the D and A along with downhill pathway involving from D^* and A, represented by the figure 2.9, is equal to the sum of free energy changes for oxidation of the donor and reduction of the acceptor.

$$\Delta G_{el} = \Delta G_{(D \rightarrow D^+)} + \Delta G_{(A \rightarrow A^-)} \quad (2.133)$$

¹ Calculations of parameters α_o , α_1 and E_1 by the two different procedures generally agreed very well. However, the possibility for systematic errors is very great and certain quantification must be made in considering the results.

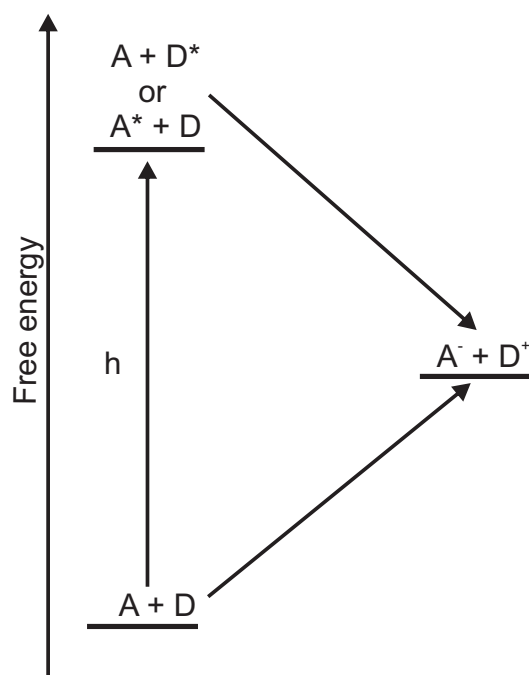


Figure 2.9.: A diagram showing the thermodynamic pathway for photoinduced electron transfer reaction.⁸⁷

In above equation ΔG_{el} specifies the standard free-energy change. As $\Delta G = nFE_{redox}$ ¹ so the above equation can be written as:

$$\Delta G_{el}(eV) = n(-E_{(D \rightarrow D^+)}) - E_{(A \rightarrow A^-)} \quad (2.134)$$

or, in keeping with the convention of writing all half-reactions as reduction and using redox potentials:

$$\Delta G_{el}(eV) = nF \left[E^\circ \left(\frac{D^+}{D} \right) - E^\circ \left(\frac{A}{A^-} \right) \right] \quad (2.135)$$

The free-energy change for an electron transfer between an excited donor and ground-state acceptor — the thermodynamically downhill reaction — can be derived in a similar manner:

$$\Delta G_{el}(eV) = nF \left[E^\circ \left(\frac{D^+}{D^*} \right) - E^\circ \left(\frac{A}{A^-} \right) \right] \quad (2.136)$$

¹ Where E_{redox} is defined as the potential of a half-reaction. It is sensitive to the direction of reaction. Positive E_{redox} means exothermic, spontaneous reaction on the other hand the negative value means an endothermic reaction.

As¹

$$E^\circ \left(\frac{D^+}{D^*} \right) = E^\circ \left(\frac{D^+}{D} \right) - E_{\infty} \quad (2.137)$$

So substituting the value of equation 2.137 into equation 2.136 following equation results:

$$\Delta G_{el}(eV) = n \left[E^\circ \left(\frac{D^+}{D} \right) - E^\circ \left(\frac{A}{A^-} \right) - \Delta G_{\infty} \right] \quad (2.138)$$

Where ΔG_{∞} is the free energy in electron volts corresponding to the equilibrium energy, E_{∞} . For most one electron transfers, $n \approx 1$, so that we can write

$$\Delta G_{el}(eV) = E^\circ \left(\frac{D^+}{D} \right) - E^\circ \left(\frac{A}{A^-} \right) - \Delta G_{\infty} \quad (2.139)$$

If the measured excited state energy is in kilo joules per mole and redox potentials in volts then the equation number 2.143 can be written as:

$$\Delta G_{el}(kJoule\,mol^{-1}) = 23.06 \left[E^\circ \left(\frac{D^+}{D} \right) - E^\circ \left(\frac{A}{A^-} \right) - \Delta G_{\infty} \right] \quad (2.140)$$

Similar equation will result if the electron transfer is between A^* and D. In above equation the experimental parameters required are the excited state energy of the photo excited molecules and the redox potentials of the ground states of both the electron donor and acceptor. Above equation is applicable to an equilibrated excited state and not a Franck-Condon state. It is assumed that the electron transfer occurs after the equilibration of the Franck-condon state to the relaxed, equilibrated state².

2.7. Factors Effecting Solution Dynamics of Exciplexes

Various short lived intermediates are formed in photoinduced electron transfer reactions as a result of interaction between an excited-and ground state molecule³. Their is rapid dissipation of excitation energy through the reactant and solvent molecules because each

¹ If it is assumed that the structure of D and D^+ and of D^* and D^+ are approximately same then free-energy is $\Delta G = \Delta H$ and $\Delta G_{(D^* \rightarrow D^+)} = \Delta G_{(D \rightarrow D^+)} - E_{\infty}$. As the free energy change is $\Delta G = -nFE_{redox}$ so the redox potentials of half-reactions involving excited states can be derived as: $E_{(D^* \rightarrow D^+)} = E_{(D \rightarrow D^+)} + E_{\infty}$.

Also by convention $E^* \left(\frac{D^+}{D} \right) = -E_{D \rightarrow D^+}$ and $E^* \left(\frac{D^+}{D^*} \right) = -E_{D^* \rightarrow D^+}$

² It should not be assumed that the electron transfer cannot take place involving unrelaxed excited states. There are examples in literature showing electron transfer in these cases but these are not considered in present discussion.

³ Here very general case is considered in which the excited state specie is electron acceptor, the reaction takes place in solution phase and the reactants are free to diffuse to the encounter distances.

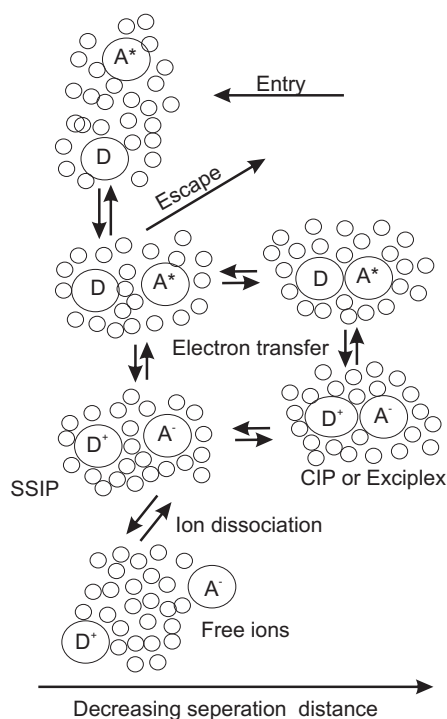


Figure 2.10.: A diagram showing the dynamic interconversion of solvent-separated ion pairs (SSIP), exciplexes, contact ion pairs (CIP), and free ions in solution. Electron transfer taking place within a cage of solvent molecules to generate a SSIP or more intimate charge-transfer complex, the latter being an exciplex or CIP. The nature of the charge-transfer intermediate generated may depend on the distance separating the reactants. The distance depends on the molecular structures of the reactants, i.e their sizes, shapes, and steric features. Free ions are produced by ion dissociation from the solvent cage.⁸⁷

ion pair intermediate is successfully transformed into another intermediate of lower energy. Depending upon its structure, the separation distance and the polarity of medium, each ion pair is stabilized by electrostatic and solvation effects. Thus in solution, the nature of the pathway leading to ionic intermediates is dictated to a large extent by the polarity of solvent as well as the shape of the excited and ground state reactants. If the reactants are spherical then they may diffuse into a solvent cage and remain for a short time within an encounter distance (see figure 2.10). Within the cage separation distances depends on the shape and sizes of molecules usually, for spherical reactants, the center to center distance d_{cc} is between ≈ 6.5 and 7.5 \AA . The planar molecules and oblate spheroidal or ellipsoidal molecules can probably approach to closer distances depending on the dimensions of their sub axes.

For exciplex formation the greater is the difference faster is its formation. The possibility of exciplex formation depends upon the structure of reacting species. Usually the planar molecules are ideal choice for exciplex formation as they can easily adapt face-to-face geometries at a distance of 3 - 4 Å. Exciplexes have also been identified in interactions in intra molecular systems linked by flexible chains. Numerous chain motions in these molecules eventually bring both donor and acceptor in favorable orientation. Thus a variety of intermolecular exciplex structures are possible. These exciplex structures which are slightly different from each other can undergo interconversion in solutions.

If there are two ground-state species in fluid medium and they are engaged in a series of collisions at a range of distances then their electronic and structural features will dictate the nature of these interactions. However there are electronic forces which are opposing these attractive interactions e.g. in ground state the repulsion between the bonding electrons in ground states of both donor and acceptor may prevent the molecules from approaching to closer distances. Steric repulsion between the molecules may be another reason which prevent a close approach. Therefore the net result is that at close separation distance the ground-state species may be repulsive in fluid media. Whereas on the other hand in excited state, the intermolecular repulsive forces may be relaxed. Therefore after photo excitation, the reactants may approach on the excited surface and form an encounter complex and finally an exciplex. Emission for the excited reactant called as "monomer emission" will be observed as long as the reactants remain well separated. When the complex equilibrates to a minimum on the excited state surface corresponding to the equilibrium separation distance of the exciplex, the exciplex may then undergo emission or radiation less decay to the ground state surface. Deactivation occurs as a vertical Franck-Condon transition from a minimum on a reaction surface to a position of high energy on the ground state, so that the reactants will separate rapidly until their energy reaches a minimum point on the surface.

As the nature and character of exciplexes in photoinduced electron transfer are strongly dependent on the polarity of medium so the exciplex solvation enthalpy in a solvent of known polarity can be calculated as¹:

$$\Delta H_{A-D^+} = -\frac{\mu^3}{\rho^3} \left(\frac{\epsilon_s - 1}{2\epsilon_s + 1} \right) N_L \quad (2.141)$$

Where μ is the dipole moment and it is calculated before by using equation 2.97 and ρ is the radius and can be calculated using the 2.95. The free energy change for exciplex

¹ This equation exists because an exciplex is a dipolar specie with a dipole moment.

formation is given by the following expression:

$$\Delta G_{EX} = E^{\circ} \left(\frac{D^+}{D} \right) - E^{\circ} \left(\frac{A}{A^-} \right) - \Delta G^* + \frac{e^2}{2} \left(\frac{1}{r_D} + \frac{1}{r_A} \right) \left(1 - \frac{1}{\epsilon_s} \right) + E_{orb} - \frac{e^2}{d_{cc}} - \frac{\mu^2}{\rho^3} \left(\frac{\epsilon_s - 1}{2\epsilon_s + 1} \right) \quad (2.142)$$

Last term appearing in above equation describes the energy of exciplex (which is dipolar in nature)¹. Thus the coulombic interactions and solvation plays a very important role in stabilization of exciplex. By having a large dipole moment and also by increasing solvent polarity the solvation energy is favored. E_{orb} appearing in the last equation is the difference between destabilizing and stabilizing orbital interactions ($E_{orb} = E_{desr} - E_{stab}$). Thus the exciplex stabilization is also enhanced by orbital interactions which favors E_{stab} . In polar solvents the pathway to free ions may proceed from the encounter or collision complex through an exciplex (or CIP), in competition with direct formation via a SSIP (see figure 2.11). Magnitudes of the Kirkwood-Onsager and Born energies, electrostatic effects and orbital interactions are used to determine the actual pathway involving the formation of exciplex is unfavorable because of a energy barrier due to large ΔG_{sol} . If ion pairing takes place at all in polar solvents², then the ions may dissociate into an SSIP and finally into free ions because polar solvents molecules may penetrate the space between ions of opposite charge and effectively weaken electrostatic attractions.

However there are some exciplexes which can be stabilized in polar solvents due to the Kirkwood-Onsager solvation energy term.⁵¹ As for example in polar solvents as exciplex structure with a large dipole moment can be stable with respect to solvent-separated and free ions(see figure 2.12). Formation of exciplex by 9 - anthracene - $(CH_2)_3$ - N, N - dimethylaniline in acetonitrile is the proof of formation and existence of exciplex in polar solvents.^{88,89} Similarly results shown by Davidson also proves the presence of exciplex for a series of naphthalene - CH_2 - N - alkylpyrroles($n = 0, 1, 2$) in polar solvents. The intermolecular systems play a role in stabilizing intra molecular exciplexes in polar solvents.

In case of non-polar solvents smaller value of ΔG_{sol} and favorable coulombic terms are responsible for the exciplex stability. In case of non-polar solvents ions preferably remain in contact for long time, i.e, ion pairing is effective because of favorable coulombic and solvent effects.

¹ This explanation is based on the Kirkwood-Onsager model (assuming formation of a spherical complex).⁵⁰

² This may occur if the Born term is equal to or less than the kirkwood-onsager term.

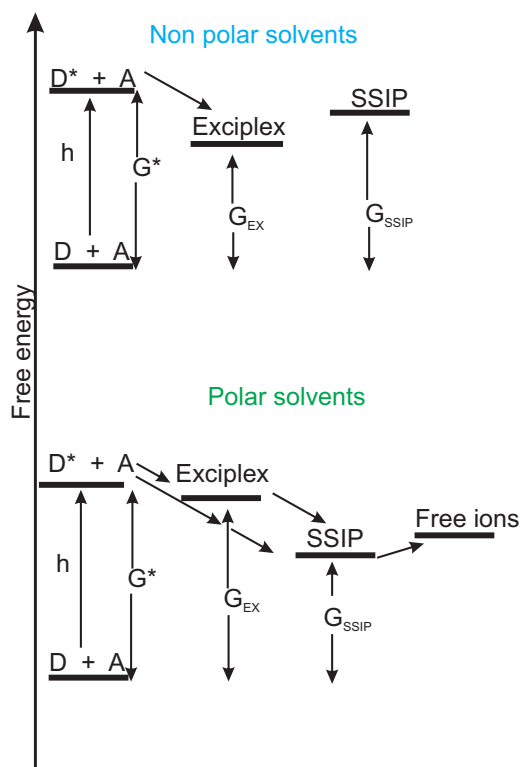


Figure 2.11.: The course of photoinduced electron transfer in solution depends on the polarity of the solvent. In non polar solvents, exciplexes are usually more stabilized than SSIP. In polar solvents, which can stabilize an SSIP and free ions, this figure shows two pathways leading to free ions. The exciplex in polar solvents may be more appropriately regarded as a contact ion pair.⁸⁷

2.8. Electron Donor and Acceptor – Electrochemical and Photophysical Properties

Successful electron transfer between electron donor and acceptor can occur if there is a perfect match between their photophysical and photochemical properties. The lifetime of the excited state (fluorophore in the present discussion) must be sufficiently long to allow quenching by electron transfer to take place¹. Knowledge of excited state energies of the sensitized and their redox potentials, wavelengths, quantum yields of important radiative and non-radiative pathways, excited state lifetimes, as well as the redox potentials of electron donating or accepting quenchers is thus an essential requirement for investigation

¹ i.e. the decay pathways should not be in competition with electron transfer. In the present context the decay pathways include the deactivation of the excited state by emissive and non-emissive processes.

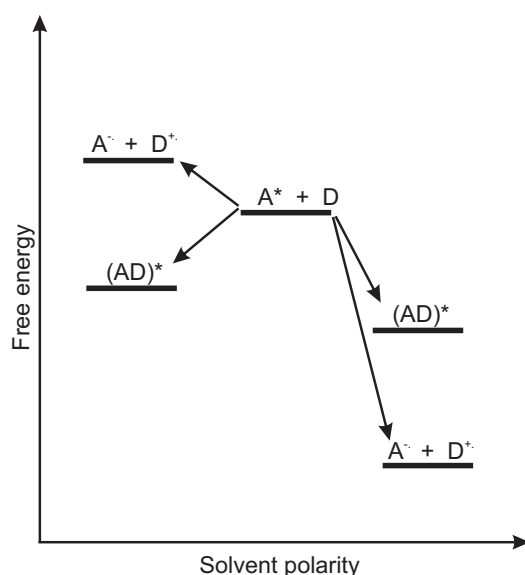


Figure 2.12.: Effects of solvent polarity on the energetics of electron transfer.⁸⁷

of photoinduced electron transfer processes. In order to get the value of rate constant, k_q , when an electron donor and acceptor quenches an excited state by electron-transfer mechanism is facilitated if the sensitizers display luminescence. In order to get the value of k_q from singlet excited state life times, following stern-volmer equation can be used:

$$\frac{1}{\tau_f} - \frac{1}{\tau_f^0} = 1 + k_q[Q] \quad (2.143)$$

In above equation τ_f and τ_f^0 are fluorescence life times in presence and absence of quencher respectively. With the increase in concentration of quencher $[Q]$ value of τ_f progressively decreases and the value of k_q can then be determined from slope by plotting $\frac{1}{\tau_f}$ Vs. $[Q]$ ¹.

2.9. Energy Transfer and Electron Transfer in Photoinduced Electron Transfer

Figure 2.13 illustrates the concept of energy transfer and the electron transfer in photoinduced electron transfer. In this figure the horizontal lines represent orbitals populated by electrons (represented by dots). In energy transfer, there are two pathways for the

¹ This reaction is very rapid and diffusion controlled. The rate determining step is diffusion of the sensitizer and quencher to a quenching sphere.

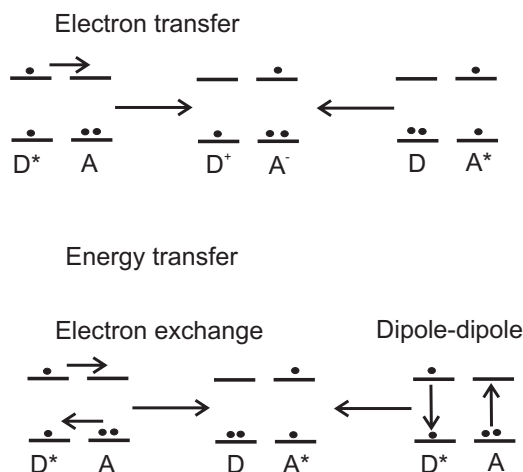


Figure 2.13.: Energy transfer versus electron transfer.⁸⁷

generation of A's excited state, A^* . First there may be a mutual exchange of electrons, a mechanism known as the energy transfer by electron exchange. The fact that D gives up an electron to A, while the latter in turn returns an electron to D, implies mutual or close proximity of D^* and A. In other words, for the electrons to travel back and forth, there must be some overlap of the electron clouds on D^* and A. In this respect, electron transfer is quite similar to energy transfer via electron exchange. In both of these pathways, overlap between the electron clouds of the reactants is an important feature. Energy transfer may also occur as a result of long-range dipole-dipole interaction. Since there is no mutual electron exchange in dipole-dipole interactions therefore the electronic transitions take place exclusively within D and A. D^* acts like an oscillating dipole— analogous to a transmitting antenna—by inducing the formation of A^* . In contrast to electron exchange, the dipole-dipole mechanism does not require D and A to be in close proximity. In fact, the dipole-dipole mechanism may be operative over many tens of angstroms.

The free-energy changes accompanying energy transfer either by electron exchange or the dipole-dipole mechanism may be formulated as:

$$\Delta G_{en} = \Delta H_{en} - T\Delta S_{en} = -\Delta G_{(D^* \rightarrow D)} + \Delta G_{(A^* \rightarrow A)} \quad (2.144)$$

$$\Delta G_{en} = -\Delta H_{(D^* \rightarrow D)} + T\Delta S_{(D^* \rightarrow D)} + \Delta H_{(A^* \rightarrow A)} - T\Delta S_{A^* \rightarrow A} \quad (2.145)$$

2. Theoretical Perspective

Above equation can be simplified as ¹:

$$\Delta G_{en} = -E_{oo}(D^*) + E_{oo}(A^*) \quad (2.146)$$

Substituting the values of $E_{oo}(D^*)$ and $E_{oo}(A^*)$ in above equation can provide the value of ΔG_{en} . Before the investigation of a new quenching reaction the redox potentials of reactants, their zero spectroscopic energies and the excited state energies of the quencher and the excited states must be known.

¹ Here it is assumed that the enthalpy difference is equal to the spectroscopic energy, E_{oo} . Further it is assumed that the entropy difference between the ground and excited states are negligible (in general $T\Delta S < 0.1 \text{ kcal mol}^{-1}$).

3. Experimental

A theory is something nobody believes, except the person who made it. An experiment is something everybody believes, except the person who made it.

(Albert Einstein)

This chapter includes information about the solvents used, fluorophores and quenchers, measurement procedures, apparatus and sample preparation. For better understanding this chapter is subdivided as. The first part posses information about the solvents used regarding their physical properties along with the purification methods used, second part will describe briefly the photo physical and photo chemical properties of fluorophores and quenchers used with their purification methods, next section will deal with the description of instruments used in the study. Steady state and time resolved measurements were performed here. Description of home build single photon counting and home build temperature regulating assembly attached with fluorimax is also included in present description. Finial part deals with the sample preparation procedure.

3.1. Solvents

Exciplex systems are studied here in non polar or slightly polar solvents over a range of temperature starting from 253.15 to 338.15 K. Dielectric constants for the selected solvents range within the limit $1.9 < \epsilon < 20.0$ because at $\epsilon > 20.0$ the exciplex dissociates into radical ion pairs.⁶ In photoinduced electron transfer process the macroscopic properties like $\rho, \eta, n_D, and \epsilon$ plays a very important role. Table 3.1 contains summary of the macroscopic properties of the solvents used, their supplier, purity and the purification method.

All solvents used were stored under argon in dark, especially carbon tetrachloride because it has low energy absorption band in the low energetics UV and is sensitive to light. It was therefore stored and distilled with black raping.

3. Experimental

Table 3.1.: Solvents used, their dielectric constant, ϵ_s (at 293.15 K), refractive index, n_D (at 293.15 K), mass density, ρ (at 298.15 K) and viscosity, η at 298.15 K. Majority of this data is taken from reference.[?] Along with this, suppliers of these solvents as well as purification (drying) methods are given.

Solvent ^a	ϵ_s	n_D	η / mPas	ρ / g/ml	Supplier	purification / drying
ACE	21.4	1.359	0.299	0.783	Fluka (99.9%)	3Å molecular sieve, distilled
ACN	36.68	1.344	0.344	0.776	Aldrich (99.9%, spectranal)	3Å molecular sieve, distilled
BUT	24.83	1.384	0.556	0.795 ^b	Fluka (\geq 99.9%)	Distilled
CYH	2.02	1.426	0.887	0.768	Roth (99.9%, UV/IR-Grade)	4Å molecular sieve, distilled
CTC	2.24	1.460	0.908	1.578	Acros Organic (99.8%,)	4Å molecular sieve, distilled
DCM	9.08	1.424	0.406	1.314	Roth(99.8%)	4 Å molecular sieve, distilled
DCE	9.97	1.444	0.451	1.244	Roth(99.5%)	4Å molecular sieve, dsitilled
ETA	6.05	1.372	0.419	0.889	Aldrich (99.5%)	4Å molecular sieve, distilled
DEE	4.35	1.352	0.235	0.879 ^c	Roth(99.5%)	4Å molecular sieve, distilled
BUA	5.01	1.394	0.685	0.876 ^d	Roth (98%)	4Å molecular sieve, distilled
PRA	6.02	1.384	0.553	0.883 ^e	Aldrich(99.5%)	4 Å molecular sieve, distilled
HEP	1.92	1.388	0.388	0.676	Roth(99.5%, HPLC)	4 Å molecular sieve, distilled
TOL	2.38	1.497	0.552	0.857	Roth(99.5%)	rotory dry, 4Å molecular sieve, c
THF	7.39	1.407	0.463	0.879	Roth(99.9%)	4Å molecular sieve, distilled

^a used acronyms: acetone (ACE), acetonitrile (ACN), butyronitrile (BUT), cyclohexane (CYH), carbon tetrachloride (CTC), dichloromethane (DCM), dichloroethane (DCE), ethylacetate (ETA), diethylether (DEE), butylacetate (BUA), propylacetate (PRA), heptane (HEP), toluene (TOL), tetrahydrofurane (THF)

^b This value is at 288.15 K

^c Data obtained from reference⁹⁰

^d Data obtained from reference⁹¹

^e Data obtained from reference⁹²

3.1.1. Propylacetate/Butyronitrile Mixture

Propylacetate/butyronitrile mixture was chosen to examine the effect of dielectric constant (ϵ) on the kinetics of exciplex. The two solvents are completely miscible over all mole fractions. This mixture was perfect for this investigation because the refractive index ($n_D = 1.3845$)⁹³ and the solvent viscosity ($\eta = 0.581cP$)⁹³ doesn't change by varying the mole fraction of mixture from 0 – 1, while the value of dielectric constant changes from 6.0 (butyronitrile) to 24.7 (propylacetate).⁹³ Solvent mixtures from $X_{PRA} = 0.9 - 0.4$ were selected because at $\epsilon > 18.0$ the exciplex dissociates into radical ion pairs. Linear dependence was observed between solvent dielectric constant and the weight fraction of propylacetate which can be described by the following equation:

$$\epsilon(w_1) = w_1\epsilon_1 + (1 - w_1)\epsilon_2 \quad (3.1)$$

Where w_1 and ϵ_1 represent the weight fraction and dielectric constant of propylacetate and ϵ_2 is the dielectric constant of butyronitrile.

3.2. Reactants

Exciplexes have been matter of interest of photo chemists for almost forty years.² The study of exciplexes with partial charge transfer makes it possible to gain a more profound understanding of the character of changes in the electronic structure of reactants and in the energetics of the electron transfer processes and corresponding reorganization of the medium.

Exciplexes that are formed by strong electron donors and acceptors and display an intense emission band well separated from that of the parent fluorophore in their emission band have also been studied here. In their structure, such exciplexes resemble contact radical-ion pairs and are characterized by almost complete charge transfer. The formation of strongly polar exciplexes is easy to observe in non polar solvents; however as solvent polarity increases, the quantum yield and the lifetime of fluorescence decreases, presumably, because of their dissociation into radical ions.⁹⁴ Exciplexes with partial charge transfer are characterized by strong overlapping of their emission spectra with those of parent fluorophore. Comparison was then made between the spectral and thermodynamic properties of partial and full charge transfer exciplexes. Effect of solvent polarity and the electron transfer driving force was also done.

3.2.1. Fluorophores

All the fluorophores selected here produce fairly intense emission in both the polar and non-polar solvents (insert figures). Structure of fluorophore used are given in figure 3.1

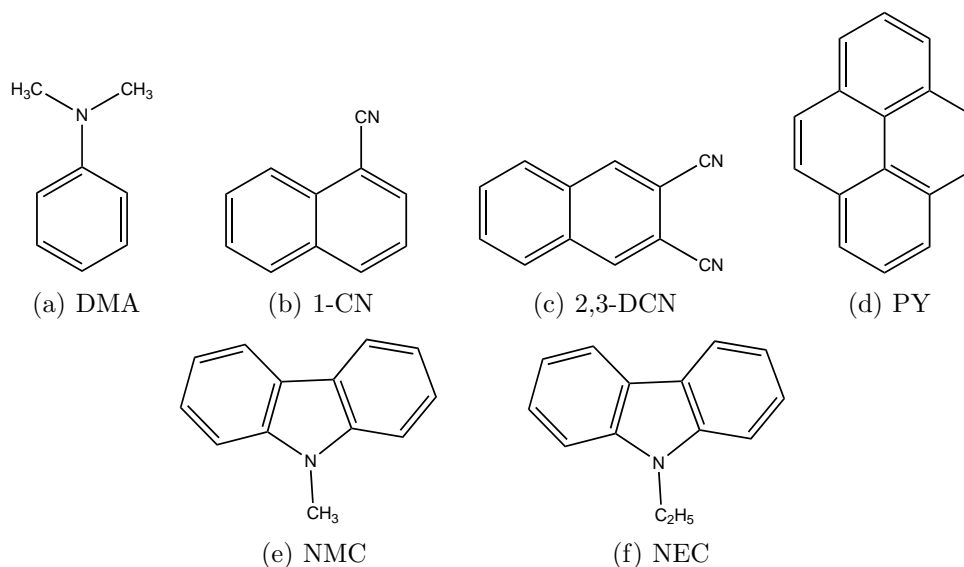


Figure 3.1.: Structures of the Fluorophore Used in the Present Studies.

In table 3.2 the fluorophore with their oxidation and reduction potentials are given. All other properties which are of interest are given in the incoming results.

3.2.2. Quenchers

The structure of quenchers used is given in figure 3.2

The redox potentials and the purification procedure used for them are reported in table 3.3.

Quenchers were selected on the basis of their redox potentials and structures, also they form exciplex with good intensity.

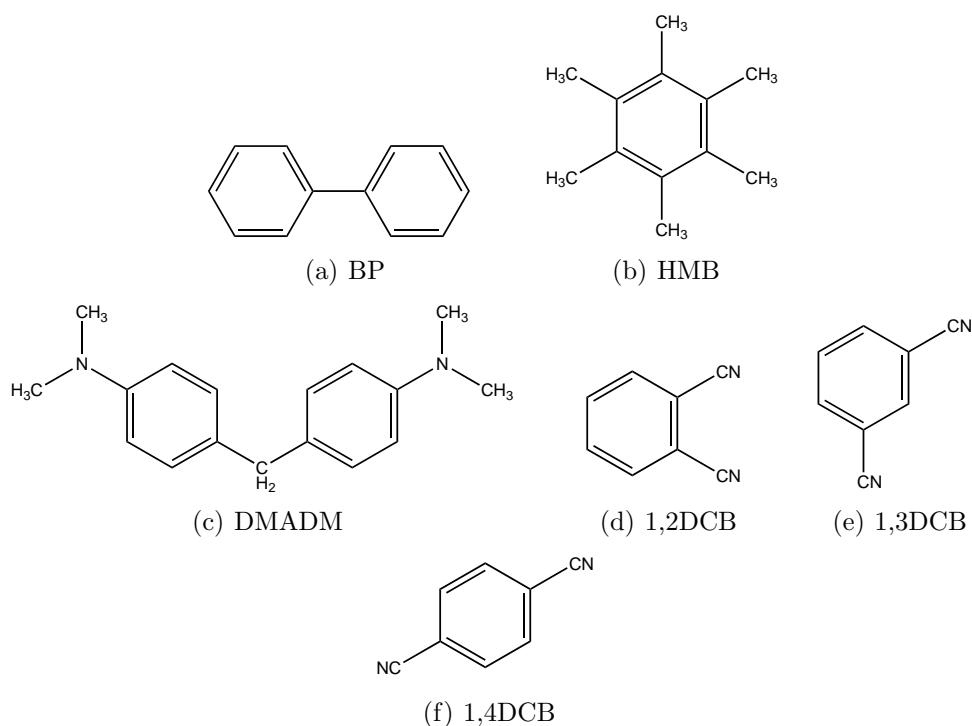
3.3. Absorption Spectroscopy

steady state absorption recording Shimadzu UV-3101PC double beam spectrometer was used.

Table 3.2.: Fluorophores used, their molecular weight, redox potentials, suppliers as well as purification methods.

Fluorophores ^a	Mol.wt <i>g.mol</i> ⁻¹	$E_{1/2}^{red}$ V vs. SCE	$E_{1/2}^{oxd}$ V vs. SCE	Supplier	purification
DMA	121.19	0.81 ⁹⁵	0.76 ⁹⁶	Aldrich (99.5%)	vacuum sublimtion
1-CN	153.18	-2.33 ⁹⁷	2.01 ⁹⁸	Aldrich (98%)	vacuum sublimtion
2,3-DCN	178.19	-1.67 ⁹⁹		Sigma-Aldrich (97%)	recrystallized from acetonitrile
PY	202.25	-2.07 ¹⁰⁰	1.16 ¹⁰⁰	Fluka	sublimated
NMC	181.24	-2.46 ¹⁰¹	1.03 ¹⁰²	Aldrich (99%)	sublimited
sublimited NEC	195.26		1.12 ¹⁰³	Aldrich	sublimated

^a used acronyms: Dimethylaniline (DMA), 1-Cyanonaphthalene (1-CN), 2,3-Dicyanonaphthalene (2,3-DCN), Pyrene (PY), N-methylcarbazole (NMC), N-ethylcarbazole (NEC),

**Figure 3.2.:** Structures of the Quenchers Used in the Present Studies.

3. Experimental

Table 3.3.: Quenchers used, their molecular weight, redox potentials, suppliers as well as purification methods.

Quenchers ^a	Mol.wt <i>g.mol</i> ⁻¹	$E_{1/2}^{red}$ V vs. SCE	$E_{1/2}^{oxd}$ V vs. SCE	Supplier	purification
BP	154.21		1.95 ¹⁰⁴	Fluka (purum)	recrystallized from 70% ethanol
HMB	162.28		1.58 ¹⁰⁵	Alfa Aesar(95%)	recrystallized from 70% ethanol
DMADM	254.38			Alfa aesar	sublimated
1,2DCB	128.13	2.05 ¹⁰⁶	1.45 ¹⁰⁷	Fluka	sublimated
1,3DCB	128.13	2.20 ¹⁰⁶	1.51 ¹⁰⁷	Alfa Aesar	recrystallized from ethanol
1,4DCB	128.13	2.00 ¹⁰⁶	-1.65 ¹⁰⁸	Fluka	recrystallized from toluene

^a used acronyms: Biphenyl (BP), Hexamethylbenzene (HMB), N,N'-bis(dimethylamino)diphenylmethane (DMADM), 1,2-dicyanobenzene (1,2DCB), 1,3-dicyanobenzene (1,3DCB), 1,4-dicyanobenzene (1,4DCB),

3.4. Fluorescence Spectroscopy

For recording steady state fluorescence spectra fluorescence spectrometer was used. As the spectra were recorded over a range of temperature starting from 253.15 K to 338.15 K therefore the sample compartment of fluorimax was connected by means of light guides with the temperature regulating assembly. Figures 3.3 and 3.4 shows the arrangement of temperature regulating assembly attached with the fluorimax.

The various important parts of this whole unit are given as:

3.4.1. Fluoromax:

Jobin Yvon Fluoro-max 2 fluorescence spectrometer was used here.

3.4.2. Thermally Insulated Box With Cuvette Holder:

Figure 3.5 shows the cuvette holder inside the thermally insulated box.

Sample holder was made of Aluminum metal because it is good conductor of heat. The sample cell can be moved in and out of the metallic cube by means of an opening present at the top of cube. For thermal insulation the opening of cube can be closed by means of a screwed cap made of Aluminum metal. On the two adjacent sides of cube are the opening for inlet and outlet of temperature regulating liquid. The liquid flows through the Polyvinyl Chloride pipes in and out of the cube. On the other two adjacent sides are the

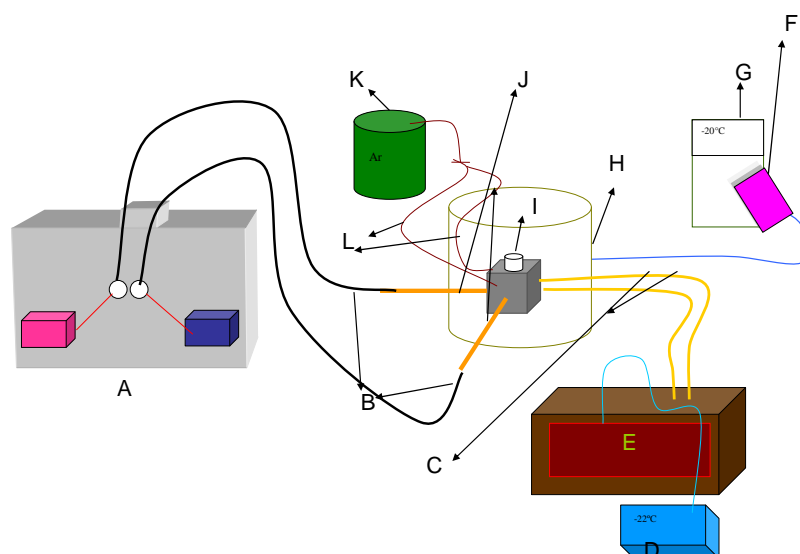


Figure 3.3.: Figure showing the generalized arrangement of temperature regulating assembly attached with fluoromax. In this figure A= fluoromax, B= liquid light guides, C= liquid mixture from the thermostat, D= thermometer, E= thermostat, F= temperature converter, G= Voltmeter, H= plastic box enclosing the cuvette holder, I= cell, J= metallic rods, K= argon cylinder, L= PVC pipes carrying the argon to the cell

Quartz rods very near to the liquid light guides. As the liquid light guides are sensitive to temperature i.e they get frozen at 268.15 K and they are destroyed at 308.15 K. therefore quartz rods are used to transmit light to the light guides because first they temperature resistant ¹and secondly they are transparent to the excitation and emission light. Argon gas was continuously flowing through the very small gap between the light guides and the Quartz rods to prevent the light guides from freezing or getting destroyed due to the low or high temperature. Argon gas was coming from the same cylinder and it was split into two paths. Argon was also flowing in the Polyvinyl Chloride pipes. The light guide used for excitation was with the wave length range of 340 - 800 nm (LUM^TEC liquid light guides) and for the emission was with the wave length range of 270 - 670 nm (LUM^TEC liquid light guides). The remaining space inside the thermally insulated box was filled with glass wool. Glass wool was used because it helps in regulating the temperature. The thermally insulated box was made of Polyvinyl Chloride. As the light guides are very sensitive therefore they were supported with small Aluminum rods out of the box. Further the light guides were clamped with stand for their protection. Openings

¹ Softening point of Quartz is approximately $1200^{\circ}C$ ¹⁰⁹

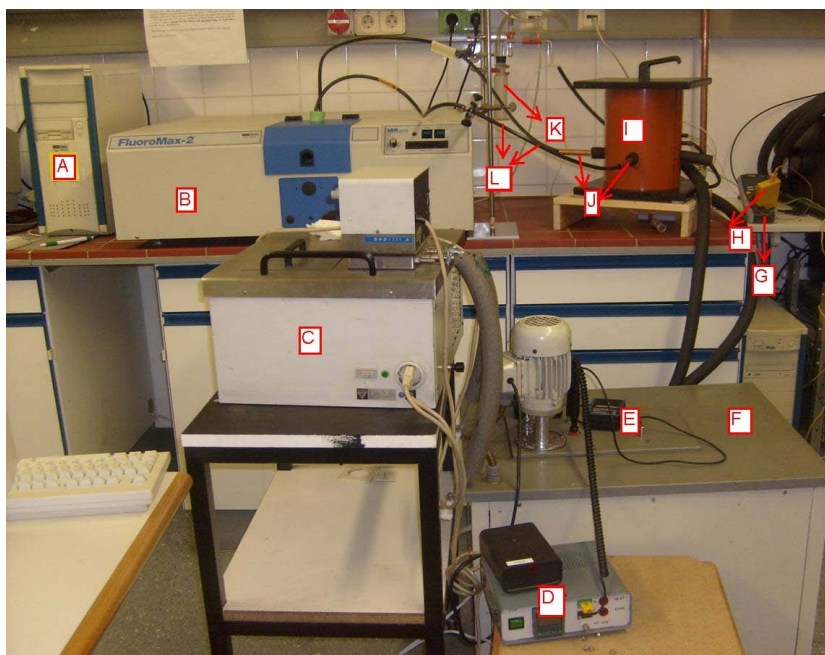


Figure 3.4.: Pictorial representation of temperature assembly attached with the fluoromax spectrometer. In this figure: A= computer connected to the fluoromax, B= Fluoromax, C= thermostat, D= digital thermometer and power supply, E= thermometer showing the temperature of the liquid for heating/cooling, F= bath for cooling the liquid (50% water-glycerol mixture), G= voltmeter, H= temperature converter, I= plastic box enclosure the cuvette holder, J= metallic rods, K= argon gas supply, L= liquid light guides,

of the thermally insulated box for the light guides and the Poly vinyl Chloride pipes were further insulated by the use of insulator sheet. The lid of the thermally insulated box was also made of thermally insulated material.

3.4.3. Temperature Regulating Liquids and Thermometers:

The cooling liquid was 50% mixture of water and glycerol along with ethanol. Ethanol was added because it prevents water and glycerol from freezing at 253.15 K. The liquid used for heating the cell was water. Thermometers were placed at two places. First of all the desired temperature is given to the power supply then the temperature of the bath and the cuvette holder is measured. The temperature of the bath is measured with the help of the thermocouple dipping inside the liquid. where as a voltmeter is attached on one side of the cuvette holder and with the help of temperature converter it shows the temperature of the cell. The difference of temperature between the power supply and the thermostat is 1.5°C and between the thermostat and the cuvette is 0.5°C , so the powers

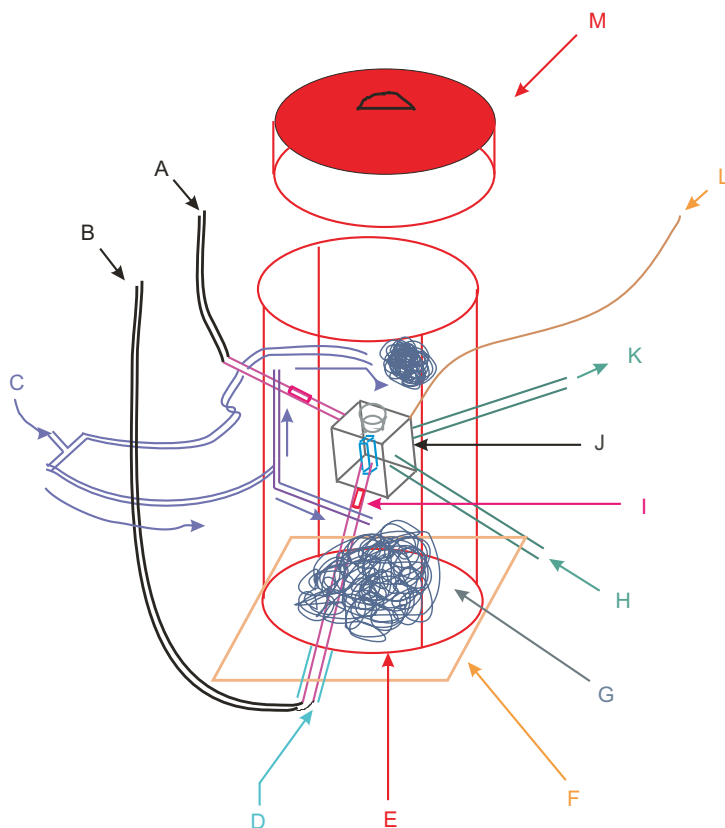


Figure 3.5.: Figure showing the arrangement of thermally insulated box with cuvette holder. In this figure A= emission light guide, B= excitation light guide, C= argon gas flow, D= metallic tubes, E= plastic box, F= wooden box, G= glass wool, H= inlet for cooling/heating liquid mixture, I= quartz rod, J= sample holder (A1), K= outlet for cooling/heating liquid, L= sensor for temperature, M= box cover with insulation.

supply and the cuvette are at the difference of $\pm 2^\circ\text{C}$. The calibration curve was plotted for the temperature regulating assembly and is given in figure 3.6. The fluorescence spectra were recorded from 253 to 340 K.

3.4.4. Light Guide Arrangement Inside the Fluoromax:

Figure 3.7 shows the arrangement of light guides inside the fluoromax for getting the excitation and emission light and spectrometer. Figure 3.8 shows the normal arrangement of the cuvette inside the Fluorimax.

Special holder is made in such a way so that it holds the two light guides just above the reflecting mirrors. The excitation light falls on one of the mirror and then it is reflected to

3. Experimental

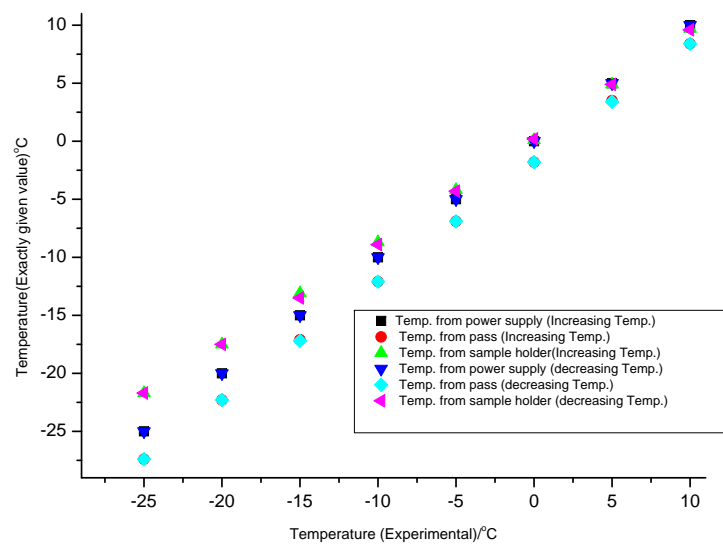


Figure 3.6.: Calibration curve for temperature regulating assembly.

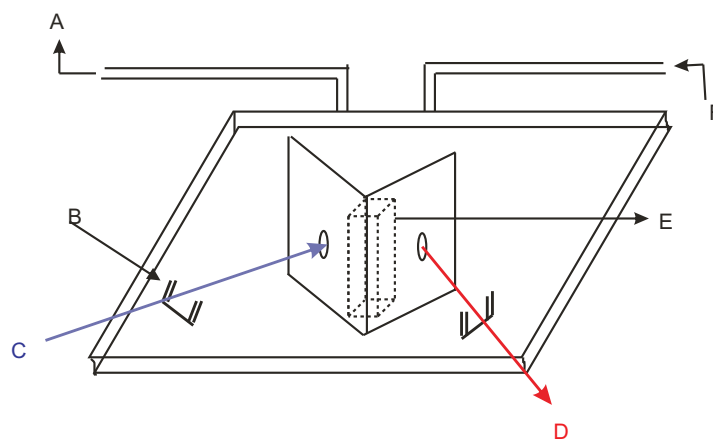


Figure 3.7.: Figure showing the arrangement of normal cuvette holder inside the fluoromax. In this figure A= outlet to water bath, B= filter holder, C= excitation light, D= emitted light, E= cuvette, F= inlet from water bath.

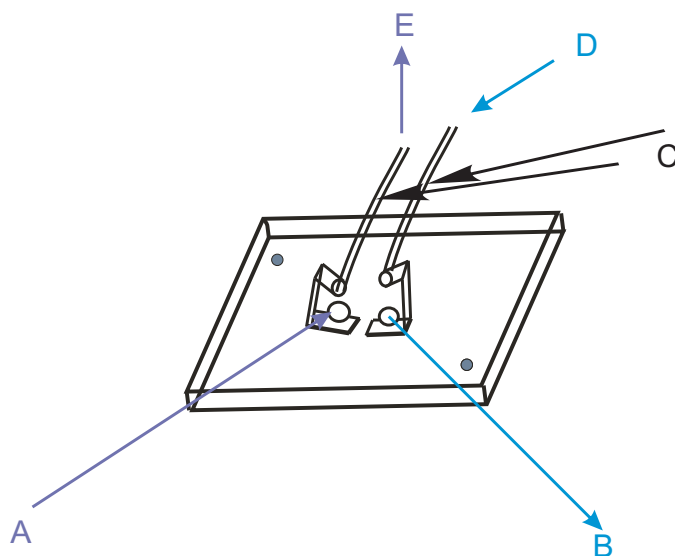


Figure 3.8.: Light guide arrangement inside the fluoromax. In this figure A= excitation light falling on the reflecting mirror and going towards the sample holder, B= emission light falling on the reflecting mirror coming for the sample holder, C= liquid light guides D= emission light coming from the cuvette, E= excitation light going towards the cuvette.

the liquid light guide which takes it to the cuvette placed inside the thermally insulated box where as the emission light coming from the cell via the liquid light guide goes to the detector for detection after reflection from the other reflecting mirror.

3.4.5. Light Lost by Liquid Light Guide

About 19% light is lost by the liquid light guide compared to the normal fluorescent cuvette. This test was performed before the start of experiment and is given in the form of figure 3.9.

3.5. Time Resolved Fluorescence Spectroscopy

Pulse fluorometry and phase-modulation fluorometry are the techniques which are used commonly for the measurement of fluorescence lifetimes. Using the pulse fluorometry the recording is done in the time domain where as the phase-modulation fluorometry is related with the frequency domain. The exciting pulse of light from the lasers or spark sources is focused to the sample and then the time dependence of fluorescence decay is recorded

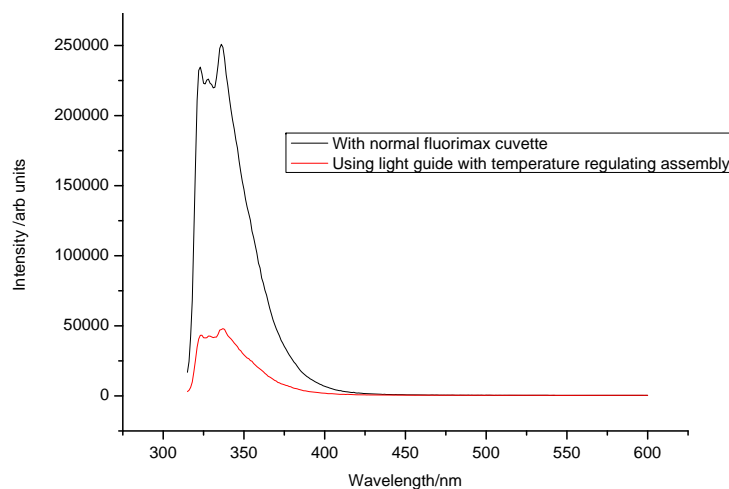


Figure 3.9.: Light lost by liquid light guide shown by fluorescence spectra of 5×10^{-5} M 1-cyanonaphthalene in diethylether

in the case of pulse fluorometry. Time correlated single photon counting (TCSPC), simply known as single photon counting (SPC), is the instrument used for time resolved spectroscopy. Phase-modulation fluorometry uses a modulated excitation source which causes the fluorescence emission waveform to be phase shifted and resultant different amplitudes are obtained with respect to the excitation waveform. Both TCSPC and Phase-modulation fluorometry are used for the measurement of fluorescence life times. The two techniques are discussed separately in upcoming discussion.

3.5.1. Time Correlated Single Photon Counting (TCSPC)

By using this instrumental method fluorescence decay curves are recorded from which the lifetime of excited state of fluorophore is measured.¹¹⁰ At a given time 't' the emission intensity is proportional to the number of fluorophores that are in the excited state at time 't'. Thus to obtain a decay curve, the sample is repeatedly excited by a pulsed light source. On each excitation pulse a single photon is detected at an angle of 90° to the excitation light and its time of interval, relative to the excitation pulse, is measured electronically. Emission intensity determines the probability of detecting a single photon therefore the detected events will be distributed in a manner that correlates with emission intensity along with the time axis. The decay curve defined by the number of detected photons is typically in the range of 10^5 to 10^6 . In order to avoid undistortion in data it is essential that only a single photon is received by the detector per excitation cycle. This condition is achieved by attenuation of the emission beam from the sample which

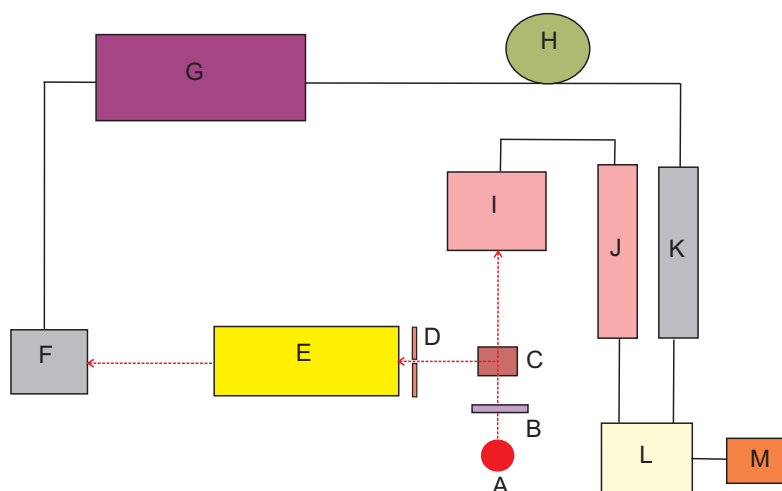


Figure 3.10.: Simplified scheme of a time correlated single photon counting fluorometer. In this figure A = excitation light source, B = filter, C = sample cell, D = slit, E = wavelength discriminator, F = stop PMT, G = amplifier, H = delay line, I = start PMT, J = start CFD, K = stop CFD, L = TAC, M = MCA.

limits the count rate of photons per excitation (stop/start ratio) at value of 0.01 to 0.10¹¹¹

Figure 3.10 shows the principal of operation and simplified scheme of SPC. Start signal is generated by photomultiplier tube (PMT) on the emission of light pulse. The constant function discriminator (CFD) normalize the signal which is then send to the time-to-amplitude converter (TAC). A single emission photon detected by the stop PMT, after being processed by another CFD, provides a ‘stop’ signal to the TAC. It is ensured by the delay cable that the ‘stop’ pulse doesn’t arrive before the ‘start’ pulse at the TAC. A voltage pulse with an amplitude proportional to the elapsed time is send by TAC between the ‘start’ and ‘stop’ signals to the multichannel analyzer (MCA). Detailed discussion related to the instrumental set-up is given in the upcoming discussion.

Important parts of instrument: Different functional subunits of SPC used in the present work can be exchanged easily, such an instrumental design is known as modular design. The equipment is classified into following three groups:

- Excitation light source including power supply and pulser
- Detection system
- Pulse-processing electronic devices

Excitation Light Source Including Power Supply and Pulser A light source having a high

3. Experimental

repetition frequency, short pulse duration, high light intensity, a constant but reproducible pulse shape over long operation times is considered to be an ideal excitation source. Additionally it should cover a wide spectral range from the UV to NIR in order to make it acceptable for a broad variety of fluorescent species. Up till now there is no such light source which is said to be universal and fulfill all the criteria mentioned before. Various systems are available with their own advantages and disadvantages. So according to the requirement of system determined by the quantum yield of the fluorescent system one has to select the excitation source. In present work light emitting diode (LED) was used as excitation light.

●Light Emitting Diode: In present work 387 nm Picoquant LED was used as excitation light source. The fluorescence lifetime of exciplex was measured with this LED. Detection System Start PMT and stop PMT, i.e the combination of excitation and emission wavelength selector, constitute the detection system in the present discussion. Below are listed the topics which will be discussed under this heading

Wavelength selector

Photomultiplier tube

Monochromator

●Wavelength selector: In order to avoid the detection of scattered and strayed light from the excitation source and also in order to make sure that only the photons originating from the fluorescence process are processed, wavelength selectors like optical filters or monochromator are placed in the path of both the excitation and emission light. It is necessary to make the excitation light monochromatic and to remove all other wavelengths before it arrives at the sample to ensure the selective excitation of the fluorophore and also to avoid the scattered light in the emission beam. This task is accomplished by placing a short-or-band pass filter in the excitation path. The observation wavelength, determined by the fluorescence spectrum of the sample, is selected by either a monochromator or a long pass filter placed in the path of emission light.

●Photomultiplier tubes: Two fast responded photomultiplier tubes (PMTs) one as the 'start' channel and the other as the 'stop' channel are required in the classical form of SPC. Purpose of start PMT is the detection of excitation light pulse and then to transfer it to the TAC in the form of an electronic signal. A function generator is used to trigger the pulsing of the excitation light source, at the same time the start signal for the TAC can be generated electronically by the function generator itself. Function of stop PMT is to detect the arrival of fluorescent photons emitted by the sample after excitation. The sensitivity of stop PMT must be very high in order to detect the single photons

also the dark count rate should be as low as possible. By using time discriminator direct processing of the output signal is not possible as it is too small therefore a fast amplifier is required to increase the pulse amplitude. As the light intensity of the excitation pulse is by orders of magnitude larger than that of a single fluorescent photon, neither amplification nor dark count selected PMT is required in the start channel.

The time respond characteristics of the photomultiplier tube determine the time resolution of the detected system as well as the shape of the excitation pulse. Following definitions will be used in upcoming explanation.¹¹² The “rise time” of the PMT is the time for the output pulse to increase from 10 to 90% of the peak pulse height. The “transient” time is the time interval between arrival of a light pulse at the photocathode and appearance of the output pulse. The transient “time” spread of a PMT refers to the fluctuation in the transient time.

●**Monochromator:** Monochromator is used here as detection system. PTI model 101, 250 to 1700 nm monochromator is mounted to an aluminum housing which takes up a Hamamatsu R928P (185 to 900nm) or IP28(185 to 650 nm) side-on PMT with its voltage dividing circuit. A Hewlett Packard HP8447A amplifier (gain +2dB) is applied to amplify the output signal. The monochromator is equipped with both a variable entrance and exist slit in order to adjust the emission light intensity hitting the stop PMT. By using a lens that can be moved perpendicular to the optical axis the incident emission beam from the fluorescent sample is focused laterally. At the entrance of monochromator a sample holder mounted on an optical bench is placed. Also the excitation source at an angle of 90% to monochromator is mounted on an optical bench. The sample holder is designed to take up a standard or an inert gas type fluorescent cuvette (10 X 10 mm or 20 X 10 mm). It includes two lenses to focus the excitation and emission beam.

The start pulse is generated by a start PMT. With the help of a light guide (d = 1 mm) a small portion of the excitation light intensity is fed to a R928 PMT (185 to 900 nm) which provides a start pulse for the TAC. The light guide is introduced into the sample chamber from The face opposite to the excitation light so that it is hit by a portion of the excitation beam that passes through the sample cuvette. This ‘classical’ way of start pulse generation in combination with the free-running Xenon discharge lamp is used in the present work.

Pulse-processing Electronic Devices This portion is subdivided into following parts:

Constant fraction timing discriminator (CFDs)

Time to amplitude converter(TAC)

Multichannel analyser (MCA)

Electronic counter

●Constant fraction timing discriminator (CFDs): Timing discriminator functions to mark the arrival time of the output pulses from the PMTs (or the function generator) with precision and consistency. From the PMT anode the negative analog pulses are fed to the discriminator either directly with the help of start channel or upon amplification using stop channel. At the output of timing discriminator the input pulses that cross a pre-set discriminator threshold are converted to standard logic pulses (NIM signal). In order to discriminate noise the discriminator threshold is set just above the noise level. If a leading-edge discriminator¹ is used then the arrival time of its output pulse will depend on the amplitude of the input pulse. This is known as the “time walk” and is represented in figure 3.11 .

Figure 3.10 shows the principal of operation and simplified scheme of SPT. In this figure two pulses are shown with same shape but with different amplitude. The higher amplitude pulse crosses the discriminator threshold earlier as compared to the smaller pulse. Therefore with a leading-edge discriminator the smaller pulses produce an output from the discriminator later compared to the large pulses. A constant fraction discriminator (CFD) is used to avoid this amplitude dependent time walk. Figure 3.12 represents the formation of constant fraction signal. Figure 3.10 shows the principal of operation and simplified scheme of SPT. This figure shows that the input signal is splitted into two parts. One part is attenuated to a fraction ‘f’ of the original amplitude where as the other part is delayed and inverted. Then these two signals are added subsequently to form a bipolar signal having a zero crossing which corresponds to the original point of fraction ‘f’ on the delayed signal. The CFD delivers zero walk as the time of zero crossing is independent of pulse amplitude. In present work EG&G ORTEC 584 CFD is used in each start and stop channel. They generate 5 ns negative output pulses which are then fed to the TAC.

●Time to amplitude converter (TAC): It is a principal device used in the time correlation processes. It measures the time difference between the CFD output pulses in the start and stop channel. In figure 3.13 it is shown that when the start pulse arrives the TAC triggers the voltage ramp and when a stop pulse arrives the voltage ramp is heated and an output pulse is generated. The voltage level of this generated pulse is directly proportional to the elapsed time between the trigger pulses. Figure 3.10 shows the principal of operation and simplified scheme of SPT.

EG&G ORTEC 566 model TAC is used here. The amplitude of 2 μ s rectangular out-

¹ i.e a simple voltage comparator that generates a logic pulse when the leading edge of the input pulse crosses the threshold voltage

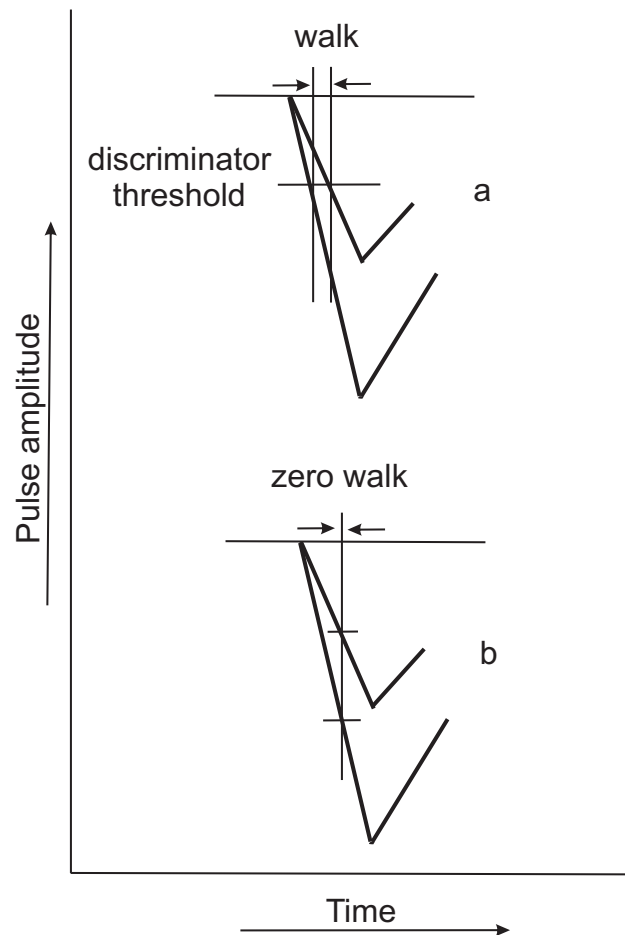


Figure 3.11.: Leading-edge timing versus constant-fraction timing.

put pulses varies from 0 to 10 V. The time range for TAC can be set from 50 ns to 2 ms in 15 subdivisions. Delay cables placed before the CFDs in both stop and start channel controls the position of excitation pulse on the TAC time axis. 1 m of additional BNC cable shifts signal by 5 ns to later times when applied in the stop channel, to earlier times when applied in the start channel.

- **Multichannel analyzer (MCA):** MCA sorts the output pulses produced by the TAC according to the amplitude and the stores them as counts in memory. The channels of the MCA correspond to increment of time because the amplitude of the TAC output pulses is directly proportional to the elapsed time. The number of counts in the memory channel is directly proportional to the fluorescence intensity. In the present work, a 4096 channel

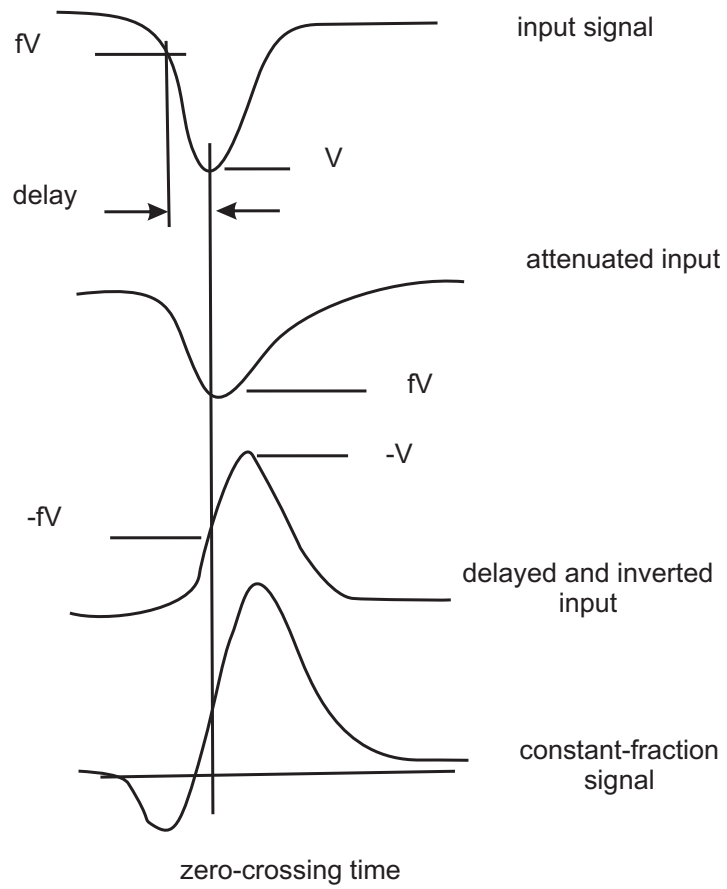


Figure 3.12.: Formation of constant-fraction signal.

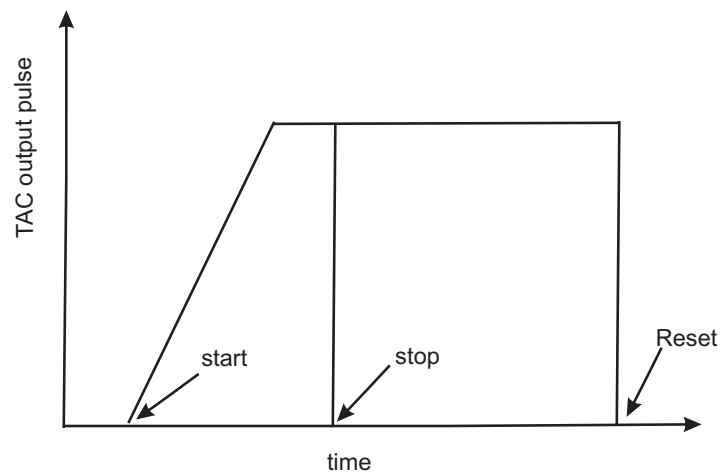


Figure 3.13.: Voltage ramp generated by time-to-amplitude converter.

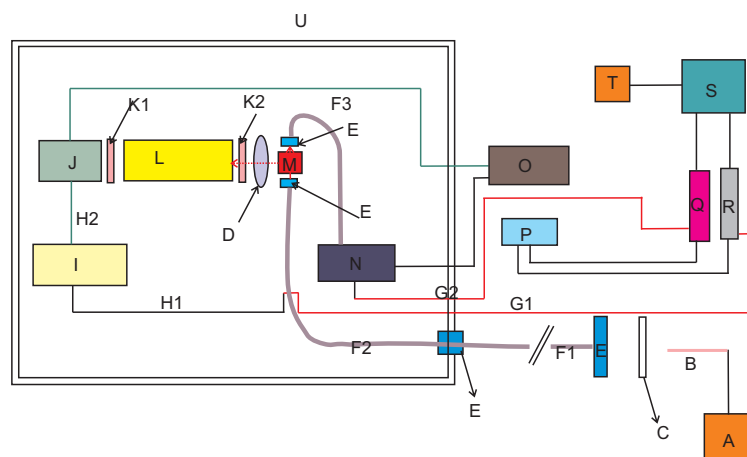


Figure 3.14.: Configuration of SPT instrument with LED and pulser as excitation source. In this figure A= Pulser, B= LED, C= excitation filter, D = lens, E= adapters, F1, F2 = light guides (1500 × 5 mm), F3 = light guide (700 × 1 mm), G1= BNC cable (5m, stop delay line), G2 = BNC cable (1m, start delay line), H1 = BNC cable (1m), H2 = BNC cable (150 mm), I= HP 8447A, J= R928P(stop), K1, K2 = slits, L= monochromator, M= sample, N=R928(start), O= HV generator (0 to 1000V), P= Counter HP 5328 B, Q= CFD 584 (start), R= CFD 584 (stop), S= TAC 566, T= MCA, U= box

MCA (EG&G ORTEC model ACE-4k) with maximum number of $(2^{24} - 1)$ counts is used. It is mounted in a personal computer. Depending on the TAC range, the timing increments per channel reach from 12 ps (50 ns time range) to 488 ns (2 ms time range).

- Electronic counter: The repetition rate of the excitation source and ratio between stop and start counts (S/S ratio) are monitored by a Hewlett-Packard 5328B two-channel counter which receives a timing output signal from each of the CFDs.

Apparatus Parameters and Instrumental Setup Figure 3.14 represents the schematic drawing of the instrument configuration with the LED and pulser as excitation source and monochromator R928P PMT as detection unit. The optimized instrumental parameters are given in table 3.4 The instrumental parameters listed in table 3.4 are discussed as following:

- CFD levels: As reported by C.Lewis, W.R.Ware et al¹¹¹ reference, the stop discriminator level should be set slightly above the threshold value. Higher levels increase the multiple to single photon detection ratio since the multiple photon events have a higher voltage distribution than the single photon pulses. Resultantly the narrowing of instru-

3. Experimental

Table 3.4.: Instrumental configuration and parameters of the SPT equipment.

Excitation source	LED
Detection system	R928P, monochromator
Stop PMT and amplifier	R928P, HP8447A
Start pulse generator	R928
S/S ratio	0.10
Start CFD ratio (mV)	50
Stop CFD level (mV)	10 - 12
Start PMT voltage (V)	900
Stop PMT voltage (V)	950
FWHM of the instrumental response (ns)	5.0
Repetition frequency (kHz)	5 (at 15 kHz)
Excitation Wavelength (nm)	250 - 750

mental response and the decay of measured curves occur. Also it leads to the shortening of the measured lifetimes. For the start CFD, the setting of the discriminator level is less critical since the pulses from the start PMT or from the function generator are much more intense than the stop pulses. In this work, the start CFD levels were set at voltage that correspond to about the half height of the discriminator input pulses.

●Stop/start ratio and number of counts collected: Accurate time correlated single photon data is obtained if no more than one emission photon is detected per excitation cycle. If multiple photon events do occur, the counts in the multichannel analyzer accumulate disproportionately faster in the early portion of the decay curve resulting in too short lifetimes. This phenomenon is known as pulse pileup and it occurs because of the inherent operating characteristics of the TAC. Start signal initiates the TAC voltage lamp and it is heated when the stop signal is received. After a preset time the TAC is recycled and is cleared before the next excitation cycle. If a second emission photon is detected later in time and before the next excitation cycle, it will be observed by the stop PMT but will not be counted because the TAC is disabled. Consequently, the decay curve is biased toward early arriving photons. In order to avoid the pulse pileup, the emission beam of photons from the sample must be attenuated so that the probability of detecting more than one photon per excitation pulse is small. Thus, the detection of a photon is a rare event, and probability P_n of detecting n photons per excitation pulse is calculated from

the Poisson's equation

$$P_n = \frac{m^n}{e^m n!} \quad (3.2)$$

In above equation m is the average number of detected photons per excitation pulse, i.e the stop/start ratio (S/S ratio). The poisson probability polygons are shown in figure They may be used to predict the frequency of occurrence of multiple photon events and appropriate S/S ratio for minimum pileup error. Usually, an S/S ratio of 0.01 to 0.10 is used, so that the probability of multiple photon events is very small. On the other hand, as too long recording times for fluorescence decay curves are undesirable, low repetition frequencies of the excitation source will set a lower limit to the S/S ratio. For the flash lamp which has the lowest frequency of all the excitation sources used in this work, an S/S ratio of 0.10 turned out to be sufficiently low. This was determined by a comparison of the decay curves recorded at S/S ratio of 0.10 and 0.05, respectively. Both the decay curves lead to the same lifetime within experimental error. When the fluorescence decay measurements are stopped after collecting different numbers of counts, The lifetime increases with increasing counts until a plateau is reached. After this limit the lifetimes are not changed significantly with the further increase of counts. This limit was found to be 400 000 counts for the flash lamp. Generally 1000 counts are collected in the peak channel for the instrumental profile. With flash lamp it takes 12 to 16 minutes to collect 400 000 counts at an S/S ration of 0.10. Taking into account eventual fluctuations in the lamp profile being more important for longer recording times, extending the number of counts collected seems to be rather disadvantageous.

- Repetition frequencies: The repetition frequency is directly proportional to the the supply voltage for the flash lamp. If the repetition frequency is high then shorter is the time to record the decay curve and the lower is the S/S ratio. In order to avoid the corrosion of the electrodes, the discharge lamp is operated continuously below the absolute maximum supply voltage of 20 kV.

- PMT voltage supply: A high voltage improves the time response and sensitivity, and contrarily it increase the dark count rate. So it should be decided that which aspect is more important for the particular measurement. The R928P is operated at voltage lower than 1000 V to decrease the dark count rate. The obtained lifetimes are generally not affected by moderately changing the PMT voltage supply.¹¹³

- Pulse energies: An important characteristic of excitation source is the energy content

3. Experimental

of the emitted pulses, expressed as energy per pulse, photons per pulse or peak power at the pulse maximum. If the investigated fluorophore has a low fluorescence quantum yield or if a photochemical reaction takes place then the information about the energy characteristic is of particular interest. Using the Newport Power /Energy meter (model 1825-C with a 818-UV detector), the mean power P_{mean} at given sets of instrumental parameters is measured for each of excitation light sources used. The flash lamp was investigated both at its emission peak wavelength with and without filter as well as in combination with an excitation filter at a wavelength usually selected for excitation. The energy per pulse E_{pulse} is calculated using the following formula by using the P_{mean} .

$$E_{pulse} = \frac{P_{mean}}{f} \quad (3.3)$$

The maximum peak power at pulse maximum is P_{max} is approximated by considering a rectangular shape.

$$P_{max} = \frac{E_{pulse}}{FWHM} \quad (3.4)$$

The number of photons per pulse n_{pulse} are calculate by using the following expression:

$$n_{pulse} = \frac{E_{pulse}}{h\nu} \quad (3.5)$$

In above equation h is the planks constant and ν is the frequency of light at which the power is measured. ν is calculated by using the following equation:

$$\nu = \frac{c}{\lambda} \quad (3.6)$$

Where c is the speed of light. The measured and calculated values along with the respective instrumental conditions are given in table 3.5

3.5.2. Phase-Modulation Fluorometry

Basic Principal: The nanosecond lifetime of fluorescent specie is measured by using the modulated light source and then by the measurement of phase of the emitted fluorescence light. Sample is excited by a sinusoidal wave and the emission which is modulated with smae frequency as the excitation is observed. As a result of delay between the excitation and the emission, the emission is delayed relative to the modulated excitation (fig.3.15).

Table 3.5.: Pulse energies characteristic of flash lamp. f represents the repetition frequency, λ means the wavelength at which the power is measured, P_{mean} is the mean power measured, E_{pulse} is the energy per pulse, P_{max} is the peak power, and n_{pulse} is the number of photons emitted per pulse

Filter	f kHz	FWHM/ ns	λ / nm	P_{mean} / μs	E_{pulse} nJ	P_{max} / W
$-^a$	4.35	6.5^b	470	26	6.0	0.92
UG1 ^c	4.35	4.6^d	360	3.6	0.83	0.18

^a $n_{pulse} = 1.4 \times 10^{10}$

^b Value obtained with monochromator-R928 PMT detection system

^c $n_{pulse} = 1.5 \times 10^9$

^d Value obtained with the filters-R5600U-01 detection system

Comparison is made between the degree of modulation and the the phase shift (Φ) of emitted light with respect to the excitation light waveform. with the increase of modulation frequency the phase shift increases from $0^\circ - 90^\circ$. Demodulation of the time by a factor m results from the finite time response of of the sample, which is decreased from 1.0 to 0.0 with the increase of modulation frequency.

The lifetime for a fluorofore (τ) which decays mono exponentially can be evaluated from the phase shift (τ_p) and the demodulation (τ_m). Mathematically it is represented as:

$$\tau_p = \frac{\tan\Phi}{\omega} \approx \frac{\Phi}{\omega} (\Phi < 0.2) \quad (3.7)$$

$$\tau_m = \frac{1}{\omega} \left(\frac{1}{m^2} - 1 \right)^{\frac{1}{2}} \quad (3.8)$$

In above equation $\tan\Phi$ is the measured phase shift, m is the measured modulation, ω is the angular frequency of light modulation $= 2\pi f$, f is the modulation frequency. For the mono exponential decay the fluorescence lifetime $\tau = \tau_p = \tau_m$. The accuracy in this case is higher than that of TCSPC. However for the multi exponential decay, the data evaluation is very complex and less accurate compared to the TCSPC. From the fittings of following equations the lifetimes τ_p and τ_m are obtained.¹¹⁴

$$\tau_p = \frac{\sum_i \left(\frac{a_i \tau_i^2}{1 + \omega^2 \tau_i^2} \right)}{\sum_i \left(\frac{a_i \tau_i}{1 + \omega^2 \tau_i^2} \right)} \quad (3.9)$$

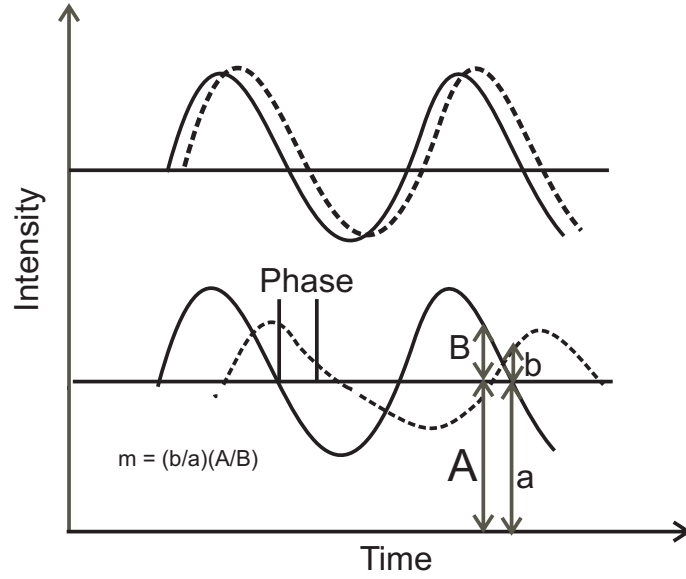


Figure 3.15.: Phase and modulation of fluorescence in response to intensity-modulated excitation using single frequency. There is delay of time (Δt) between excitation and emission signal which relates to the phase shift (Φ). In addition, the amplitude signal is decreased ($b \neq B$) which is called demodulation.⁸¹

$$\tau_m = \frac{1}{\omega} \left[\frac{\sum_i \left(\frac{a_i \tau_i}{1 + \omega^2 \tau_i^2} \right) + \sum_i \left(\frac{a_i \tau_i^2 \omega}{1 + \omega^2 \tau_i^2} \right)}{\sum_i a_i \tau_i} \right]^{-1} \times \left[1 - \frac{\sum_i \left(\frac{a_i \tau_i}{1 + \omega^2 \tau_i^2} \right) + \sum_i \left(\frac{a_i \tau_i^2 \omega}{1 + \omega^2 \tau_i^2} \right)}{\sum_i a_i \tau_i} \right]^{\frac{1}{2}} \quad (3.10)$$

a_i and τ_i are exponential functions and are represented in equation 3.11

$$I(t) = \sum_{i=1}^n a_i \exp - \left(\frac{1}{\tau} \right) t \quad (3.11)$$

With the increase of modulation frequency the phase angle of emission increases and the modulation decreases. This relationship is shown in.¹¹⁵

Digital Oscilloscope attached with modulation technique: In 1995 this technique

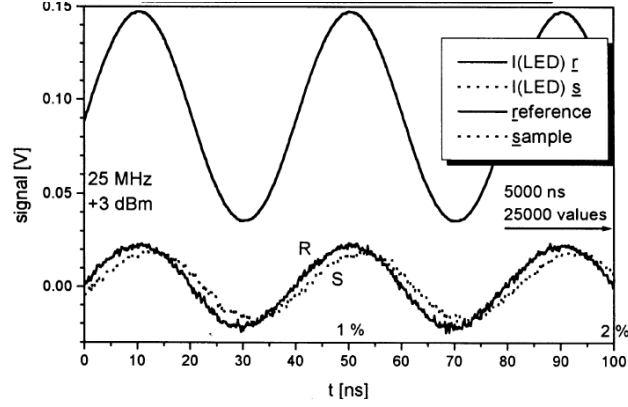


Figure 3.17.: Example of original data recorded on DSO. Curve R and S refer to the reference signal and sample signal, respectively which are different in phase and modulation amplitude. $I(\text{LED})_r$ and $I(\text{LED})_s$ are the recorded data from the measurements through the LED during the measurement of reference and sample, respectively. They both are identical and are used for triggering the oscilloscope ¹¹⁴.

Data analysis of modulated technique with the help of digital storage oscilloscope:

The excitation light source, reference and fluorescence signals are recorded on the DSO and the data files comprises of following four sinusoidal waves:

- Curve 1: electronic signals of light source for exciting the reference.
- Curve 2: amplified signal from the reference
- Curve 3: electronic signal from the reference
- Curve 4: amplified fluorescent signal from the sample

An example of original data is given in figure3.17. Sample analysis is accomplished by finding the zero point crossing in all the four curves. the time value $t_1 - t_4$ are optimized by a linear regression of the data point within a phase angle $\Phi = \pm 0.1$, where the approximation $\sin\Phi \approx \Phi$ is valid. This procedure is used to calculate the values with a resolution better than one from the oscilloscope but even in frequency scans of 10 different modulation frequencies results are rather poor. In order to solve this problem a new method has been developed. In this method a mathematical fit using a simple logarithm optimizes the following function to a complete data set including all experimental values.

$$E_{1-4}(t) = A_{1-4}\sin(t2\pi f + \Delta t_{1-4}) \quad (3.12)$$

Curves $E_{1-4}(t)$ in figure3.17 are the experimental curves. The A_{1-4} are the amplitude factors and f is the modulation frequency which is optimized for only curve 1 and 3. Δt_{1-4} is the delay time. In order to obtain the solution of equation 3.7 and 3.8 Φ and m

must be known. The phase shift can be calculated from the equation:

$$\Phi = (\Delta t_3 - \Delta t_1 + (\delta t_4 - \Delta t_2))2\pi f \quad (3.13)$$

where

$$m = \left(\frac{A_3}{A_1}\right) \left(\frac{A_4}{A_2}\right) \quad (3.14)$$

In majority of experiments $\Delta t_3 - \Delta t_1 \approx 0$ and $\frac{\Delta A_3}{\Delta A_1} \approx 1$. In order to get information that whether the decay is mono exponential or not and also to get value of fluorescence lifetime it is necessary to measure at different modulation frequencies. The measured lifetimes are expected to be independent of varied frequencies. In order to calculate the fluorescence lifetime from the frequency response it is necessary to consider the phase angle. The most precise results are between $10^\circ - 40^\circ$. If it is less than 10° then errors might occur from the limited number of points on the DSO and if it is above 40° then the signal is decreasing significantly by demodulation.

3.6. Sample Preparation

For measurement of absorption and emission spectra quartz cell was used. All solutions were out gassed by bubbling Argon gas through the solution. As many solvents used were volatile therefore the Argon gas was first saturated with the solvent. As pyrene is very sensitive to air ¹ therefore special quartz cell, whose walls were molded rather than jointed, was used.

¹ Pyrene is quenched very easily by oxygen present in air

4. Results and Discussion

One must not attempt to justify them, but rather to sense their nature simply and clearly.

(Albert Einstein)

Interactions between the electron donor and acceptor in ground state results in the formation of charge transfer (CT) complex which is characterized by the appearance of a new absorption band at lower energies. Where as an exciplex is formed as a result of bimolecular interactions between an excited fluorophore (acting as electron acceptor (A)) and a ground state quencher acting as electron donor (D) and vice versa.¹ An exciplex is a two component system in which both the components (donor and acceptor) share charge and electronic distribution.

Previously the classical mechanism of electron transfer, based on the model proposed by Marcus^{3,4} was used to describe the electron transfer from the donor to excited acceptor after preliminary reorganization of reactants and media. This electron jump provides degenerate electronic terms for reactants and products along with subsequent relaxation of product and media. Later it was concluded⁵ that electron transfer between donor and excited acceptor involves transient formation of exciplex and a gradual concerted shift of electron density from electron donor to acceptor and changes in the nuclear coordinates of the reactant and media, rather than a diabatic jump. Thus the formation of exciplex occurs with the change in the electronic structure of excited fluorophore and quencher, at the same time changes in medium reorganization also occur.⁸

On photo excitation all the fluorophores show intense emission and upon addition of respective quenchers into solution a broad structure less emission band appears. This band is the exciplex. Absorption properties and chemical reactivity may also be used for the assignment of exciplexes. Emission from exciplex is preceded by vertical Franck-Condon allowed transitions from a minimum on an excited-state surface to a low lying repulsive ground state surface. Emission from exciplex may not be observed if there is a significant nuclear change during the transition to the low-lying ground state surfaces. Such a non emitting exciplex has properties similar to contact ion pair. The exciplex formation is

represented by the kinetic schemes 2.5 and 2.6 which are discussed already. The exciplex formed can decay either radiatively and non radiatively. Fluorescence spectra were measured between 253 and 340K.

The exciplex systems of 1-cyanonaphthalene with hexamethylbenzene (1-CN/HMB), 2,3-dicyanonaphthalene with hexamethylbenzene (2,3-DCN/HMB), biphenyl with N,N-dimethylaniline (BP/DMA), pyrene with 4,4'-bis(dimethylamino)diphenylmethane (PY/DMADM), N-methylcarbazole with 1,2-dicyanobenzene (NMC/1,2-DCB), N-methylcarbazole with 1,3-dicyanobenzene (NMC/1,3-DCB), N-methylcarbazole with 1,4-dicyanobenzene (NMC/1,4-DCB), and N-ethylcarbazole with 1,2-dicyanobenzene (NEC/1,2-DCB) are discussed as a function of solvent polarity and temperature. The factors effecting the exciplex formation and decay are discussed in upcoming sections.

4.1. Spectral Shifts

Present section describes the exciplex formation and the exciplex emission spectral shift with respect to fluorophore for all the exciplex systems. This shift value is the difference of the average frequencies of fluorophore and exciplex. Its mathematical representation is given already in equation number 2.91.

4.1.1. 1-Cyanonaphthalene/Hexamethylbenzene Exciplex System(1-CN/HMB)

5.5×10^{-5} M solution of 1-CN was photo excited at 305nm and then on the addition of HMB intensity of 1-CN decreases and a broad structureless band representing the exciplex appears at the bathochromic side. Figure 4.1 represents the fluorescence of 1-CN, decrease in its intensity due to quenching with HMB and the isolated emission spectra of the exciplex. The fluorescence spectra of 1-CN/HMB in all solvents used are given in A.1.1.

No change in the excitation wavelength was observed in this system with the change of solvent polarity. The exciplexes formed in all the solvents are strongly emissive thus representing the large electronic coupling and therefore they are contact radical ion pairs (CRIPs). These exciplexes are dipolar in nature because they all are red shifted.

Direct relation between $h\Delta\nu$ and function of solvent polarity $f(\epsilon)$ was observed for 1-CN/HMB exciplexes in solvents of all polarity (table: 4.1). Where $f(\epsilon)$ is the Debye-Lorentz function. Similar relations are reported by Kuzmin et al for many systems.⁶⁹ The positive slope of graph between $h\Delta\nu$ and ϵ indicates that they have highly polar charge

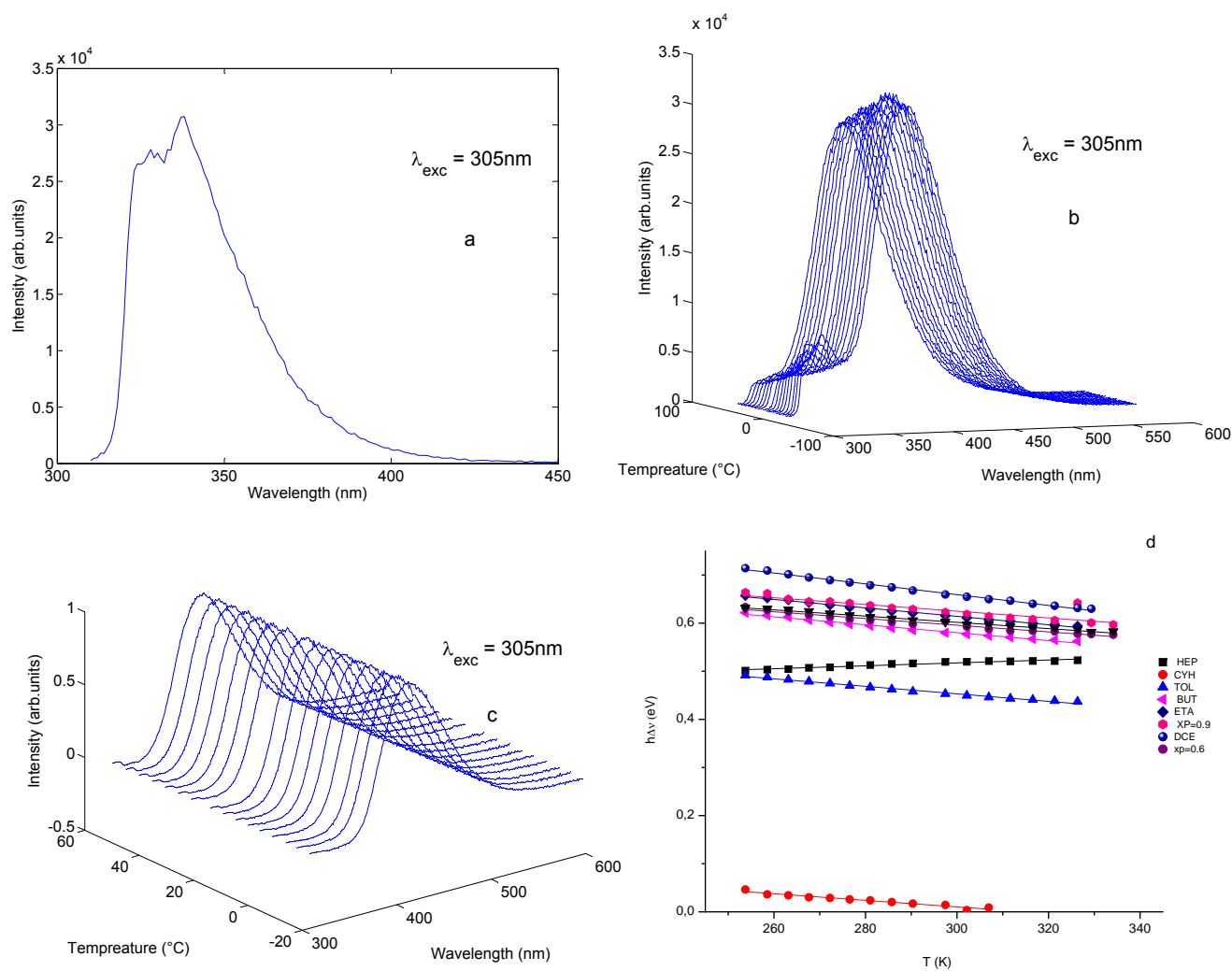


Figure 4.1.: Fig a: fluorescence spectra of 5×10^{-5} M 1-CN in butylacetate, fig b: quenching of 1-CN with HMB at various temperatures in butylacetate, fig c: isolated emission spectra of 1-CN/HMB in butylacetate at various temperatures and fig d: spectral shift vs. temperature for the same exciplex system in solvents of different polarity.

Table 4.1.: Table representing exciplex emission spectral shift with respect to fluorophore ($h\Delta\nu(\text{eV})$) for exciplex ^a in solvents^b of different polarity at 297K. The solvents are arranged in the order of increasing solvent polarity from top of list to bottom.

Solvent	1-CN/HMB	2,3-DCN/HMB	DMA/ BP	PY/DMADM
HEP	0.01	0.53	0.43	0.88
CYH	0.52	-	0.42	0.79
TOL	0.45	0.54	0.52	0.64
DEE	0.59	0.57	0.59	0.63
BUT	0.58	0.69	0.60	0.64
PRA	0.59	0.78	0.65	0.63
ETA	0.62	0.80	0.70	0.64
THF	0.59	0.78	0.72	0.74
$x_P=0.9$	0.62	0.70	0.70	0.48
$x_P=0.8$	0.63	0.70	0.72	0.35
DCE	0.66	0.75	0.61	-
$x_P=0.7$	0.60	0.66	0.74	0.32
$x_P=0.6$	0.62	0.74	0.85	0.30
$x_P=0.5$	0.60	0.73	0.75	0.21
$x_P=0.4$	0.65	0.70	0.79	0.15
$x_P=0.3$	0.59	0.68	0.79	-

^a Used acronyms: 1-Cyanonaphthalene (1-CN), Hexamethylbenzene (HMB), 2,3-Dicyanonaphthalene (2,3-DCN), Biphenyl (BP), Dimethylaniline (DMA), Pyrene (PY), N,N'-bis(dimethylamino)diphenylmethane (DMADM)

^b Used acronyms: heptane (HEP), cyclohexane (CYH), toluene (TOL), diethylether (DEE), butyronitrile (BUT), propylacetate (PRA), ethylacetate (ETA), tetrahydrofuran (THF), propylacetate mole fraction in propylacetate/butyronitrile mixture (x_P), dichloroethane (DCE)

transfer emission. Inverse relationship was observed between $h\Delta\nu$ and temperature for 1-CN/HMB in all solvents (figure 4.1). Change in shift values on changing the solvent polarity and temperature is observed because the exciplexes are considered as a resonance hybrid of the charge transfer (CT) configuration (A^-D^+) mixed with the locally excited (LE) configuration (AD^*) and its wave function is already described in 2.4.3. Variation in the temperature and solvent polarity may change the geometrical structure of exciplex resultantly the electronic delocalization interactions are changed between A and D. Thus the change in the extent of charge transfer is observed by changing these parameters. Dependence of solvent polarity and temperature on $h\Delta\nu$ is also reflected by the equation 2.105. The H_{12} appearing in this equation is the matrix element of the electronic coupling of the LE and CT states. With the increase of temperature there should be a decrease in the value of H_{12} because of decrease of radiative process and increase in non-radiative decay,¹²⁰ and thus a corresponding decrease in the value of

$h\Delta\nu$ is observed. U_s is the energy of the polarization of the solvation shell and it depends upon the extent of charge transfer (z) in exciplex and dielectric constant of solvent. Also U_s is related to the energy associated with the high frequency component of dielectric constant which is approximated by the square of the refractive index. There is decrease in the refractive index with increase of temperature and therefore the value of U_s also decreases. So resultantly an inverse relation is observed between $h\Delta\nu$ and temperature, therefore with the decrease of temperature the exciplex is destabilized. With the increase of solvent polarity the exciplex is red shifted i.e it is destabilized due to the dissociation of exciplex into radical ion pairs and result is observation of direct relationship between $h\Delta\nu$ and $f(\epsilon)$.¹²¹

4.1.2. 2,3-Dicyanonaphthalene/Hexamethylbenzene Exciplex System(2,3-DCN/HMB)

Intense fluorescence peak was observed for 5×10^{-5} M 2,3-DCN after photo excitation at 300 nm. Later on the addition of 0.08 M HMB in the same solution results in the decrease in intensity of 2,3-DCN due to the formation of 2,3-DCN/HMB exciplex (figure:4.2). Remaining emission spectra of 2,3-DCN with HMB are given in A.1.2.

The excitation wavelength was found to be independent of the solvent polarity as there was no change in the excitation wavelength with the change of solvents. Like 1-CN/HMB exciplex here also direct relation was observed between $h\Delta\nu$ and function of solvent polarity $f(\epsilon)$ (table 4.1) and the reason is also the same as mentioned before i.e the exciplex becomes destable due to the increase of solvent polarity. The positive slope between $h\Delta\nu$ and ϵ indicates highly polar charge transfer emission

Inverse relation is observed between $h\Delta\nu$ and temperature for solvents in polarity range $\epsilon = 1.91$ to 4.91 and then with the increase of solvent polarity ($\epsilon = 6$ to 17.22) direct relation is observed (figure 4.3).

Two factors named solvent's orientation and distortion polarizations are responsible for thermochromic shifts. Direct relation between $h\Delta\nu$ and temperature is observed when distortion polarization dominates as observed in solvents with dipole moments ranging from 6 to 17.2. For these systems the exciplex is destabilized with the increase of temperature. Inverse relation is observed when the solvent's orientation dominates and here the exciplex is destabilized with decreasing temperature.

4.1.3. N,N-dimethylaniline and biphenyl System (DMA/BP)

Intense fluorescence peaks were observed for 1.1×10^{-4} M DMA between 305 to 324 nm in various solvents. On the addition of 0.05 M BP decrease in intensity of fluorophore is

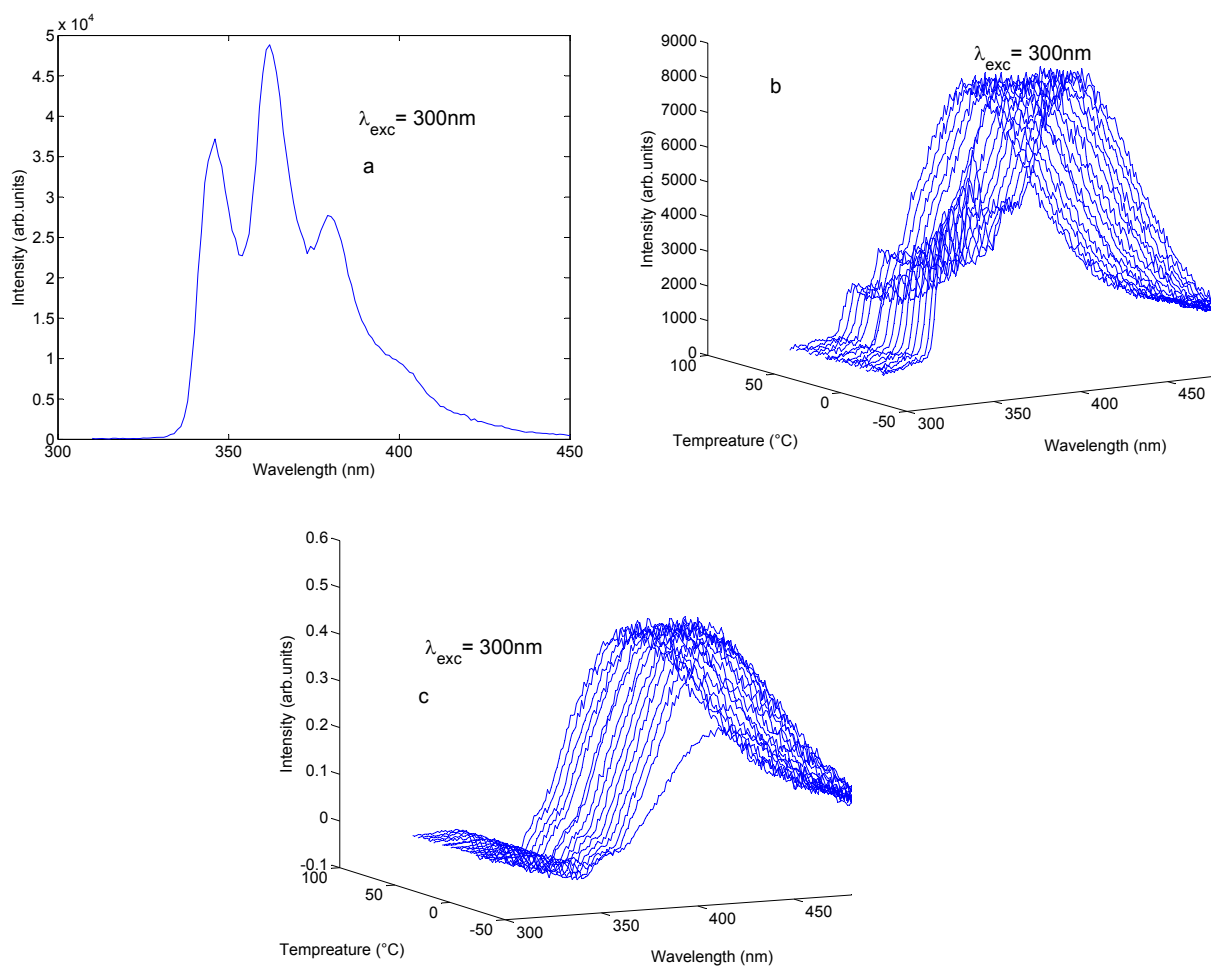


Figure 4.2.: Fig a: fluorescence spectra of 5×10^{-5} M 2,3-DCN in toluene, fig b: quenching of 2,3-DCN with HMB at various temperatures in toluene and fig c: isolated emission spectra of 2,3-DCN/HMB in n-butyl acetate at various temperatures.

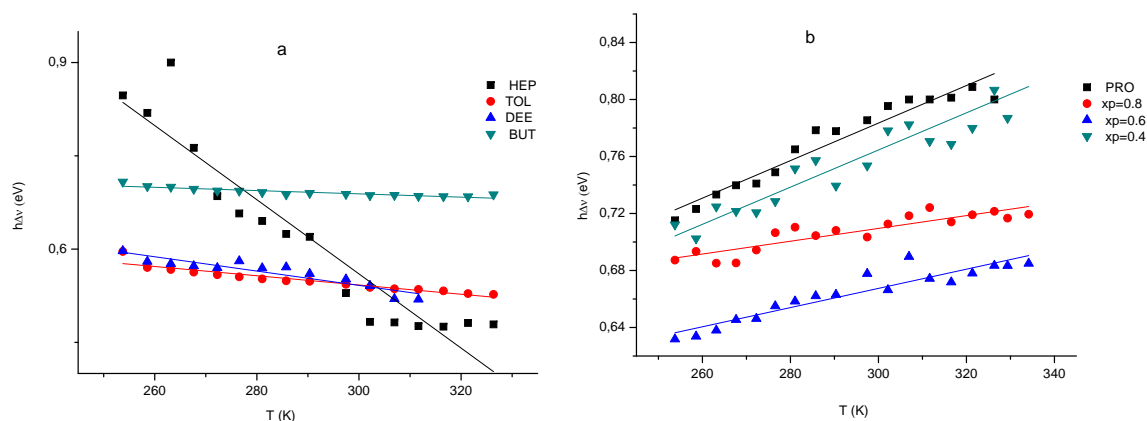


Figure 4.3.: Spectral shift for 2,3-DCN/HMB exciplexes in fig a: solvents with $\epsilon = 1.91 - 4.91$, fig b: in solvents from $\epsilon = 6 - 17.2$.

observed due to the formation of exciplex. The exciplex formed is red shifted i.e towards the bathochromic side and thus all the exciplexes are dipolar. The fluorophore fluorescence spectra, quenching of fluorophore with HMB and the isolated emission spectra are given in figure 4.4. For all other solvents the emission spectra of DMA with BP are given in A.1.3.

A decrease in the fluorophore excitation wavelength was observed with increasing the solvent polarity from 1.91 to 4.18 and then with the further increase in solvent polarity from 4.91 to 19.09 there is an increase in the excitation wavelength. Here again the increase in $h\Delta\nu$ results due to the increase in the function of solvent polarity and the reason is the exciplex destabilization due to the change in the geometrical structure with changing the solvent polarity (table : 4.1). Similarly the exciplex becomes destabilized with the decrease of temperature in all the solvents and the result is an inverse relation between $h\Delta\nu$ and temperature (figure 4.4(d)).

4.1.4. Pyrene and N,N'-bis(dimethylamino)diphenylmethane system(PY/DMDPM)

1×10^{-4} M PY shows intense fluorescence in all solvents used when photo excited at 337 nm. No shift in the fluorophore excitation wavelength was observed here with the increase in the solvent polarity. Upon addition of 0.004 M DMDPM an exciplex appears towards the bathochromic side (figure4.5). Emission spectra of PY with DMDPM in all other solvents are given in A.1.4.

Inverse relation between $h\Delta\nu$ and temperature is observed in all the solvents except

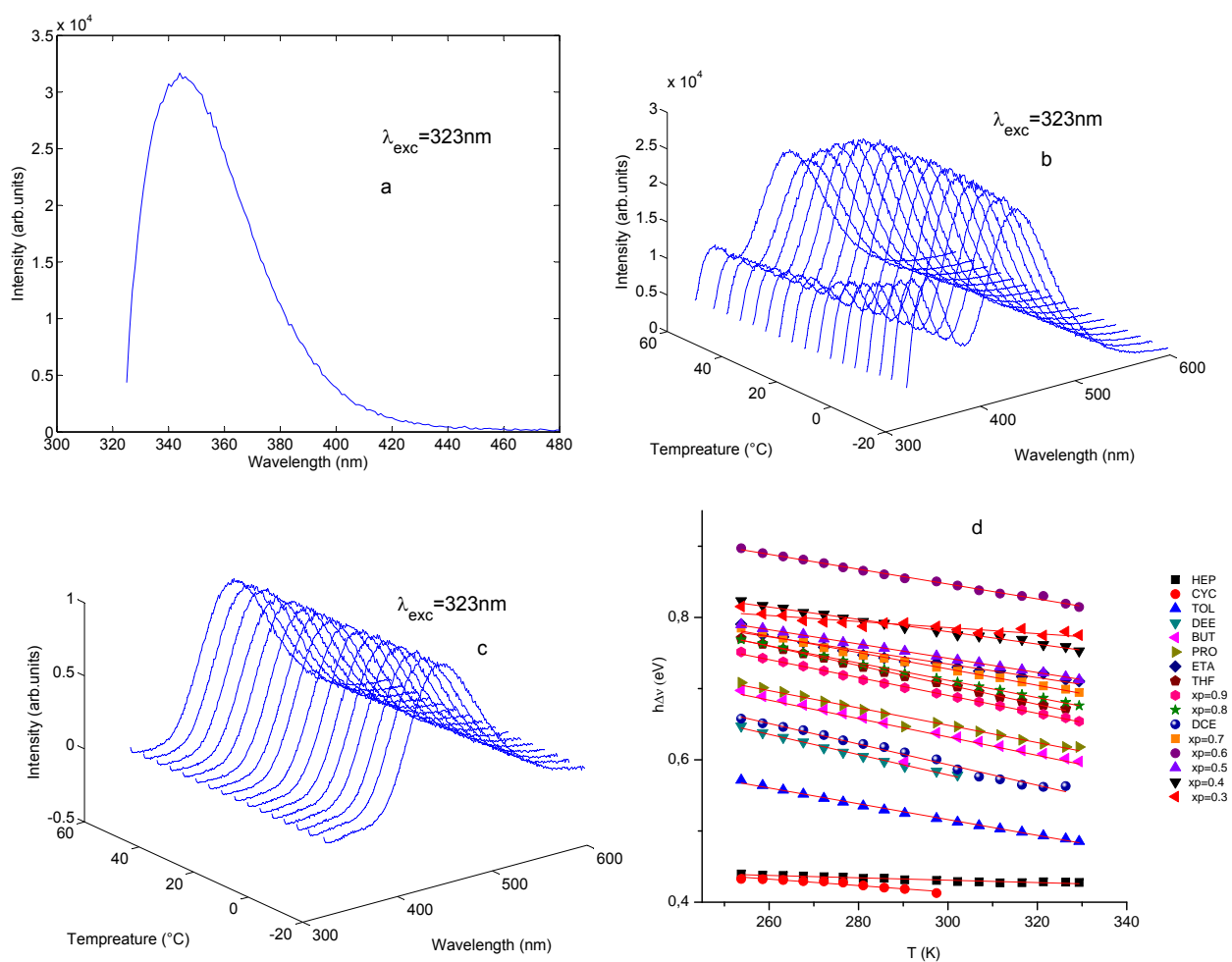


Figure 4.4.: Fig a: fluorescence spectra of 1.1×10^{-4} M DMA in propylacetate, fig b: quenching of DMA with BP at various temperatures in propylacetate, fig c: isolated emission spectra of DMA/BP in propylacetate at various temperatures and fig d: spectral shift vs. temperature for the same exciplex system in solvents of different polarity.

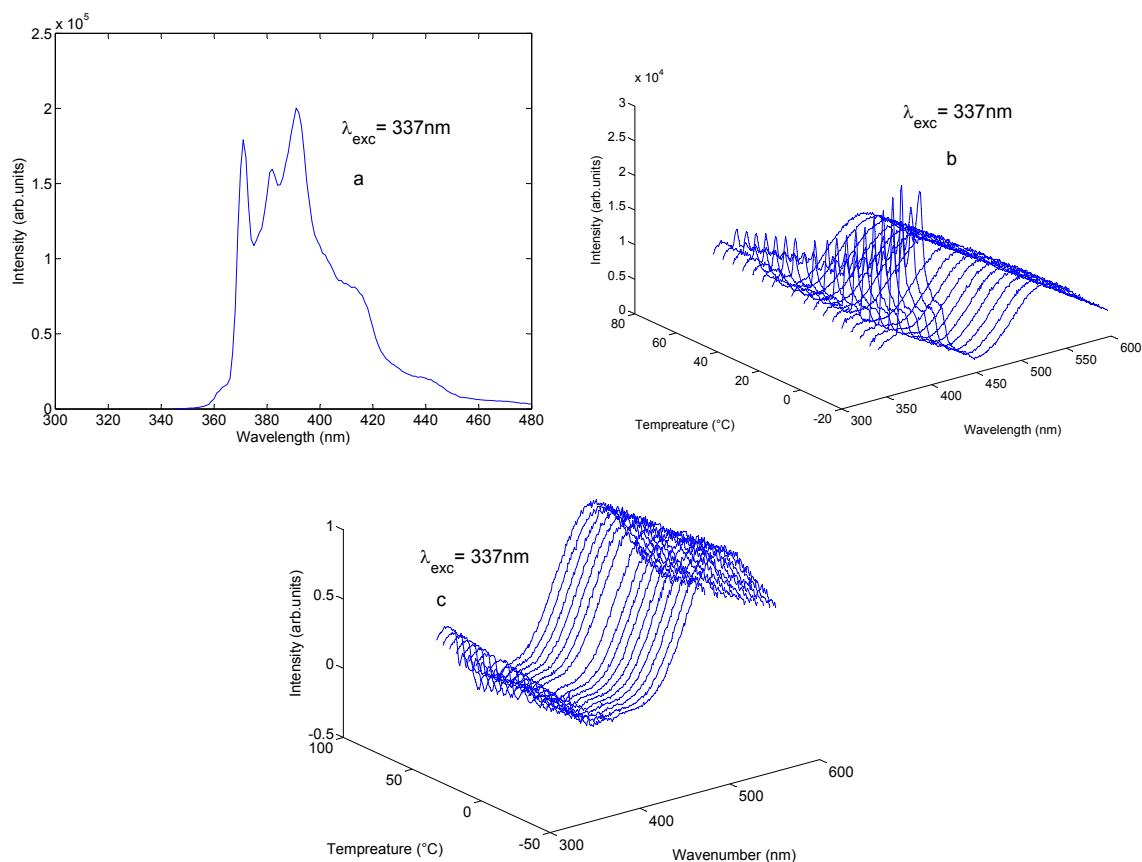


Figure 4.5.: Fig a: fluorescence spectra of 1×10^{-4} M PY in $x_p = 0.9$, fig b: quenching of PY with DMDPM at various temperatures in $x_p = 0.9$ and fig c: isolated emission spectra of PY/DMDPM in $x_p = 0.9$ at various temperatures.

n-heptane and cyclohexane (figure 4.6).

In the case of n-heptane from 255K till 310K the distortion polarization dominates and the result is direct relation between $h\Delta\nu$ and temperature. Where as for the rest of higher temperature range i.e from 310K till 325K the inverse relation is observed showing that the solvent orientation dominates and the exciplex is destabilized with the further increase of temperature. For PY/DMDPM exciplex in cyclohexane only the distortion polarization dominates and it was reflected from the direct relation between $h\Delta\nu$ and temperature therefore here the exciplex is destabilized with increase of temperature. The solution was just heated up till 310K because the boiling point of cyclohexane is 354K. For all rest solvents the exciplex is destabilized with the increase of temperature and this behavior is reflected from the inverse relation between $h\Delta\nu$ and temperature (figure 4.6(b)). For this exciplex system surprisingly inverse relation is observed between $h\Delta\nu$

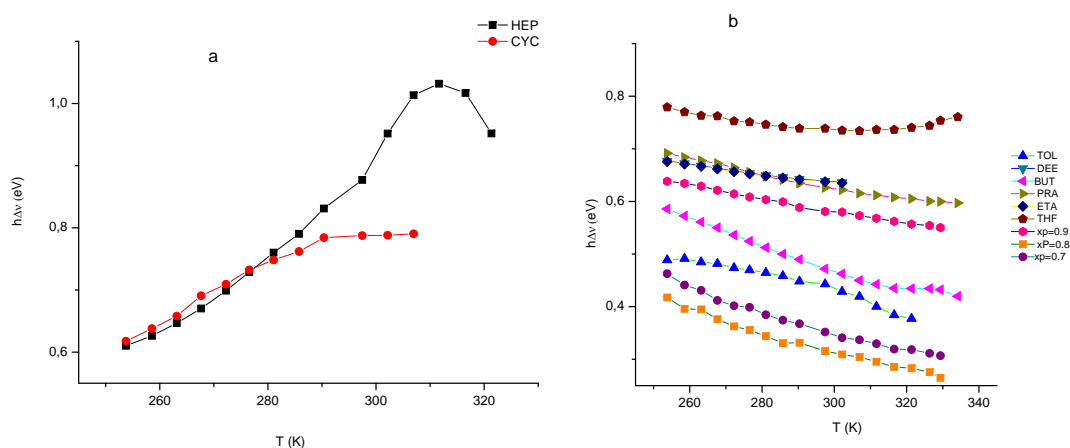


Figure 4.6.: Spectral shifts Vs. temperatures for PY/DMDPM in fig a: HEP and CYC, fig b: in all other solvents.

and $f\epsilon$ (table 4.1) and the reason for this behavior is unknown.

4.1.5. N-alkylated Carbazoles with Dicyanobenzenes

N-MC and N-EC shows intense fluorescence when excited at 320nm. But upon addition of 1,2-DCN, 1,3-DCB and 1,4-DCB into N-MC, and addition of 1,2-DCB into N-EC very weak exciplex is formed which is shifted towards the bathochromic side (figure:4.7). Remaining all emission spectra of n-alkylated carbazoles with dicyanobenzene are given in A.1.5.

These exciplex systems were studied only in tetrahydrofuran solvent. With the increase of solvent polarity the exciplex becomes destabilizes and the result is inverse relation between the $h\Delta\nu$ and temperature (figure 4.7). From table (4.2) it is observed that at 297K the NMC/1,4-DCB exciplex has the highest shift value and NMC/1,3-DCB has the smallest shift value (see table 4.2)so the exciplex system with higher polar charge transfer character is NMC/1,4-DCB. All these exciplex systems gets destabilized with lowering of temperature and this behavior is reflected from the inverse relation between $h\Delta\nu$ and temperature.

4.2. Fluorophore and Exciplex Peak Intensities

4.2.1. Fluorophore peak intensities in absence of quencher

For all the systems considered here, with the increase of temperature, the fluorophore peak intensities in the absence of quencher (I_{flu}) was considered constant. An inverse

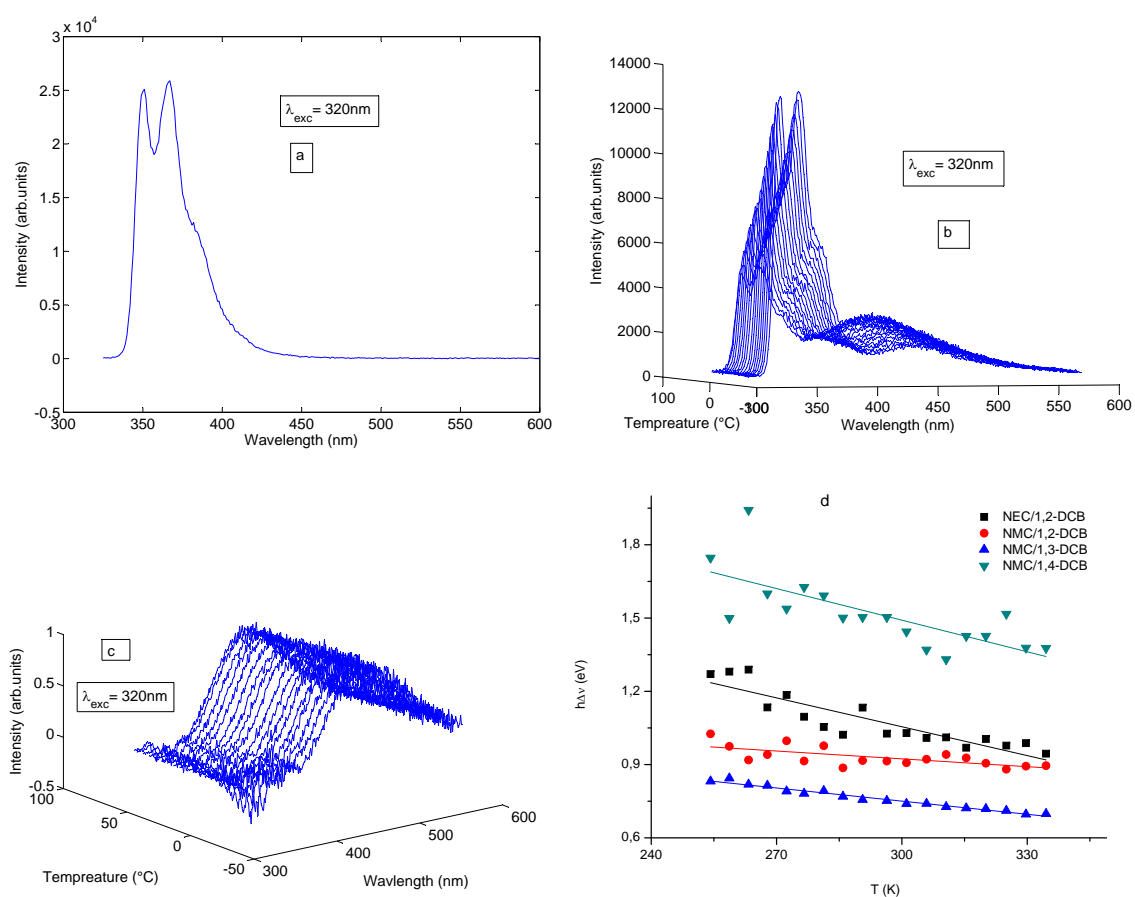


Figure 4.7.: fig a: fluorescence spectra of 5×10^{-5} M NMC in tetrahydrofuran, fig b: quenching of NMC with 1,3-DCB at various temperatures in tetrahydrofuran, fig c: isolated emission spectra of NMC/1,3-DCB in THF at various temperatures and fig d: spectral shift vs. temperature for carbazoles/DCB in tetrahydrofuran at various temperatures.

Table 4.2.: Data of N-alkylcarbazol/dicyanobenzenes^a showing exciplex spectral shift ($h\Delta\nu$ eV), fluorophore peak intensity (I_f) and ratio of exciplex peak intensity to fluorophore peak intensity ((I_{ex}/I'_{flu})) in tetrahydrofuran (THF) at 297K.

Exciplex	$h\Delta\nu$ eV	I_f (arbitrary units)* 10^4	(I_{ex}/I'_{flu})
NEC/1,2DCB	1.03	2.99	0.09
NMC/1,2DCB	0.91	3.01	0.08
NMC/1,3DCB	0.75	3.01	0.29
NMC/1,4DCB	1.50	3.01	0.17

^a Used acronyms: N-ethylcarbazole (NEC), 1,2-dicyanobenzene (1,2DCB), N-methylcarbazole (NMC), 1,3-dicyanobenzene (1,3DCB), 1,4-dicyanobenzene (1,4DCB)

relation was observed between fluorophore peak intensity without quencher and solvent polarity, except for pyrene system (see table 4.4).

In the case of pyrene from $\epsilon = 1.91$ till 6 direct relation was obtained between I_{flu} and function of dielectric constant and from $\epsilon = 6.06$ till 19.09 inverse relation was observed. Reason for this strange behavior of pyrene is unknown. Whereas the inverse relation between I_{flu} and $f(\epsilon)$ is obtained because in solution phase the ground state fluorophore possess a dipole moment and the dipole moment of solvent molecules interact with it to yield an ordered distribution of solvent molecules around the fluorophore. On photo excitation the dipole moment of fluorophore is changed and resultantly rearrangement is observed in the solvent molecules surrounding it. But according to the Franck-Condon principle the molecule is excited to a higher electronic energy level in a far shorter time frame than it takes for the fluorophore and solvent molecules to reorient themselves within the solvent-solute interactive environment. Resultantly there appears a time lag between the excitation event and the reorientation of solvent molecules around the excited fluorophore. The excited fluorophore has usually a larger dipole moment compared with the ground state fluorophore. Soon after photo excitation of the fluorophore to higher vibrational levels of the first excited singlet state ($S_{(1)}$), excess vibrational energy is lost to surrounding solvent molecules because the fluorophore slowly relaxes to the lowest vibrational energy level. Then by a much slower process of solvent relaxation the solvent molecules help in stabilizing and lowering the energy level of the excited state by reorienting themselves around the excited fluorophore. Therefore, the fluorophore peak intensity is highly sensitive to the interactions that occur in the local environment during the excited state lifetime. Increasing the solvent polarity produces a correspondingly larger reduction in the energy level of the excited state, while decreasing the solvent

Table 4.3.: Fluorophore^a peak intensity I_f (arbunits) $\times 10^4$ in solvents^b of different polarity at 297K. The solvents are arranged in the order of increasing solvent polarity from top of list to bottom.

Solvent	1-CN	2,3-DCN	BP	PY
HEP	3.76	3.68	4.07	0.84
CYH	3.69	-	3.88	1.51
TOL	3.59	2.89	3.18	2.47
DEE	3.76	2.66	3.28	5.72
BUT	3.07	2.83	3.88	7.23
PRA	3.24	2.93	3.17	20.02
ETA	3.81	2.51	3.10	13.08
THF	2.54	2.47	3.02	19.19
$x_P=0.9$	2.34	2.27	2.61	20.22
$x_P=0.8$	2.05	2.29	2.51	18.25
DCE	1.98	3.00	2.48	-
$x_P=0.7$	1.41	2.53	2.49	15.83
$x_P=0.6$	1.36	2.19	2.35	15.06
$x_P=0.5$	1.66	2.10	2.60	16.87
$x_P=0.4$	1.66	1.80	2.36	17.74
$x_P=0.3$	1.60	1.68	2.33	16.01

^a Used acronyms: 1-Cyanonaphthalene (1-CN), 2,3-Dicyanonaphthalene (2,3-DCN), Biphenyl (BP), Pyrene (PY)

^b Used acronyms: heptane (HEP), cyclohexane (CYH), toluene (TOL), diethylether (DEE), butyronitrile (BUT), propylacetate (PRA), ethylacetate (ETA), tetrahydrofuran (THF), propylacetate mole fraction in propylacetate/butyronitrile mixture (x_P), dichloroethane (DCE)

polarity reduces the solvent effect on the excited state energy level. Thus the excited fluorophore is highly sensitive to solvent effects.

4.2.2. Ratio of Exciplex Peak Intensity to the Fluorophore Peak Intensity in Presence of Quencher

An inverse relation is observed between ratio of exciplex peak intensity to the fluorophore peak intensity in presence of quencher (I_{ex}/I'_{flu}) and $f(\epsilon)$ (see table 4.4). Similar behavior was observed in many other systems.^{122,123} The reason for this behavior is that photoinduced electron transfer between neutral molecules forms contact radical ion pairs (CRIPs) which may recombine in the solvent cage or may form solvent separated and free solvated ions depending upon the solvent polarity. These species formed from CRIPs decay non-radiatively to ground state i.e no fluorescence is observed. Radiative emission is observed only if the excited state is a contact ion pair. Reduction in the intensity

4. Results and Discussion

Table 4.4.: Ratio of exciplex ^a peak intensity to the fluorophore peak intensity in the presence of quenchers (I_{ex}/I'_{flu}) in solvents^b of different polarity at 297K. The solvents are arranged in the order of increasing solvent polarity from top of list to bottom.

Solvent	1-CN/HMB	2,3-DCN/HMB	DMA/ BP	PY/DMADM
HEP	17.68	4.33	3.11	8.65
CYH	14.13	2.39	2.37	4.96
TOL	7.70	2.38	2.00	3.60
DEE	14.30	1.31	-	2.38
BUT	7.52	-	2.12	1.70
PRA	6.12	-	2.23	0.83
ETA	9.05	-	2.29	0.31
THF	8.61	-	2.41	1.18
$x_P=0.9$	6.17	-	2.25	0.63
$x_P=0.8$	4.16	-	2.30	1.18
DCE	2.96	0.90	1.03	-
$x_P=0.7$	5.74	-	1.83	0.29
$x_P=0.6$	4.63	-	1.33	0.33
$x_P=0.5$	4.60	-	1.04	0.21
$x_P=0.4$	1.94	-	0.62	0.1
$x_P=0.3$	1.80	-	0.42	-

^a Used acronyms: 1-Cyanonaphthalene (1-CN), Hexamethylbenzene (HMB), 2,3-Dicyanonaphthalene (2,3-DCN), Biphenyl (BP), Dimethylaniline (DMA), Pyrene (PY), N,N'-bis(dimethylamino)diphenylmethane (DMADM)

^b Used acronyms: heptane (HEP), cyclohexane (CYH), toluene (TOL), diethylether (DEE), butyronitrile (BUT), propylacetate (PRA), ethylacetate (ETA), tetrahydrofuran (THF), propylacetate mole fraction in propylacetate/butyronitrile mixture (x_P), dichloroethane (DCE)

of fluorophore band with the increase of solvent polarity is observed due to the formation of such solvated ion radical pairs in competition with exciplex formation.¹²⁰ Thus this decrease in the emission intensity of exciplex is due to the decrease in the radiative probability of exciplex fluorescence and as increase in the corresponding radiation less transition probability.¹²⁴ Different relation was observed between (I_{ex}/I'_{flu}) and temperature in all selected solvents for different exciplex systems therefore each exciplex system is described separately as:

•1-cyanonaphthalene/hexamethylbenzene exciplex system: Direct relation was observed between (I_{ex}/I'_{flu}) and temperature for all solvents except n-heptane and cyclohexane (figure:4.8). For n-heptane first a direct and then an inverse relation was observed whereas for cyclohexane only inverse relation was observed. As already mentioned, the polar nature of exciplex is due to the charge transfer character and it exhibits solvatochromic fluorescence due to this highly polar nature. On photo excitation a dynamic process is

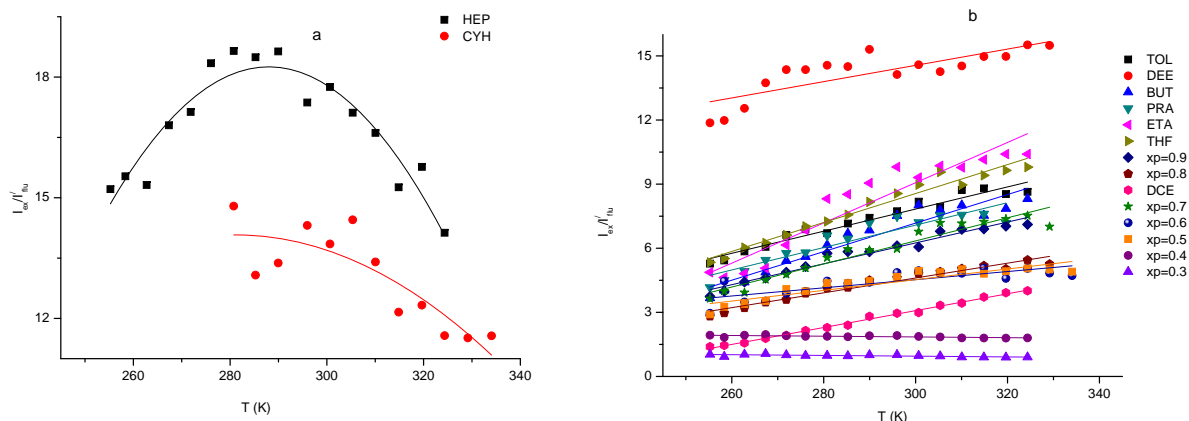


Figure 4.8.: Ratio of peak intensities of exciplex to fluorophore in the presence of quencher (I_{ex}/I'_{flu}) vs. temperature for exciplex of 1-CN/HMB in fig a: n-heptane and cyclohexane, fig b: in all other solvents.

initiated to stabilize the charge separated excited state. The donor and acceptor undergo internal reorganization to adopt the most favorable conformation for exciplex formation, while the solvent molecules surrounding them also reorganize to stabilize the polar exciplex. Lowering the temperature retards these processes and result is decrease in the rate of charge transfer and exciplex intensity also decreases.¹ On the other hand in the case of cyclohexane reason of decrease in intensity with the increase of temperature may be that at higher temperature the the deactivation process by collision is enhanced in exciplex. Thus at higher temperature the 1-CN and HMB molecules modify their configuration that there is a decrease in the intensity of exciplex. Whereas for n-heptane from 255 till 290 K, a direct relation is observed, whereas from 298 till 325 K an inverse relation is observed for (I_{ex}/I'_{flu}). From 255 - 290 K the lowering of temperature retards the solvent reorganization around the exciplexes and from 298 to 325 K the deactivation process due to collision is dominated with rise of temperature.

- 2,3-dicyanonaphthalene/hexamethylbenzene and N-alkylated carbazoles/cyanobenzene exciplex systems: Figure 4.9 shows that direct relation is present between (I_{ex}/I'_{flu}) and temperature for 2,3-DCN/HMB and N-alkylated carbazoles/cyanobenzene exciplexes and the reason for this behavior is again that with the increase of temperature the solvent molecules can reorient themselves more efficiently around the dipolar exciplex and result is increase in the rate of charge transfer along with the increase of exciplex intensity.
- N,N'-dimethylaniline/biphenyl exciplex system: For this exciplex system in non-polar solvents (n-heptane and cyclohexane) the increase of temperature leads to a deactiva-

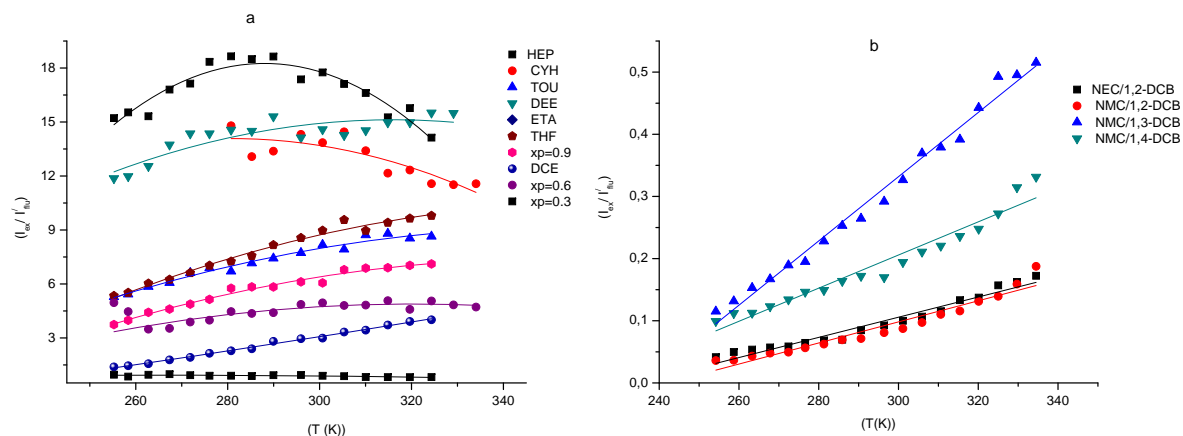


Figure 4.9.: Ratio of peak intensities of exciplex to fluorophore in the presence of quencher (I_{ex}/I'_{flu}) vs. temperature for exciplexes of fig a: 2,3-DCN/HMB, fig b: N-alkylated carbazoles/Cyanobenzenes.

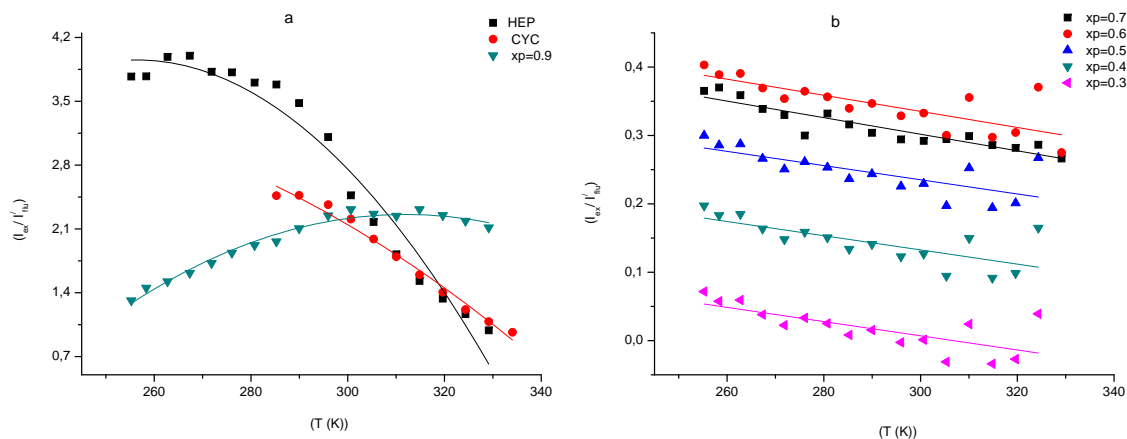


Figure 4.10.: Ratio of peak intensities of exciplex to fluorophore in the presence of quencher (I_{ex}/I'_{flu}) vs. temperature for exciplexes of DMA/BP in fig a: n-heptane, cyclohexane, propylacetate and mixture of propylacetate and butyronitrile with 0.9 and 0.8 mole fraction of propylacetate b: in rest solvents.

tion process by collision and at higher temperatures the BP and DMA molecules modify their configuration in such a way that there is a decrease in the fluorescence intensity (fig:4.10). In the case of toluene and cyclohexane inverse relation was observed between (I_{ex}/I'_{flu}) and temperature. Whereas for propylacetate from 255 till 290 K direct relation was found between (I_{ex}/I'_{flu}) and temperature and then with further increase of

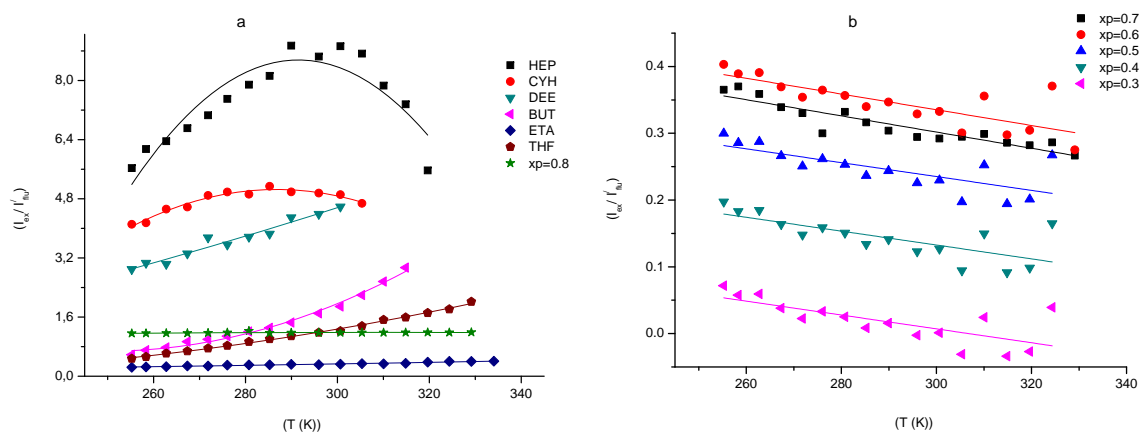


Figure 4.11.: Ratio of peak intensities of exciplex to fluorophore in the presence of quencher (I_{ex}/I'_{flu}) vs. temperature for exciplexes of PY/DMDPM in solvents with dielectric constant from fig a: from 1.91 - 9.74 b: from 10.43 - 19.09.

temperature from 296 - 329 K inverse relation was observed. Same behavior was also reflected in the solvent mixture of propylacetate and butyronitrile with 0.9 and 0.8 mole fraction of propylacetate. Thus in these systems from 255 - 290 K with the increase of temperature solvent molecules rearrange themselves around the polar exciplex in such a way that they are stabilized with more charge transfer and with further increase in temperature, i.e. from 305 till 329 K the deactivation process by collision is enhanced and result is decrease in intensity. In all other solvents with the increase of temperature exciplex intensity is increased due to the orientation of solvents in such away that the exciplex stabilizes (fig:4.10).

•Pyrene and N,N'-bis(dimethylamino)diphenylmethane system: In the case of n-heptane is an increase in the (I_{ex}/I'_{flu}) with the increase of temperature from 255 to 295 K and then from 300 to 319 K and a decrease in the (I_{ex}/I'_{flu}) by further increase of temperature. In cyclohexane from 255 till 285 K the (I_{ex}/I'_{flu}) increases with the increase of temperature and then from 285 to 305 K its value decreases with increase of temperature (figure: 4.11). Direct relation was observed between (I_{ex}/I'_{flu}) and temperature in solvents with dielectric constant from 2.41 till 9.74 and then with the increase of solvent dielectric constant i.e from 11.61 till 19.09 inverse relation was observed (figure: 4.11). In this system inverse relation between (I_{ex}/I'_{flu}) and temperature was observed in solvents with larger dielectric constant whereas in all previous mentioned systems inverse relation was observed in non-polar solvents. Reason of this behavior is unknown. When with the increase of temperature, the donor and acceptor molecules adopt the most stable confor-

mation in exciplex and the solvent molecules also reorient themselves in such a way that exciplex is stabilized then direct relation is observed between (I_{ex}/I'_{flu}) and temperature. When with the increase of temperature the exciplex is desatblized due to the increase in the deactivation process by collision, the exciplex modify its configuration in such a way that their is decrease in intensity then inverse relation is observed between (I_{ex}/I'_{flu}) and temperature.

4.3. Exciplex Energetics–Band Parameters Obtained from Excited Emission Spectra:

As mentioned already that direct information about the energetics of exciplex can be obtained from the temperature dependent exciplex emission spectra. Theory about the band parameters obtained from the excited emission spectra was already discussed in the subsection 2.6.7. Now the results obtained from these fittings are discussed in this subsection. The emission spectra gives information about the vibronic level (ΔE_{CR}) and thus the information about the dominant high frequency vibration can be obtained. In order to obtain these informations the isolated emission spectra of all exciplexes of different systems were fitted according to the Kuzmin’s model of self-consistent polarization. All the fittings were done over a range of temperature i.e from 253 till 340 K. The equation representing the Kuzmin’s model of self-consistent polarization is already given in subsection 2.6.7 of theory. In this model the emission spectra line is given as a sum of vibronic transitions with Gauss band shape. Equation 2.110 was fitted to the exciplex spectra with ν'_0 and σ being optimized and setting S and ν_v equals to 1 and 0.1 eV respectively. The parameters obtained due to these fittings are discussed as a function of solvent polarity and temperature. Figures 4.12 represents the emission spectra of all the systems discussed here in tetrahydrofuran at 297.15 K. For N-alkytaled carbazoles/dicyanobenzene systems only the fittings were done for NMC/1,3-DCB system because for rest all systems the exciplex obtained was not intense enough for fittings according to this model.

4.3.1. Energy of zero-zero Transitions and Gauss Broadening of Vibronic Level

Table 4.5 represents the energy of zero-zero transitions ($h\nu'_0$) as a function of solvent polarity for all systems studied. An inverse relation is observed between $h\nu'_0$ and $f(\epsilon)$ for all exciplex systems except for 2,3-DCN/HMB. A similar inverse relation was also observed previously for 9-cyanonaphthalene with 1,2,3-trimethoxybenzene and 1,3,5-trimethoxybenzene¹¹ and also for 9,10-dimethylanthracene/ N,N-dimethylaniline system.¹²⁵ This inverse rela-

4.3. Exciplex Energetics–Band Parameters Obtained from Excited Emission Spectra:

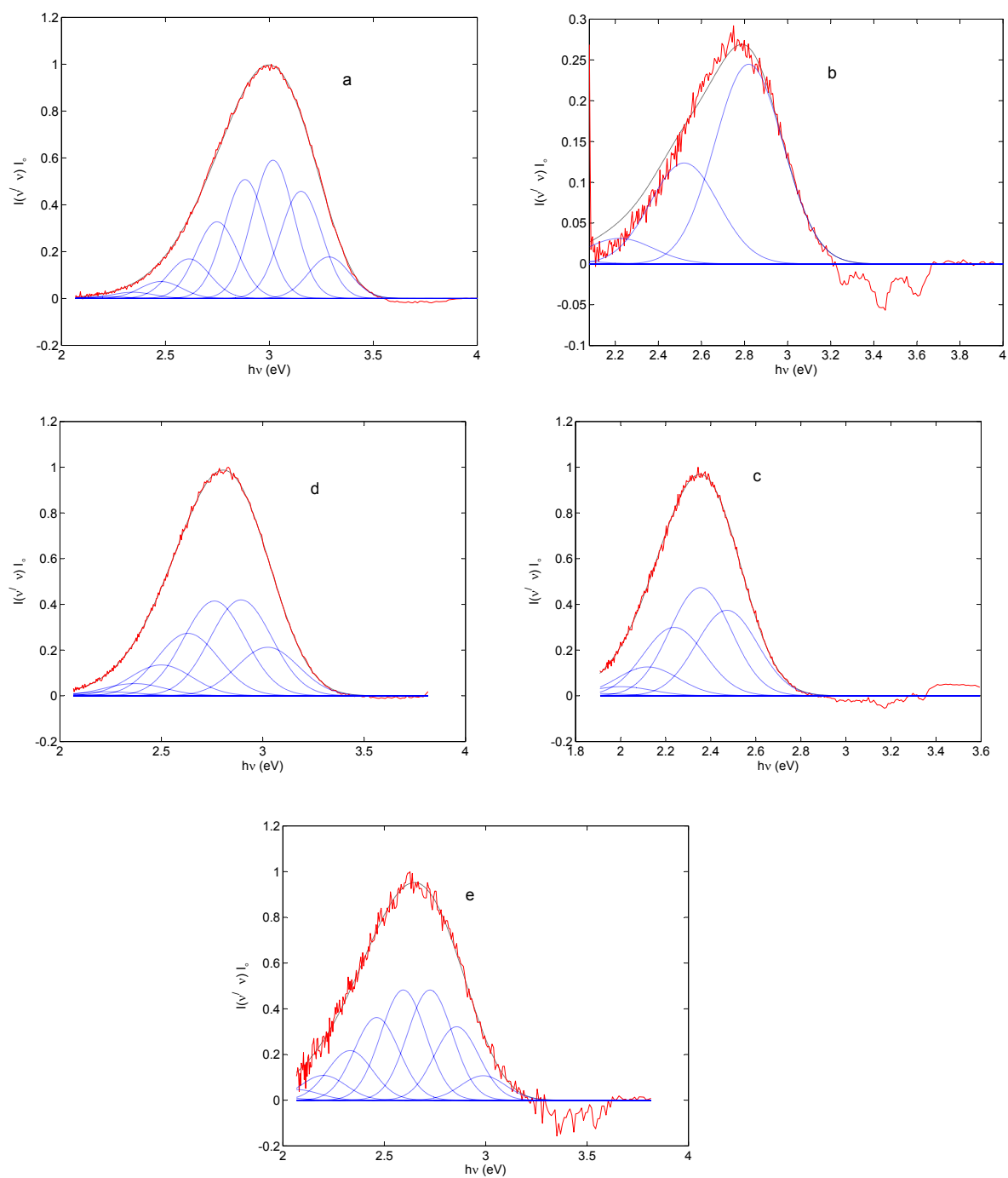


Figure 4.12.: Exciplex emission spectra and result of its fittings to equation 2.110 for a: 1-CN/HMB, b: 2,3-DCN/HMB, c: DMA/BP, d: PY/DMDPM and e: NMC/1,3-DCB in tetrahydrofuran at 297K. contributions of 0-0, 0-1, 0-2, 0-3 0-4 and 0-5 vibronic transitions are shown by blue lines.

Table 4.5.: Zero-zero transition energy ($h\nu'_0$ (eV)) for exciplexes ^a in solvents^b of different polarity at 297K. The solvents are arranged in the order of increasing solvent polarity from top of list to bottom.

Solvent	1-CN/HMB	2,3-DCN/HMB	DMA/ BP	PY/DMADM
HEP	3.15	3.16	3.36	2.72
CYH	3.34	-	3.37	2.74
TOL	3.26	3.10	3.23	2.62
DEE	3.27	3.13	3.26	2.66
BUT	3.30	2.90	3.15	2.62
PRA	3.29	2.98	3.09	2.62
ETA	3.30	3.10	3.14	2.66
THF	3.29	3.04	2.98	2.47
$x_P=0.9$	3.28	3.07	3.01	2.55
$x_P=0.8$	3.29	3.07	2.94	-
DCE	3.21	2.82	2.80	-
$x_P=0.7$	3.25	2.85	2.91	2.50
$x_P=0.6$	3.26	3.08	2.82	2.46
$x_P=0.5$	3.25	3.00	2.81	2.40
$x_P=0.4$	3.17	2.88	3.00	2.41
$x_P=0.3$	3.10	2.56	2.99	-

^a Used acronyms: 1-Cyanonaphthalene (1-CN), Hexamethylbenzene (HMB), 2,3-Dicyanonaphthalene (2,3-DCN), Biphenyl (BP), Dimethylaniline (DMA), Pyrene (PY), N,N'-bis(dimethylamino)diphenylmethane (DMADM)

^b Used acronyms: heptane (HEP), cyclohexane (CYH), toluene (TOL), diethylether (DEE), butyronitrile (BUT), propylacetate (PRA), ethylacetate (ETA), tetrahydrofuran (THF), propylacetate mole fraction in propylacetate/butyronitrile mixture (x_P), dichloroethane (DCE)

tion shows that the extent of charge transfer (z) is independent of the solvent polarity.¹²⁵ Also this inverse behavior represents the decrease in the energy gap of charge recombination (ΔE_{CT}) and thus with the increase of solvent polarity the decrease in exciplex intensity is due to charge recombination. Whereas for 2,3-DCN/HMB no satisfying relation is obtained between $h\nu'_0$ and solvent polarity and therefore no generalization could be drawn here.

Increase in the value of $h\nu'_0$ and also ΔE_{CT} was observed with increase in temperature for all exciplex systems (figure4.13) considered here thus representing the fact that at low temperature the decreased in intensity is due to the charge recombination of the CRIPs. At low temperature this increase in deactivation of exciplex due to formation of CRIPs was predicted before in sub-section 4.2.2. Change in the value of Gauss broadening of vibronic level (σ) with $f(\epsilon)$ and temperature is observed for all systems (tabel :4.6). Graphs representing the change of σ with temperature are given in A.2.1. This

4.3. Exciplex Energetics–Band Parameters Obtained from Excited Emission Spectra:

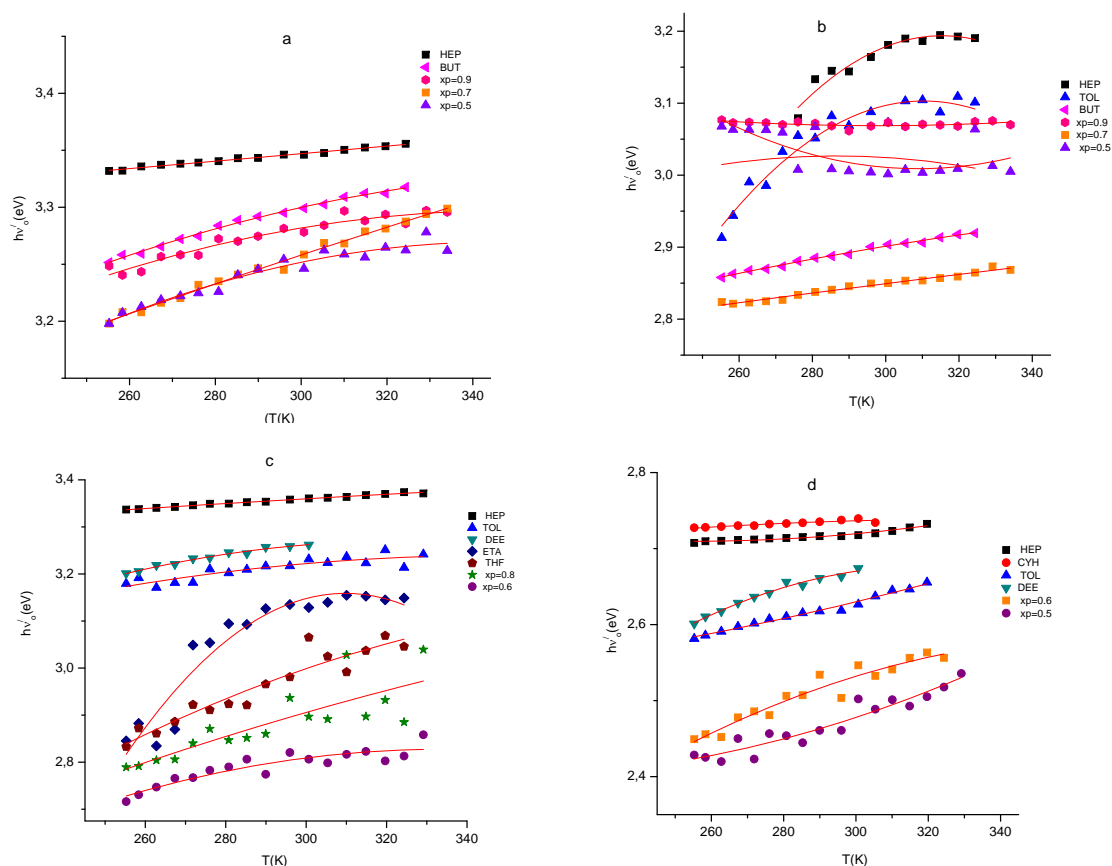


Figure 4.13.: Energy of zero-zero transition vs.temperature for exciplex of a: 1-CN/HMB, b: 2,3-DCN/HMB, c: DMA/PB and d: PY/DMDPM in solvents of different polarity.

change in the value of σ represents that the coupling of the ground and excited molecular electronic levels to surrounding solvent molecules are dependent on the solvent reorganization energy by $\sigma^2 = 2\lambda_o/k_B T$. Where λ_o describes the solvent reorganization energy. The reorganization energy appearing in equation 2.110 is sum of following two terms:

- **Inner reorganization energy:** The solvent independent term λ_v is known as the inner reorganization term. It arises from the structural differences of the molecule in reactant and product state. This term is usually very small and therefore it is ignored.
- **Solvent reorganization term:** The symbol for this reorganization term is λ_o . It arises from the differences in orientation and polarization of the solvent molecules around the solute molecules of interest.^{11,126} As mentioned already that various kinds of intermolecular interactions beside the medium reorganization are responsible for inhomogeneous broadening of vibronic levels for solids and liquids. Therefore the value of σ depends

Table 4.6.: Gauss broadening of vibronic level (σ (eV)) for exciplexes ^a in solvents^b of different polarity at 297K. The solvents are arranged in the order of increasing solvent polarity from top of list to bottom..

Solvent	1-CN/HMB	2,3-DCN/HMB	DMA/ BP	PY/DMADM
HEP	0.10	0.10	0.10	0.10
CYH	0.10	-	0.10	0.10
TOL	0.11	0.10	0.11	0.10
DEE	0.11	0.10	0.10	0.10
BUT	0.10	0.17	0.13	0.10
PRA	0.11	0.10	0.14	0.11
ETA	0.10	0.11	0.10	0.10
THF	0.10	0.11	0.16	0.13
$x_P=0.9$	0.11	0.10	0.15	0.10
$x_P=0.8$	0.12	0.10	0.17	-
DCE	0.10	0.16	0.24	-
$x_P=0.7$	0.14	0.22	0.16	0.10
$x_P=0.6$	0.11	0.11	0.18	0.10
$x_P=0.5$	0.13	0.13	0.19	-
$x_P=0.4$	0.2	0.12	0.14	-
$x_P=0.3$	0.21	0.11	0.10	-

^a Used acronyms: 1-Cyanonaphthalene (1-CN), Hexamethylbenzene (HMB), 2,3-Dicyanonaphthalene (2,3-DCN), Biphenyl (BP), Dimethylaniline (DMA), Pyrene (PY), N,N'-bis(dimethylamino)diphenylmethane (DMADM)

^b Used acronyms: heptane (HEP), cyclohexane (CYH), toluene (TOL), diethylether (DEE), butyronitrile (BUT), propylacetate (PRA), ethylacetate (ETA), tetrahydrofuran (THF), propylacetate mole fraction in propylacetate/butyronitrile mixture (x_P), dichloroethane (DCE)

upon many factors and therefore it should exceed ($2\lambda_0 k_B T$). Consequently the energy gap ΔE_{CR} along with energy of 0-0 transition and $h\nu'_0$ are related directly to the medium reorganization energy. Pictorial representation of this dependence of vibronic level is already mentioned in figure 2.7.

According to chart 2.7 a shift in the value of $h\nu'_0$ in a given solvent ($h\nu'_0(r)$) relative to some non polar solvent ($h\nu'_0(s)$) is equal to the difference of their reorganization energies ($h\nu'_0(r) - (h\nu'_0(s)) = \lambda_0(s) - \lambda_0(r)$).

Table 4.7 (only the results for 1-CN/HMB exciplex are represented here) does not show the same behavior. Differences in the values of zero- zero transition energies are much smaller compared to the difference in the values of $\sigma^2/k_B T$, thus representing that the spectral broadening and spectral shifts have different origin. Similar differences between the spectral broadening and spectral shifts was observed by Kuzmin and coworkers in 9-cyanophenanthrene with 1,2,3-trimethoxybenzene and 1,3,5-trimethoxybenzene and also

4.3. Exciplex Energetics–Band Parameters Obtained from Excited Emission Spectra:

Table 4.7.: Difference of shift values with respect to non-polar solvents for 1-CN/HMB in solvents^a of different polarity at 297K. The solvents are arranged in the order of increasing solvent polarity from top of list to bottom.

Solvent	$h\nu'_o$ eV	$\sigma^2/2k_B T$ eV	$h\nu'_o(r) - h\nu'_o(s)$ eV	$\sigma(r)^2/2k_B T - \sigma(r)^2/2k_B T$ eV
HEP	3.35	0.20	0.00	0.00
CYH	3.34	0.18	0.10	-0.02
TOL	3.26	0.24	0.09	0.04
DEE	3.27	0.27	0.08	0.07
BUT	3.20	0.20	0.15	0.00
PRA	3.29	0.20	0.06	0.00
ETA	3.30	0.19	0.05	-0.01
THF	3.20	0.20	0.15	0.00
$x_P=0.9$	3.28	0.20	0.07	0.00
$x_P=0.8$	3.29	0.20	0.06	0.00
DCE	3.21	0.27	0.14	0.07
$x_P=0.7$	3.25	0.25	0.10	0.05
$x_P=0.6$	3.26	0.20	0.09	0.00
$x_P=0.5$	3.25	0.20	0.10	0.00
$x_P=0.4$	3.17	0.98	0.18	0.78
$x_P=0.3$	3.17	0.98	0.18	0.78

^a Used acronyms: heptane (HEP), cyclohexane (CYH), toluene (TOL), diethylether (DEE), butyronitrile (BUT), propylacetate (PRA), ethylacetate (ETA), tetrahydrofuran (THF), propylacetate mole fraction in propylacetate/butyronitrile mixture (x_P), dichloroethane (DCE)

by Ulstrup and coworkers for the absorption spectra of betins in various solvents.

An inverse relation is observed between $h\nu'_o$ and $f(\epsilon)$ for all exciplex systems except for 2,3-DCN/HMB (tabel : 4.5). A similar inverse relation was also observed previously for 9-cyanonaphthalene with 1,2,3-trimethoxybenzene and 1,3,5-trimethoxybenzene¹¹ and also for 9,10-dimethylanthracene/ N,N-dimethylaniline system.¹²⁵ This inverse relation shows that the extent of charge transfer (z) is independent of the solvent polarity.¹²⁵ Also this inverse behavior represents the decrease in the energy gap of charge recombination (ΔE_{CT}) and thus with the increase of solvent polarity the decrease in exciplex intensity is due to charge recombination. Whereas for 2,3-DCN/HMB no satisfying relation is obtained between $h\nu'_o$ and solvent polarity and therefore no generalization could be drawn here.

Table 4.8.: Huang-Rhys factor (S) for exciplexes ^a in solvents^b of different polarity at 297 K. The solvents are arranged in the order of increasing solvent polarity from top of list to bottom.

Solvent	1-CN/HMB	2,3-DCN/HMB	DMA/ BP	PY/DMADM
HEP	1.10	1.10	1.23	0.72
CYH	0.96	-	1.19	0.68
TOL	1.28	1.36	1.73	1.09
DEE	1.25	1.79	2.53	1.93
BUT	2.27	2.22	3.00	3.00
PRA	2.38	2.36	2.61	3.00
ETA	2.71	1.24	3.00	1.93
THF	2.73	1.29	1.69	1.26
$x_P=0.9$	2.57	2.54	2.04	2.18
$x_P=0.8$	3.00	1.71	1.51	-
DCE	3.00	0.51	0.09	-
$x_P=0.7$	3.00	0.46	1.44	2.14
$x_P=0.6$	3.00	1.32	0.74	1.69
$x_P=0.5$	3.00	0.94	0.79	-
$x_P=0.4$	2.73	0.98	3.00	-
$x_P=0.3$	3.00	0.99	0.12	-

^a Used acronyms: 1-Cyanonaphthalene (1-CN), Hexamethylbenzene (HMB), 2,3-Dicyanonaphthalene (2,3-DCN), Biphenyl (BP), Dimethylaniline (DMA), Pyrene (PY), N,N'-bis(dimethylamino)diphenylmethane (DMADM)

^b Used acronyms: heptane (HEP), cyclohexane (CYH), toluene (TOL), diethylether (DEE), butyronitrile (BUT), propylacetate (PRA), ethylacetate (ETA), tetrahydrofuran (THF), propylacetate mole fraction in propylacetate/butyronitrile mixture (x_P), dichloroethane (DCE)

4.3.2. Huang-Rhys Factor (S) and Energy of Dominant High-Frequency Vibration

Huang-Rhys factor (S) describes the extent to which geometrical deformations take place in the excited state and corresponds to the average number of phonon involved in the relaxation process.¹²⁷ Direct relation was observed between S and function of solvent polarity for 1-CN/HMB exciplex system showing an increase in geometrical deformations and also increase in the number of phonon in the excited states.¹²⁸ This means that for present system increase in the magnitude of S increases the magnitude of vibrational overlap factors and therefore the exciplex destabilizes and their is reduction in the emission intensity of exciplex (table:4.8). No good relation is observed between S and function of solvent polarity for 2,3-DCN/HMB exciplex system and therefore no generalization could be made here (table: 4.8). For DMA/BP direct relation is observed between S and

solvent polarity in solvents with dielectric constant from 1.91 to 6.06. Thus in this range of solvent polarity there is reduction in the emission intensity of exciplex with increase of solvent polarity due to the increase in the magnitude of vibrational overlap factors where as inverse relation is observed in solvents with dielectric constant 7.36 to 19.09 (table:4.8). Explanation for this inverse relation is unknown and is also not in agreement with the previous results for this system. For PY/DMDPM system increase in the value of S with the increase in the dielectric constant of solvent was observed in solvents with dielectric constant from 1.91 till 4.91 so here again there is reduction in the intensity with increase of solvent polarity (table:huang-Rhys factor). From 4.91 till 19.09 no relation is observed between S and solvent polarity so no generalization could be drawn for this range of solvent polarity.

Inverse relation between S and temperature was observed for 1-CN/HMB and 2,3-DCN/HMB exciplex system (fig:A.15) again conforming that with the decrease in temperature the exciplex is destabilized due to increased geometrical deformations and also increase in vibrational overlap.

For the DMA/BP inverse relation is observed between S and temperature in solvents with dielectric constant from 1.91 till 4.18 representing the increased geometrical deformations and vibrational overlap with decrease of temperature. In solvents with dielectric constant from 4.91 till 11.61 direct relation is observed between S and temperature showing the reverse behavior and reason for this trend is still unknown. In solvents with dielectric constant from 13.48 till 17.22 no relation was obtained between these parameters therefore in this solvent range no generalization could be drawn. In solvent with dielectric constant 19.09 again inverse behavior is observed thus representing that there is increase in geometrical deformations and vibrational overlap (figure:A.15)

For the PY/DMDPM exciplex system inverse relation is observed between S and the temperature in solvents with dielectric constant between 1.91 and 2.40 and also in propylacetate/butyronitrile mixture with 0.9 propylacetate mole fraction. Thus in these solvents the exciplex is destabilized with decrease in temperature. Where as direct relation was observed in propylacetate and in rest all solvents no relation was observed (figure:A.15). In the case of n-alkylated carbazoles with dicyanobenzenes only results were obtained for NMC/1,3-DCB because for all systems exciplex formed were quite weak. For this exciplex system no relation was observed and therefore no generalization could be drawn here (figure:A.15).

Table 4.9 represents inverse relation between $h\nu_v$ and function of solvent polarity for 1-CN/HMB and BP/DMA exciplex systems. The inverse relation for these systems confirm the decrease in the energy of high-frequency vibration with an increase of solvent polarity, resultantly the increased non radiative decay of exciplex with increase of solvent polarity

Table 4.9.: Energy of dominant high-frequency vibration ($h\nu_v(eV)$) for exciplexes ^a in solvents^b of different polarity at 297 K. The solvents are arranged in the order of increasing solvent polarity from top of list to bottom.

Solvent	1-CN/HMB	2,3-DCN/HMB	DMA/ BP	PY/DMADM
HEP	0.17	0.19	0.17	0.17
CYH	0.19	-	0.18	0.18
TOL	0.17	0.17	0.15	0.14
DEE	0.17	0.15	0.13	0.11
BUT	0.14	0.30	0.11	0.09
PRA	0.14	0.20	0.12	0.09
ETA	0.13	0.21	0.13	0.01
THF	0.13	0.22	0.13	0.02
$x_P=0.9$	0.14	0.19	0.14	0.01
$x_P=0.8$	0.13	0.18	0.29	-
DCE	0.12	0.30	0.14	-
$x_P=0.7$	0.12	0.24	0.19	0.11
$x_P=0.6$	0.13	0.28	0.18	0.11
$x_P=0.5$	0.13	0.24	0.11	-
$x_P=0.4$	0.09	0.23	0.12	-
$x_P=0.3$	0.08	0.23	0.12	-

^a Used acronyms: 1-Cyanonaphthalene (1-CN), Hexamethylbenzene (HMB), 2,3-Dicyanonaphthalene (2,3-DCN), Biphenyl (BP), Dimethylaniline (DMA), Pyrene (PY), N,N'-bis(dimethylamino)diphenylmethane (DMADM)

^b Used acronyms: heptane (HEP), cyclohexane (CYH), toluene (TOL), diethylether (DEE), butyronitrile (BUT), propylacetate (PRA), ethylacetate (ETA), tetrahydrofuran (THF), propylacetate mole fraction in propylacetate/butyronitrile mixture (x_P), dichloroethane (DCE)

and decrease in the fluorescence intensity of exciplex. No relation was observed between $h\nu_v$ and solvent polarity for 2,3-DCN/HMB and NMC/1,3-DCB systems therefore no generalization could be drawn here (table: 4.9). Direct relation was observed between $h\nu_v$ and temperature for 1-CN/HMB exciplex system (fig: A.16) thus representing that these exciplex systems are more stable at low temperature.

For 2,3-DCN/HMB exciplexes inverse relation was observed between $h\nu_v$ and temperature in solvents with dielectric constant from 1.91 till 2.40 (fig: A.16). Reason for this inverse behavior is unknown whereas in rest all solvents direct relation was observed between rest of all solvents showing the increased non radiative decay with decrease of solvent temperature and therefore reduced fluorescence intensity at low temperature.

For DMA/BP, in solvents with dielectric constant from 1.91 till 4.18, their was observed an increased non radiative decay with the decrease of temperature and this behavior was reflected from direct relation between $h\nu_v$ and temperature. In solvents with polarity

from 4.19 till 9.74 inverse relation was observed between the $h\nu_v$ and temperature. Again reason for this behavior is unknown. In solvents with dielectric constant from 10.43 till 19.09 no good relation was observed between $h\nu_v$ and temperature (fig: A.16).

For PY/DMDPM an increase was observed in the non-radiative decay with decrease of temperature in solvents with dielectric constant from 1.91 till 6.06 except propylacetate and conformation to this behavior was obtained from direct relation between $h\nu_v$ and temperature. In propylacetate no relation was observed between the parameters. Where as in solvents with dielectric constant from 7.36 till 13.48 no relation was observed between the parameters except in propylacetate/butyronitrile mixture with 0.9 propylacetate mole fraction. In this solvent range as no relation was observed therefore no generalization could be drawn here. In propylacetate/butyronitrile mixture with 0.9 propylacetate mole fraction direct relation was observed between $h\nu_v$ and temperature thus representing decreased non radiative decay with increase of temperature (fig: A.16). For NMC/1,2-DCB no generalization could be drawn from these parameters because no relation was observed between them.

4.4. Fluorescence Life Times

Measurements of fluorescence lifetimes were performed with two different techniques depending upon the excitation wavelength. The fluorescence lifetimes of fluorophores with wavelength from 300nm till 337nm were measured with the help of frequency modulation. For the exciplex systems with maximum wavelength in the range of early 400 nm the lifetimes were measured with the help of time-correlated single photon counting techniques. Different long pass and short pass filters were used which are written in the tables which describe the results. The aim of measuring fluorescence lifetimes for fluorophore and exciplex was to calculate the extent of charge transfer (Z), entropy of exciplex formation ΔS_{EX}^* and equilibrium constant for complex formation K_c . In this chapter only fluorescence lifetime of 1-CN and 1-CN/HMB exciplex will be discussed. For rest all fluorophores and exciplexes systems only data is given in table4.10 and ... (data of appendix)

4.4.1. Fluorescence Lifetime of Fluorophore

Fluorophore is the species which plays a central role in fluorescence spectroscopy. It is the component that absorbs light of specific wavelength and then it is excited later on it re-emits light at different but equal specific wavelength. The amount of light absorbed and emitted by the fluorophore depends upon the nature of fluorophore and also on the chemical environment in which it is present. In old times the fluorophore was known as

Table 4.10.: Fluorescence lifetimes of fluorophores (ns) ^a in solvents^b of different polarity at 297K. The solvents are arranged in the order of increasing solvent polarity from top of list to bottom.

Solvent	1-CN	2,3-DCN	PY
HEP	17.66	31.23	405.48
CYH	15.90	-	341.16
TOL	12.79	29.13	296.91
DEE	13.65	29.24	308.14
BUT	12.94	27.52	288.65
PRA	12.84	26.74	295.47
ETA	11.86	27.62	307.57
THF	10.96	26.51	271.01
$x_P=0.9$	11.77	26.22	268.56
$x_P=0.8$	11.84	25.25	266.51
DCE	-	-	-
$x_P=0.7$	11.12	24.99	265.02
$x_P=0.6$	11.42	23.88	263.15
$x_P=0.5$	10.96	23.24	262.33
$x_P=0.4$	10.94	22.48	259.45
$x_P=0.3$	10.80	22.62	251.04

^a Used acronyms: 1-Cyanonaphthalene (1-CN) (long pass filter: 375nm, Short pass filter: 320nm), 2,3-Dicyanonaphthalene (2,3-DCN)(long pass filter: 375nm, Short pass filter: 320nm), Pyrene (PY)(long pass filter: 375nm, Short pass filter: 320nm)

^b Used acronyms: heptane (HEP), cyclohexane (CYH), toluene (TOL), diethylether (DEE), butyronitrile (BUT), propylacetate (PRA), ethylacetate (ETA), tetrahydrofurane (THF), propylacetate mole fraction in propylacetate/butyronitrile mixture (x_P), dichloroethane (DCE)

chromophore because it was considered at that time that they are the part of molecule which is responsible for its colour. But chromophore is the molecule which absorbs light but fluorophore is the molecule which re emits the light after absorption. The umbrella term used in light emission is the luminescence, whereas fluorescence denotes allowed transitions with a lifetime in the nanosecond range from higher to lower excited singlet states of molecules.

The lifetime measurements were done at 297 K (i.e at constant temperature) and it was assumed that it remain constant for all the temperature range used for exciplexes. As mentioned previously that the solvent polarity and local environment have strong effects on the emission spectral properties of fluorophores. The effects of solvent polarity and environment are complex on the emission spectra. All the factors which influence the emission spectra are given as:

- Solvent polarity and viscosity

- Rate of solvent relaxation
- Rigidity of local environment
- Internal charge transfer
- Excited state reactions
- Probe-probe interactions
- Changes in radiative and non-radiative decay rates

All of these factors mentioned before help to investigate the local environment surrounding the fluorophore. However it is difficult to know that which effect is dominant in particular environmental system, and usually more than one factors are simultaneously effecting the fluorophore. When ever their is change in the emission spectra of fluorofore due to change in local environment around the fluorophore the quantum yields and the lifetimes are also changed so all the factors changing the emission spectra are also changing the fluorescence lifetimes.

All the fluorophores considered here are excited to the first singlet state (S_1). The excess vibrational energy is lost to the solvent and the solvent effects shift the emission to lower energy due to the stabilization of the excited state by the solvent molecules. Typically the fluorophores have larger dipole moment in excited state (μ_E) than in the ground state (μ_G). Soon after excitation the solvent dipoles can reorient or relax to (μ_E), which lowers the energy of excited state. In present discussion all those fluorophores are considered that are themselves polar and therefore, they display sensitivity to the solvent molecules. Only the fluorescence lifetime of 1-CN will be discussed here. The values of lifetimes are given in table: 4.10. With the increase of solvent polarity their is found decrease in the value of lifetime. The value of lifetime in non polar solvent was 17.66 ns with dielectric constant 1.91 and then in most polar solvent with dielectric constant 19.09 the value of lifetime decreases to 10.80 ns thus a decrease of 6.42 ns is observed for the fluorescence lifetime of fluorophore. This decrease in the value was due to the reduction in the radiative transition probability of fluorophore along with an increase in radiation less transition probability with increase of solvent polarity.¹²⁴ The reason of former decrease is the change in the electronic and geometrical structures of fluorophores with increase of solvent polarity and the reason behind the later mentioned increase is the decrease of the relevant energy gap owing to the lowering of the CT state energy by solvations.

In polar solvents the molecules of 1-CN are oriented in such away that their dipole moments compensate for the dipole moment of 1-CN in order to minimize the total energy of the system i.e fluorophore + solvation and resultantly decreasing the lifetimes as compared to lifetime in non polar solvents.

Another reason for the decrease in the fluorescence lifetime may be the solvent relaxation. This effect introduces an additional redshift to the stokes shift of the fluorophore

Table 4.11.: Fluorescence lifetimes for exciplex system 1-CN/HMB in solvents^a of different polarity at 297K. LED used is 340nm and long pass filter: 435nm. The solvents are arranged in the order of increasing solvent polarity from top of list to bottom.

Solvent	χ	t_1	t_2	Residue
		ns	ns	
HEP	1.20	0.98	13.06	4.72
CYH	0.91	1.05	12.15	3.75
TOL	0.82	1.21	14.29	4.99
DEE	0.94	1.01	15.31	5.00
BUT	0.99	0.99	15.97	4.09
PRA	0.93	1.12	16.15	3.99
ETA	1.18	1.08	16.98	4.71
THF	1.04	1.18	17.29	4.04
$x_P=0.9$	0.71	1.16	15.35	3.12
$x_P=0.8$	0.95	1.14	16.67	4.82
$x_P=0.7$	0.88	1.15	15.91	5.01
$x_P=0.6$	0.99	1.13	14.89	4.08
$x_P=0.5$	1.01	1.13	14.41	4.79
$x_P=0.4$	0.89	1.17	14.18	3.99
$x_P=0.3$	1.05	1.15	14.73	4.09

^a Used acronyms: heptane (HEP), cyclohexane (CYH), toluene (TOL), diethylether (DEE), butyronitrile (BUT), propylacetate (PRA), ethylacetate (ETA), tetrahydrofuran (THF), propylacetate mole fraction in propylacetate/butyronitrile mixture (x_P), dichloroethane (DCE)

and resultantly the 1-CN spectra tends to be more red shifted in more polar solvent. Consequently the lifetime decreases with increase in solvent polarity.

4.4.2. Fluorescence Lifetime of Exciplex

Here again only the exciplex system 1-CN/HMB is discussed. Exciplex lifetimes for rest of all exciplex systems are tabulated in section A.3.1. The fluorescence lifetimes for 1-CN/HMB exciplex system in solvents of different polarity are tabulated in table 4.11.

For exciplex formation and ET between 1-CN and HMB both the fluorophore and quencher diffuse to a shorter distance which requires a higher concentration of HMB and also long lifetimes of 1-CN. For this reason the selected concentration of 1-CN was $5 \times 10^{-5}M$ and the concentration of HMB was 0.08M. Also in sub-section 4.4.1 it is shown that 1-CN has relatively long lifetime. The extent of charge transfer and thus the lifetime depends strongly upon the environment in which the exciplex is formed. In this section it is again assumed that the fluorescence lifetime of exciplex is independent of

temperature and therefore only measurements were made by changing solvent polarity. In electron transfer reactions the solvent polarity is the major factor effecting the free energy of activation, the solvent influences an outer sphere reorganization energy. Also the dynamic solvent effect also plays an important role for the extent of electron transfer in photoinduced electron transfer reactions. This effect refers to the friction between the reactants and solvents molecules. Since the solvent environment and the reacting molecules in electron transfer are coupled electrostatically, the rates of electron transfer are influenced more dramatically and resultantly the lifetimes of exciplexes are also strongly effected by solvent polarity⁸⁶

Biexponential decay curves were obtained for 1-CN/HMB exciplex system (table: 4.11). Shorter component of lifetime was almost constant in all solvents and its value was approximately 1 ns. It is therefore suggested that this is the portion due to some unknown impurity, although the solvents were purified again but still it was not possible to get rid of this impurity. Whereas the other component i.e the longer component was observed to be changing with change in solvent polarity so this is the component which is considered as the lifetime of exciplex. On comparison between the lifetimes of 1-CN and 1-CN/HMB reduction in the lifetime of fluorophore (i.e 1-CN) is observed. Thus the lifetimes of exciplex are smaller than those of the fluorophores.

Gradual increase is observed in the lifetime of 1-CN/HMB exciplex in solvent with dielectric constant 1.91 till 7.36. Later with further increase of solvent dielectric constant (from 7.36 till 19.09) decrease is found in the lifetime values. The reason of decrease in exciplex lifetime with increase of solvent polarity may be that the exciplex is a charge transfer state and therefore it is polar and has a dipole moment. Therefore the energy of charge transfer state depends upon the polarity and upon the distance between A^- and D^+ due to the presence of columbic attractions between A^- and D^+ . Result of all these interactions is bathochromic shift of exciplex maxima upon increasing solvent polarity.⁴⁴ Therefore reduction is observed in fluorescence lifetime of exciplex with increase of solvent polarity. Also this decrease in lifetime may be due to the dissociation of exciplex into solvated radical ion pair. According to Weller^{16,51} this reduction is due to the competition between the formation of a solvated radical ion pair and exciplex formation from the encounter complex. Where as according to Mataga¹²⁹⁻¹³¹ this effect was due to the solvent dependence of electronic structure of exciplex. With increase of solvent polarity the energy gap between the zeroth-order CT state and the different non polar locally excited states increases and the different non polar locally excited states leads to a less extensive mixing of those locally excited states in exciplexes.¹³²

Whereas it appears that in solvent polarity range from 1.91 till 7.36 the radiative transition probability of fluorescence appears to decrease with increase of solvent polarity.

Exact reasons of this behavior are unknown, but it may be due to the change in the values for extent of charge transfer with change of solvent polarity. This will be discussed in up-coming sections.

4.5. Equilibrium constant for exciplex formation

The exciplex stability is supposed to be related with the concept, whether a particular excited state acceptor and donor can be converted into exciplex easily or not. As a matter of fact this is a kinetic aspect of stability which deals with the rate of the reaction and its mechanism. The other aspect of stability is thermodynamic aspect, in which stability of a complex is related with the amount of energy released during its formation or the amount of energy required to break it. In this section equilibrium constant for exciplex formation and the factors effecting it are discussed. The values of equilibrium constant for exciplex formation K_c was calculated by using equation number 2.56 of theory. The obtained values are given in table 4.12.

Thermodynamic stability and kinetic stability comes under the broad heading of formation of complexes in solution. These both terms are discussed as:

- Thermodynamic stability: This is a measure of the extent to which the complex (here exciplex) will form or will be transformed into another species under certain conditions, when the system has reached equilibrium state. This type of stability deals with the bond energies between the molecules of exciplex and also it deals with the stability constant.
- Kinetic stability: This refers to the speed with which transformation leading to the attainment of equilibrium will occur. This kinetic stability deals with the rate and mechanism of chemical reactions. For exciplex formation this reaction is electron transfer from donor to excited state acceptor.

In present section the thermodynamic stability is discussed because equilibrium constant for exciplex formation is under consideration. The factors effecting the equilibrium constant of formation are

- Size of donor and acceptor
- Charge present on donor or acceptor
- Polarizability of donor and acceptor
- Electronegativities of reacting species
- Ionization energies of reacting molecules
- steric effects
- Solvent dipole moment

Here stabilization constants of 1-CN/HMB exciplex in solvent of different polarity is discussed. Therefore size of donor and acceptor, electronegativity of reacting species and

Table 4.12.: Equilibrium constant for exciplex formation (K_c) and extent of charge transfer between donor and acceptor (z) for exciplex system 1-CN/HMB in solvents^a of different polarity at 297 K. The solvents are arranged in the order of increasing solvent polarity from top of list to bottom.

Solvent	K_c	z
HEP	0.74	-
CYH	0.76	0.66
TOL	1.12	0.61
DEE	1.12	0.75
BUT	1.23	0.56
PRA	1.26	0.67
ETA	1.43	0.56
THF	1.58	0.53
$x_P=0.9$	1.31	0.53
$x_P=0.8$	1.41	0.54
$x_P=0.7$	1.43	0.54
$x_P=0.6$	1.30	0.59
$x_P=0.5$	1.31	0.59
$x_P=0.4$	1.29	0.62
$x_P=0.3$	1.36	0.65

^a Used acronyms: heptane (HEP), cyclohexane (CYH), toluene (TOL), diethylether (DEE), butyronitrile (BUT), propylacetate (PRA), ethylacetate (ETA), tetrahydrofuran (THF), propylacetate mole fraction in propylacetate/butyronitrile mixture (x_P), dichloroethane (DCE)

ionization energies of reacting species are constant. No charges are present either on donor or acceptor so this factor cannot be effecting here. As large bulky groups are not attached with neither donor nor acceptor therefore this effect is also not effecting in this discussion. The parameters effecting the equilibrium constant of formation are polarizability of donor and acceptor because the solvent polarity changes the polarizability and the dipole moment of solvent.

Except in n-heptane and cyclohexane values of equilibrium constant greater than one are observed. Values of equilibrium constant smaller than one means that the fluorophore lifetimes in theses solvents have values smaller than the exciplex lifetimes in these solvents. Equilibrium constants with values larger than one were observed by Ji Hoon Lee et all for exciplex of pyrene with silverperchlorate¹³³ and also by Pierre Valat and co for exciplexes of dibenzoylmethanatoboron difluoride with benzene.¹³⁴ The exciplex systems with value of equilibrium constant lower than one were observed by Sadhan Basu for exciplexes of pyrene with benzene, p-xyiene and mesitylene. Also for exciplexes of

Anthracene with benzene, p-xylene and mesitylene.¹³⁵ By looking at the table: 4.12 it is observed that there is an increase in the value of equilibrium constant of formation in solvents with solvent polarity from 1.91 till 7.36. The solvent in which highly stable exciplexes are formed is tetrahydrofuran because this is the system in which the highest value of equilibrium constant is observed. Then with further increase of solvent polarity there is a slight decrease in the value of equilibrium constant because with further increase of solvent polarity the exciplex dissociates into radical ion pairs. The solvent in which the exciplex system is most stabilized should be n-heptane because this is the solvent with least dipole moment (non polar solvent) and also in previous discussion it was found to be most stable. But the reason for getting stable exciplex systems in tetrahydrofuran is not known.

4.6. Extent of charge transfer between donor and acceptor

Extent of charge transfer cannot be calculated by using A.Weller's mechanism. Kuzmin defines exciplex systems on the basis of extent of charge transfer. According to him exciplex systems are either:

- Partial charge transfer with value for extent of charge transfer less than one or they can be.
- Full charge transfer with value for extent of charge transfer greater than one.

This nomenclature is described in section 2.6.6 of theory. According to Kuzmin's scheme equation 2.90 or 2.91 can be used to categorize the exciplexes as full or partial charge transfer. Strange values were obtained by using both of equations. By using equation 2.90 negative values for "z" were obtained which are simply not possible. The reason for getting a negative value is that the ratio of exciplex lifetime and fluorophore lifetime has a value greater than one and the value for ratio of exciplex fluorescence frequency to the fluorescence frequency of fluorophore is less than one and by taking ratios of these two quantities the resultant digit is larger than one. Upon subtraction of this quantity from one the result is a negative value. This negative value of "z" shows that the exciplex system is formed with full charge transfer between donor and acceptor. Whereas when value of "z" is calculated by using equation 2.91 positive values are obtained but these values are greater than one. The maximum value of "z" obtained here is 2.3 (in n-heptane) and the minimum value of "z" obtained is 1.1 (in n-butylacetate). In system 1-CN/HMB only one electron can be donated from donor to acceptor and therefore the maximum value of "z" which can be obtained is 1 but here all values obtained are larger than 1 so these values cannot be used for further calculations. Thus values obtained by these equations just show that the exciplex formed is full charge transfer therefore another equation should

be used which is suitable for system with partial charge transfer exciplex. Also the values of K_c greater than 1 (discussed in section 4.12) shows that the 1-CN/HMB exciplex is formed with full charge transfer between donor and acceptor. Therefore in order to get the value of “z” the Kuzmin’s model for partial charge transfer is used and according to this model the value of “z” is calculated by using the equation :2.105.

Now comparison can be made between the equations used to calculate the value of “z”. By looking at equations 2.90, 2.91 and 2.105 it is observed that the value of extent of charge transfer depends upon different factors if the exciplex system is with partial charge transfer or with full charge transfer. The factors effecting the extent of charge transfer in partial and full charge transfer exciplex system are discussed separately as.

Factors effecting “z” for full charge transfer exciplexes: For full charge transfer exciplexes according to equation number 2.90 the value of “z” depends directly upon the rate constant for exciplex formation and average fluorophore frequency thus with increase in the value of these two parameters larger will be extent of charge transfer. The value of “z” is inversely proportional to the rate constant of fluorophore formation and the average fluorophore frequency so here decrease will be observed in “z” with decrease in these two values. According to equation number 2.91 the value of extent of charge transfer depends directly on the under root of shift of exciplex peak with respect to fluorophore peak and the enthalpy of charge transfer. Therefore if their is larger shift value and larger enthalpy the larger will be extent of charge transfer observed here. The value of “z” according to this equation depends inversely upon the square root of destabilization factor “a” and function of solvent polarity and temperature. Thus with the increase of solvent polarity, solvent refractive index and destabilization energy their should be a decrease in the value of extent of charge transfer.

Factors effecting “z” for partial charge transfer exciplexes: The extent of charge transfer depends upon less factors if the exciplex system is with full charge transfer. According to equation number 2.105 it depends directly upon the exciplex spectral shift with respect to fluorophore and inversely it depends upon the H_{12} i.e the matrix element coupling charge transfer and the locally excited states, m which itself depends upon the square root of dipole moment and radius of solvation shell (see equation number 2.94) and also on the function of refractive index. Thus for exciplexes with partial charge transfer the extent of charge transfer doesn’t depends upon the solvent polarity. In section 4.3.1 it is mentioned that the extent of charge transfer is independent of solvent polarity because inverse relation was obtained between zero-zero-transition energy and solvent polarity. The value of extent of charge transfer used in further calculations are given in table 4.12. By looking at this table it is observed that no good relation is present between “z” and solvent polarity thus confirming the comment made before that extent of charge transfer

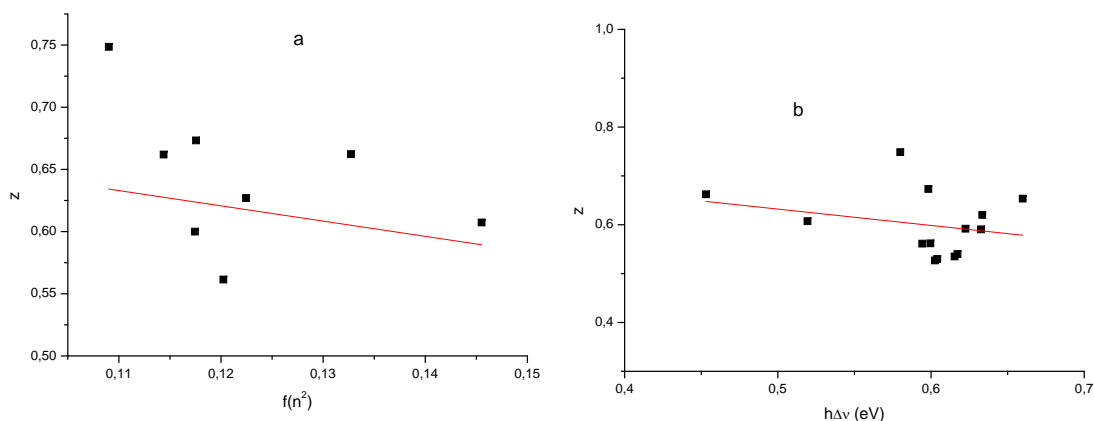


Figure 4.14.: Extent of charge transfer for 1-CN/HMB exciplex system as a function of a: function of refractive index, b: exciplex spectral shift with respect to fluorophore.

is independent of solvent polarity. The graph between function of refractive index and extent of charge transfer is given in figure 4.14(a). This figure shows an inverse relation between both parameters. For propylacetate/butyronitrile solvent mixture the value of refractive index remains constant for all mole fractions but the value of “z” obtained was in the range of 0.5 to 0.6. This small change in the value was due to the fact that other parameters like exciplex spectral shift with respect to fluorophore, m and the matrix element coupling charge transfer and the locally excited states also effects the value of “z”.

Another parameter on which extent of charge transfer depends is the exciplex spectral shift with respect to fluorophore. Figure 4.14(b) represents the relationship between these two parameters. An inverse relation is observed between these two quantities for 1-CN/HMB. Reason for obtaining this inverse relation between these two parameters is unknown. Relation between H_{12} and “z” is discussed in upcoming discussion.

4.7. Parameters appearing in Kuzmin’s equations:

As mentioned already that the exciplex formed shows full charge transfer from donor to acceptor so the calculations mentioned in paragraph 2.6.6 of theory will be used for further calculations of thermodynamic parameters. Some parameters are also appearing in these calculations which are given as under.

- Destabilization energy (a)
- Value of m

Table 4.13.: Kuzmin's parameters for exciplex system 1-CN/HMB in solvents^a of different polarity used in further calculations. The solvents are arranged in the order of increasing solvent polarity from top of list to bottom.

Solvent	a	m	$H_{22} - H_{11}$	H_{12}
	eV	eV	eV	eV
HEP	-	0.48	-	-
CYH	-0.14	0.48	0.06	0.03
TOL	-0.16	0.48	-0.08	0.39
DEE	0.26	0.48	-0.24	0.36
BUT	-0.15	0.48	0.03	0.53
PRA	0.16	0.48	-0.12	0.44
ETA	0.08	0.48	0.03	0.56
THF	-0.01	0.48	0.11	0.58
$x_P=0.9$	0.00	0.48	0.10	0.60
$x_P=0.8$	0.00	0.48	0.10	0.61
$x_P=0.7$	-0.07	0.48	0.10	0.59
$x_P=0.6$	0.00	0.48	0.03	0.52
$x_P=0.5$	-0.03	0.48	0.04	0.53
$x_P=0.4$	-0.08	0.48	0.01	0.49
$x_P=0.3$	0.07	0.48	-0.01	0.53

^a Used acronyms: heptane (HEP), cyclohexane (CYH), toluene (TOL), diethylether (DEE), butyronitrile (BUT), propylacetate (PRA), ethylacetate (ETA), tetrahydrofuran (THF), propylacetate mole fraction in propylacetate/butyronitrile mixture (x_P), dichloroethane (DCE)

•Difference between the matrix element coupling of charge transfer and locally excited state ($H_{22}^{\circ} - H_{11}^{\circ}$) representing the energies of ψ_1 and ψ_2 at the exciplex.

The values of all these parameters in solvents of different polarity are tabulated in table reftab:kuzmin-para-(1-CN/HMB).

•Coupling matrix element between the locally excited and charge transfer states (H_{12}) These parameters are discussed separately as under:

Destabilization energy (a) The equation used to calculate this parameter is discussed already in equation 2.104. The values of this parameter is given in table number 4.13. Thus it is observed that the destabilization energy depends directly upon the difference between the matrix element coupling of charge transfer and locally excited state ($H_{22}^{\circ} - H_{11}^{\circ}$), matrix element coupling between the locally excited and charge transfer states (H_{12}) and extent of charge transfer (z). From figure ?? it is seen that a direct relation is present between the dielectric constant and the extent of charge transfer. Direct relation between these parameters is also confirmed from equation 2.104. Although their should

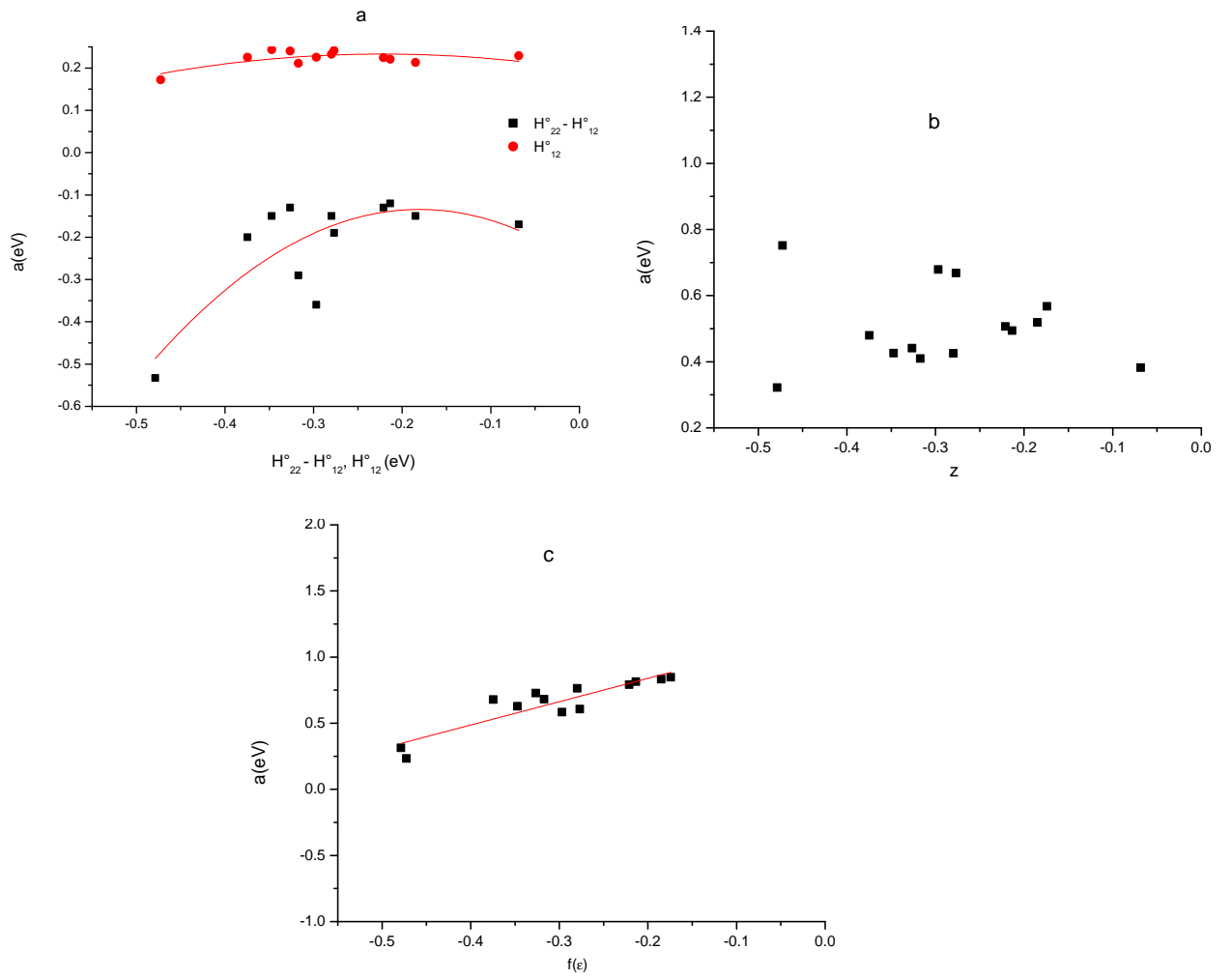


Figure 4.15.: Dependence of destabilization energy on Fig a: $H_{22} - H_{11}, H_{12}$ fig b: z and fig c: function of dielectric constant.

Table 4.14.: Dipole moment (μ_{EX} (D)) and hypothetical gas phase exciplex fluorescence maximum (μ_{EX}° (D)) for exciplex system 1-CN/HMB in solvents^a of different polarity. $r_{exc} = 8.13 \times 10^{-8} cm$, slope from graph between ν_{max} and $f - 1/2f' = -8278.9 cm^{-1}$, $\mu_{EX} = 5.94D$. The solvents are arranged in the order of increasing solvent polarity from top of list to bottom.

Solvent	μ_{EX}° D
HEP	5.41
CYH	5.33
TOL	5.10
DEE	5.06
BUT	4.91
PRA	4.86
ETA	4.89
THF	4.76
$x_P=0.9$	4.79
$x_P=0.8$	4.75
$x_P=0.7$	4.72
$x_P=0.6$	4.69
$x_P=0.5$	4.68
$x_P=0.4$	4.67
$x_P=0.3$	4.66

^a Used acronyms: heptane (HEP), cyclohexane (CYH), toluene (TOL), diethylether (DEE), butyronitrile (BUT), propylacetate (PRA), ethylacetate (ETA), tetrahydrofuran (THF), propylacetate mole fraction in propylacetate/butyronitrile mixture (x_P), dichloroethane (DCE)

be a direct relation between destabilization energy and $(H_{22}^{\circ} - H_{11}^{\circ})$, (H_{12}) , but due to the unknown reasons inverse relation is found between them.

Value of m: Value of m can be calculated by using equation number 2.103 mentioned in theory. Value of m for partial charge transfer exciplexes depends upon the exciplex dipole moment and also on the radius of solvation shell (as mentioned in equation number 2.94). So for calculation of "m" first the dipole moment is calculated by using the equation 2.97. The value of dipole moment is given in given in table 4.14 and the graph between ν_{max} and $f - 1/2f'$ is given in appendix A.4 .

By looking at table 4.14 it is observed that with the increase of solvent polarity there is a slight decrease in the value of hypothetical gas phase exciplex fluorescence maximum thus showing that the exciplex is destabilized with increase of solvent polarity. The value of μ_{EX} obtained from the solvatochromic method represents an average value in solution, while for the purpose of comparison the exciplex dipole moments in the gas phase, μ_{EX}° ,

are given. The value of μ_{EX}° reflects the intrinsic donor-acceptor interactions without solvent effects. The relationships between μ_{EX}° and μ_{EX} is given by the relation:

$$\mu_{EX} = \mu_{EX}^{\circ} \phi(\epsilon, n^2) \quad (4.1)$$

where $\phi(\epsilon, n^2)$ a classical correction term for a polarizable dipole in a spherical cavity immersed in a dielectric isotropic medium. For exciplexes that are essentially CRIPs, solvent induced polarization is insignificant ($\mu_{EX} = \mu_{EX}^{\circ}$). For exciplexes with less than full electron transfer (those with low μ_{EX}) solvent-induced enlargement of μ_{EX} is known to be substantial owing to the reaction field set up by the solvent in opposing the electrical field generated by the exciplex dipole moment. For 1-CN/HMB exciplex system larger values of μ_{EX} , larger value of extent of charge transfer and appearance of strongly emissive exciplex peak in emission spectra shows that this exciplex system is CRIP and therefore ($\mu_{EX} \approx \mu_{EX}^{\circ}$) the CRIPs are not polarizable.

So now after calculating the value of dipole moment and putting values in equation 2.94 the value of “m” is found to be 0.48 eV. This value is used for further calculations.

Value of ($H_{22}^{\circ} - H_{11}^{\circ}$): This parameter was calculated by using equation 2.103. As already mentioned that this parameter represents the energies of ψ_1 and ψ_2 at the exciplex. As already mentioned that the exciplex is a resonance hybrid of locally excited and charge transfer states. ψ_1 is the wave function representing the locally excited state and ψ_2 is the wave function for charge transfer state so the parameter ($H_{22}^{\circ} - H_{11}^{\circ}$) represents the energy difference between these two states. This parameter depends upon many factors and graphically for the exciplex system 1-CN/HMB the dependence of this parameter on many factors is given in figure 4.16. According to equation 2.103 there should be a direct relation between solvent polarity and ($H_{22}^{\circ} - H_{11}^{\circ}$) and looking on figure 4.16 it is observed that same behavior was followed by the system under discussion (fig: 4.16). Similarly this parameter depends directly upon the H_{12} and same behavior was observed here.

Value of H_{12} : As already mentioned that this parameter is the matrix element coupling between the locally excited and charge transfer states. Graphical representation of many factors effecting H_{12} is given in figure 4.17. As larger the coupling between the locally excited and charge transfer states as larger will be the value of H_{12} . Equation number 2.106 is used to calculate the value of this parameter. This parameter should depend directly upon the shift of exciplex peak with respect to fluorophore and by looking at figure 4.17 it was observed that same relation is observed. Similarly this parameter should depend directly upon the function of refractive index and same relation was observed here.

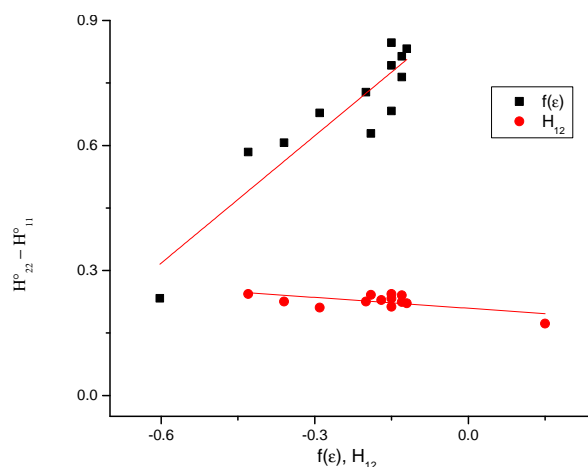


Figure 4.16.: Dependence of $(H_{22}^o - H_{11}^o)$ on various factors for 1-CN/HMB.

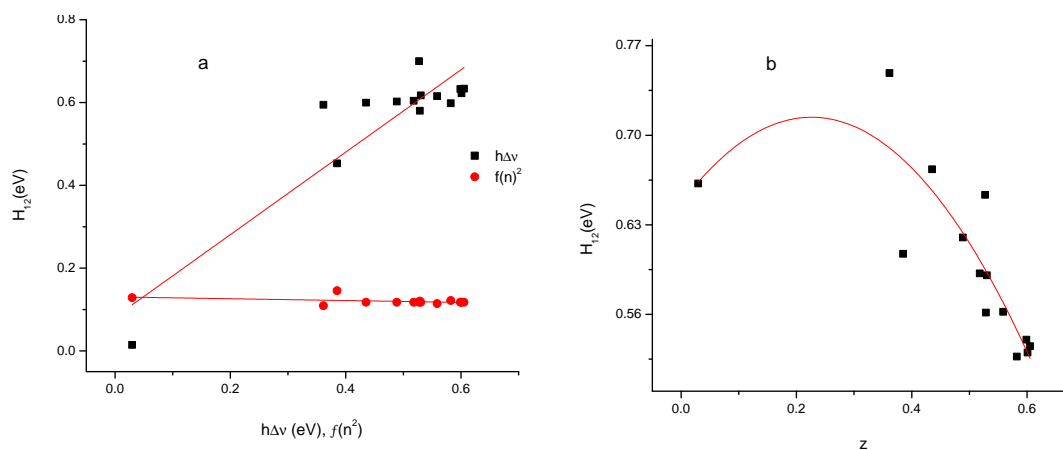


Figure 4.17.: Dependence of (H_{12}) on fig a: function of dielectric constant and spectral shifts, and b: extent of charge transfer.

According to figure 2.103. H_{12} depends directly upon the extent of charge transfer but by looking the figure 4.17 it is observed that an inverse relation is present for present system and the reason for this relation is unknown.

4.8. Enthalpy of Exciplex Formation

In this section the enthalpy of exciplex formation calculated according to the model of A.Weller and the M.G.Kuzmin will be discussed. Both these models are discussed already in theory. The Term enthalpy includes the internal energy, i.e, the energy required to create a system, thus it is the total energy of system therefore it is a thermodynamic

Table 4.15.: Enthalpy of exciplex formation (ΔH_{EX}^* (kJ/mol)) for exciplex system 1-CN/HMB calculated according to model proposed by A.Weller and M.G.Kuz'min in solvents^a of different polarity. The solvents are arranged in the order of increasing solvent polarity from top of list to bottom.

Solvent	ΔH_{EX}^* (kJ/mol)	ΔH_{EX}^* (kJ/mol)
	A.Weller model	M.G-Kuz'imn's model
HEP	-6.86	-
CYH	-6.76	-15.76
TOL	-7.13	-33.38
DEE	-5.14	-13.04
BUT	-3.15	-31.09
PRA	-3.31	-16.78
ETA	-3.47	-9.18
THF	-3.19	-12.51
$x_P=0.9$	-2.91	-12.21
$x_P=0.8$	-0.69	-13.82
$x_P=0.7$	-0.40	-21.78
$x_P=0.6$	-2.72	-22.29
$x_P=0.5$	-2.71	-25.86
$x_P=0.4$	-3.17	-34.17
$x_P=0.3$	-5.67	-27.61

^a Used acronyms: heptane (HEP), cyclohexane (CYH), toluene (TOL), diethylether (DEE), butyronitrile (BUT), propylacetate (PRA), ethylacetate (ETA), tetrahydrofurane (THF), propylacetate mole fraction in propylacetate/butyronitrile mixture (x_P), dichloroethane (DCE)

potential, a state function and an extensive quantity. Equation 2.54 is used to calculate this value according to Weller's mechanism and equation 2.102 is used to calculate this value according to Kuzmin's mechanism. The resulting values obtained are given in table 4.15. According to A.Weller mechanism the enthalpy of exciplex formation was determined from the temperature dependence of quantum yields and the ratio of quantum yield of exciplex emission and fluorophore emission in presence of quencher is plotted against reciprocal of temperature. The plotted graphs are given in figure A.19. Graphs in remaining solvents are given in A.19. In majority of solvents both branches of the temperature dependence were obtained but for cyclohexane, dichloroethane, diethylether and n-heptane only one branch for temperature dependence was obtained and reason for this was that T_{max} for a exciplex here was beyond the experimentally accessible range of temperature.⁶⁹ For this model the enthalpy of exciplex formation depends upon following factors:

- ratio of quantum yield of exciplex emission and fluorophore emission in presence of

4.8. Enthalpy of Exciplex Formation

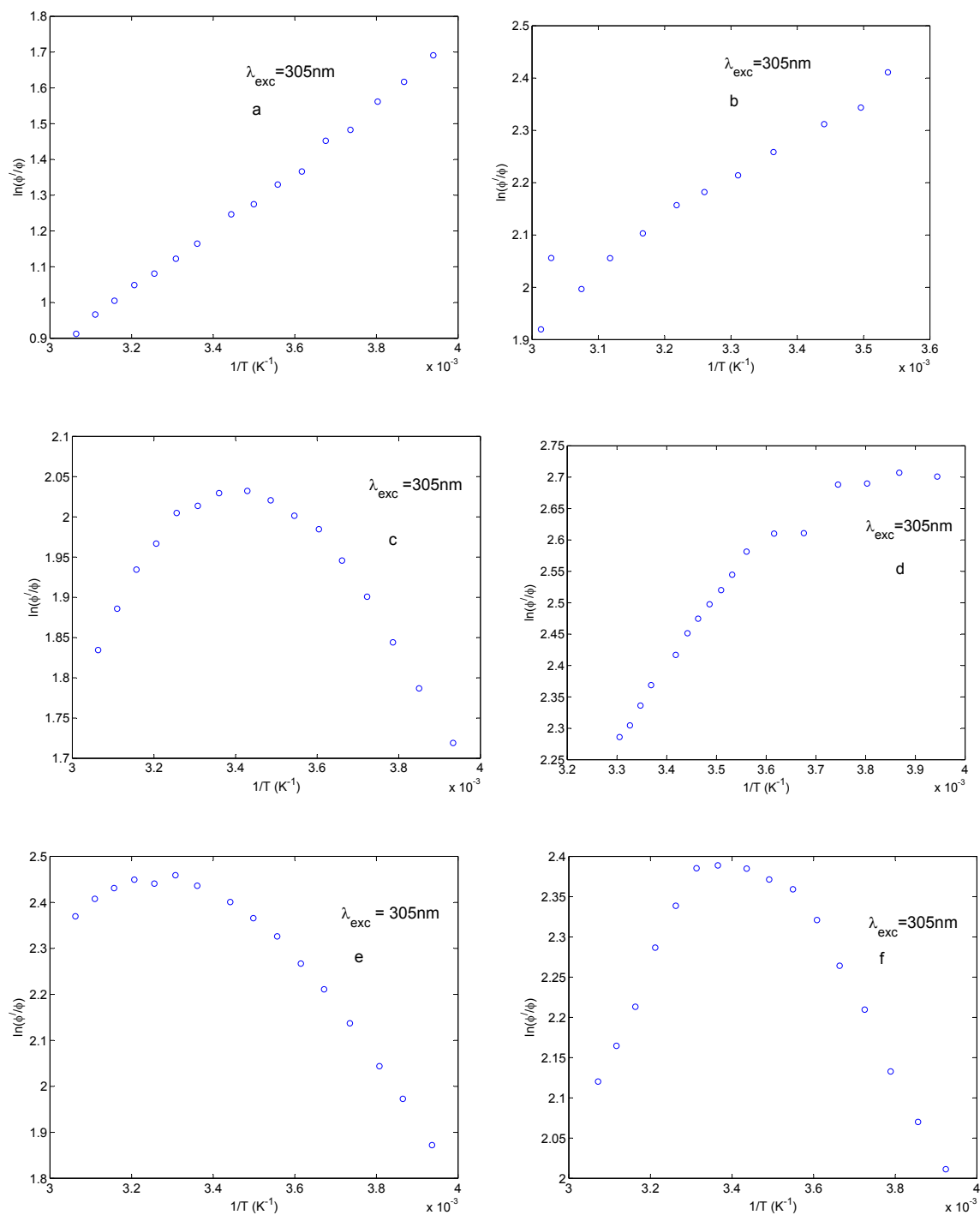


Figure 4.18.: The reciprocal temperature dependence of $\ln(\phi'/\phi)$ for the exciplexes of 1-CN/HMB in a:n-heptane, b:cyclohexane, c:toluene, d:diethylether, e:n-butylacetate, f:propylacetate.

quencher.

- quencher concentration.
- ratio of lifetime of exciplex to fluorophore.
- entropy of exciplex formation.

For 1-CN/HMB exciplex system the concentration of quencher was constant in all solvents therefore this factor was constant for the whole system. Whereas no temperature dependence was used for calculation of enthalpy for the M.G-Kuzmin's model. Here the enthalpy of exciplex formation depends upon the following factors:

- difference between the matrix element coupling of charge transfer and locally excited state ($H_{22}^o - H_{11}^o$)
- destabilization energy (a).
- Parameter m.
- Function of refractive index and dipolemoment.

Thus all the factors mentioned above depends upon the solvent polarity so the entropy values for all the systems depends upon the solvent polarity. Looking at the table number 4.15 it is observed that negative values are obtained for both the models. Their should be decrease in the enthalpy values on increase of solvent polarity and this trend was for the calculations obtained from A.Weller, but for the values obtained from M.G.Kuzmin's model no relation was observed between enthalpy and solvent polarity and therefore no generalization could be drawn here. Thus the A.Weller model was proved to be more applicable compared to the M.G.Kuzmin's model.

4.9. Entropy of Exciplex Formation

This section deals with the entropy of exciplex formation calculated according to A.Weller and M.G.Kuzmin's model. According to A.Weller model equation number 2.54 is used to calculate this value and according to M.G.Kuzmin's model equation number 2.109 is used to calculate the value of entropy of exciplex formation. The obtained values are given in table 4.16. For calculation of entropy of exciplex formation according to A.Weller's model lifetimes for both radiative and non radiative decay of fluorophore and exciplex are required. In our lab we can measure the fluorescence lifetime of fluorophore and exciplex, therefore by ignoring the lifetime of non radiative decay and considering only the radiative decay of fluorophore and exciplex the entropy values are calculated therefore these values can give just a rough idea about the entropy of exciplex formation. The entropy values according to A.Weller model depend upon following factors:

- ratio of quantum yield of exciplex emission and fluorophore emission in presence of quencher.

Table 4.16.: Entropy of exciplex formation (ΔH_{EX}^* (kJ/mol)) for exciplex system 1-CN/HMB calculated according to model proposed by A.Weller and M.G.Kuzmin in solvents^a of different polarity. The solvents are arranged in the order of increasing solvent polarity from top of list to bottom.

Solvent	ΔS_{EX}^* (J/mol K)	ΔS_{EX}^* (J/mol K)
	A.Weller model	M.G-Kuzmin's model
HEP	-15.86	-0.02
CYH	-6.19	-0.03
TOL	-6.06	-0.03
DEE	-0.94	-0.05
BUT	-11.91	-0.06
PRA	1.89	-0.06
ETA	14.3	-0.06
THF	27.38	-0.07
$x_P=0.9$	11.48	-0.07
$x_P=0.8$	18.03	-0.07
$x_P=0.7$	21.83	-0.08
$x_P=0.6$	9.49	-0.08
$x_P=0.5$	9.62	-0.08
$x_P=0.4$	1.79	-0.08
$x_P=0.3$	-10.46	-0.09

^a Used acronyms: heptane (HEP), cyclohexane (CYH), toluene (TOL), diethylether (DEE), butyronitrile (BUT), propylacetate (PRA), ethylacetate (ETA), tetrahydrofuran (THF), propylacetate mole fraction in propylacetate/butyronitrile mixture (x_P), dichloroethane (DCE)

- quencher concentration.
- ratio of radiative lifetimes of exciplex to fluorophore.
- ratio of non radiative lifetimes of exciplex to fluorophore.
- enthalpy of exciplex formation.

Here the concentration of quencher was constant in all solvents so this factor is constant for this system. Although the non radiative decay lifetimes of fluorophore and exciplex increases with the increase of solvent polarity due to the decrease of exciplex and fluorophore radiative rates and dissociation of exciplex finally into radical ion pairs, but due to the unavailability of data this factor was ignored and approximate entropy values were calculated. Intercept of graph between ratio of quantum yield of exciplex emission and fluorophore emission in presence of quencher ($\ln(\phi'/\phi)$) and reciprocal of temperature is used for calculation of entropy value. The graph between these parameters are already discussed in section 4.8. The entropy values according to M.G.Kuzmin depend upon following factors

- parameter m
- function of dielectric constant
- temperature

By looking at table 4.16 it is observed that negative values are obtained from the calculations of both the models. These negative values are not surprising as these are characteristic of charge transfer complex. Slightly higher values are obtained from the A.Weller's mechanism compared to the M.G.Kuzmin's value and the reason is that the non radiative rates are ignored for A.Weller mechanism. With the increase of solvent polarity there is first an increase in the value of entropy (from n-heptane to tetrahydrofuran) and then with further increase of solvent polarity there is decrease in the value (from 0.9 mole fraction of propylacetate in propylacetate/butyronitrile mixture till the highest polar solvent i.e 0.3 mole fraction of propylacetate in propylacetate/butyronitrile mixture). The reason of first increase in entropy value is not known but the reason of decrease in value is that the exciplex is destabilized with increase of solvent polarity and finally it dissociates into radical ion pairs. Whereas for entropy values according to M.G.Kuzmin there is found to be a gradual decrease in the value with increase of solvent polarity thus showing that slow destabilization of exciplex between 1-CN and HMB.

4.10. Gibb's Energy of Exciplex Formation

Equation 2.58 is used to calculate the Gibb's free energy of exciplex formation according to A.Weller and equation 2.107 is used to calculate the Gibb's free energy according to M.G-Kuzmin's mechanism. The values of Gibb's free energy calculated by using these equations are tabulated in table: 4.17. Looking at table 4.17 it is observed that no reasonable relation is obtained between function of dielectric constant and Gibb's free energy. According to A.Weller the Gibb's energy of electron transfer depends upon following factors:

- temperature
- equilibrium constant of exciplex formation
- lifetime of exciplex formation
- lifetime of fluorophore

Temperature was constant at 297.15 K so this parameter was constant in present situation. According to equation number 2.58 there should be a direct relation between equilibrium constant of exciplex formation, lifetime of exciplex formation and Gibb's energy of electron transfer, but for present system direct relation is present between Gibb's energy of electron transfer and fluorescence lifetime of fluorophore, reason of this behavior is unknown (figure:4.19). Similarly due to unknown reasons inverse relation is observed

Table 4.17.: Gibb's energy of exciplex formation (ΔH_{EX}^* (kJ/mol)) for exciplex system 1-CN/HMB calculated according to model proposed by A.Weller and M.G.Kuz'min in solvents^a of different polarity. The solvents are arranged in the order of increasing solvent polarity from top of list to bottom.

Solvent	ΔG_{EX}^* (kJ/mol)	ΔG_{EX}^* (kJ/mol)
	A.Weller model	M.G-Kuz'min's model
HEP	0.70	-
CYH	0.63	-15.51
TOL	-0.26	-32.69
DEE	-0.27	-12.59
BUT	-0.49	-30.52
PRA	-0.53	-16.22
ETA	-0.83	-9.97
THF	-1.06	-11.88
$x_P=0.9$	-0.62	-11.59
$x_P=0.8$	-0.79	-13.15
$x_P=0.7$	-0.83	-21.07
$x_P=0.6$	-0.62	-21.55
$x_P=0.5$	-0.64	-25.09
$x_P=0.4$	-0.60	-33.38
$x_P=0.3$	-0.72	-26.81

^a Used acronyms: heptane (HEP), cyclohexane (CYH), toluene (TOL), diethylether (DEE), butyronitrile (BUT), propylacetate (PRA), ethylacetate (ETA), tetrahydrofuran (THF), propylacetate mole fraction in propylacetate/butyronitrile mixture (x_P), dichloroethane (DCE)

between Gibb's energy of electron transfer, fluorescence lifetime of exciplex and equilibrium constant of exciplex formation (figure: 4.19). According to M.G-Kuzmin the Gibb's free energy of exciplex formation depends upon following factors: •difference between the matrix element coupling of charge transfer and locally excited state ($H_{22} - H_{11}$)

•destabilization energy (a)

•factor m

•function of dielectric constant $m(\epsilon)$

Equation 2.107 shows that Gibb's energy of electron transfer directly depends upon all the factors mentioned before. Figure:4.19 shows that no good relation is obtained between all the parameters mentioned before and Gibb's energy of electron transfer therefore no generalization could be drawn here.

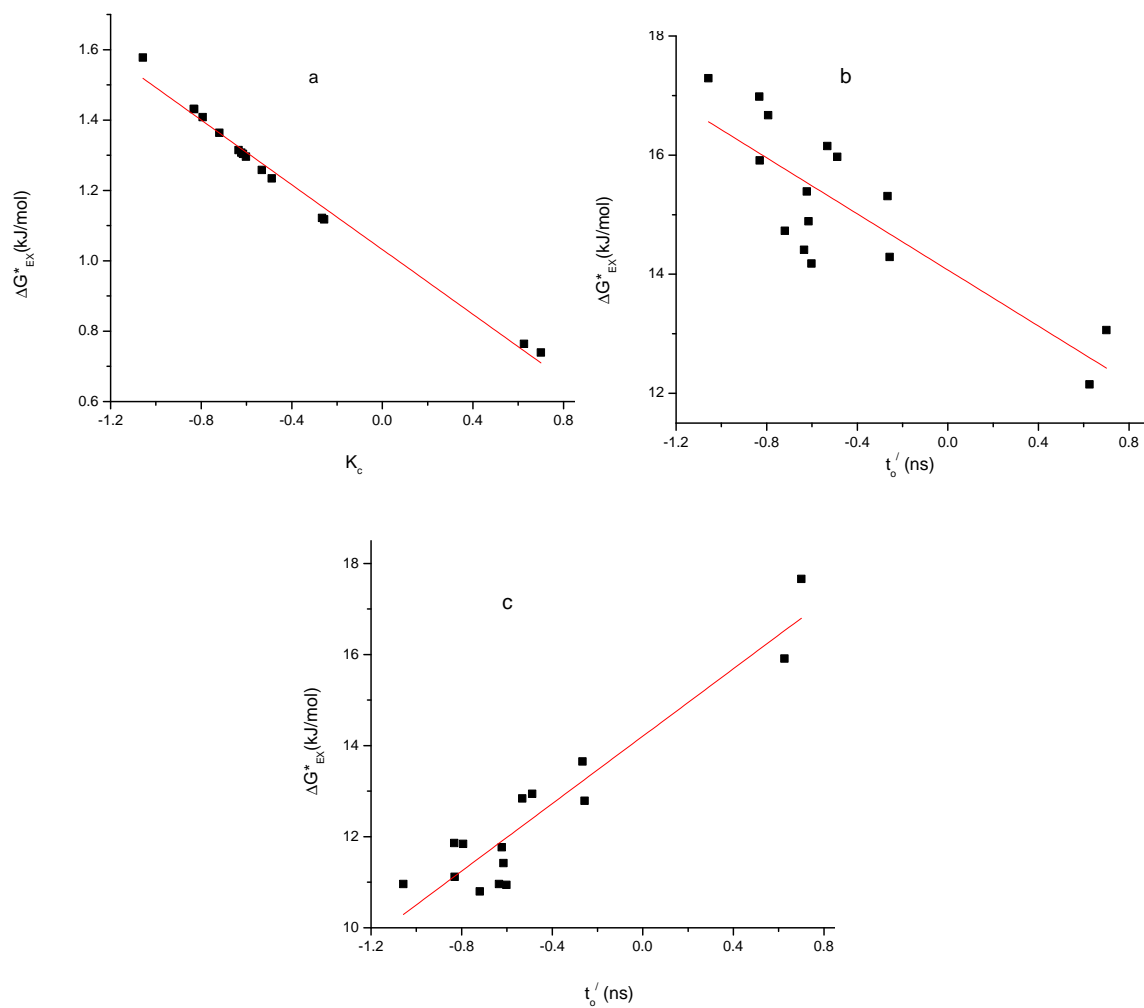


Figure 4.19.: Dependence of Gibb's energy of electron transfer on fig a: Stabilization energy, fig b: fluorescence lifetime of exciplex and fig c: fluorescece lifetime of fluorophore.

5. Conclusions and Outlooks

Everyone is a genius at least once a year. The real geniuses simply have their bright ideas closer together.

(Georg Christoph Lichtenberg)

5.1. Concluding Remarks

Main focus of present thesis was on the photoinduced electron transfer from the donor to acceptor as a result of which an exciplex is formed. Later on the effect of solvent polarity and temperature was studied on the stability and energetics of the formed exciplexes. Then comparison was made between the kinetic models proposed by A.Weller and M.G.Kuz'min. As a first step the mechanism of exciplex formation and the factors effecting it were studied from literature. The first step of experiment was development of thermally insulated box with cuvette holder inside it, later on this thermally insulated box was attached with the fluoromax and the thermostat. Tricky part of this construction was attachment of liquid light guides with the cuvette holder present inside the box because the light guides are very sensitive to temperature and they get frozen at 268.15 and they are destroyed at 308.15 K. Details about the construction of this assembly are given in section 3.4.1. Then the calibration of assembly was performed. As a first step of experimental work the fluorescence spectra of fluorophore was recorded and then the effect of solvent polarity and temperature was observed on it. The fluorophore peak intensity was observed to be unaffected with the change of temperature. Only inverse relation was observed for the intensity and peak position of fluorophore upon increase of solvent polarity thus reflecting the destabilization of fluorophore with the increase of solvent polarity due to the reduction in the energy levels of excited states. Next step of work was the selection of appropriate quenchers and then adding them into the fluorophore solutions. The excitation wavelengths were observed to be constant upon the addition of quencher into the solution. Appearance of broad structureless band towards the bathochromic side represents the formation of exciplex. All the exciplexes observed were strongly emissive

and they were dipolar as they all were red shifted. Change in the behavior of exciplex was observed on increase of solvent polarity and temperature. For some exciplex systems the distortion polarization dominates and result is the appearance of direct relation between shift of exciplex peak with respect to fluorophore and temperature and, for other systems the orientation polarization dominates and resultantly inverse relation is found between shifts values and temperature. With the increase of solvent polarity at constant temperature for most of systems their was observed an increase in shift values due to the changes in the geometrical structure of exciplex and as a result of it the electronic delocalization interactions are also changed, therefore the exciplex is destabilized at high solvent polarity. Details about the further emission intensity and the reason about the behavior of pyrene is discussed further in section 4.1. Then ratio of exciplex peak intensity to the fluorophore peak intensity with quencher was discussed in 4.2.2.

In the next part of thesis the effect of temperature and solvent polarity was observed on the parameters obtained from the fittings of Kuzmin's model of self-consistent polarization. The obtained parameters were the zero-zero transition energy, huang-rhys factor, gauss broadening of vibronic level and the energy of the dominant high-frequency vibration. In order to obtain all these parameters fittings were performed on the isolated emission spectra of exciplexes in all solvents, over a range of temperatures. From results an inverse relation was observed between zero-zero transition energy and reason of it was the increase in the charge recombination of CRIPs. Couplings between the ground and excited state were observed to be dependent on the solvent's reorganization energy because the gauss broadening of vibronic level was also dependent on solvent polarity and temperature. Spectral broadenings and spectral shifts were observed to have different origin. Increase in the non-radiative decay of exciplex on the increase of solvent polarity was confirmed due to inverse relation between energy of maximum high frequency vibration and solvent polarity.

Later on the fluorescence lifetimes for fluorophore and exciplex were discussed as a function of solvent polarity. It was assumed here that the fluorescence lifetimes were unaffected with the change of temperature. Also only the results for 1-CN/HMB were discussed. Some unexpected behaviors were obtained here and these are discussed in this sections. The mono exponential decay curves were observed for fluorophore and the lifetimes were observed to dependent upon solvent polarity, rate of solvent relaxation, internal charge transfer, and changes in radiative and non-radiative decays. For 1-CN/HMB exciplex system bi exponential decay curves were obtained and the reason for obtaining these bi exponential curves was the presence of some unknown impurity in the system. Gradual increase was observed in the lifetimes of exciplex with dielectric constant from 1.91 till 7.36 and then in solutions with dielectric constant from 7.36 till

19.09 decrease in lifetimes were observed. Reasons for this behavior is discussed in this portion.

Then the equilibrium constant for exciplex formation was calculated and in section 4.5 the effect of charge present on donor and acceptor, electronegativities of reacting species, ionization energies of reacting molecules, and solvent dipole moment were discussed. Extent of charge transfer was then discussed and it was observed that the system under discussion (i.e 1-CN/HMB) was full charge transfer exciplex system because the value of extent of charge transfer was observed to be larger than one. In this section the factors effecting the extent of charge transfer along with the obtained results were discussed. The value of extent of charge transfer was observed to be increasing with the the increase of solvent polarity representing the destabilization of exciplex and then final dissociation of exciplex into radical ion pairs.

In last part of of thesis Comparison was made between the kinetics models proposed by A.Weller and M.G.Kuz'min. In start of thesis mathematical details about theses models along with the proposed schemes were discussed and then in last part of results and discussions comparison was made between the entropy, enthalpy and gibb's energy of exciplex formation calculated from these models. Some additional parameters were appearing in Kuz'min's equation, all these parameters were dependent on one another along with their dependence on solvent polarity and temperature; it was tried to explain their interdependence graphically. The calculation of dipole moment of exciplex was also done and then the various factors effecting it were also discussed.

Thus in conclusion the author of this thesis will say that soon after the exciplex formation the solvent molecules rearrange them selves around it and they may stabilize or destabilized the reactant exciplex. In case of non polar solvents the solvent stabilization between the ion pair state is weak and therefore the donor and acceptor of exciplex remain tightly held together due to the absence of significant solvent stabilization. Resultantly stronger exciplex with larger stability is observed in non polar solvents.

5.2. Outlook

In present thesis the organic exciplexes were studied in organic solvents and the effect of solvent polarity and temperature was studied on their spectral and energetic properties. Still lots of more work could be performed in this contest. Some suggested work is given as:

- The exciplex kinetics strongly depends upon the solvent viscosity therefore such system should be selected for which wide range of dynamic viscosities can be observed but the Pekar factor (representing the solvent polarity and refractive index) remains constant.

One such solvent mixture is Dimethylsulfoxide / Glycerol. So need is to check that weather the exciplex exists in this solvent mixture because both the solvents have high dielectric constant ($\epsilon_{dimethylsulfoxide} = 50.0$ and $\epsilon_{glycerol} = 43.0$ and usually the exciplex dissociates at high polarity.

- The fluorescence lifetimes for both the exciplex and fluorophores were calculated at constant temperature. In another experiment the lifetimes over a range of temperatures should be observed in order to find the effect of temperature on the time resolved measurements. Due to the technical reasons it is impossible to find the lifetimes at very low temperatures but still experiment can be performed in the limited range of temperature. For this a special thermally insulated cell is to be constructed and then it should be attached with the cell holder inside the single photon counting and frequency modulation instrument.

- ionic liquids

- use of bio exciplexes

- In present thesis only organic exciplexes were studied. It will be interesting if now inorganic exciplexes are studied and then comparison is made between the properties of organic and inorganic exciplexes.

- ...

A. Appendix

A.1. Spectral Shifts

A.1.1. 1-cyanonaphthalene/hexamethylbenzene Exciplex System (1-CN/HMB)

Emission spectras of 1-CN with HMB in all solvents are given in this appendix.

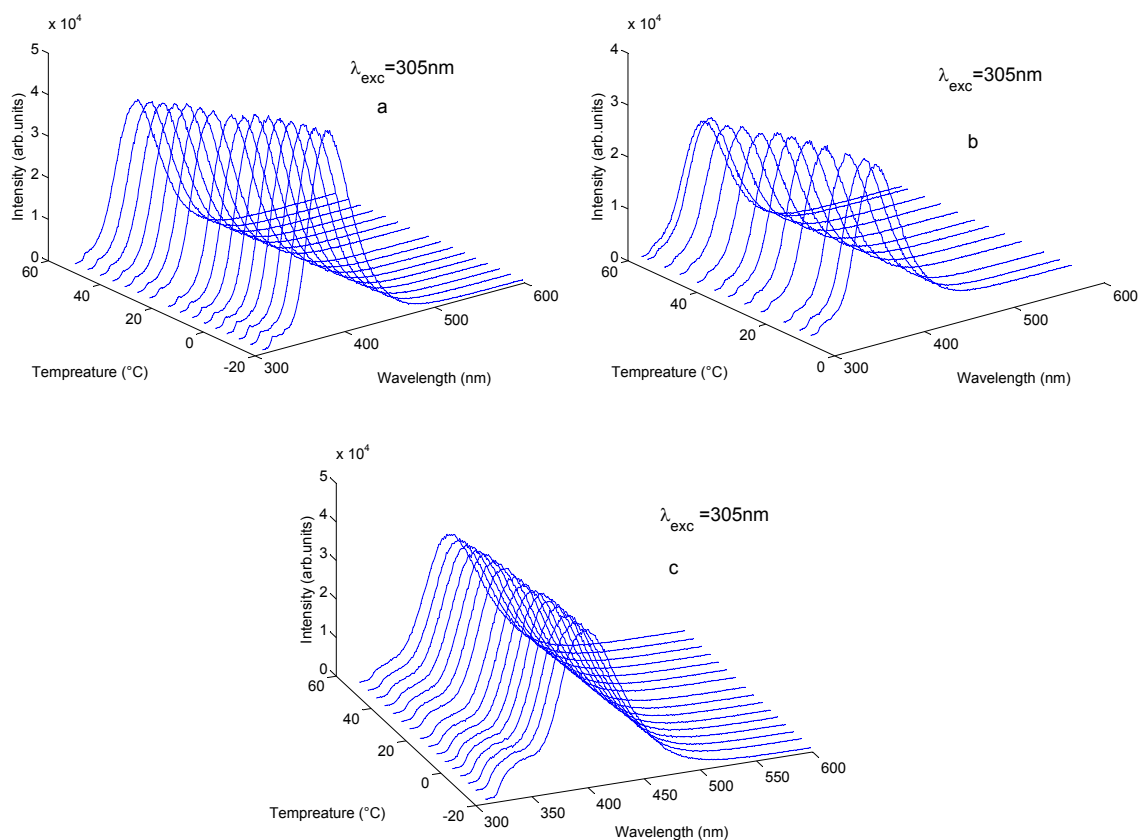


Figure A.1.: Emssion spectras of 5×10^{-5} M 1-CN with 0.08 M HMB in a:n-heptane, b: cyclohexane, and c:toluene from 253.15 to 338.15 K.

A. Appendix

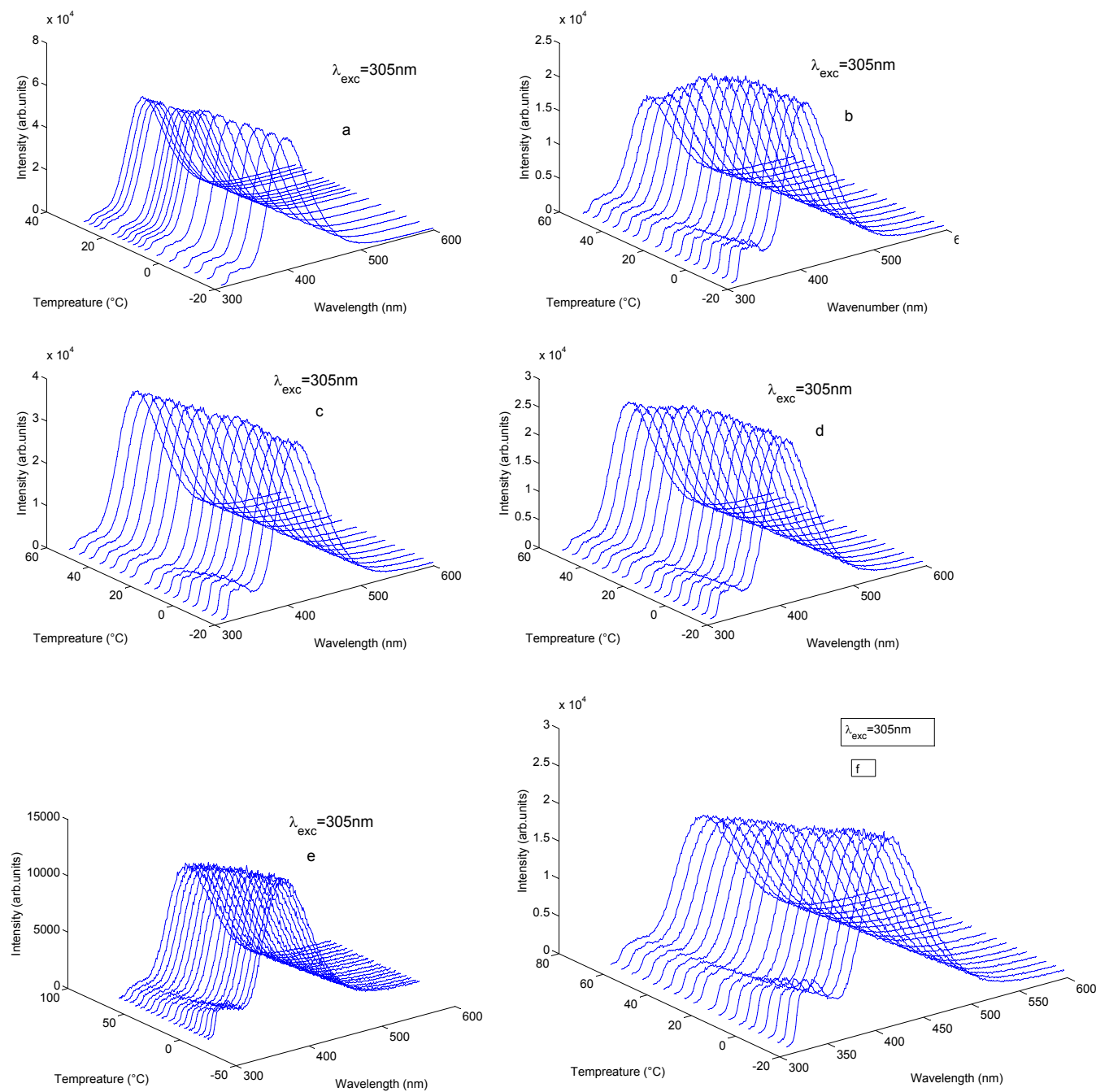


Figure A.2.: Emission spectra of 5×10^{-5} M 1-CN with 0.08 M HMB in a:diethylether, b:propylacetate, c:ethylacetate, d:tetrahydrofurane, e:propylacetate/butyronitrile mixture with 0.9 propylacetate mole fraction and f:propylacetate/butyronitrile mixture with 0.8 propylacetate mole fraction from 253.15 to 338.15 K.

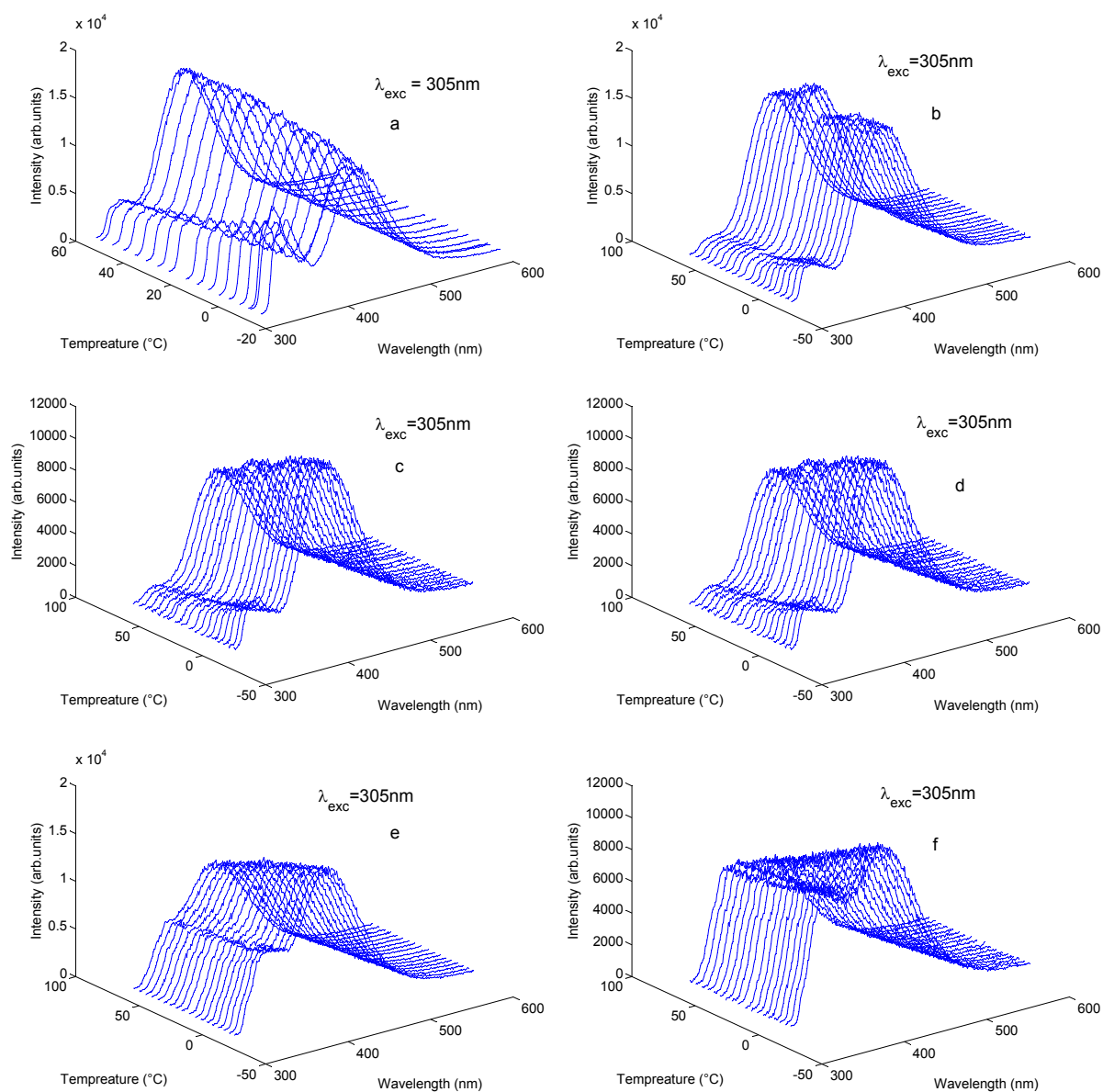


Figure A.3.: Emssion spectra of 5×10^{-5} M 1-CN with 0.08 M HMB in a: dichloroethane b: propylacetate/butyronitrile mixture with 0.7 propylacetate mole fraction, c: propylacetate/butyronitrile mixture with 0.6 propylacetate mole fraction, d: propylacetate/butyronitrile mixture with 0.5 propylacetate mole fraction, e: propylacetate/butyronitrile mixture with 0.4 propylacetate mole fraction, and f: propylacetate/butyronitrile mixture with 0.3 propylacetate mole fraction from 253.15 to 338.15 K.

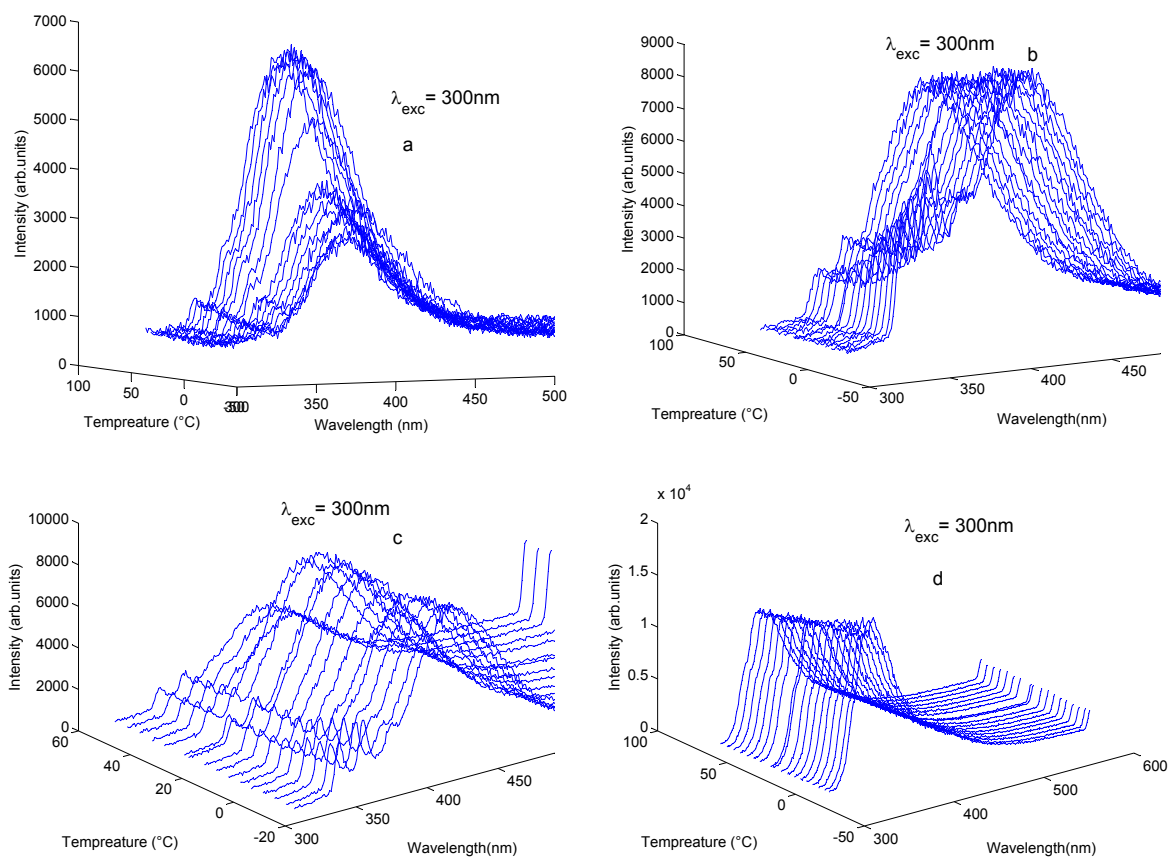


Figure A.4.: Emission spectra of 5×10^{-5} M 2,3-DCN with 0.08 M HMB in a:n-heptane, b:toluene, c:diethylether, and d:propylacetate from 253.15 to 338.15 K.

A.1.2. 2,3-dicyanonaphthalene/hexamethylbenzene Exciplex System(2,3-DCN/HMB)

Emission spectras of 1-CN with HMB in all solvents are given in this appendix.

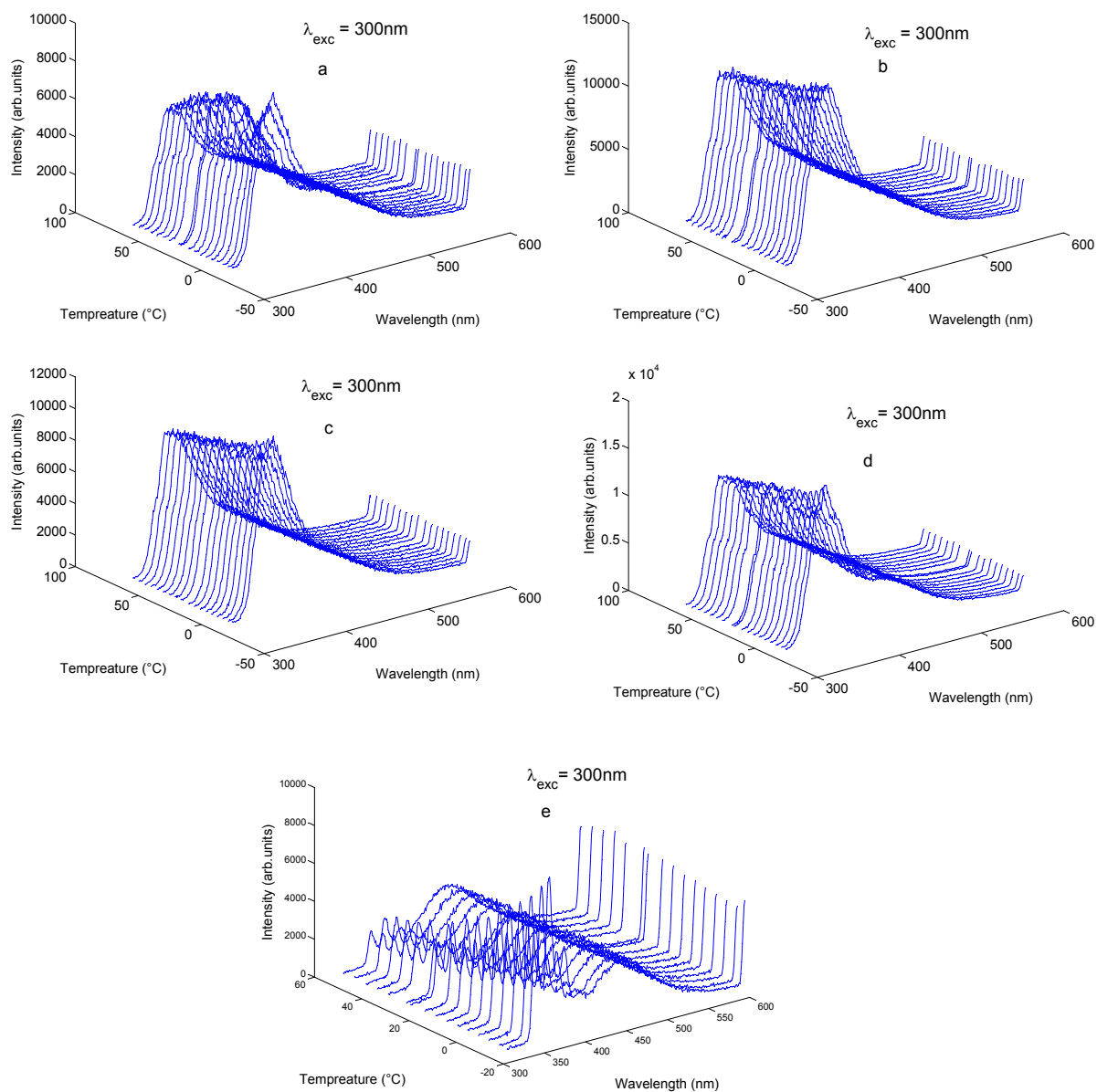


Figure A.5.: Emission spectra of 5×10^{-5} M 2,3-DCN with 0.08 M HMB in a:ethylacetate, b:tetrahydrofuran, c:propylacetate/butyronitrile mixture with 0.9 propylacetate mole fraction and d:propylacetate/butyronitrile mixture with 0.8 propylacetate mole fraction, e:dichloroethane from 253.15 to 338.15 K.

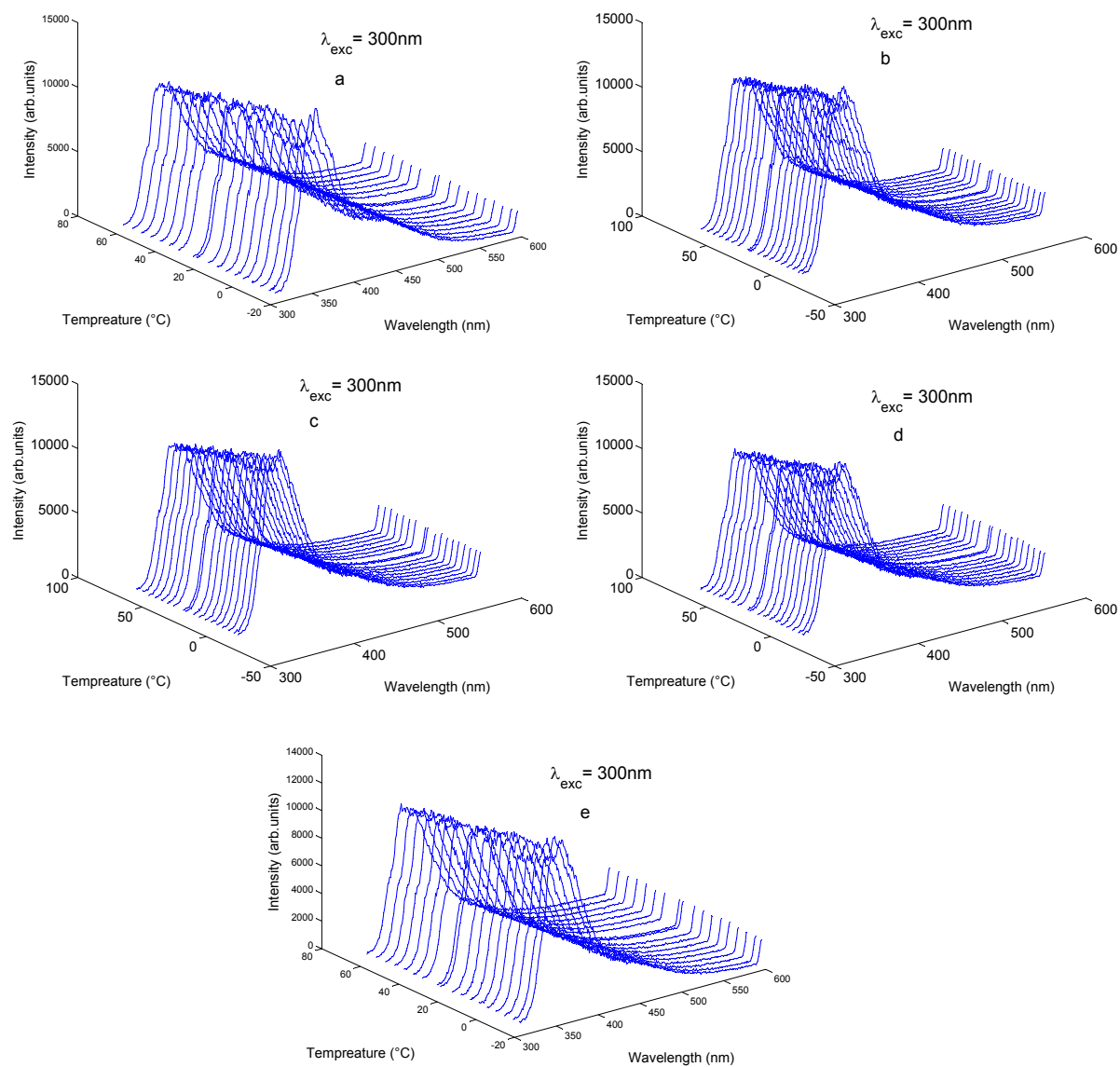


Figure A.6.: Emission spectra of 5×10^{-5} M 2,3-DCN with 0.08 M HMB in a:propylacetate/butyronitrile mixture with 0.7 propylacetate mole fraction, b:propylacetate/butyronitrile mixture with 0.6 propylacetate mole fraction, c:propylacetate/butyronitrile mixture with 0.5 propylacetate mole fraction, d:propylacetate/butyronitrile mixture with 0.4 propylacetate mole fraction and e:propylacetate/butyronitrile mixture with 0.3 propylacetate mole fraction from 253.15 to 338.15 K.

A.1.3. N,N'-dimethylaniline and biphenyl System (DMA/BP)

The emission spectras of DMA with BP as a function of temperature in all solvents is given as under:

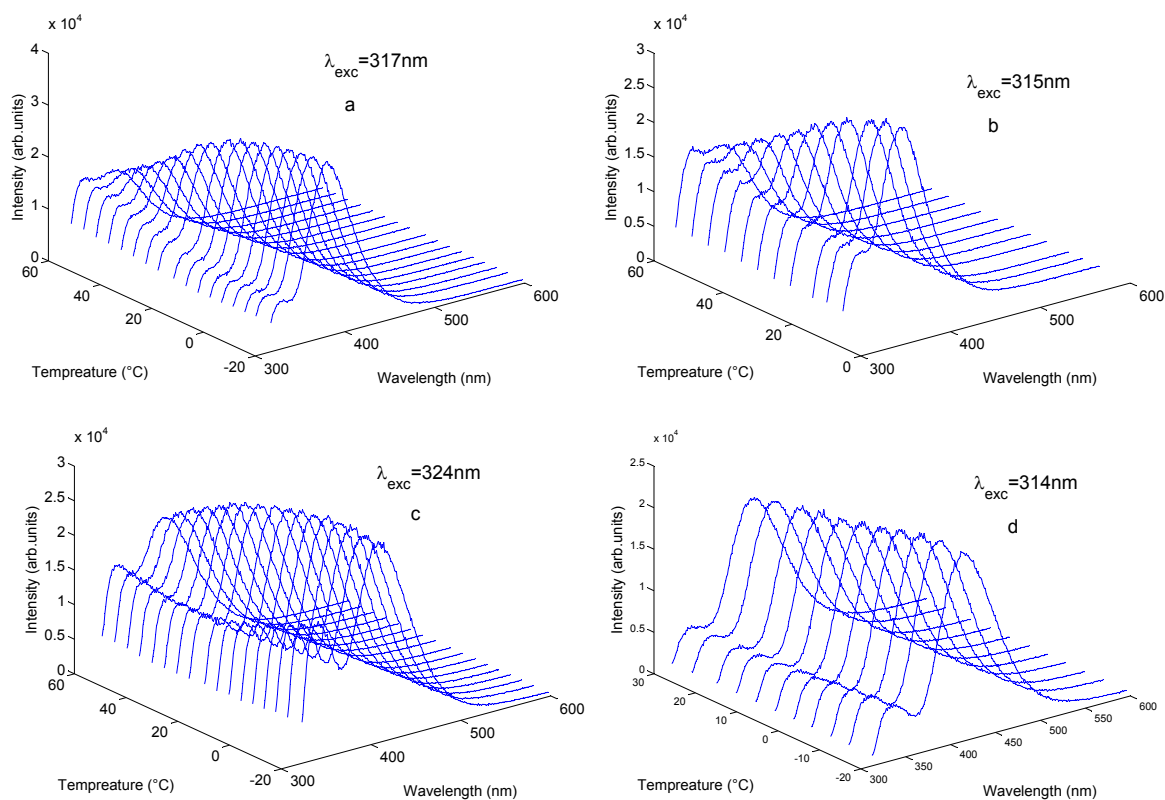


Figure A.7.: Emssion spectras of 1.1×10^{-4} M DMA with 0.05 M BP in a:n-heptane, b:cyclohexane, c:toluene and d:diethylether from 253.15 to 338.15 K.

A. Appendix

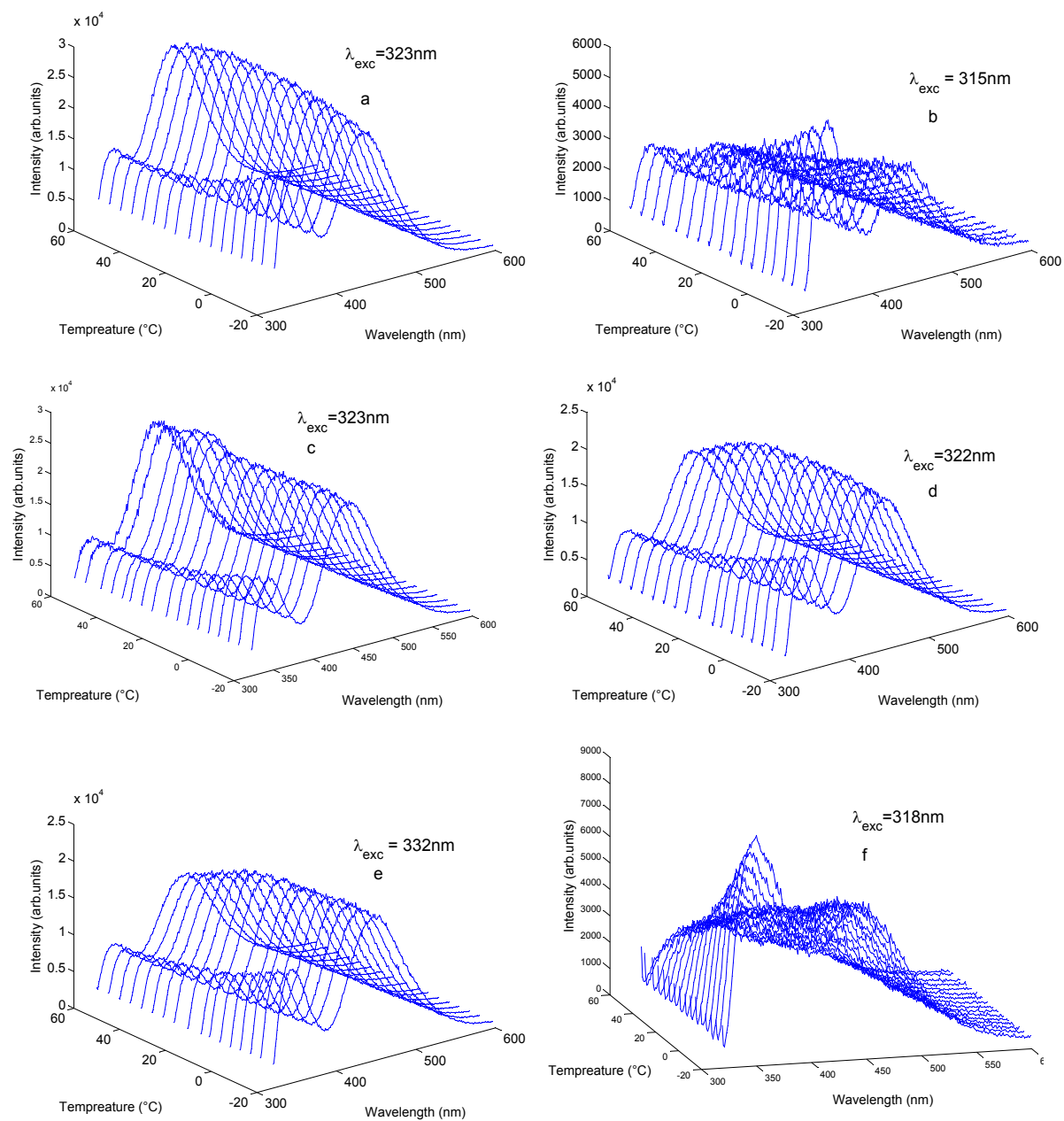


Figure A.8.: Emission spectra of 1.1×10^{-4} M DMA with 0.05 M BP in a:butylacetate, b:ethylacetate, d:tetrahydrofuran and e:propylacetate/butyronitrile mixture with 0.9 propylacetate mole fraction, f:propylacetate/butyronitrile mixture with 0.8 propylacetate mole fraction and g:dichloroethane from 253.15 to 338.15 K.

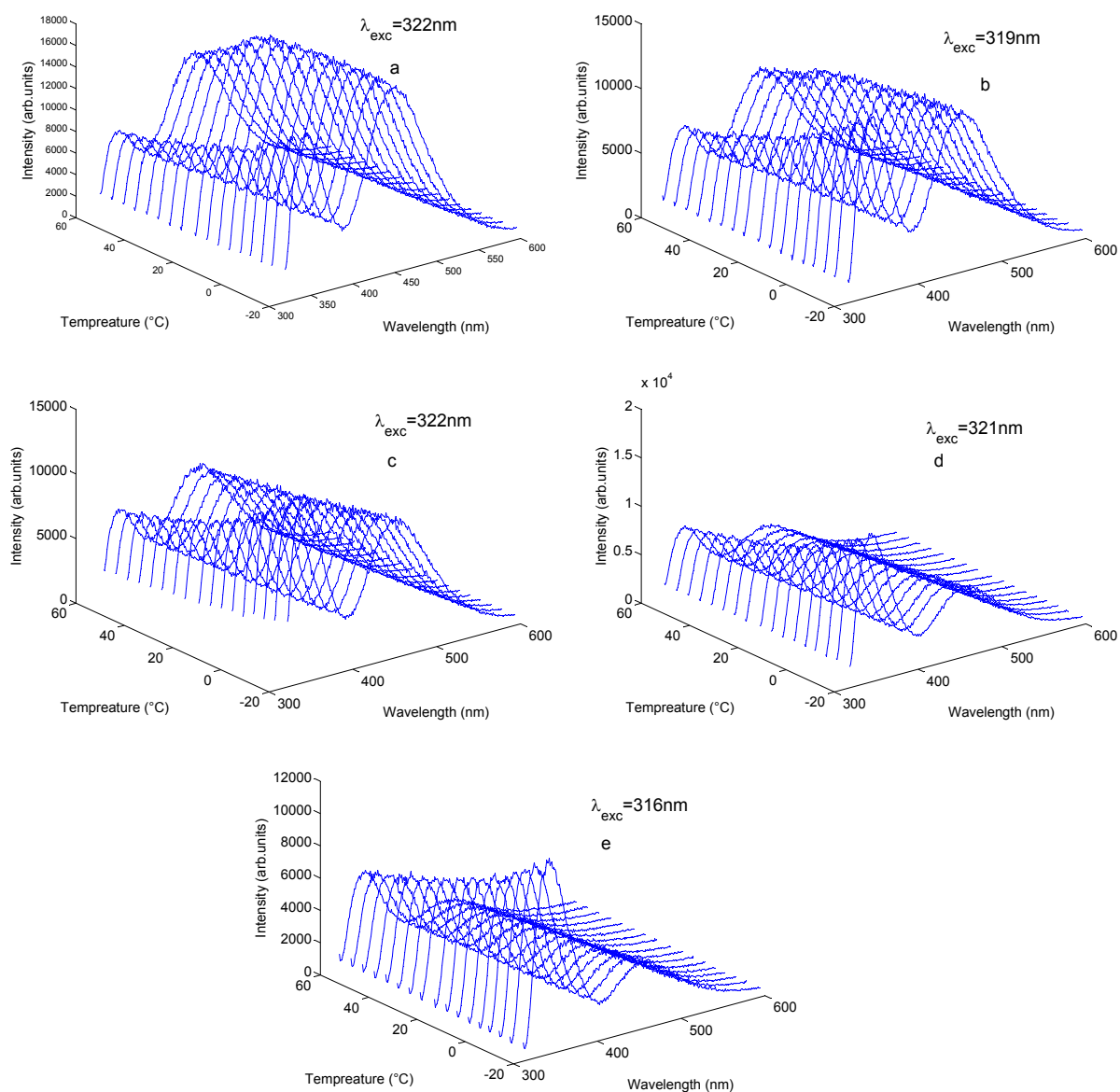


Figure A.9.: Emission spectra of 1.1×10^{-4} M DMA with 0.05 M BP in a:propylacetate/butyronitrile mixture with 0.7 propylacetate mole fraction, b:propylacetate/butyronitrile mixture with 0.6 propylacetate mole fraction, c:propylacetate/butyronitrile mixture with 0.5 propylacetate mole fraction d:propylacetate/butyronitrile mixture with 0.4 propylacetate mole fraction, e:propylacetate/butyronitrile mixture with 0.3 propylacetate mole fraction from 253.15 to 338.15 K.

A.1.4. Pyrene and N,N'-bis(dimethylamino)diphenylmethane system(PY/DMDPM)

The emission spectra of PY with DMDPM as a function of temperature in all solvents is given as under:

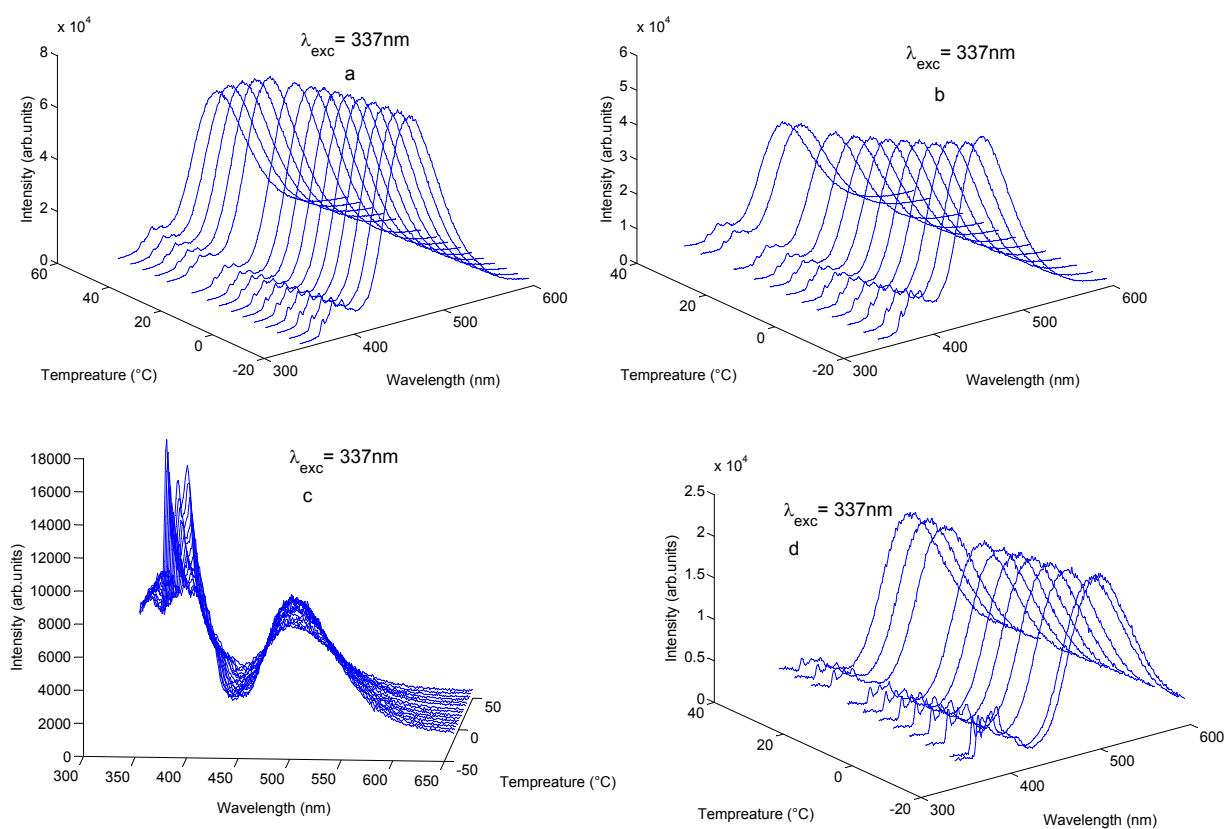


Figure A.10.: Emission spectra of 1×10^{-4} M PY with 0.004 M DMDPM in a:n-heptane, b:cyclohexane, c:toluene, and d:diethylether from 253.15 to 338.15 K.

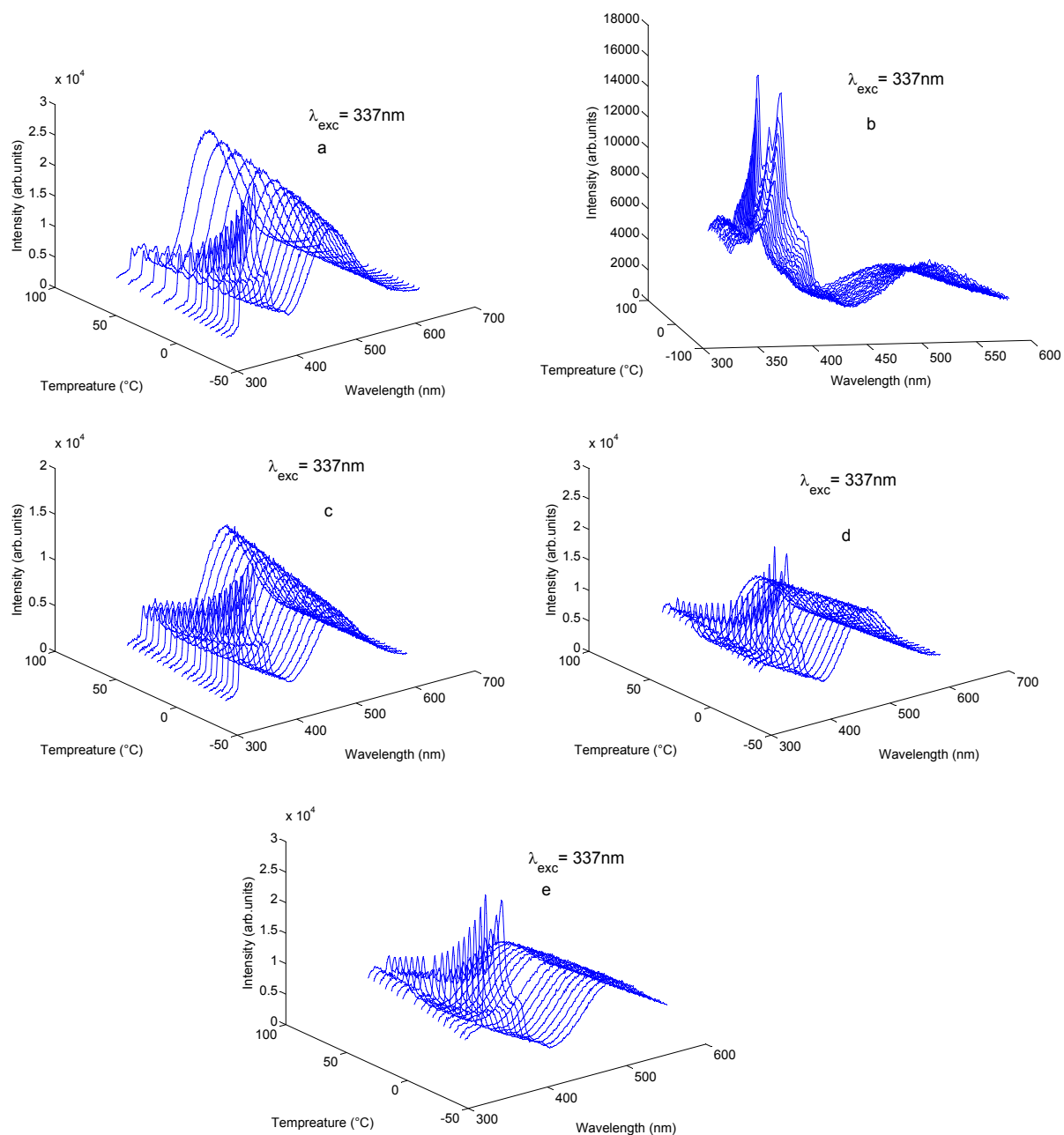


Figure A.11.: Emission spectra of 1×10^{-4} M PY with 0.004 M DMDPM in a:butylacetate, b:ethylacetate, c:tetrahydrofuran, d:propylacetate, and e:propylacetate/butyronitrile mixture with 0.8 molefraction of propylacetate from 253.15 to 338.15 K.

A. Appendix

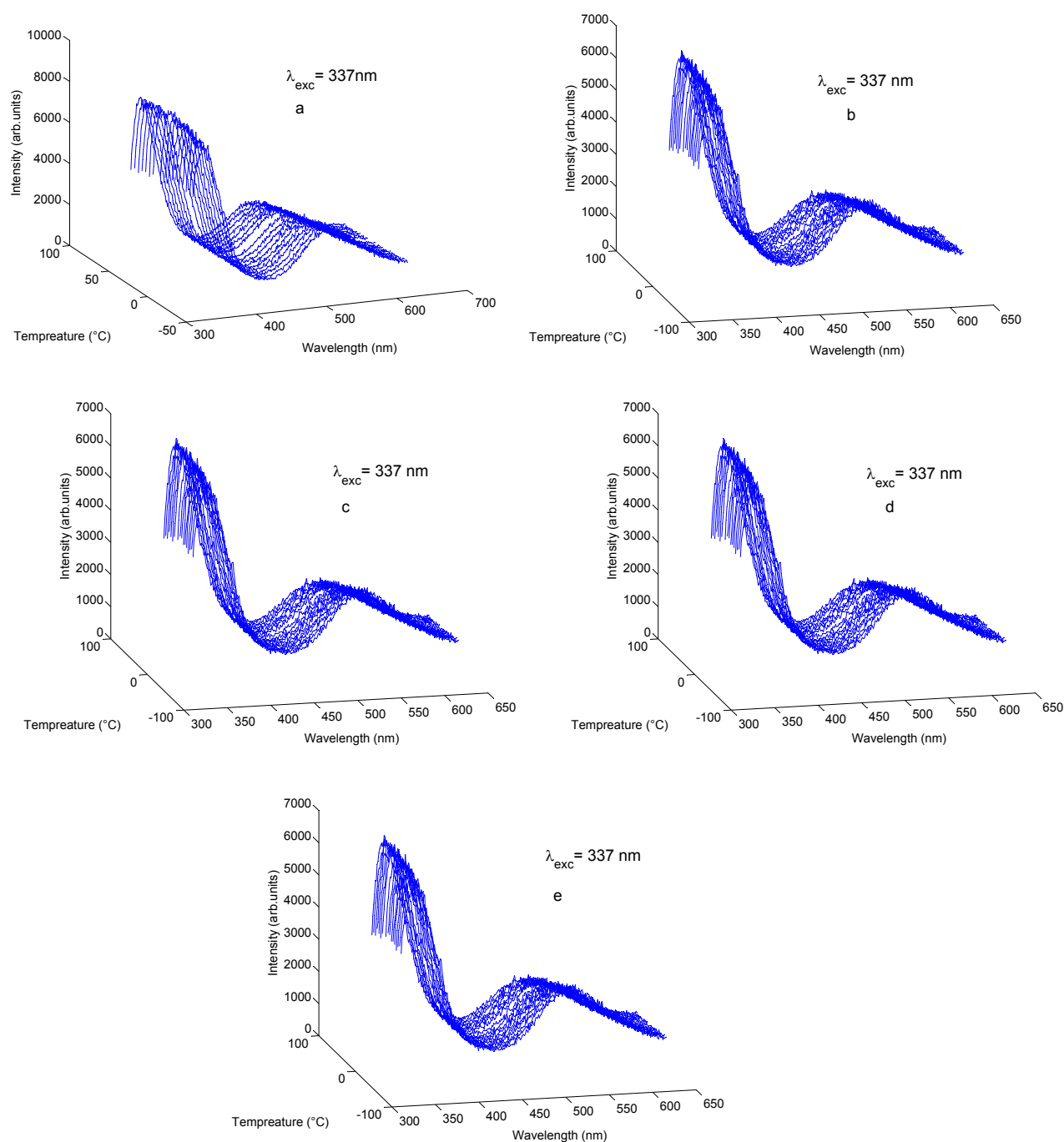
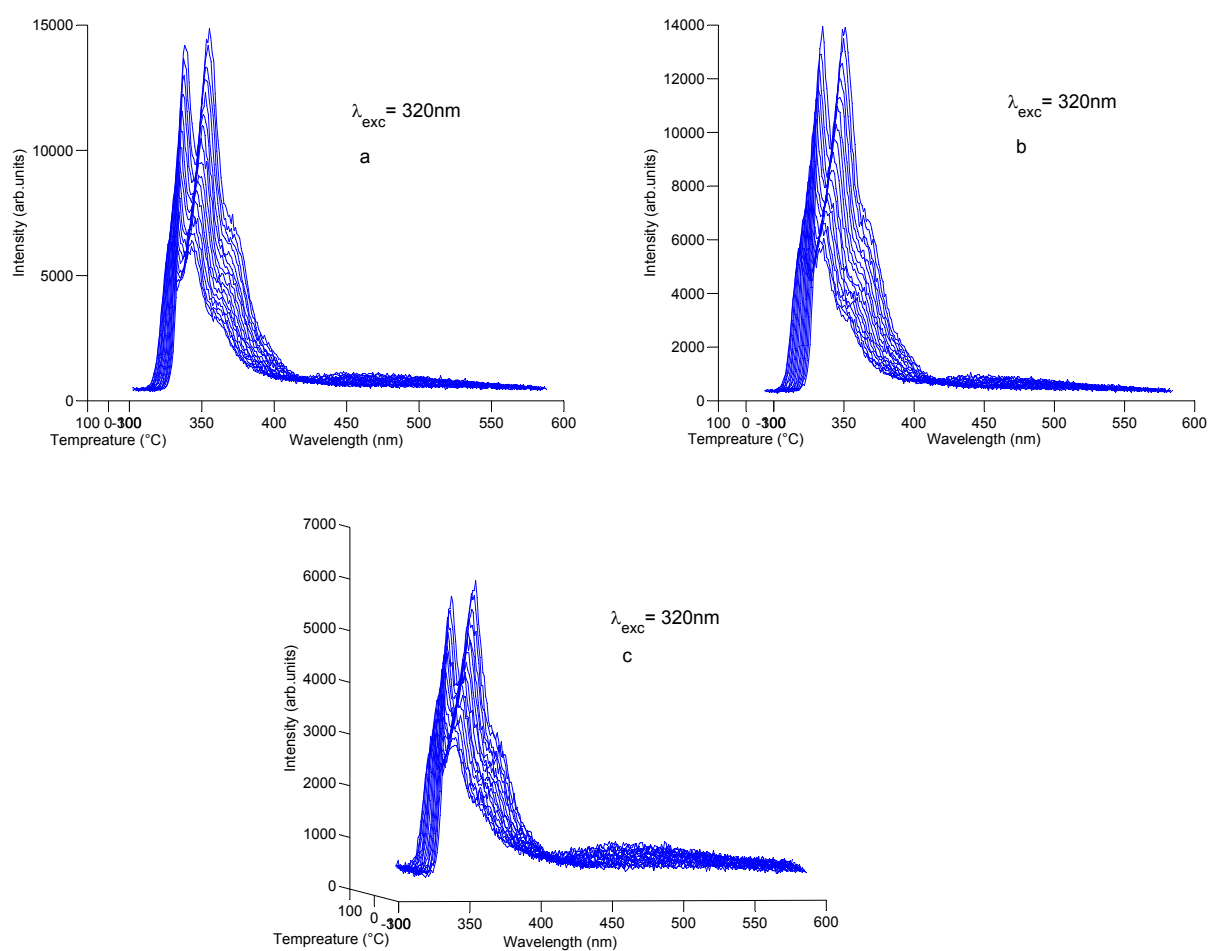


Figure A.12.: Emission spectra of 1×10^{-4} M PY with 0.004 M DMDPM in a:propylacetate/butyronitrile mixture with 0.7 propylacetate mole fraction, b:propylacetate/butyronitrile mixture with 0.6 propylacetate mole fraction, c:propylacetate/butyronitrile mixture with 0.5 propylacetate mole fraction, d:propylacetate/butyronitrile mixture with 0.4 propylacetate mole fraction, e:propylacetate/butyronitrile mixture with 0.3 propylacetate mole fraction from 142.53.15 to 338.15 K.

A.1.5. N-alkylated Carbazoles With Dicyanobenzenes

Emission spectra of N-alkylated carbazoles with dicyanobenzenes are given in this chapter



5

Figure A.13.: Emission spectra of a: 5×10^{-5} M NEC with 0.02 M 1,2-DCB, b: 5×10^{-5} M NMC with 0.02 M 1,2-DCB and c: 5×10^{-5} M NMC with 0.02 M 1,4-DCB from 253.15 to 338.15 K.

A.2. Exciplex Energetics–Band Parameters Obtained from Excited Emission Spectra:

A.2.1. Energy of zero-zero transitions and Gauss broadening of Vibronic level

Graphs for all systems showing the change in the gauss broadening of Vibronic level with change of temperature are given as under:

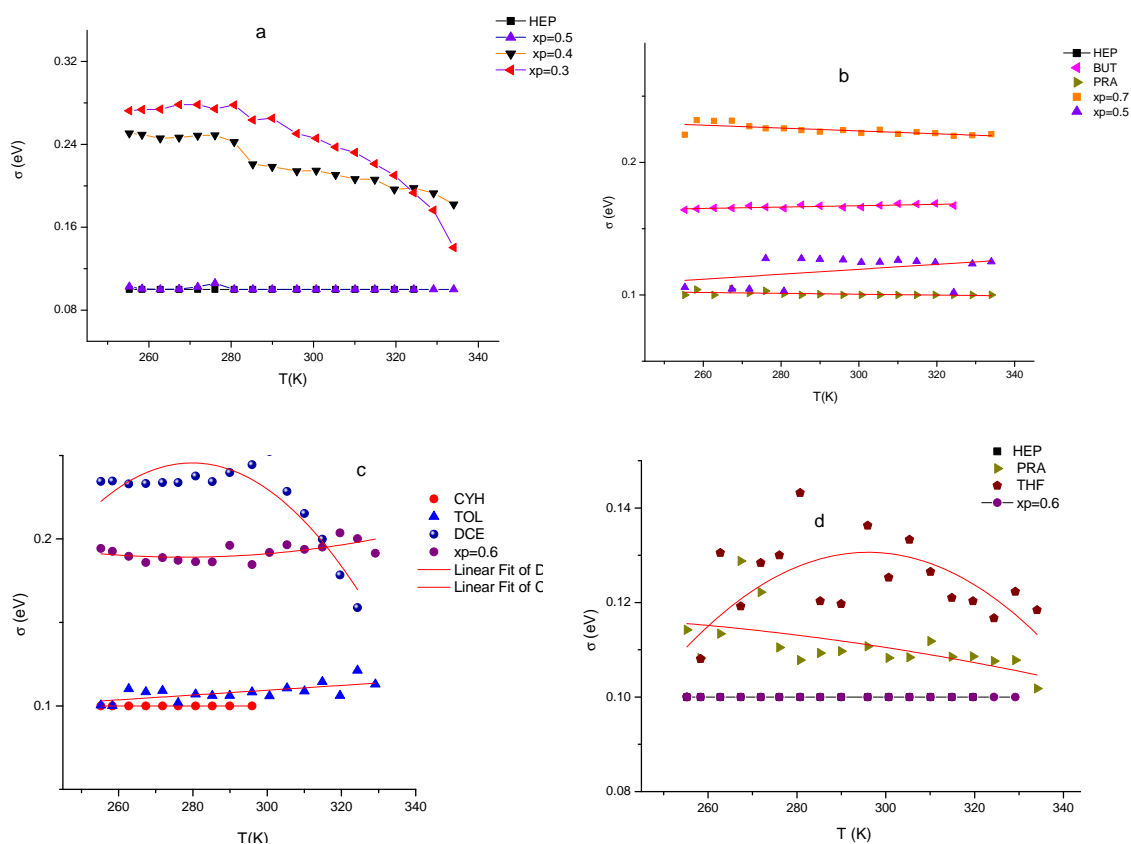


Figure A.14.: Gauss broadening of vibronic level vs. temperature for a:1-CN/HMB, b:2,3-DCN/HMB, c:DMA/BP and d:PY/DMDPM.

A.2.2. Huang-Rhys factor (S) and energy of dominant high-frequency vibration

For all the systems, graphical representation of Huang-Rhys factor as a function of temperature are given as under

A.2. Exciplex Energetics–Band Parameters Obtained from Excited Emission Spectra:

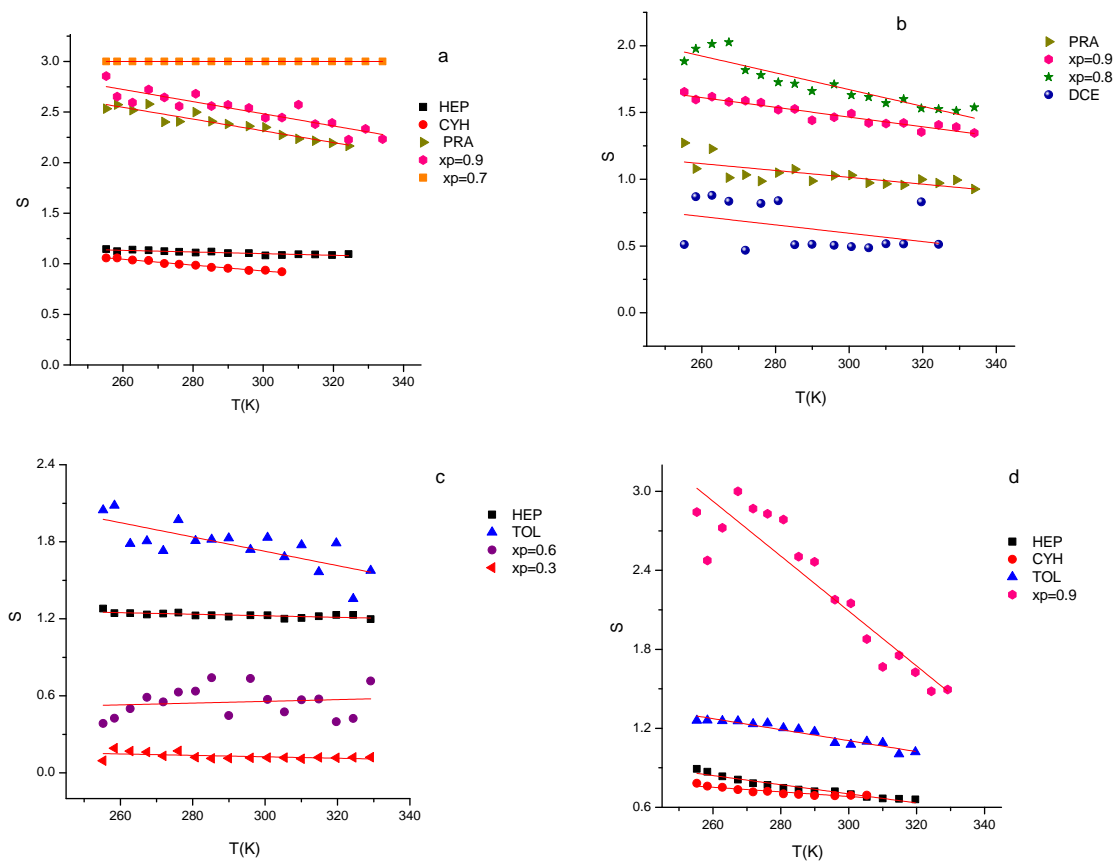


Figure A.15.: Spectral Huang-Rhys factor as a function of temperature for a:1-CN/HMB, b:2,3-DCN/HMB, c:DMA/BP, d:PY/DMDPM and e:NMC/1,3-DCB exciplex systems.

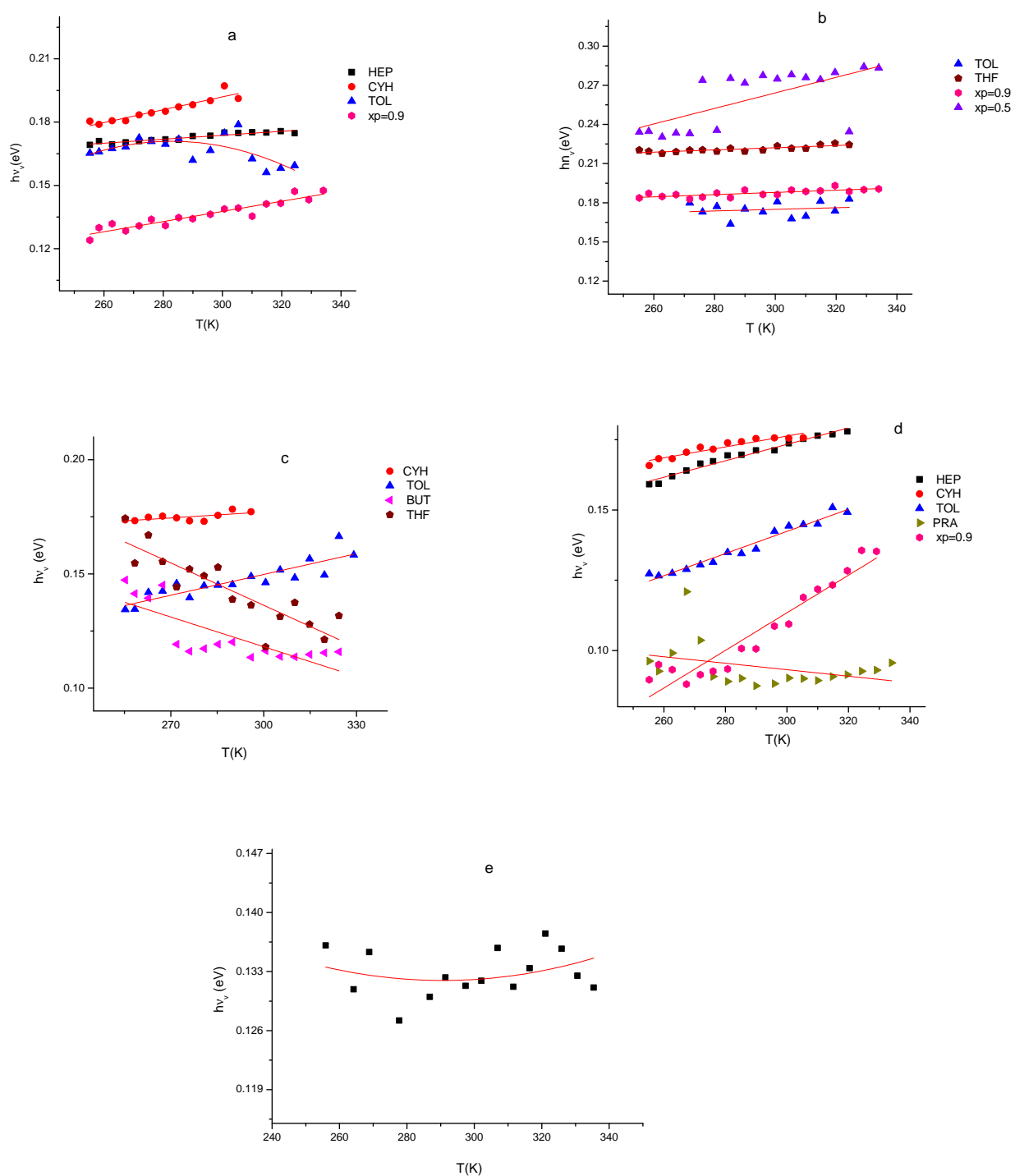


Figure A.16.: Energy of high-frequency vibration $h\nu_v$ (eV)) as a function of temperature for a:1-CN/HMB, b:2,3-DCN/HMB, c:DMA/BP, d:PY/DMDPM and e:NMC/1,3-DCB exciplex systems.

A.3. Fluorescence Life Times

A.3.1. Fluorescence Lifetime of Exciplex

The fluorescence lifetimes for exciplexes of 2,3-DCN/HMB, DMA/BP and PY/DMDPM are tabulated in this section:

Table A.1.: Fluorescence lifetimes for exciplex system 2,3-DCN/HMB in solvents^a of different polarity at 297K. LED used is 340nm and long pass filter: 400nm. The solvents are arranged in the order of increasing solvent polarity from top of list to bottom

Solvent	χ	t_1	t_2	Residue
		ns	ns	
HEP	0.86	1.11	13.01	4.54
TOL	0.84	1.96	13.78	3.95
DEE	0.88	1.03	14.82	3.81
BUT	0.64	0.94	15.91	4.29
PRA	0.63	0.93	17.56	4.90
ETA	0.92	1.09	18.24	3.39
THF	0.73	0.91	17.27	3.79
$x_P=0.9$	0.73	0.95	16.99	3.70
$x_P=0.8$	0.64	0.95	16.68	3.47
$x_P=0.7$	0.75	0.95	16.57	3.85
$x_P=0.6$	0.68	0.95	15.52	3.56
$x_P=0.5$	0.67	0.98	12.06	4.33
$x_P=0.4$	0.73	0.96	12.74	3.02
$x_P=0.3$	0.62	0.98	10.99	4.41

^a Used acronyms: heptane (HEP), cyclohexane (CYH), toluene (TOL), diethylether (DEE), butyronitrile (BUT), propylacetate (PRA), ethylacetate (ETA), tetrahydrofuran (THF), propylacetate mole fraction in propylacetate/butyronitrile mixture (x_P), dichloroethane (DCE)

Table A.2.: Fluorescence lifetimes for exciplex system DMA/BP in solvents^a of different polarity at 297K. LED used is 340nm and long pass filter: 450nm. The solvents are arranged in the order of increasing solvent polarity from top of list to bottom

Solvent	χ	t_1	Residue	
		ns		
HEP	0.61	6.86	3.44	
CYH	0.65	7.02	3.19	3.75
TOL	0.76	11.87	4.05	
DEE	0.67	13.68	4.11	
BUT	0.73	14.19	5.01	
PRA	0.58	15.89	3.25	
ETA	0.56	27.65	2.85	
THF	0.58	25.59	3.26	
$x_P=0.9$	0.71	24.64	3.88	
$x_P=0.8$	0.54	23.46	2.83	
$x_P=0.7$	0.71	19.57	2.93	
$x_P=0.6$	0.55	18.45	2.89	
$x_P=0.5$	0.56	14.06	3.45	
$x_P=0.4$	0.61	10.39	3.02	
$x_P=0.3$	0.59	7.23	3.80	

^a Used acronyms: heptane (HEP), cyclohexane (CYH), toluene (TOL), diethylether (DEE), butyronitrile (BUT), propylacetate (PRA), ethylacetate (ETA), tetrahydrofuran (THF), propylacetate mole fraction in propylacetate/butyronitrile mixture (x_P), dichloroethane (DCE)

Table A.3.: Fluorescence lifetimes for exciplex system DMA/BP in solvents^a of different polarity at 297K. LED used is 340nm and long pass filter: 450nm. The solvents are arranged in the order of increasing solvent polarity from top of list to bottom

Solvent	χ	t_1	Residue	
		ns		
HEP	0.61	6.86	3.44	
CYH	0.65	7.02	3.19	3.75
TOL	0.76	11.87	4.05	
DEE	0.67	13.68	4.11	
BUT	0.73	14.19	5.01	
PRA	0.58	15.89	3.25	
ETA	0.56	27.65	2.85	
THF	0.58	25.59	3.26	
$x_P=0.9$	0.71	24.64	3.88	
$x_P=0.8$	0.54	23.46	2.83	
$x_P=0.7$	0.71	19.57	2.93	
$x_P=0.6$	0.55	18.45	2.89	
$x_P=0.5$	0.56	14.06	3.45	
$x_P=0.4$	0.61	10.39	3.02	
$x_P=0.3$	0.59	7.23	3.80	

^a Used acronyms: heptane (HEP), cyclohexane (CYH), toluene (TOL), diethylether (DEE), butyronitrile (BUT), propylacetate (PRA), ethylacetate (ETA), tetrahydrofuran (THF), propylacetate mole fraction in propylacetate/butyronitrile mixture (x_P), dichloroethane (DCE)

Table A.4.: Fluorescence lifetimes for exciplex system PY/DMDPM in solvents^a of different polarity at 297K. LED used is 340nm and long pass filter: 500nm. The solvents are arranged in the order of increasing solvent polarity from top of list to bottom

Solvent	χ	t_1 ns	Residue
HEP	0.51	66.09	3.39
CYH	0.66	65.90	4.23
TOL	0.75	63.81	3.29
DEE	0.57	61.89	3.83
BUT	0.52	55.79	5.81
PRA	0.56	49.68	3.26
ETA	0.56	49.55	3.92
THF	0.63	48.09	5.22
$x_P=0.9$	0.58	47.89	4.13
$x_P=0.8$	0.57	43.84	2.95
$x_P=0.7$	0.52	38.32	3.53
$x_P=0.6$	0.59	31.70	4.75
$x_P=0.5$	0.68	24.52	4.26
$x_P=0.4$	0.666	19.01	5.26
$x_P=0.3$	0.56	18.22	5.52

^a Used acronyms: heptane (HEP), cyclohexane (CYH), toluene (TOL), diethylether (DEE), butyronitrile (BUT), propylacetate (PRA), ethylacetate (ETA), tetrahydrofuran (THF), propylacetate mole fraction in propylacetate/butyronitrile mixture (x_P), dichloroethane (DCE)

A.4. Parameters appearing in Kuzmin's equations:

Value of m:

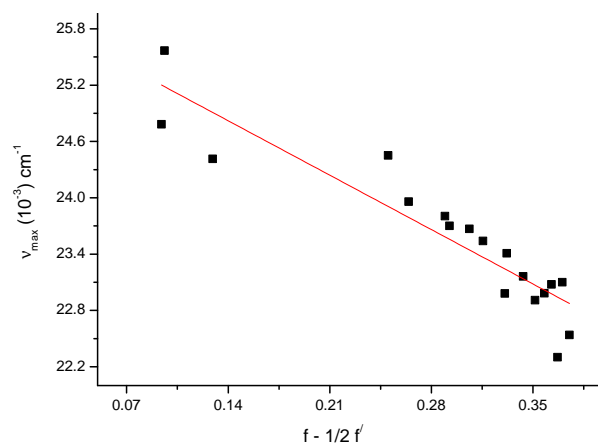


Figure A.17.: Graph between ν_{max} and $f - 1/2f'$ used for the calculation of dipolemoment for 1-CN/HMB exciplex system.

A.5. Enthalpy of exciplex formation

Graphs in remaining solvents are given as : A.19. Graphs in remaining solvents are given in .

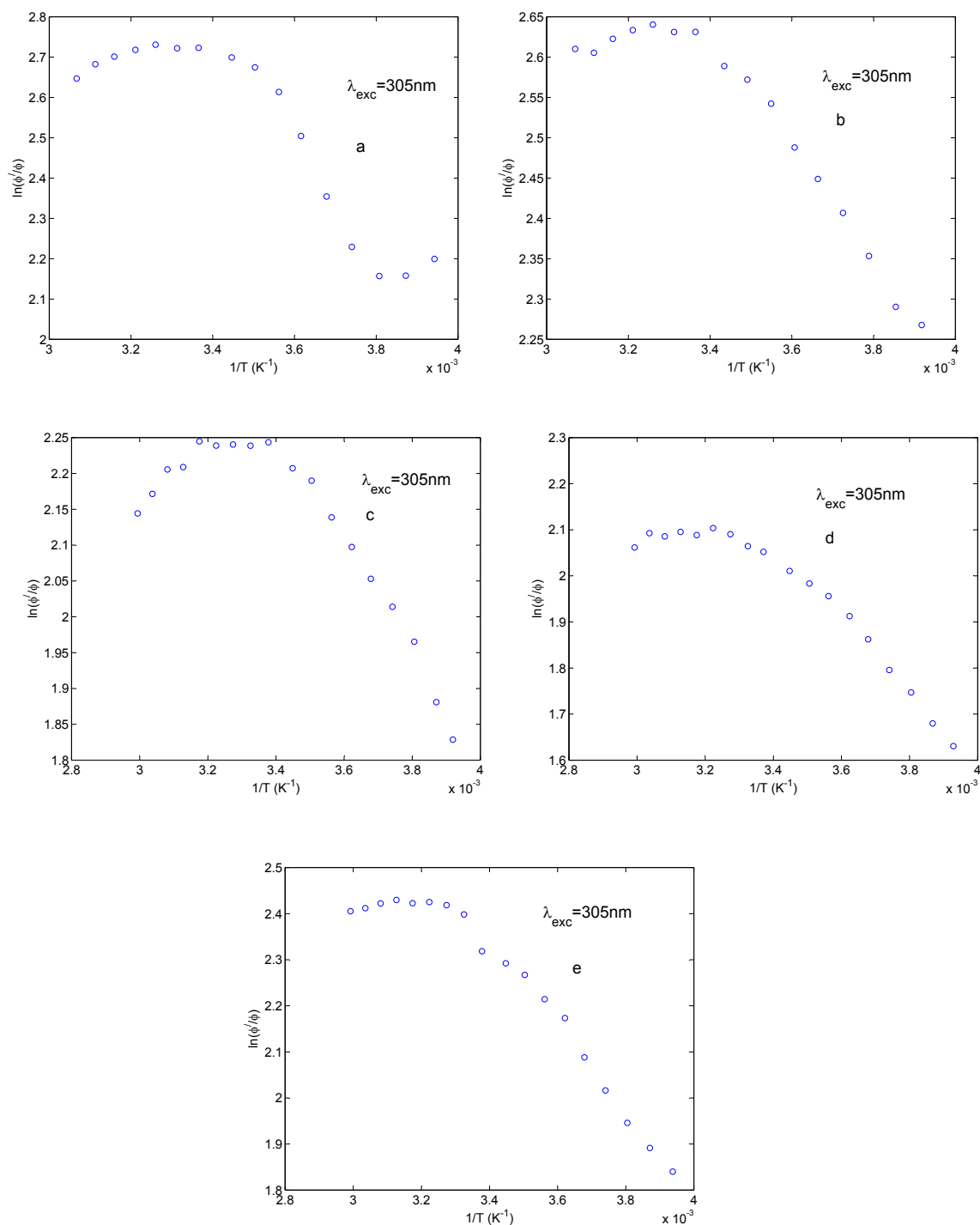


Figure A.18.: The reciprocal temperature dependence of $\ln(\phi'/\phi)$ for the exciplexes of 1-CN/HMB in a:ethylacetate, b:tetrahydrofuran, c:propylacetate/butyronitrile mixture with $x_p = 0.9$, d:propylacetate/butyronitrile mixture with $x_p = 0.8$, e:propylacetate/butyronitrile mixture with $x_p = 0.7$.

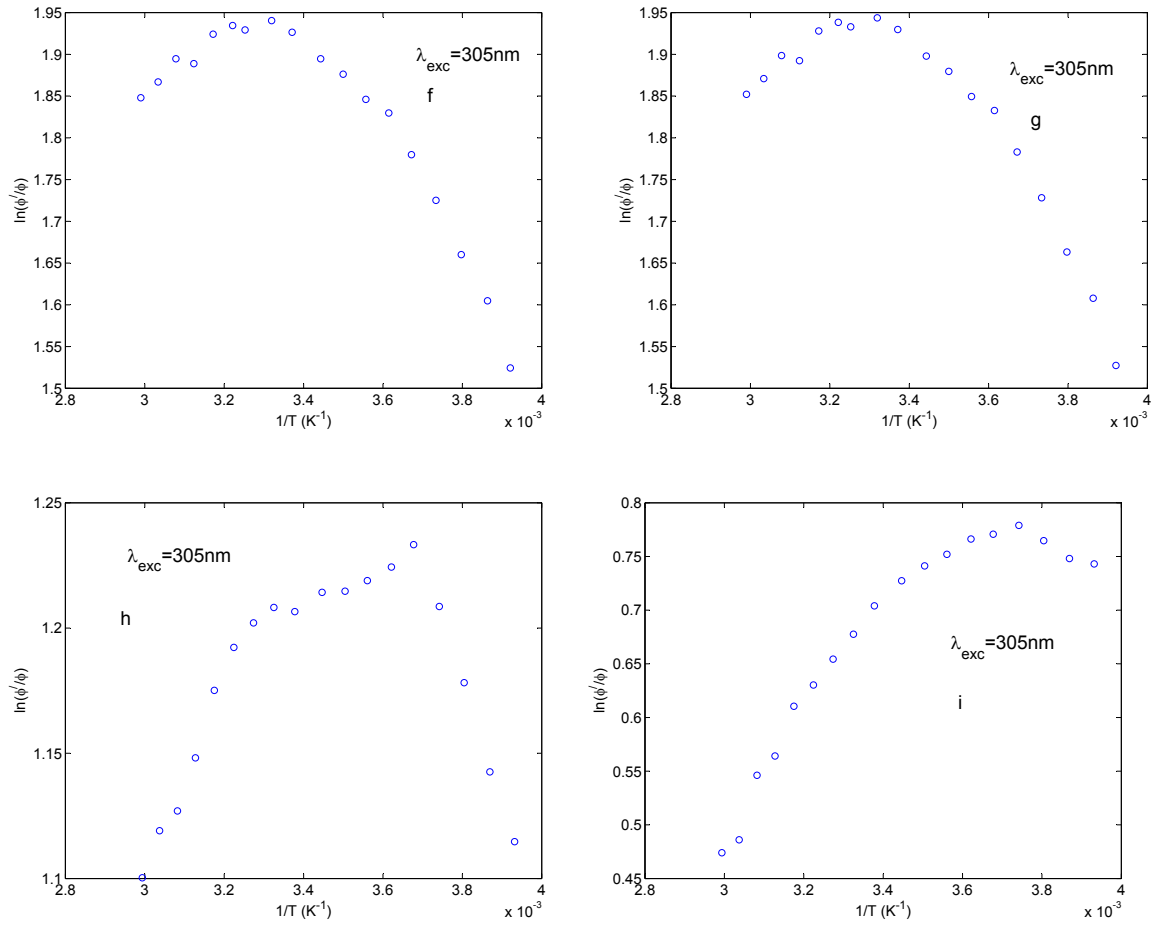


Figure A.19.: The reciprocal temperature dependence of $\ln(\phi'/\phi)$ for the exciplexes of 1-CN/HMB in f:propylacetate/butyronitrile mixture with $x_p = 0.6$, g:propylacetate/butyronitrile mixture with $x_p = 0.5$, h:propylacetate/butyronitrile mixture with $x_p = 0.4$, i:propylacetate/butyronitrile mixture with $x_p = 0.3$.

B. Acronyms

Solvents			
ACE	acetone	DMA	Dimethylaniline
ACN	acetonitrile	1-CN	1-Cyanonaphthalene
BUT	butyronitrile	2,3-DCN	2,3-Dicyanonaphthalene
CYH	cyclohexane	PY	Pyrene
CTC	carbon tetrachloride	NMC	N-methylcarbazole
DCM	dichloromethane	NEC	N-ethylcarbazole
DCE	dichloroethane	HMB	Hexamethylbenzene
ETA	ethylacetate	DMADM	N,N'-bis(dimethylamino)diphenylmethane
DEE	diethylether	1,2DCB	1,2-dicyanobenzene
BUA	butylacetate	1,3DCB	1,3-dicyanobenzene
PRA	propylacetate	1,4DCB	1,4-dicyanobenzene
HEP	heptane		
TOL	toluene		
THF	tetrahydrofuran		
x_P	propylacetate mole fraction in propylacetate/butyronitrile mixture		
Reactants		Solutes	
BP	Biphenyl	BQ	1,4-benzoquinone
		Others	
		CIDEP	chemically induced dynamic electron polarization

Spectral Shifts

1-CN/HMB 1-cyanoanthracene with
hexamethylbenzene

2,3-DCN/HMB 2,3-dicyanoanthracene
with hexamethylbenzene

BP/DMA biphenyl with
N,N'-dimethylaniline

PY/DMADM pyrene with 4,4'-
bis(dimethylamino)diphenylmethane

NMC/1,2-DCB N-methylcarbazole with
1,2-dicyanobenzene

NMC/1,3-DCB N-methylcarbazole with
1,3-dicyanobenzene

NMC/1,4-DCB N-methylcarbazole with
1,4-dicyanobenzene

NEC/1,2-DCB N-ethylcarbazole with
1,2-dicyanobenzene

Bibliography

- [1] Kwan, P. H.; Swager, T. M. *J. Am. Chem. Soc.* **2005**, *127*, 5902–5909.
- [2] Leonhardt, H.; Weller, A. *Ber. Bunsen-Ges.* **1963**, *67*, 791–5.
- [3] Marcus, R. A. *J. Chem. Phys.* **1956**, *24*, 966–78.
- [4] Marcus, R. A.; Eyring, H. *Annu. Rev. Phys. Chem.* **1964**, *15*, 155–96.
- [5] Kuzmin, M. G. *Pure Appl. Chem.* **1993**, *65*, 1653–8.
- [6] Kuzmin, M. G. *J. Photochem. Photobiol., A* **1996**, *102*, 51–57.
- [7] Kinoshita, I.; Hamazawa, A.; Nishioka, T.; Adachi, H.; Suzuki, H.; Miyazaki, Y.; Tsuboyama, A.; Okada, S.; Hoshino, M. *Chem. Phys. Lett.* **2003**, *371*, 451–457.
- [8] Gould, I. R.; Young, R. H.; Mueller, L. J.; Albrecht, A. C.; Farid, S. *J. Am. Chem. Soc.* **1994**, *116*, 8188–99.
- [9] Gould, I. R.; Young, R. H.; Mueller, L. J.; Albrecht, A. C.; Farid, S. *J. Am. Chem. Soc.* **1994**, *116*, 3147–8.
- [10] Knibbe, H.; Weller, A. *Z. Phys. Chem. (Leipzig)* **1967**, *56*, 99–102.
- [11] Kuzmin, M. G.; Soboleva, I. V.; Dolotova, E. V. *J. Phys. Chem. A* **2007**, *111*, 206–215.
- [12] Kjaer, A. M.; Ulstrup, J. *J. Am. Chem. Soc.* **1987**, *109*, 1934–42.
- [13] Iwakura, I.; Yabushita, A.; Kobayashi, T. *J. Am. Chem. Soc.* **2009**, *131*, 688–696.
- [14] Miyasaka, H.; Kotani, S.; Itaya, A.; Schweitzer, G.; De Schryver, F. C.; Mataga, N. *J. Phys. Chem. B* **1997**, *101*, 7978–7984.
- [15] Parsons, B. J.; Beaumont, P. C.; Harrison, W. D.; Navaratnam, S.; Othman, M.; Akasheh, T. S. *Inorg. Chem.* **1994**, *33*, 157–63.
- [16] Knibbe, H.; Rehm, D.; Weller, A. *Ber. Bunsenges. Phys. Chem.* **1968**, *72*, 257–63.

- [17] Mylon, S. E.; Smirnov, S. N.; Braun, C. L. *J. Phys. Chem. A* **1998**, *102*, 6558–6564.
- [18] Findley, B. R.; Smirnov, S. N.; Braun, C. L. *J. Phys. Chem. A* **1998**, *102*, 6385–6389.
- [19] Smirnov, S. N.; Braun, C. L. *Rev. Sci. Instrum.* **1998**, *69*, 2875–2887.
- [20] Masuhara, H.; Shioyama, H.; Saito, T.; Hamada, K.; Yasoshima, S.; Mataga, N. *J. Phys. Chem.* **1984**, *88*, 5868–73.
- [21] Foerster, T. *Pure Appl. Chem.* **1970**, *24*, 443–9.
- [22] Asaoka, S.; Wada, T.; Inoue, Y. *J. Am. Chem. Soc.* **2003**, *125*, 3008–3027.
- [23] Niemi, M.; Tkachenko, N. V.; Efimov, A.; Lehtivuori, H.; Ohkubo, K.; Fukuzumi, S.; Lemmetyinen, H. *J. Phys. Chem. A* **2008**, *112*, 6884–6892.
- [24] Stevens, B.; Hutton, E. *Nature (London, U. K.)* **1960**, *186*, 1045–6.
- [25] Hopfield, J. J. *Phys. Rev.* **1930**, *36*, 784.
- [26] Kautsky, H.; Merkel, H. *Naturwissenschaften* **1939**, *27*, 195–6.
- [27] Foerster, T.; Kasper, K. *Z. Phys. Chem., N. F.* **1954**, *1*, 275.
- [28] Walker, M. S.; Bednar, T. W.; Lumry, R. *J. Chem. Phys.* **1966**, *45*, 3455–6.
- [29] Walker, M. S.; Bednar, T. W.; Lumry, R. *J. Chem. Phys.* **1967**, *47*, 1020–8.
- [30] Birks, J. B.; Christophorou, L. G. *Nature (London, U. K.)* **1962**, *194*, 442–4.
- [31] Selinger, B. K. *Nature (London, U. K.)* **1964**, *203*, 1062–3.
- [32] Forster, T.; Kasper, K. *Z. Elektrochem. Angew. Phys. Chem.* **1955**, *59*, 976–80.
- [33] Ferguson, J. *J. Chem. Phys.* **1958**, *28*, 765–8.
- [34] Murrell, J. N.; Tanaka, J. *Mol. Phys.* **1964**, *7*, 363–80.
- [35] Stevens, B. *Spectrochim. Acta* **1962**, *18*, 439–48.
- [36] Hirayama, F. *J. Chem. Phys.* **1965**, *42*, 3163–71.
- [37] Kloepffer, W. *J. Chem. Phys.* **1969**, *50*, 2337–43.
- [38] Foerster, T. In *The Exciplex*; Gordon, M., Ware, W. R., Eds.; Academic Press Rapid Manuscript Reproduction, 1975.

-
- [39] Parker, C. A.; Hatchard, C. G. *Nature (London, U. K.)* **1961**, *190*, 165–6.
- [40] Chandross, E. A.; Longworth, J. W.; Visco, R. E. *J. Am. Chem. Soc.* **1965**, *87*, 3259–60.
- [41] Mulliken, R. S. *J. Am. Chem. Soc.* **1950**, *72*, 600–8.
- [42] Beens, H. Ph.D. thesis, Free university, Amsterdam, 1969.
- [43] Beens, H.; Weller, A. *Acta Phys. Pol.* **1968**, *34*, 593–602.
- [44] Beens, H.; Knibbe, H.; Weller, A. *J. Chem. Phys.* **1967**, *47*, 1183–4.
- [45] Kavarnos, G. J.; Turro, N. J. *Chem. Rev.* **1986**, *86*, 401–49.
- [46] Kuz'min, M. G.; Sadovskii, N. A.; Vaynshtein, Y. A.; Soloveychik, O. M. *Khim. Vys. Energ.* **1992**, *26*, 522–30.
- [47] Kuzmin, M. G.; Sadovskii, N. A.; Weinstein, J.; Kutsenok, O. *Proc. - Indian Acad. Sci., Chem. Sci.* **1993**, *105*, 637–49.
- [48] Vainshtein, Y. A.; Sadovskii, N. A.; Kuz'min, M. G. *Khim. Vys. Energ.* **1994**, *28*, 244–51.
- [49] Mataga, N. *Pure Appl. Chem.* **1997**, *69*, 729–734.
- [50] Chibisov, A. K. *Usp. Khim.* **1981**, *50*, 1169–96.
- [51] Weller, A. *Z. Phys. Chem. (Wiesbaden)* **1982**, *133*, 93–8.
- [52] Beecroft, R. A.; Davidson, R. S.; Goodwin, D.; Pratt, J. E. *Pure Appl. Chem.* **1982**, *54*, 1605–21.
- [53] Ottolenghi, M. *Accounts Chem. Res.* **1973**, *6*, 153–60.
- [54] S., M. R.; B., P. W. *A Lecture and Reprint Volume*; Wiley-Interscience: New York, 1969.
- [55] H., B.; A., W. In *Inorganic molecular Photophysics*; B., B. J., Ed.; 1975; vol. 2.
- [56] .R., W. M. In *In photoinduced Electron Transfer, Part A. conceptual basis*; fox M. A., M., C., Eds.; Elsevier: amsterdam, 1988.
- [57] Birks, J. B. *Photophysics of Aromatic Molecules (Wiley Monographs in Chemical Physics)*. 1970.

- [58] Rehm, D.; Weller, A. *Isr. J. Chem.* **1970**, *8*, 259–71.
- [59] Jacques, P.; Haselbach, E.; Henseler, A.; Pilloud, D.; Suppan, P. *J. Chem. Soc., Faraday Trans.* **1991**, *87*, 3811–13.
- [60] Ghoneim, N.; Hammer, C.; Haselbach, E.; Pilloud, D.; Suppan, P.; Jacques, P. *J. Chem. Soc., Faraday Trans.* **1993**, *89*, 4271–3.
- [61] Wang, Y.; Haze, O.; Dinnocenzo, J. P.; Farid, S.; Farid, R. S.; Gould, I. R. *J. Org. Chem.* **2007**, *72*, 6970–6981.
- [62] Strickler, S. J.; Berg, R. A. *J. Chem. Phys.* **1962**, *37*, 814–22.
- [63] Foerster, T.; Seidel, H. P. *Z. Phys. Chem. (Muenchen, Ger.)* **1965**, *45*, 58–71.
- [64] Knibbe, H.; Rehm, D.; Weller, A. *Ber. Bunsenges. Phys. Chem.* **1969**, *73*, 839–45.
- [65] Suppan, P. *Chem. Phys. Lett.* **1983**, *94*, 272–5.
- [66] Grampp, G.; Justinek, M.; Landgraf, S.; Angulo, G.; Lukzen, N. *Photochem. Photobiol. Sci.* **2009**, *8*, 1595–1602.
- [67] Mladenova, B.; Kattnig, D. R.; Grampp, G. *Z. Phys. Chem. (Muenchen, Ger.)* **2006**, *220*, 543–562.
- [68] Soboleva, I. V.; Dolotova, E. V.; Kuz'min, M. G. *High Energy Chem.* **2002**, *36*, 98–102.
- [69] Soboleva, I. V.; Dolotova, E. V.; Kuz'min, M. G. *High Energy Chem.* **2002**, *36*, 29–37.
- [70] Dogadkin, D. N.; Soboleva, I. V.; Kuz'min, M. G. *High Energy Chem.* **2002**, *36*, 383–390.
- [71] Chow, Y. L.; Johansson, C. I. *J. Phys. Chem.* **1995**, *99*, 17558–65.
- [72] Dolotova, E. V.; Soboleva, I. V.; Kuz'min, M. G. *High Energy Chem.* **2003**, *37*, 231–240.
- [73] Huang, K.; Rhys, A. *Proc. R. Soc. London, Ser. A* **1950**, *204*, 406–23.
- [74] Marcus, R. A. *J. Phys. Chem.* **1989**, *93*, 3078–86.
- [75] Gould, I. R.; Boiani, J. A.; Gaillard, E. B.; Goodman, J. L.; Farid, S. *J. Phys. Chem. A* **2003**, *107*, 3515–3524.

- [76] Asahi, T.; Ohkohchi, M.; Mataga, N. *J. Phys. Chem.* **1993**, *97*, 13132–7.
- [77] Vauthey, E. *J. Phys. Chem. A* **2001**, *105*, 340–348.
- [78] Levy, D.; Arnold, B. R. *J. Phys. Chem. A* **2005**, *109*, 2113–2119.
- [79] Gould, I. R.; Noukakis, D.; Gomez-Jahn, L.; Young, R. H.; Goodman, J. L.; Farid, S. *Chem. Phys.* **1993**, *176*, 439–56.
- [80] Valeur, B.; Editor., *Molecular Fluorescence - An Introduction: Principles and Applications*, 1st Edition 2000. 2000.
- [81] Albrecht, C. *Anal. Bioanal. Chem.* **2008**, *390*, 1223–1224.
- [82] Lakowicz, J. R. *Principles of Fluorescence Spectroscopy*. 1983.
- [83] Querner, J.; Wolff, T. *Angew. Chem., Int. Ed.* **2002**, *41*, 3063–3064.
- [84] McPhie, P. *Anal. Biochem.* **2000**, *287*, 353–354.
- [85] Kirby, E. P.; Steiner, R. F. *J. Phys. Chem.* **1970**, *74*, 4480–90.
- [86] Kavarnos, G. J. *Fundamentals of Photoinduced Electron Transfer*. 1993.
- [87] Kavarnos, G. J. *Top. Curr. Chem.* **1990**, *156*, 21–58.
- [88] Crawford, M. K.; Wang, Y.; Eisenthal, K. B. *Chem. Phys. Lett.* **1981**, *79*, 529–33.
- [89] Wang, Y.; Crawford, M. C.; Eisenthal, K. B. *J. Am. Chem. Soc.* **1982**, *104*, 5874–8.
- [90] Zhong, Q.; Fourkas, J. T. *J. Phys. Chem. B* **2008**, *112*, 8656–8663.
- [91] Djojoputro, H.; Ismadji, S. *J. Chem. Eng. Data* **2005**, *50*, 727–731.
- [92] Oswal, S. L.; Oswal, P.; Gardas, R. L.; Patel, S. G.; Shinde, R. G. *Fluid Phase Equilib.* **2004**, *216*, 33–45.
- [93] Rosspointner, A. *Experimental Observations of Diffusional Effects on Photoinduced Electron Transfer Reactions*. Ph.D. thesis, Technical university Graz (Austria), 2008.
- [94] Kuzmin, M. G.; Soboleva, I. V. *Prog. React. Kinet.* **1986**, *14*, 157–218.
- [95] Nad, S.; Pal, H. *J. Phys. Chem. A* **2000**, *104*, 673–680.
- [96] Pan, Y.; Tang, W.; Yu, T.; Wang, J.; Fu, Y.; Wang, G.; Yu, S. *J. Lumin.* **2007**, *126*, 421–426.

- [97] Arnold, D. R.; Maroulis, A. J. *J. Am. Chem. Soc.* **1976**, *98*, 5931–7.
- [98] Schmidt, R. *J. Phys. Chem. A* **2006**, *110*, 5990–5997.
- [99] Brancaleon, L.; Brousmiche, D.; Johnston, L. J. *Can. J. Chem.* **1999**, *77*, 787–791.
- [100] Abreu, A. S.; Castanheira, E. M. S.; Ferreira, P. M. T.; Monteiro, L. S.; Pereira, G.; Queiroz, M.-J. R. P. *Eur. J. Org. Chem.* **2008**, 5697–5703.
- [101] Sundararajan, C.; Falvey, D. E. *J. Org. Chem.* **2004**, *69*, 5547–5554.
- [102] Bonesi, S. M.; Erra-Balsells, R. *Perkin 2* **2000**, 1583–1595.
- [103] Caspar, J. V.; Wang, Y. *Chem. Phys. Lett.* **1994**, *218*, 221–8.
- [104] Guirado, G.; Fleming, C. N.; Lingenfelter, T. G.; Williams, M. L.; Zuilhof, H.; Dinnocenzo, J. P. *J. Am. Chem. Soc.* **2004**, *126*, 14086–14094.
- [105] Merkel, P. B.; Luo, P.; Dinnocenzo, J. P.; Farid, S. *J. Org. Chem.* **2009**, *74*, 5163–5173.
- [106] Borg, R. M.; Arnold, D. R.; Cameron, T. S. *Can. J. Chem.* **1984**, *62*, 1785–802.
- [107] Dossot, M.; Burget, D.; Allonas, X.; Jacques, P. *New J. Chem.* **2001**, *25*, 194–196.
- [108] Aich, S.; Basu, S. *J. Chem. Soc., Faraday Trans.* **1995**, *91*, 1593–600.
- [109] Kosugi, R.; Suzuki, K.; Takao, K.; Hayashi, Y.; Yatsuo, T.; Fukuda, K.; Ohashi, H.; Arai, K. *Mater. Sci. Forum* **2006**, *527-529*, 1309–1312.
- [110] Love, L. J. C.; Shaver, L. A. *Anal. Chem.* **1976**, *48*, 364A–368A, 370A–371A.
- [111] Lewis, C.; Ware, W. R.; Doemeny, L. J.; Nemzek, T. L. *Rev. Sci. Instrum.* **1973**, *44*, 107–14.
- [112] Photomultiplier Tube - Principle to Application. Hamamatsu Photonics K.K, 1994.
- [113] Justinek, M. Magnetic field effects used for the determination of electron self-exchange kinetics. M.Sc. thesis, Institut für Physikalische und Theoretische Chemie der Technischen Universität Graz., 2003.
- [114] Landgraf, S. *Spectrochim. Acta, Part A* **2001**, *57A*, 2029–2048.
- [115] Rosspeintner, A. Kinetics of photoinduced electron transfer reactions between 2,6-Dicyano-N,N,N,N Tetramethyl-p-Phenylenediamine and various solvents,. M.Sc. thesis, Graz, Austria, 2002.

- [116] Landgraf, S. *Rev. Fluoresc.* **2004**, *1*, 341–363.
- [117] Landgraf, S.; Grampp, G. *J. Inf. Rec.* **1996**, *23*, 203–207.
- [118] Landgraf, S.; Grampp, G. *Monatsh. Chem.* **2000**, *131*, 839–848.
- [119] Landgraf, S. *J. Biochem. Biophys. Methods* **2004**, *61*, 125–134.
- [120] Ghoneim, N. *Spectrochim. Acta, Part A* **2001**, *57A*, 483–489.
- [121] Deperasinska, I.; Gaweda, E.; Mandziuk, M.; Prochorow, J. *Adv. Mol. Relax. Interact. Processes* **1982**, *23*, 45–67.
- [122] Haselbach, E.; Pilloud, D.; Suppan, P. *J. Chem. Soc., Faraday Trans.* **1995**, *91*, 3123–5.
- [123] Aspari, P.; Ghoneim, N.; Haselbach, E.; von Raumer, M.; Suppan, P.; Vauthey, E. *J. Chem. Soc., Faraday Trans.* **1996**, *92*, 1689–1691.
- [124] Mataga, N. *Pure Appl. Chem.* **1993**, *65*, 1605–10.
- [125] Kattnig, D. R.; Rosspeintner, A.; Grampp, G. *Angew. Chem., Int. Ed.* **2008**, *47*, 960–962.
- [126] Lemmetyinen, H.; Tkachenko, N. V.; Efimov, A.; Niemi, M. *J. Phys. Chem. C* **2009**, *113*, 11475–11483.
- [127] Cornil, J.; Beljonne, D.; dos Santos, D. A.; Shuai, Z.; Bredas, J. L. *Synth. Met.* **1996**, *78*, 209–217.
- [128] Scaltrito, D. V.; Thompson, D. W.; O’Callaghan, J. A.; Meyer, G. J. *Coord. Chem. Rev.* **2000**, *208*, 243–266.
- [129] Kakitani, T.; Mataga, N. *Chem. Phys.* **1985**, *93*, 381–97.
- [130] Kakitani, T.; Mataga, N. *J. Phys. Chem.* **1985**, *89*, 8–10.
- [131] Mataga, N.; Okada, T.; Yamamoto, N. *Bull. Chem. Soc. Jpn.* **1966**, *39*, 2562.
- [132] Van Haver, P.; Helsen, N.; Depaemelaere, S.; Van der Auweraer, M.; De Schryver, F. C. *J. Am. Chem. Soc.* **1991**, *113*, 6849–57.
- [133] Lee, J. H.; Carraway, E. R.; Schlautman, M. A.; Yim, S.; Herbert, B. E. *J. Photochem. Photobiol., A* **2004**, *167*, 141–148.

Bibliography

- [134] Valat, P.; Wintgens, V.; Chow, Y. L.; Kossanyi, J. *Can. J. Chem.* **1995**, *73*, 1902–13.
- [135] Purkayastha, A. K.; Basu, S. *J. Photochem.* **1979**, *11*, 261–72.